MICROBIAL COMMUNITY SUCCESSION DURING DECOMPOSITION AND POTENTIAL FORENSIC APPLICATIONS.

by

EBIAKPO AKPOS APERE

A thesis submitted in partial fulfilment for the requirements for the degree of a Doctor of Philosophy at the University of Central Lancashire

November 2024

RESEARCH STUDENT DECLARATION FORM

Type of Award Doctor of Philosophy

School School of Law and Policing

*I declare that while registered as a candidate for the research degree, I have not been a registered candidate or enrolled student for another award of the University or other academic or professional institution

*****I declare that no material contained in the thesis has been used in any other submission for an academic award and is solely my own work.

*****I declare that no candidate's research programme is part of a collaborative project.

* I declare that no proof-reading service was used in the compilation of this thesis.

Print name: Ebiakpo Akpos Apere

ABSTRACT

Reliable estimation of post-mortem interval can be crucial in criminal investigations and required distinguishing different stages of decomposition. Microbial communities play a vital function in decomposition processes and can act as biomarkers to show predictable patterns of succession throughout the period of decomposition. Microbial biomarkers therefore have potential in estimating post-mortem interval (PMI) and developing an additional, reliable approach for determining PMI via microbial community succession. This study investigates the spatial and temporal dynamics of microbial taxa during swine carcass decomposition, examining microbial succession as potential biomarkers for post-mortem interval (PMI) estimation. Swine carcasses, which were used as proxies for this research, gave a comprehensive exploration of microbial communities across various ecological niches, with samples collected from body sites (mouth, belly, anus), internal organs (liver, lung), and surrounding environments (soil, seawater, freshwater, brackish water). Genomic DNA was extracted, quantified, and followed by a 16S rRNA gene amplification using next-generation sequencing (Illumina MiSeq). The bacterial composition and biodiversity were analysed using the EzbioCloud microbiome profiling tool, with statistical analyses revealing the microbial dynamics throughout decomposition. The result of this research advances the current understanding of microbial succession patterns in decomposition ecology, highlighting the challenging yet promising nature of identifying suitable microbial biomarkers for PMI estimation. No significant differences in overall community composition were revealed over time, however significant differences in specific bacterial taxa that can be used as post-mortem biomarkers were identified among body sites [belly: Bacteroidetes and families from Firmicutes (Clostridiaceae, Tissierellaceae), Actinobacteria (Corynebacteriaceae)], internal organs [liver: Firmicutes (Lactobacillaceae), and lung: Actinobacteria and Bacteroidetes], and environmental niches [Aquatic samples: Pseudomonadaceae (Proteobacteria), Bacteroidaceae (Bacteroidetes) and Acidaminococcaceae (Firmicutes), and soil: Chthoniobacteraceae (Verrucomicrobia) and Chitinophagaceae (Bacteriodetes)] as decomposition progresses. The identification of these specific bacterial taxa during different stages of decomposition offers further approach for estimating PMI, presenting microbial succession as a potential forensic tool.

TABLE OF CONTENTS

ACKNOWLEDGEMENT

First and foremost, I express my gratitude to the Almighty God, the author and finisher of my faith, for His boundless goodness and mercies that have sustained me throughout this project and in my daily pursuits.

I extend profound appreciation to my supervisor, Dr. Judith Alexis Smith (Senior Lecturer, School of Law and Policing, University of Central Lancashire) for her patience, guidance, and invaluable advice during the completion of this research. I also want to acknowledge the contributions of my second supervisor, Dr. William H. Godwin (Senior Lecturer, School of Law and Policing, University of Central Lancashire), and my Research Degree Tutor, Dr. Chandrashekhar Vishwanath Kulkarni (Senior Lecturer at the School of Pharmacy and Biomedical Sciences, University of Central Lancashire) for their thorough review during the project and their kind assistance in the absence of my primary supervisor.

I sincerely appreciate the contributions of my former supervisor, Dr. Athanasios (Thanos) Rizoulis, during the initial phase of this project and the assistance provided by the laboratory and TRACES technicians (including Christine Woodcock and her colleagues in the LIS Learning & Technical Resources department, Peter Cross and his colleagues at the Taphonomic Research in Anthropology: Centre for Experimental Studies) whose role were crucial in ensuring the success of this project.

Special thanks go to my fellow PhD colleagues, and friends whose moral and technical support proved indispensable. Being away from home presented its challenges, but their encouragement and love bolstered my confidence in the fulfilment of this project.

Ultimate appreciation is extended to my parents, Dr. Apere Embeleakpo and Mrs. Apere Beauty, whose prayers and advice have been instrumental in my academic pursuits. Their parental love has provided strength in shaping and realising my ambitions. Gratitude is also expressed to my siblings (Tamarakarela-Emi Apere, Oyindebamo Apere, Tamaratare Apere, Ebi-Eyerin Apere, Oyintarela Apere) for their unwavering encouragement and love, without which this project may have not reached completion.

LIST OF TABLES AND FIGURES

LIST OF ABBREVIATIONS

BLAST - Basic Local Alignment Search Tool

CMN - Corynebacteriaceae- Mycobacteriaceae- Nocardiaceae Bacteria

CPR - Candidate Phylum Radiation

DNA - Deoxyribonucleic acid

gDNA - Genomic Deoxyribonucleic Acid

GI - Gastrointestinal Tract

HSD - The Tukey's Honestly Significant Difference

HTA - The Human Tissue Act

JGI - Joint Genome Institute

LAB - Lactic acid bacteria

NCBI - National Centre for Biotechnology Information

NGS - Next-generation sequencing

PCR - Polymerase Chain Reaction

PD - phylogenetic diversity

pH – power of hydrogen

PM - Post-Mortem

PMSI - Postmortem submersion interval

MSA - Multiple Sequence Alignment

PMI - Post-Mortem Interval

QC – Quality Control

SCFAs – Short Chain Fatty Acid Producing Bacteria

TRACES - Taphonomic Research in Anthropology: Centre for Experimental Studies

UCLAN – University of Central Lancashire

1.0 CHAPTER ONE: INTRODUCTION

1.1 DECOMPOSITION

When a person dies, the heart stops beating, the body starts to break down via the process of autolysis, putrefaction, and anthropophagy, with nutrients being recycled back into the environment, generating a cadaver decomposition island (Pope, 2010; Carter *et al*., 2006). Dead humans undergo lots of physical and chemical changes; the changes that occur are distinct as time progresses between weeks to months and years later. The rate, process and stages of decay also depends on different biotic factors (such as microbial communities, invertebrate or vertebrate scavengers) and abiotic factors (such as weather conditions, temperature, humidity, oxygen abundance, wounds) (Bugelli *et al*., 2018; Guo *et al*., 2016; Verheggen *et al*., 2017; Singh *et al*., 2018; Rubenstein *et al*., 2017). Many researchers use pig carcasses to study, monitor and establish a prediction of the post-mortem interval, because of their physiology and comparable body size to humans (Ehrenfellner *et al*., 2017) but using animal carcasses to study decomposition as a model for estimating the post-mortem interval for human cadaver could bring some disparities between the suggested time and stages of decomposition and limit the findings of the study compared to using an actual human cadaver (Matuszewski *et al*., 2019; DeBruyn *et al*., 2021). It would be ideal to use a human carcass in this study, but there are various limitations, such as the ethical and legal frameworks required for such research and the reliance on the donation of human remains. The Human Tissue Act (HTA) 2004, sets out a framework for the use and storage of human tissues and organs, research facilities are expected to be licensed with the HT license to store and it might be difficult to store organs if the storage facilities operate without a 'Human Tissue License'. Taphonomy facilities in the UK focus on mostly pig research, as there are no human taphonomy facilities in the UK at the time of this study. Considering the limitation using human corpses, pigs would be considered a suitable proxy for the study. By the late 1980s, domestic pigs were recommended in forensic entomology study and training workshops as an analogue for humans (Matuszewski *et al*., 2019). Pigs are easy to get at low cost, have some comparable features with humans such as; similar skin and flesh, organ size and physiology, as they are omnivores which would influence the gut microbial content.

1.1.1 Stages of Decomposition

Vass (2001) showed that as death progresses, there are four stages of decomposition: fresh (autolysis), bloat (putrefaction), decay (putrefaction and carnivores), and dry (diagenesis). Other research went further to recognise decomposition as five different stages: fresh, bloated, active decay, advanced decay and dry (Guo *et al*., 2016; Almulhim and Menezes, 2020; Cláudia-Ferreira *et al*., 2023) (Figure 1.2), which

are highly influenced by physical and chemical changes in the carcass. The scientific process of decomposition starts with autolysis (Singh *et al*., 2018; Guo *et al*., 2016) or self-digestion roughly about four minutes after death (Vass 2001; Guo *et al*., 2016). Without the heart pumping blood, cells are not provided with oxygen and cannot carry out biosynthesis (Pope, 2016), and as the absence of oxygen and carbon dioxide in the blood increases, intracellular pH declines which makes the cell become more acidic and wastes build-up which eventually poisons the cells (Vass, 2001) in the process of breaking down its membranes. Without the body maintaining its homeostatic mechanism, the body acclimates to ambient temperature at the rate 1.5 - 1.6^{o}C per hour until ambient temperature is attained via a process known as *algor mortis* (Chisiu, 2018; Dillon, 2019) which is a Latin word for "the coldness of death". Since blood is not circulating from the heart anymore, post-mortem red blood cells settle at the bottom of the body by a gravitational pool, which results in a discoloration. This colour change known as *livor mortis* occurs as the lack of oxygen prevents binding with the haemoglobin in red blood cells, eventually producing deoxyhaemoglobin, which is visible as a bluish-purple colour. (Pope *et al*., 2010; Clark *et al*., 1997). This process may begin within 30 minutes after death and fully emerges approximately from 10 to 12 hours after death (Brooks, 2016). The next stage is *rigor mortis* which is a Latin word for the "the stiffness of Death" is the post-mortem stiffness of muscles that occur as a result of the chemical effects of autolysis (Pope, 2010; Clark 1997). It starts around 2-6 hours after death, and it is noticeable first in the facial muscle, then spreads to the entire body about 24 hours later, and as chemical interactions in the muscles occurs (Clark, 1997; Brooks, 2016), the muscles then relax.

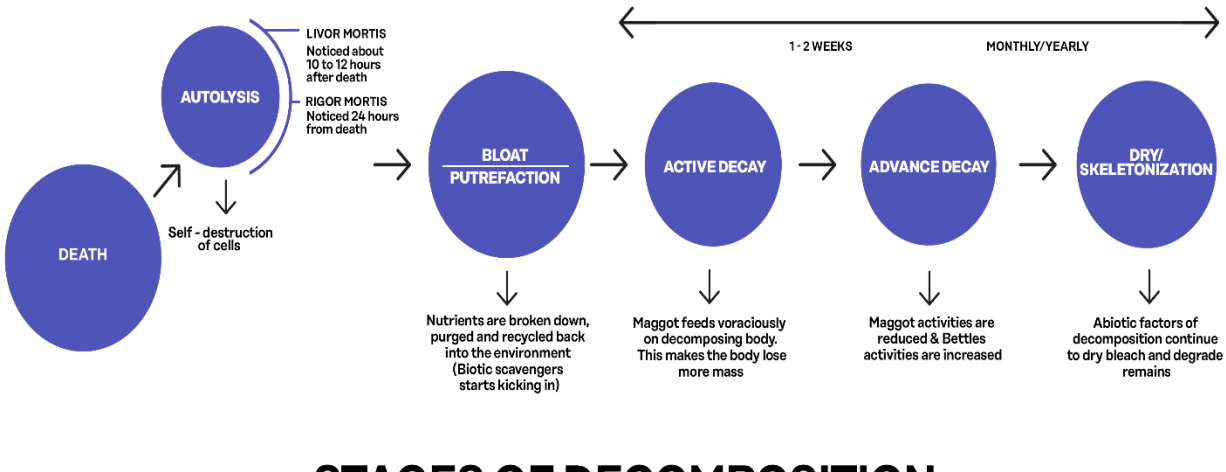

Figure 1.1 showing various stages of decomposition that can occur in an animal carcass or human cadaver (Guo et al. 2016; Almulhim and Menezes, 2020; Cláudia-Ferreira et al., 2023)

As decomposition process progresses, anaerobic bacteria resident in the gut starts to take over and commences the decay process known as putrefaction (Hyde *et al*., 2013). Putrefaction is the intrinsic cessation of body tissues by the action of microorganism (Pope, 2010; Vass, 2001). These microbes break down the left-over tissues, digesting the carbohydrates, fats and proteins released by autolysis (Clark, 1997) producing gases like carbon dioxide, methane, ammonia, hydrogen sulfide, and hydrogen sulphide, cadaverine, and putrescine (Pinheiro, 2006; Saraswat, 2008; Vass 2001; Hyde *et al*., 2013; Joseph *et al*., 2011) and the release of such volatile organic compounds is a key attractant for insects to oviposit on the decaying body (Verheggen *et al*., 2017; Joseph *et al*., 2011). The gas accumulates inside the body causing what is known as bloat which is the first visible sign of putrefaction, and it begins slightly after autolysis (Brooks, 2016). At this stage, the skin cells are broken down, therefore, the accumulated gasses and fluid in the intestine and other body parts can escape out of the body (sometimes referred to as post-mortem purging) and recycled to the environment. Not long after the purging of the gases and fluid, active decay begins. Outside microbial post-mortem activities that are evidently seen at the putrefaction stage; if a cadaver or corpse is exposed to the atmosphere, it attracts vertebrate scavengers and if not exposed to the atmosphere, invertebrate scavengers such as maggots continue to feed voraciously on the remains (Clark, 1997) and that notches decomposition into the active decay stage which commences a week or two after death depending on the environmental conditions (Brook, 2016; Joseph *et al*., 2011). After a week or two of the active decay stages, larvae that are fully matured vacates the remains of the host to experience adulthood (Pope, 2010), reducing maggot activity and indicating the beginning of the advanced decay stage (alternatively known as dry decay), this stage leads to skeletonization and can last anywhere from a few months to several years depending on the environmental conditions (Brook, 2016; Vass, 2001). Skeletonization is regarded as the ending phase of decomposition, in which the bones of the decomposing body are exposed because its soft tissues are decayed or dried.

1.1.2 Terrestrial and Aquatic conditions of Decomposition

Examining cadavers left different conditions (buried underneath the soil or submerged in water), will arguably undergo similar decomposition phases but at varying rate. According to a rule known as Casper's law, a body will take eight times longer to decompose if buried underneath the soil and twice the time to decompose in water than it would when exposed to the atmosphere (Hau *et al*., 2014). This is based on the fact that post-mortem scavengers cannot easily access the corpse when buried underneath the soil or immersed in water. Moreover, when immersed in water, the temperature might be cooler, and extreme cold and can reduce the rate or inhibit decomposition process or not allowing the body to pass the phases

of autolysis (Vass, 2001). As mentioned earlier in Casper's law, decomposition in water and buried in the soil may be slower compared to when exposed to the atmosphere. Sometimes, soil may tend to act as a primitive refrigerator for corpse buried in it, thus altering the rate of decomposition due to the inaccessibility of predators, absence of air and low temperature (Pinheiro, 2006). Due to the altered decomposition process, bodies buried in the soil, or deposited in warm or cold water (Pinherio, 2006) may undergo an entirely different process known as saponification. In saponification, microorganisms in the soil interacts with the oil and fats present in the corpse and, synonymous to the reaction in soap-making, it produces a consistent, greasy, waxy material known as adipocere or grave wax (Clark, 1991; Hau *et al*., 2014), with the colour ranging from yellowish white to grey colour (Hau *et al*., 2014). This begins to wrap the body, and if sufficient, the pH drops and bacterial activity is limited, thus inhibiting decomposition, and forming a so-called "soap mummy" (Clark, 1997). The buoyancy of the body is lost via the emission of putrefactive gases during decomposition and eventually, the body sinks to the bottom of the water source hence, forming adipocere in the absence of aquatic scavengers, (Pope, 2010). Cadaver submerged in water tend to develop adipocere due to low level of oxygen (Clark, 1997). Hau *et al*. (2014) highlights that in warmer waters, adipocere forms in the interval of two to three months, when compared to cooler water; it forms in the interval of twelve to eighteen months. Saponification changes can preserve the corpse for a period of time, making it difficult for the deceased to be identified and estimation of the post-mortem interval (Hau *et al*., 2014). Anaerobic Gram-negative Bacteria, especially putrefactive species such as *Clostridium*: *Clostridium perfringens* and *Clostridium frigidicanes* has been found to accelerate the formation of Adipocere and it entails several weeks to months (Vass, 2001; Pinheiro 2006; Hau *et al*., 2014)

In terrestrial habitats, succession of saprophytic organisms on decomposing carrion are mostly used as indicators during post-mortem interval investigations (He *et al*., 2019). However, post-mortem analysis in aquatic environments can be more challenging compared to terrestrial environment (Wallace *et al*., 2021). This can be attributed to complexities of factors in aquatic habitat such as such as tide effect salinity, water temperature, the deepness at which the carcass is located, carcass movability in the water, bacterial and chemical content of the water before carcass decomposition, and scavengers (He *et al*., 2019). Biotic organisms such as invertebrates and scavenging vertebrates, algae, and diatoms have been the focus of Postmortem submersion interval indicators in fresh and marine water with little insight to bacterial and fungal communities (Wallace *et al*., 2021). In aquatic environments, there are also metabolic function which are influenced by the interaction of post-mortem microbes in all stage of carrion decompositions.

Therefore, similar to terrestrial habitats, sequencing bacterial DNA of epinecrotic microbiota could serve as a biotic indicator which can reveal the PMI by connecting the successional changes of the epinecrotic microbiome on the carcass (He *et al*., 2019). In aquatic environments, microorganism usually co-exist in biofilms rather than in a free-floating planktonic state within the water column (Lang *et al*., 2016; Benbow *et al*., 2015: Wang *et al*., 2022). Biofilms are clusters of diverse microbial cells enclosed in a matrix (extracellular polymeric substance) that could be phylogenetically or non-phylogenetically related and adhere to various surfaces such as soil environments, natural aquatic habitats, industrial or potable water piping systems, medical devices, and even living tissues (Hassan et al., 2011; Benbow et al., 2015). This matrix that houses the microorganisms adheres to surfaces and is responsible for protecting the organism against non-favourable environmental conditions, which includes temperature and pH changes, desiccation, predation and competition, UV exposure (de Carvalho, 2018). The EPS also trap and saves nutrient and accrues enzymes that disintegrate organic matter (Benbow *et al*., 2015). The substrate (either biological or non-biological) on which the biofilm grows on usually classifies it and influences the community members and energy dynamics by dictating the prevalent community. For instance, epilithic biofilms that forms on inorganic materials such as rock might be autotrophically characterized and be typified by substantial agal microbiota while epixylic biofilms forms on decomposing plant matter are heterotrophically characterised and represents an abundant fungal community (Benbow *et al*., 2015). Within biofilms examined on piglet carcasses, diatoms (unicellular algae with a silica cell wall) exhibited patterns of diversity and richness all through decomposition but figuring out these organisms is taxonomically ferocious and demand environmental conditions with adequate sunlight. Biofilms founds on dead/decaying carrion are classified as epinecrotic which is equally diverse and rich and experience a shift during marine decomposition. As aquatic decomposition progresses, tracking the change of biofilm community composition on carrion substrate can be useful in forensics. (Benbow *et al*., 2015).

In an aquatic setting, predicting the time interval at which remains have been fully or partly submerged is one of the tasks for a medicolegal investigator, mostly in cases involving drowning or aquatic body disposal (Benbow et al., 2015). This time interval is referred to as post-mortem submersion interval (PMSI) which can simply be defined as the time between the carcass submerged until it is discovered (He *et al*., 2019). Initially described, submerged vertebrate remains undergo from a fresh to floating stage and eventually ending with sunken remains decomposition. Notwithstanding, these visual assessment and wide categorization of decomposition can vary based on some crucial biotic factors. Hence, biotic agent of aquatic decomposition such as the microbial colonies which are known to be ubiquitous within habitats

and might be more promising in forecasting the PMSI extent (Benbow *et al*., 2015). Microbial communities can equally stand more accurate as indicators than insects. This is because the body of water prevents most terrestrial insects from operations and are most only capable of colonialising the carcass when its floatation starts and can only provide a PMI from that point which is different from the time of interval since the dead and submerged (Wang *et al*., 2022). Scientific investigators have examined the successional activities of bacterial communities in biofilm on submerged animal carcass and epilithic communities (Benbow *et al*., 2015; He *et al*., 2019). The researchers discovered that microbial community on animal carcass varies in different seasons (Benbow *et al*., 2015) and equally differs greatly from the succession pattern of the epilithic communities on the rock and ceramic tiles (He *et al*., 2019; lang *et al*., 2016).

1.2 THE POTENTIAL OF MICROBIAL FORENSICS

Forensic Microbiology (also known as Microbial Forensics) was conceived from the knowledge and expertise from Forensic science and Microbiology, given that virtually everywhere on earth, diverse and ubiquitous communities of microorganisms (e.g bacteria, fungi, and viruses) can be found (Oliveira & Amorim, 2018; Kuiper, 2018; Yuan *et al*., 2023). Microbes exist in large number; hence, they can be recovered from limited trace material in a forensic investigation and provide the potential to carry out in-depth analyses of microbial communities and molecular ecology (Kupier, 2016; Roy *et al*., 2021). The concept of Forensic Microbiology is to utilise microbiological methods for the analysis of evidence related to a criminal case, ranging from fraud and bioterrorism to the transmission or outbreaks of pathogens, as well as the accidental, intentional, or hoax release of a biological agent and/or a toxin (Oliveira & Amorim, 2018; Oliveira *et al*., 2020; Budowle *et al*., 2005; Elshafei, 2020; Mir *et al*., 2022). The investigation process of Forensic Microbiology is the same as any other Forensic investigation process, which involves crime scene investigation, establishing chain of custody (collecting, documenting, processing, and protecting evidence), analysis of evidence and court presentation (Budowle *et al*., 2005). Forensic Microbiology should not be limited to biocrime (bioterrorism) but can be broadened to the application skin, body fluid microbiome for human identification which could help crime related investigations.

1.2.1 Skin Bacterial Microbiome: An Important Forensic Tool for Identification.

Identification of humans is important in forensic science (Leake, 2013) and will continue to be so. Notwithstanding minimal evidence such as insubstantial quality and inadequate copy number of DNA cannot be identified with stringency used for crime prosecution along with those associating violence. A smart criminal or offender may take cautious steps to contaminate or reduce trace evidence (such as

fingerprint, blood sweat, semen, hair, or anybody fluid) in the crime scene which could lead to investigation complications (Lee *et al*., 2015). Via environmental interaction, sloughing of skin, and bodily emission, distinctive microbial imprints are left behind (Bishop, 2019). Given that bacterial microbiome is peculiar to an individual, researchers have hypothesized that it is possible to utilise the resident bacteria of the skin transferred to object (personal items) for forensic investigation and identification (Fierer *et al*., 2010; Lee *et al*., 2015; Meadow, Altrichter and Green, 2014; Knight *et al*., 2018). These objects might be regular tools used by individuals such as mobile phones, personal computer gadgets such as computer keyboard and mice. Fierer *et al*., (2010) revealed skin-associated bacteria can be retrieved from the surface of an object regularly in contact with an individual, even up to 2 weeks after the last contact, at room temperature. Fierer *et al*., (2010) equally showed that skin bacterial are comparatively stable and can be recovered from palm surface within hours of hand washing.

On average, interpersonal variations in the microbiome constituent supersede temporal variation within individuals even when these people are sampled many months in isolation (Costello *et al*., 2009). Bacterial DNA is a neoteric avenue for forensic science, and it is of great potential, bacterial DNA is more resistant to environmental factors than the human DNA and can last for a longer period on contact surfaces (Gouello *et al*., 2021; Leake, 2013). Environmental surroundings can affect the configuration of the bacterial DNA and the individual's microbiome and therefore be likely that the distinct bacterial patterns could stereotype individuals with various lifestyles (Lee *et al*., 2015). Fierer *et al*., (2010) hypothesised that bacterial fingerprint could be used as a significant tool in forensic investigation given that people harbour skin-associated bacterial microbiome that are peculiar to that individual and are equally stable and transferrable. Lee *et al*., 2015 equally hypothesised that bacterial DNA analysis could stereotype the distinctive bacterial profile amongst individuals in a significant forensic way.

1.2.2 Body fluid Bacterial Microbiome: An Important Forensic Tool for Identification.

At crime scenes, body fluids such as blood, saliva and semen are commonly found (Zapico *et al*., 2022). However, other fluids such as sweat, vaginal fluid and urine can also be found and all these body fluids may play essential roles in forensic investigations (Oliveira and Amorim, 2018; Zou *et al*., 2016; Díez López *et al*., 2019). For example, to identify a bite process in a crime investigation, the saliva can be used so also, in cases of sexual intercourse, harassment or assault, the presence of vaginal fluid on a suspect's penis can support such investigation (Zou *et al*., 2016). The oral cavity hosts the second most diverse microbial communities in the body after the gastrointestinal tract (Adserias-Garriga *et al*., 2017).

Yao *et al*., (2020) conducted as research on body fluid via microbial profiling and its potentials for forensic investigation. They demonstrated that microbial 16S gene sequencing can be used to sequence forensic trace samples and results as regards to the microbial composition profiles that can be applied for discerning saliva from skin. It has been proposed that fluid shows distinct constitution of microorganism that can be used as bioindicators, being able to deduce the available body fluid based on its microbial composition (Oliveira and Amorim, 2018).

1.3 CRIME SCENE AND MICROBIAL FORENSIC TECHNIQUE

Bacterial cells from diverse areas of the body can be examined regarding the type of crime and the readily available evidence in the crime scene (Gadiraju & Oberle, 2021). For a criminal case investigation using microbial forensic technique to be successful, the efficient collection and preservation of microbial forensic sample and evidence is paramount (Budowle *et al*., 2006). Investigations may be compromised, if evidence or samples degrade or is contaminated at the point of collection, not collected or available when needed or transported and stored poorly. Arguably, forensic microbiology should maintain quality chain of custody as do other traditional forensic processes in order to maintain the integrity of evidence. Budowle *et al*., (2005) revealed that a biocrime can either be covert or overt. If the investigation is covert, law enforcement agencies may not be immediately involved. If the investigation is overt, law enforcement agency holds strong control of the investigation and works closely with the investigating officer or public health authorities as appropriate (Budowle *et al*., 2005).

Crime scene investigators usually accompany the first responders (such as police, health care workers, paramedics, veterinarians, or hazardous materials personnel) or a surveillance team that has knowledge or has gathered some preliminary data about the crime event. As such, the forensic investigator has an idea or prior knowledge before arrival at the crime scene. This knowledge will be an added advantage in operational planning phase of the crime investigation (Budowle *et al*., 2005). Planning is a necessity, and in biocrime investigations, a comprehensive executional plan showing a strategic approach to sample collection, storage and transportation of evidence should be developed. The procedure in which a biological agent is stored and transported can affect the analysed result of an investigation (Budowle *et al*., 2005) so it is of the utmost importance that the forensic examiner knows the conditions of storing and transporting a biological agent that would be used as a sample for forensic investigation.

1.4 POST-MORTEM MICROBIOME PROJECT

Recent research has revealed massive expansion in the field, operation, and scope of forensic microbiology (Schmedes *et al*., 2016; Arenas *et al*., 2017) as mentioned earlier in section 1.1 of this chapter. These expansions in Forensic microbiology may be useful in medicolegal investigation involving estimations of post-mortem interval. The human body is a host to over a trillion microbial cells (Guinane and Cotter, 2013; Dash and Das, 2020; Cryan *et al*., 2019; Ursell *et al*., 2012; Wang *et al*., 2017), when the host organisms die, these taxa undergo a fundamental succession as they constantly interact with host organism (Dash and Das, 2020). In an autopsy of a cadaver, these successions might be revealed and can be used as a bioindicator to estimate the post-mortem interval of the cadaver. Human Microbiome research has concentrated mainly on commensal and pathogenic microbes (Ogunrinola *et al*., 2020; Javan *et al*., 2016b) and their impact on health, but little research is geared towards the succession of microbes when a human die (Javan *et al*., 2016a). Death of living organisms is inevitable. Therefore, it is worthy to study the life that continues on a dead human. When a dead body is found, knowing the time of death is as important as knowing the reason of death. When a living organism dies, decomposition takes place, microorganisms break down, biodegrade and recycles its molecular components back to nature (Kowalski, 2014). During this process, nutrients and the minerals are broken down and returned to the environment. Researchers have shown via culture-independent methods that there are microbial successions on a dead organism. These microorganisms that act as key players during decomposition can be described as the thanatomicrobiome, derived from 'thanatos' a Greek word meaning death (Javan *et al*., 2016a; Javan *et al*., 2016b; Zhou and Bain, 2018) and microbiome, a term microbiologist use in describing the community of microorganisms in an environment. Thanatomicrobiome communities in a general definition is said to be the study of microorganism and its succession on internal organs while epinecrotic communities is the external succession of microorganisms on skin or other body part and cavities upon death (Hauther *et al*., 2015; Javan *et al*., 2016; Zhou and Bain, 2018; Roy *et al*., 2021) (Figure 1.2).

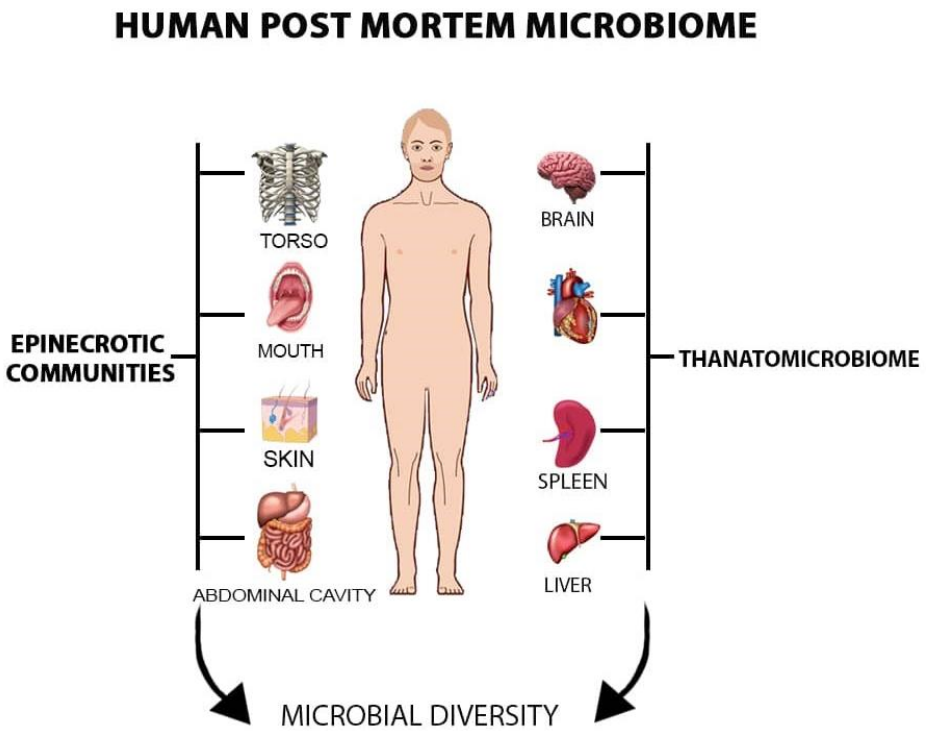

Figure 1.2 Showing the various locations of Thanatomicrobiome and Epinecrotic Communities (Javan et al., 2016a)

Forensic microbiology has the potential to answer legal questions such as where a death occurred, or how long ago did the death occur? Projects on the human microbiome have shown that in and on the surface on the human body, microbial cells are ten times more abundant than human cells. In healthy humans, the internal organs such as the heart, brain, liver, and spleen are devoid of microorganism (Can *et al*., 2014). Nevertheless, in 35% cases of post-mortem anatomical dissection, culturable organism(s) were discovered by Fredette (1916) as cited in Javan *et al*., (2016a). As the post-mortem interval (PMI) increased, the ratio of positive cases where microbes were detected also increased. Thus, the microorganisms found in these internal organs probably consist of those that are directly linked with decomposition. When a human die, decomposition begins, microbes from internal organs such as the lung and gut that are not sterile (Zhou and Bain, 2018) can readily spread and colonise the liver and other organs previously devoid of microorganism (Sibulesky, 2013; Can *et al*., 2014; Zhou and Bain, 2018). The microbiome of the human large intestine is occupied mostly by Firmicutes (for example, Lactobacillus spp.) and Bacteroidetes (for example, Bacteroides spp.) with smaller populations of Proteobacteria (for example, Escherichia spp.) and Actinobacteria (for example, Bifidobacterium spp.) (Hauther *et al*., 2015); upon death, there is a decline in anaerobic taxa such as Bacteroidetes and Lactobacillus that were

abundant when the host was living (regardless of the disparity in the respective proportions of these species between individuals as a result of diet and lifestyle).

1.4.1 Soil microbial forensics

Soil microbial forensics can be defined as the study of microorganism in or on the soil, its ecological system and how it can be applied to forensic science (Santiago-Rodriguez & Cano 2016). Soil can play a vital role in solving criminal case investigations, both in evidential and intelligence context, as a result of its complexity and transferability (Ritz, Dawson, and Lorna, 2009). Since the field of forensic microbiology evolved, research on soil microbial communities and its environment have potentially strengthened and added value on crime investigations as soil can provide knowledge of the origin of unknown sample (Melo *et al*., 2019; Demanèche *et al*., 2017; Franklin & Mills 2003). When executing a crime, movements of the suspect e.g., if they have stepped on a soil, may be recovered from the suspect's footwear and be used to link the suspect to a specific location. An investigation may not be complete if the movement of the suspect or object being investigated is not studied. Arguably, this aspect of forensic microbiology can help predict the current location of a suspect or where they have been recently by the technique of microbial assemblage. Microbial assemblages refer to communities of microorganisms residing together in a particular habitat or environment (Hosoda *et al*., 2020) and microbial assemblage techniques examines the makeup, variety, and role of microbial communities within a specific environment. However, Lax *et al*., (2015) suggested that it might be less likely to use the technique of microbial assemblage to track the recent location of an individual as a result of rapid turnover of the microbial community associated to the surface. Microbial communities found in the soil may not only link a person/body to a location but can also include how changes in soil microbial communities could relate to decomposition/time since death or help identify clandestine graves (even if a body had been subsequently moved) (Ralebitso-Senior, Thompson and Carney, 2016). Decomposition of a body on soil would be expected to influence the microbial communities in the soils. Environmental factors like moisture levels, soil acidity, and oxygen levels (Cholewa, Bonar and Kadej, 2022) can influence the interaction between the microbial communities in the carcasses and soil and even if the decomposing body is subsequently removed, signatures of decomposition could still be present and depending on the microbial succession patterns the taxa identified might provide insights into PMI.

1.5 GENETIC IDENTIFICATION OF MICROBIAL COMMUNITIES DURING DECOMPOSITION

The process of isolating nucleic acids, followed by downstream sequencing, offers an understanding of the makeup of microbial communities in complex samples (Lever *et al*., 2015). Nucleic acid isolation techniques involve a variety of strategies. However, most techniques share similar objectives: the thorough lysis of cells and extraction of intracellular nucleic acids into aqueous solution, the elimination of non-nucleic acid organic and inorganic compounds from the resulting aqueous extracts, and the reduction of nucleic acid losses during this purification process (Lever *et al*., 2015). Traditionally, DNA extraction from microbial communities were achieved via procedures, such as phenol-chloroform extraction and ethanol precipitation and were time-consuming, arduous, and posed the risk of sample contamination (Hwang *et al*., 2012; Dairawan and Shetty, 2020). In recent years, commercial DNA extraction kits have transformed the DNA extraction procedure. These kits include the use of spin column or magnetic bead technology to streamline the extraction process and reduce hands-on time. Extraction kits provide better reproducibility and yield than traditional procedures since they include pre-optimised protocols and reagents for streamlined protocols (Lever *et al*., 2015). Furthermore, extraction kits are automation-compatible, allowing for high-throughput sample processing, which is required for large-scale studies. Extraction kits have become an indispensable tool in decomposition studies as they are designed to efficiently lyse a wide range of microbial cells, including those with tough cell walls or that live in biofilms, assuring complete DNA recovery and enhancing the robustness and reproducibility of DNA extraction (Knüpfer *et al*., 2020; Oldham *et al*., 2012; Claassen *et al.,* 2013). DNA extraction kits can provide high DNA yield from challenging samples with low-biomass or highly degraded organic matter (Sui *et al*., 2020), indulgencing the detection of rare or low-abundance microbial species in the context of decomposition. Regardless the benefits of extraction kit, no extraction kit has been manufactured that is universally suitable for all sample types and research objectives (Lever *et al*., 2015). Quantification of extracted DNA is crucial for ensuring the success of downstream applications such as PCR and NGS sequencing (Sedlackova *et al*., 2013). Several methods exist for DNA quantification, including spectrophotometry, fluorometry, and gel electrophoresis (Khetan *et al*., 2019). The UV spectrophotometry like the nanodrop instrument is particularly advantageous because it saves time when quantifying a vast amount of DNA extract and it requires only a small volume of the sample (1-2 µL) to provide information about DNA purity by calculating the A260/A280 ratio, which indicates protein contamination (discussed further in chapter 3). Decomposition samples often contain various organic and inorganic contaminants that can affect DNA purity and subsequent analyses, hence the Nanodrop not only quantifies DNA but also provides a quick assessment of sample purity by measuring absorbance ratios

(A260/A280 and A260/A230) (Olson and Morrow, 2012). The capabilities of the nanodrop instrument are advantageous in decomposition studies as it ensures that the DNA is sufficiently pure for PCR amplification and NGS sequencing for microbial profiling.

1.5.1 16S rRNA gene and its Amplification

The 16S rRNA gene is a key functional molecule in the machinery for gene expression and as such provide a homologous sequence for phylogenetic comparisons across species. This has made the 16S rRNA gene widely embraced for identifying, and classifying prokaryotes (Ibal *et al*., 2019). This includes prokaryotes within complex microbial communities, such as environmental samples, gut microbiomes and post-mortem microbiomes. Analysis of the 16S rRNA gene can reveal the phylogenetic affiliations and relative abundance among taxa (Vetrovsky and Baldrian, 2013). The 16S rRNA gene is about 1600 base pair long (Bukin *et al*., 2019) and comprises of nine "hypervariable regions" which are represented as V1-V9 and are separated by conserved regions (Chakravorty *et al*., 2007; Osman *et al*., 2018) (Figure 1.3). These hypervariable regions serve as useful targets in scientific research, diagnostic assays and in the identification of microbial communities because their DNA sequence can be specific to certain genera or species (Chakravorty *et al*., 2007; Osman *et al*., 2018). Sequencing of the 16S rRNA gene involves amplification of specific (selected) variable regions through Polymerase Chain Reaction (PCR) after the DNA isolation from intended sample. For taxonomic classification, it is satisfactory to sequence a single or conjoined hypervariable region rather than the whole gene length (Liu *et al*., 2008)

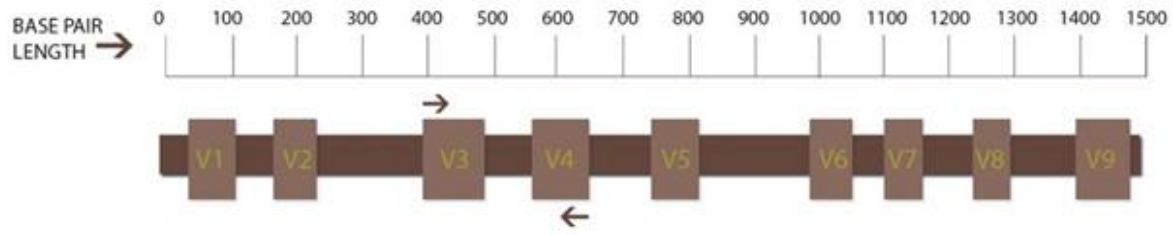

Figure 1.3 Structure of the 16rRNA gene showing the base pair length (the arrows on V3 and V4 indicates the target region) (Fasesan et al., 2020)

The V3/V4 hypervariable region of 16S rRNA gene has been exploited and used more often by researchers for profiling microbial communities since these regions accommodates the maximum nucleotide heterogeneity and maximum distinguishing power (Chakravorty *et al*., 2008) and because of their shorter length, the V3 or V4 region is considered befitting for small-length read sequencing technologies such as

the HiSeq and the MiSeq Illumina platforms (García-López *et al*., 2020). These regions have become the conventional amplicon target as Illumina has recommended a library preparation protocol for sequencing on the Miseq platform. To target the V3 and V4 region, specific set of primers are used during the amplification that targets both Bacteria and Archaea and generate an appropriate amplicon length for Next-generation sequencing (also known as high-throughput sequencing). The sequences can also be used for comparison and analysis of species composition both among and across environments (Apprill *et al*., 2015).

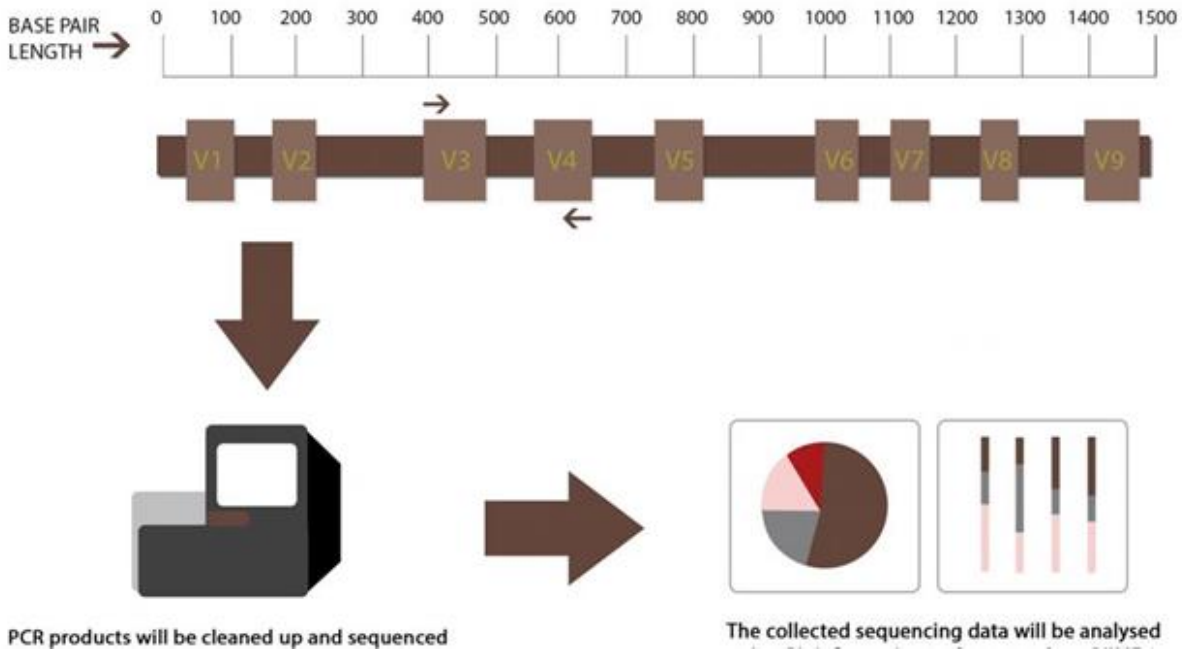

Figure 1.4 Showing post gDNA extraction workflow. General amplification and sequencing workflow for microbial metagenomics using Illumina Miseq platform (Metcalf et al., 2013) and collected sequenced data will be analysed using bioinformatic package such as EZbioCloud.

Culture-dependent methods, which have long been employed in microbiology, rely on the growth of microorganisms on particular media in controlled environments. However, culture-dependent method is selective and may not promote the growth of all microorganisms, resulting in an incorrect or biased representation of microbial communities in a sample (Al-Awadhi *et al*., 2013; Kisand and Wikner, 2003; Carraro et al., 2011). Culture-dependent approaches also favour fast-growing organisms (Medina *et al*., 2017; Perito and Cavalieri, 2018; Vartoukian, Palmer and Wade, 2010), which further leads to a biased capture of microbial community in a sample. Also, culture-dependent approaches may have lower taxonomic resolution and take longer to complete than NGS technology (Boers, Jansen and Hays, 2019; Acharya *et al*., 2019). Next-generation sequencing technologies are more advanced than the traditional

Sanger sequencing technology, and it enables sequencing of millions or billions of DNA fragments. Sanger sequencing, while a pioneering approach for DNA sequencing, has drawbacks when compared to next-generation sequencing (NGS) technologies such as Illumina MiSeq. Sanger sequencing involves sequencing one DNA fragment at a time, which is slower and more expensive per base pair sequenced than NGS (Yang, Xie and Yan, 2014). Its throughput is significantly lower, rendering it unsuitable for large-scale sequencing projects or studies with high sequencing volume (Levy and Boone, 2018; Yang, Xie and Yan, 2014). Additionally, Sanger sequencing requires a single source amplicon for sequencing, making it inappropriate for community-based or metagenomic analyses where mixed DNA from diverse organisms in a sample need to be sequenced simultaneously (Levy and Boone, 2018; Besser *et al*., 2018). Furthermore, while Sanger sequencing often produces shorter read lengths than some NGS technologies, this limitation may not necessarily apply to all contexts or applications (Yang, Xie and Yan, 2014; Besser *et al*., 2018; Heather and Chain, 2016). Illumina MiSeq is the most used platform for sequencing of 16S rRNA gene amplicons, due to its longer read depth, cost-effectiveness, and high multiplicity. Employing MiSeq sequencing platform for microbiome studies was first reported by Caporaso *et al*. (2012) as cited in Unno *et al*. (2015) in which 1.5 Gb (5 million 150 bp paired-end reads) were produced in a day. In recent times, Illumina's MiSeq platform has the potentials of generating paired 250–300 bp reads accompanied by high sequencing volume (7.5–8.5 Gb), equal to the topmost 25 million paired-end reads (Unno, 2015). Kozich *et al*., 2013 accessed the efficacy of data generated by the MiSeq platform in comparison to the 454-sequencing platform. They used the 16S rRNA gene for their sequencing and showed that data generated by the MiSeq platform can be curated to be good as data generated via the 454 platform.

1.5.2 Exploration of bacterial composition after NGS procedure

After sequencing and raw sequence data files generated from NGS are obtained, the primary step to follow is performed using bioinformatics tools (Kumar *et al*., 2023). Utilizing pipelines for exploration of different microbial composition is a revolutionary transformation in microbial studies (Ciuffreda, Rodríguez-Pérez and Flores, 2021). The limitations of the classical microbiological techniques, such as culture-dependent methods have been overcome with the inception of bioinformatics pipelines. Open-source bioinformatics pipelines such as QIIME 2, Mothur (Caporaso *et al*., 2010; López-García *et al*., 2018; Schloss *et al*., 2009), EzbioCloud (Yoon *et al*., 2017) has made high-throughput analysis of microbial populations is now more comprehensive. Activities for microbial communities' exploration via these

pipelines include, importing data into the software (pipeline), denoising and quality filtering, clustering sequences into operational taxonomic units (OTUs), assigning taxonomy using classifiers trained on databases (e.g., Greengenes, SILVA), generating diversity analyses (alpha and beta diversity) and taxonomic composition tables (Cameron *et al*., 2021; Estaki *et al*., 2020; Kaszubinski *et al*., 2019)

1.6 ETHICAL CONSIDERATIONS

Besides individual identify, procedures in a human microbiome investigation may go beyond discerning individuals but also revealing disclosed unpredicted information. Hence, human microbiome investigation may pose some challenges such as ethical, legal and social challenges (Oliveira and Amorim, 2018). Gut microbiome may be used to reveal an ethnic background, origin (Nieves Delgado and Baedke, 2021), and recent or past geographical location (Dwiyanto *et al*., 2021) of an individual. This intelligence/information may be used to accentuate the person of interest for law enforcement/security services; breaching privacy rights of the individual (Oliveira and Amorim, 2018). The existence of some specific microorganism may disclose the predisposition or susceptibility of an individual to some certain clinical conditions such as diabetes or obesity (Liu *et al*., 2021; Geng *et al*., 2022; Gaël Toubon *et al*., 2023; Hegde and Dhurandhar, 2013), contributing to socioeconomic stigmatisation or discrimination (Yadav and Jawahar, 2023). Some microbial sample collection methods such as vaginal swabs, collection of stool samples can be considered as invasive and may not be accepted by some cultures of the society. At the initial stage of human microbiome research/investigation, it is essential to put in considerations the ethical, legal and social implications and that the investigation should be conducted to meet the highest ethical standards (McGire *et al*., 2008).

1.7 AIMS AND OBJECTIVES

The aim of this study was to investigate microbial community succession as biomarkers for post-mortem interval during body decomposition and its potential forensic applications.

The objective of this study is:

- To sample microbial communities from body sites (mouth, belly, anus), internal organs (liver and lung), and environmental samples (water and soil) of pig carcases at observed time points of decomposition.
- To amplify the 16S ribosomal RNA targeting the V3 and V4 regions of extracted DNA from body site, internal organ, and environmental samples of pig carcasses at observed time points for NGS using the MiSeq platform.
- To investigate the Quantitative NGS data results using an appropriate bioinformatic database software to access the operational taxonomic unit (OTUs).

- To investigate the data from the bioinformatic database analysis through relevant statistical model and to present the data in a clear and interpretable format.

1.8 NOVELTY OF RESEARCH

This study takes a novel approach by investigating the holistic microbial successions on all body parts of adult pigs decomposing in the summer under different water condition and on soil. The study includes examination of the microbial community of the pigs, on land and in aquatic environments, correlating the 16S taxa distribution across both the body and the environment which to the best of the authors knowledge has not been previously examined.

2.0 CHAPTER TWO: MATERIALS AND METHODS

2.1 INTRODUCTION

This chapter describes the sampling and analysis methodologies used for bacterial taxonomic profiling. The experimental design is categorised into eight stages: sampling, which involved the collection of biological (body sites and tissues) and environmental (soil and water) samples from pig carcasses throughout the process of decomposition; DNA Extraction: Following sample collection, DNA extraction was carried out to isolate genetic material from the samples; Nanodrop Quantification: After DNA extraction, the quantification of DNA extracts was conducted using a Nanodrop spectrophotometer, which provided information about the concentration and purity of DNA samples; Polymerase Chain Reaction (PCR): PCR amplification was employed to target the V3 V4 region of the 16S rRNA gene, (See Chapter 1, section 1.6) Gel Electrophoresis: PCR amplicons were visualised using agarose gel electrophoresis, which allowed for the confirmation of successful DNA amplification; Next Generation Sequencing (NGS): A total of 96 samples were sent for the NGS sequencing providing high-throughput and comprehensive data on microbial taxa present in the samples; Microbiome Taxonomic Profiling (MTP): involved bioinformatic analysis to assign taxonomic identities to sequenced DNA fragments in each sample, was performed; Statistical Data Analysis: Finally, statistical data analysis was conducted to interpret the results obtained from the taxonomic profiling, allowing the assessment of any significant spatial or temporal relationships between microbial taxa.

2.2 SAMPLING

All sampling were carried at “Taphonomic Research in Anthropology: Centre for Experimental Studies” (TRACES) research facility of the University of Central Lancashire, UK. Ethical approval was granted by the Animal Welfare Ethical Review Body (AWERB) before any experiments were performed. In addition, risk/COSHH assessments for field work and laboratory experiments were also in place. The sum of 2 and 9 swine carcasses (weighing 8.9 -70kg) were used for the pilot and main sampling respectively and were provided from W. Taylor and Sons Farm (Midge Hall, Leyland), with a post-mortem interval of 2 hours. The number of two pigs for the preliminary study (which ran between 3rd July 2019 and 29th August 2019) allowed the piloting of experimental procedures, assess feasibility, and refine methodologies to help identify any potential issues or challenges before conducting a larger-scale investigation. Ethical guidelines for animal research prepared by the National Committee for Research Ethics in Science and Technology (NENT) emphasise the principle of minimising the number of animals used while still obtaining scientifically valuable (The Norwegian National Research Ethics Committees, 2019; Kiani, 2022). The

allocation of resources, including funding, also played a role in determining the size of pig for the preliminary study. An increased number of nine pigs for the main study was aimed to achieve adequate statistical power to detect any significant patterns or trends in the microbial composition of samples. Environmental parameters such as temperature, humidity and pressure were obtained from a weather forecast website as it was a convenient and time-efficient approach, since TRACES was not always accessible, measuring the environmental parameters and did not require continuous monitoring or calibration compared to an *in situ* probe. Also, data form weather monitoring websites are accurate and dependable since, it is aggregated from established meteorological stations and has undergone quality control methods to a standard point of consistency, making it acceptable for scientific research.

2.2.1 Sampling for the Principal Experiment

The principal experiment began 12th July 2021 and terminated 4th August 2021. Pig carcasses were set up in triplicate for soil experiments (pigs 1,2,3) which were provided same day sampling began. For the water experiments duplicate carcasses were set up for each water type (Pigs 4 - 9). Pigs were transferred to the sampling site using a tractor and were immediately washed with water from the tap. The work area, table and other apparatus was wiped and disinfected with 5% Decon 90 (Decon Laboratories Ltd) before swabbing and dissection of tissues proceeded. The pigs were laid out 4 meters apart from each other and covered with a mesh (Figure 2.1) to deter external scavengers. Sampling days were selected to cover the key stages of decomposition (fresh, early bloat, late bloat, active decay and skeletonization – Table 2.1). The average weather conditions during the sampling period were temperature: 18°C, Humidity: 79% and Pressure: 1014 mbar (https://www.timeanddate.com).

2.2.1.1 Sampling of Body Sites and Internal Organs of Pigs

After washing the swine carcasses with water, sterile swab heads were dipped into a 5ml tube containing distilled water and wet swabbing was done for 30 seconds on each body part for all pig carcasses, care was taken to ensure same area were not resampled. The belly, anus, and mouth of the pigs were swabbed for this experiment. Swab heads were immediately cut off with sterile scissors and placed into sterile collection tubes. Pigs were autopsied in the indoor facility of TRACES at room temperature. An incision of about 15 and 10cm was made with a disposable Feather #11 scalpel in the ventral (the front) of the belly and heart region respectively. 10g of the internal organs (liver and lung) were dissected, collected using a sterile scalpel (Javan *et al*., 2017; Javan *et al*., 2023) and placed into sterile 50ml falcon tubes. Utensils used at each point to collect tissues were sterilised at each with 5% of Decon 90 (Decon Laboratories Ltd). All incisions were sealed by standard stitching procedures and the animal carcasses were kept on the table before depositing on top of the soil on its second day of decomposition. The effect of performing autopsy

on the pig carcasses during the sample collection can introduce some biases to the study in several ways that will be discussed in chapter 8, section 8.8 (Biases of this study).

Figure 2.1 Showing the pigs in its fresh stage laid out on the soil and protected with mesh.

2.2.1.2 Sampling of environmental samples

Soil and aquatic environments are rich in microbial communities that play vital roles in decomposition. Hence, this section outlines the procedures employed for sampling the environmental samples collected at various intervals to monitor microbial community succession during the decomposition process.

2.2.1.2.1 Soil

Approximately 5g of soil was collected using sterile scoop from the deposition site before the carcases were deposited. Same weight of soil was collected from a 0-5 cm depth underneath the animal carcass at subsequence sampling intervals. Sampling was done on days 2, 4, 7, 14 and 23 covering the period of active decay (Table 2.1). All samples were placed in sterile tubes, kept in ice cooler, and transported to the laboratory where they were stored at -20^{o}C until DNA extraction.

2.2.2.2.2 Sampling of Aquatic samples

Six pigs and 83L boxes (Argos Home®, U.K.) were respectively set up for this sampling. The boxes were filled with water and dissolved with different amount salt to simulate a *normal river water* (*Control), brackish water and seawater*. The boxes were labelled in accordance with their stimulated environments and group into three segments with each segment containing two boxes. On day 0 of decomposition (July 2021) pigs were submerged into their respectively boxes and placed outdoors in a field setting while they decompose. A mesh that was outstretch when placed on the box was set, and the pigs were deposited on the mesh (Figure 2.2). The boxes were then covered with its lid, clipped on top of it, heavy stones were then placed on top of the lip to weigh it down in other to avoid leakage or water ingress from rain. Sampling of water samples from submerged pigs was carried out at seven-day intervals and were initially performed by using a 1000ul pipette (NICHIRYO, Nichipet Premium) to suction out 20ml of water from the container of the submerged pig carcasses and placed in a sterile 50ul falcon. All samples were kept in an ice cooler for transport to the laboratory where they were stored at -20^{o}C until DNA extraction (Cristina *et al*., 2022; Majaneva *et al*., 2018). All sampling procedures (including pigs and environmental samples) were repeated according at subsequent sampling interval.

Figure 2.2 Pig carcass at the fresh stage submerged in water.

2.2.2.2.2.1 Salt Concentration

Seawater and brackish concentrations were fashioned with Ocean Reef Pro Coral Salt (iQuatics®, U.K.). 2.1 Kg and 1.2 Kg of salt was dissolved in 60 L of water to create the seawater and brackish water simulated saline environments. Water from the tap was utilised for the group to represent freshwater habitat.

Table 2.1 Expressing all samples utilised from body part, internal organs, and environments of pig carcasses at the various stages of decomposition for the primary study of this research. N.s signifies no samples on the respective days (Samples were collected but unavailable because they didn't pass through the PCR amplification stage). Pig for water sampling were provided a week after sampling began, hence water samples were collected once weekly. After day 14, sampling was not done a week later (Day 21) due to inaccessibility to TRACES, hence on day 23 sampling continued when the facility was accessible.

Sampling Days	Stage of Decomposition	Dissected Internal Organs		Swabs of Body Site			Environmental Samples	
		Lung	Liver	Mouth	Anus	Belly	Water	Soil
0	Fresh	Pig 1, 2, 3	Pig 1, 2, 3	Pig 1, 2, 3	Pig 1, 3	Pig 1, 2, 3	Pig 4 & 5 (sea), Pig 6 & 7 (brackish), Pig 8 &9 (fresh)	N.s.
2	Early bloat	Pig 1, 2, 3	Pig 1, 2, 3	Pig 1, 2, 3	Pig 1, 2	Pig 1, 3	N.s.	Soil sample from the belly region
4	End bloat	Pig 1, 2, 3	Pig 1, 2, 3	Pig 1, 2, 3	Pig 1, 3	Pig 1, 2, 3	N.s.	Soil sample from the belly region
7	Putrefaction/Active Decay	N.s.	N.s.	Pig 1, 2,	N.s.	Pig 1, 3	Pig 4 & 5 (sea), Pig 6 & 7 (brackish), Pig 8 &9 (fresh)	Soil sample from the belly region
14	Advanced Decay	N.s.	N.s.	N.s.	N.s.	N.s.	Pig 4 & 5 (sea), Pig 6 & 7 (brackish), Pig 8 &9 (fresh)	Soil sample from the belly region
23	Dried Decay/Skeletonization	N.s.	N.s.	Pig 1, 2, 3	Pig 1, 2, 3	Pig 1, 2, 3	N.s.	Soil sample from the belly region

2.3 DNA EXTRACTIONS

Samples were allocated codes which was designed to tell which pig, sample region, type and time point it is for and given an extraction number to enable tracking of samples. Samples were further grouped into four distinct groups: water, soils, tissues, and external body part (includes the orifices) (as seen in the

table 2.1). Before extraction utensils such as racks, pipettes, scissors not provided in the extraction kit were sterilised using a cross linker (CL-1000 Ultraviolet Crosslinker). Soils, and tissues were weighed out in accordance with the manufacture's weight prescription. All swabs and tissues were extracted using the DNeasy Blood and Tissue kit (Qiagen), DNeasy Powersoil Pro extraction kit (Qiagen) for the soils and all modifications to the manufacturer's instructions are described below. The different extraction protocol for each sample (swabs and soils) permits for the optimisation of DNA extraction potentially improving the yield and quality of extracted DNA. For example, soil samples often contain inhibitors that can interfere with DNA extraction, necessitating specialised extraction kits designed for soil samples. Similarly, swab samples may require methods optimised for recovering DNA from bacterial cells present on surfaces.

2.3.1 Water sample and swabs of external body part

DNA extraction of water and external body part was performed via swab extraction. Each water sample type with its duplicate were allowed to defrost at room temperature for about forty-five minutes. Samples were vortexed prior to sampling with sterile swabs. Swabs were dipped into each tube containing water samples and allowed to soak for 30 seconds. Swab heads were cut into a 1.5µl Eppendorf tube. Scissors were cleaned with 5% Decon 90 (Decon Laboratories Ltd) in between cutting swab heads to avoid/reduce cross contamination between samples. Control samples were established during the DNA extraction stage by performing DNA extractions on a blank swab.

2.3.2 Tissue Extraction

15mg of tissue samples were first weighed out using OHAUS PR series machine. Weighting plates were sterilised with 5% Decon 90 (Decon Laboratories Ltd) in between weighing each dissected tissue. Extractions were done in accordance with the manufacturer's instructions with the following modifications: samples were left to lyse overnight, the elution volume was reduced to 50 µl and 100 µl of Buffer AE for swab and tissue samples respectively.

2.3.3 Soil Extraction

Soil samples were extracted using the DNeasy Powersoil Pro extraction kit (Qiagen). Extraction procedures were carried out in accordance with manufacturer's instructions with some minor modifications. Although the manufacturer recommended 0.25g of soil sample, the amount of soil weighed (OHAUS PR series machine) and used was approximately 0.24-0.26g. Weighting plates were sterilised with 5% Decon 90 (Decon Laboratories Ltd) in between weighing each soil sample. Samples were vortexed vertically using an Eppendorf thermomixer rather than horizontally as instructed.

2.4 NANODROP QUANTIFICATION

DNA extracts were quantified using a Thermo Scientific, NANODROP ONE Spectrophotometer. Blanks were established using same buffer of DNA extract.

2.5 PCR AMPLIFICATION OF gDNA EXTRACT

In addition to the DNA samples, extraction negative and bacterial positive control, a PCR control was set up with H_20 as a negative control. A 460 bp 16S rRNA target was amplified using primers as described in Klindworth et. al (2013) with 5′ tags recommended for Illumina paired end sequencing (Table 2.2). 30 µl PCR reaction was set up with the final concentration of 1X platinum master mix (Thermo Fisher) (for soil samples), or 1X SuperFi polymerase (Invitrogen Thermo Fisher Scientific) (for swabs and dissected samples), 0.4 µM forward and reverse primer, 3.4 µl of dH_20, and an average of 47.94 ng/µl of DNA template. The Illumina primers are those recommended by the for the MiSeq 16S analysis of the V3 and V4 regions. The amplification was executed using the Veriti Thermal Cycler (Applied Biosystems). During the PCR amplification stage, negative control samples were obtained by performing DNA amplification on distilled water samples (which were known to contain no extracted genetic material). The thermal cycling conditions were established and carried out for 35 cycles according to the PCR parameters (Table 2.3).

Table 2.2 showing Primer information used for PCR reaction. The sequence coloured in red are overhanging adapter sequence attached to the primer sequence.

Forward and Reverse Primers (5′-3′)	Melting Temperature (Tm)	Primers length	Amplicon Length (bp)	Reference
ILLUMINA FOR TCGTCGGCAGCGTCAGATGTGTATAAGAGACAGCCT ACGGGNGGCWGCAG	50	50	~460	Klindworth *et al.*, (2013)
ILLUMINA REV GTCTCGTGGGCTCGGAGATGTGTATAAGAGACAGG ACTACHVGGGTATCTA	50	52		Klindworth *et al.*, (2013)

Table 2.3 Thermal cycling parameters for PCR amplification reaction.

PCR Stages	Temperature (°C)	Time (mins)
Initial Denaturation	**95**	**10**
Denaturation	**95**	**1**
Annealing	**55**	**1**
Extension	**72**	**1**
Final Extension	**72**	**5**
Hold	**12**	**∞**

2.6 GEL ELECTROPHORESIS OF PCR AMPLICONS

To assess the success of PCR amplification ,50x TAE stock solution was diluted to make a 1x working solution by adding 20 ml of 50x TAE into 980ml of water. 1.2 % gels were prepared with 0.72g of agarose added to 60ml of 1x TAE buffer (40 mM Tris, 20 mM acetic acid, and 1 mM EDTA). The agarose gel was left to solidify after preparation and placed in the electrophoresis tank and covered with 1x TAE running buffer. Each sample (5µl of amplified product) were loaded into the gel and ran at 100v for approximately 20 minutes After DNA extractions and examined and captured on BioRad GelDoc XR+ image viewer.

2.7 NEXT GENERATION SEQUENCING

25µl of amplified 16rRNA gene was transferred to a 96 well plate, and covered with an adhesive plate seal, kept in frozen and then transported to Bristol University Genomic Laboratory where they were cleaned-up, removing excess primer band and fragments below 200bp. They continued the second step PCR to add dual indices and Illumina sequencing adapters using the Nextera XT Index Kit, before purifying, quantifying, normalising and pooling the barcoded products and then products were sequenced using the Illumina Miseq platform (150bp read). The raw data in a FASTA file format was provided through a link available for download.

2.8 MICROBIOME TAXONOMIC PROFILING (MTP)

Microbial taxonomic profiling was done with the use of a web-based bioinformatic tool called EzBiocloud (https://www.ezbiocloud.net). The EzBioCloud Genome Database is part of EzBioCloud.net. CJ Bioscience, Inc. maintains it in order to give the best-curated genome databases available. The database's data sources include NCBI and other public domain resources (for example, Joint Genome Institute [JGI]). The EzBioCloud database entails an integrated system (figure 2.3) that host a taxonomic hierarchy of bacterial and archaeal which consist of over 207 phyla, 433 classes, 1019 orders, 2805 families, 11446 genera, 61700 species and 387 subspecies. This taxonomy grading was established mainly on the highest possible phylogeny for 16S rRNA gene sequence data, where 97 % similarity threshold was deployed for the identification of phylotypes. Taxa which do not have its type or reference 16S rRNA gene sequences were not constituted in the database (Yoon *et al.*, 2017).

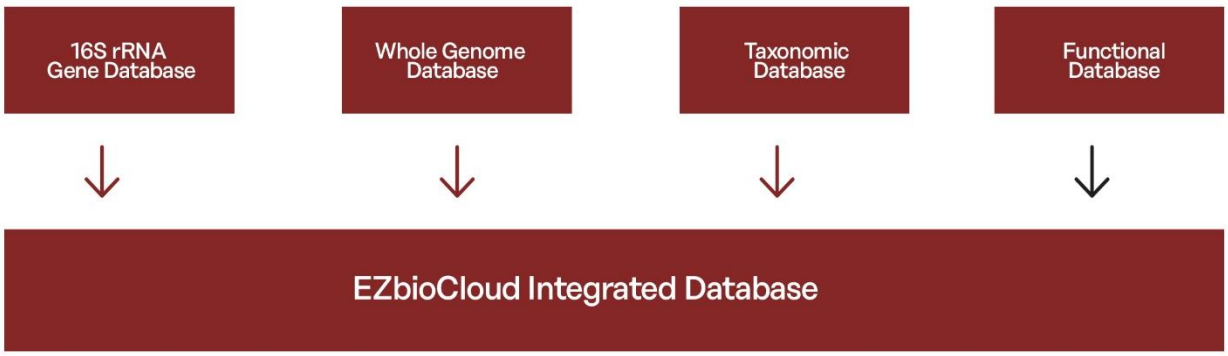

Figure 2.3 Diagram of the EZBioCloud Integrated Database: Incorporating the 16S rRNA Gene, Whole Genome, Taxonomic, and Functional Databases, this platform enables comprehensive taxonomic classification, comparative genomics, gene annotation, and functional profiling of microbial communities, all with curated reference sequences and up-to-date taxonomy.

Raw NGS data presented in FASTAQ were uploaded to the EZBioCloud website. This automatically process and converts it to a unit called MTP (microbial taxonomy profiling). Each MTP comprises of details about run QC for instance, read length and number reads matched (EzBioCloud, 2019). Non-redundant reads are identified and extracted. Taxonomic profiling is then performed on dereplicated sequences using the PKSSU4.0 database, as it is the most updated database for bacteria and Archaea available on the EzBioCloud website. Chimeras were automatically detected and removed if any with the reference to the UCHIME program. OTU's were selected and data grouped according to sample parameters for taxonomic assignment within the EzbioCloud pipeline. Statistical analysis such as the alpha- diversity, comparison within and across the data set were made via the interactive and visual inbuilt application in the EzBioCloud 16S-based MTP.

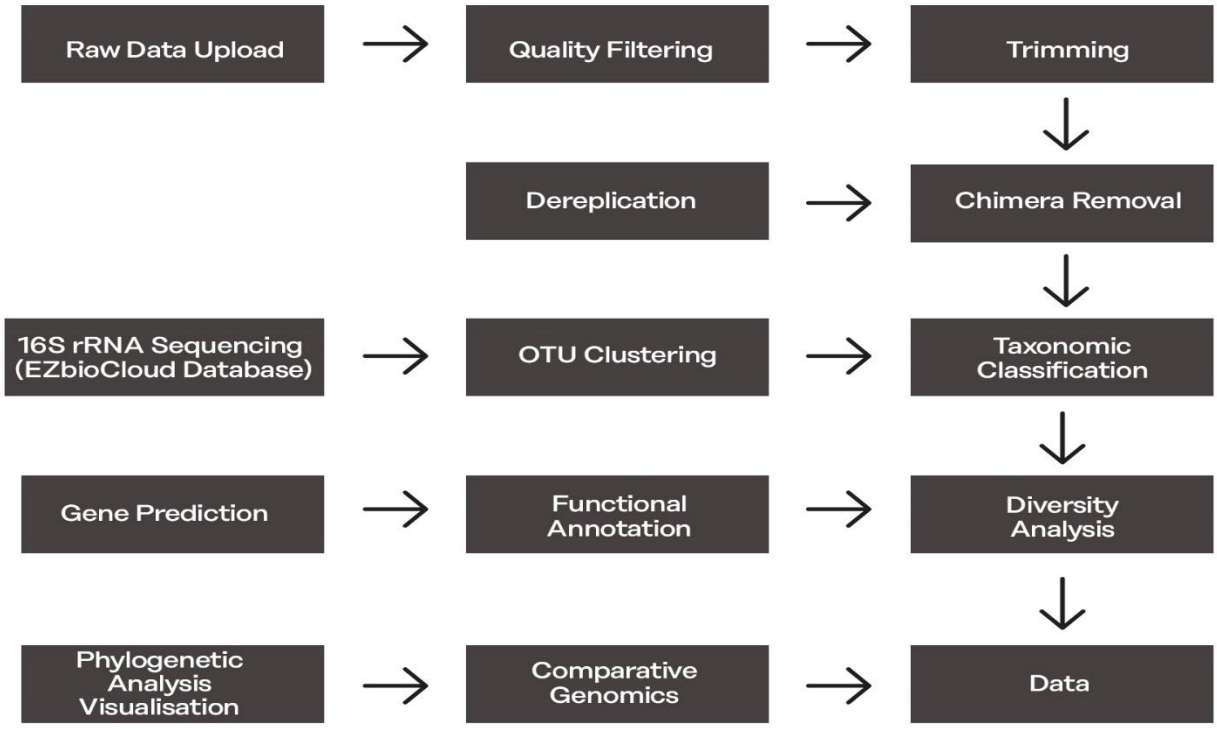

Figure 2.4 outlines the EZbioCloud pipeline for processing microbial sequencing data. Starting with Raw Data Upload, the data undergoes Quality Filtering and Trimming to ensure high-quality sequences. Dereplication removes redundant community composition. The final steps include Comparative Genomics and Phylogenetic Analysis Visualisation, yielding comprehensive insights into evolutionary relationships and functional diversity. All stages culminate in the generation of Data for further interpretation and research sequences, followed by Chimera Removal to eliminate false positive sequences. The processed data is then clustered into Operational Taxonomic Units (OTUs) using 16S rRNA sequencing (EZBioCloud Database). Functional analysis involves Gene Prediction and Functional Annotation, linking genes to biological pathways and roles. This is followed by Diversity Analysis to assess microbial.

2.9 STATISTICAL DATA ANALYSIS

Significant relationships between alpha diversity measurements (which also includes phylogenetic diversity) across all samples and over time were assessed using Regression analysis (with Day as a factor to account for potential non-linear relationships) in R Studio software. No significant differences were observed at phyla level between the preliminary and principal studies (using a subset of samples matched by day/sample type) therefore all statistical analyses were based on samples collected for the principal study only.

In chapter 3, Alpha diversity measures (species evenness, richness and phylogenetic diversity) were explored. Correlation of alpha diversity measurements was performed using the Pearson's product-moment correlation in R. Regression analysis (with day as a factor) was used for alpha diversity over time, and to assess changes in specific taxa over time. Analysis of variance was used to test for differences between the different sample types - this was used to test for differences in alpha diversity measures

between the different sample types and testing for significant differences in the abundance of specific taxa between the different sample types. Tukeys Honest Significant Differences test was used to assess pairwise comparisons. Differences in overall composition (Beta diversity) were tested using the betadisper and permutest (with 999 permutations) functions in the R-package vegan. Residuals for each model were tested for normality in R using the Shapiro-Wilks test.

In chapter 4, Analysis of Variance (ANOVA) was used to compare the alpha diversity measure across different sample types on day 0. ANOVA was also used to examine the alpha diversity measure over days of decomposition. Linear regression was also employed to model the relationship between diversity and time, with day as a categorical variable.

In Chapter 5, ANOVA was applied to compare the abundance of bacterial taxa across different sample types. Tukey's HSD test was used for post-hoc pairwise comparisons to identify specific differences between sample types.

In Chapter 6 and 7, ANOVA was used to compare the abundance of bacterial taxa over time. The Multiple Dispersion Analysis over time of decomposition was used to assess the variability or dispersion of bacterial family compositions within samples over different time points (Dayf).

3.0 CHAPTER THREE: DATA OVERVIEW

3.1 INTRODUCTION

This chapter focuses on the general integrity of the DNA extracted suitable for PCR amplification and the quality of the NGS data received. Nanodrop was employed for this evaluation because it can, via the Beer-Lambert law, reveal the purity ratios of the DNA extracts which is necessary to assess the integrity of the samples. The Beer-Lambert law shows the direct relationship between absorbance and concentration of a solution and allows the concentration of the solution to be evaluated by measuring the absorbance. Nucleic acid absorbs UV light at different wavelengths, absorbance at 260 nm indicates the aromatic base moieties such as Pyrimidines (adenine and guanine) and Purines (thymine, cytosine and uracil) present in its structure and can absorb UV light at 260nm (Lucena-Aguilar *et al*., 2016). Hence, absorbance at 260 nm has become a standard for quantifying nucleic acid samples (Lucena-Aguilar *et al*., 2016, García-Alegría *et al*., 2020). Other proteins and phenolic compounds have strong absorbance at 280 nm and aromatic amino acids side chains such as phenylalanine, tryptophan, histidine and tyrosine within their sequence are no different. Also, at 230 nm absorbance, the peptide bond of proteins and many other organic compounds such as polysaccharides, chaotropic salts, EDTA and phenol can absorb at this peak (Koetsier and Cantor 2019). Therefore, ratios of 260/280 and 260/230 give an indication of extract purity.

3.2 RESULTS AND DISCUSSION

3.2.1 DNA Extraction – Nanodrop Results.

DNA was successfully extracted from all sample types and the average DNA recovered was 49ng/µl and was of sufficient quantity for PCR amplification (Chapter 2, section 2.6). Table A1 in the appendix 1 displays the overall yield and purity of DNA recovered as measure with the Nanodrop (Thermo Scientific, NANODROP ONE). Protein contamination of DNA extracts was examined using the A260/280 ratio; values around 1.8 and 2.1 are considered pure for DNA and RNA respectively (Wang *et al*., 2020; Kanani *et al*., 2019). A lower ratio of less than or equal to 1.6 might indicate the presence of protein contamination which might impact on downstream applications (Lucena-Aguilar *et al*., 2016) of the DNA extracts. A260/230 ratio below the value of 1.8 suggests that there might be a significant quantity of organic contaminants mentioned above and absorbs near 200 and 230 nm. A pure nucleic acid should have an A260/230 ratio close to 2.0 (Lucena-Aguilar *et al*., 2016).

At this stage, samples were grouped into various types, internal organs, external body parts, soil, and water samples. As shown in Nanodrop data (appendix 1, table A1), the average A260/280 ratio for the water, external body part and samples 0.81 - 2.05 which are within the recommended range. The total

amount of DNA recovered after extraction as reflected in its Nucleic acid concentration on the nanodrop data was sufficient for PCR amplification. Although samples with low concentrations, below 1 ng/µL, did not affect amplification success.

The external body samples had a total average A260/230 ratio of 1.94 which is close to the 2.0 ideal value indicative of pure DNA, the slightly low ratio might indicate contamination of organic substances which absorb at 230nm. This might be caused by the presence of humic compounds resulting from the decay process and may have been co-extracted (Albers *et al*., 2013) with the DNA extracts. When a saline elution buffer is utilised to dissolve DNA during extraction, the salt concentration might be elevated over DNA concentration (Lucena-Aguilar *et al*., 2016). Although, internal organs had an average A260/230 ratio of 0.58 suggesting that there might be some protein contamination, however PCR amplification was still performed on DNA extracts because as revealed by the manufacturer the elution buffer used for extraction contained very low concentration of EDTA hence, a reduced inhibition during PCR amplification (Schrader *et al*., 2012) was expected.

3.2.2 Amplification results

PCR product was successfully amplified (Figure 3.1,). Amplification results suggest that samples with over 1.4ng/µl are at a sufficient concentration needed for successful NGS sequencing.

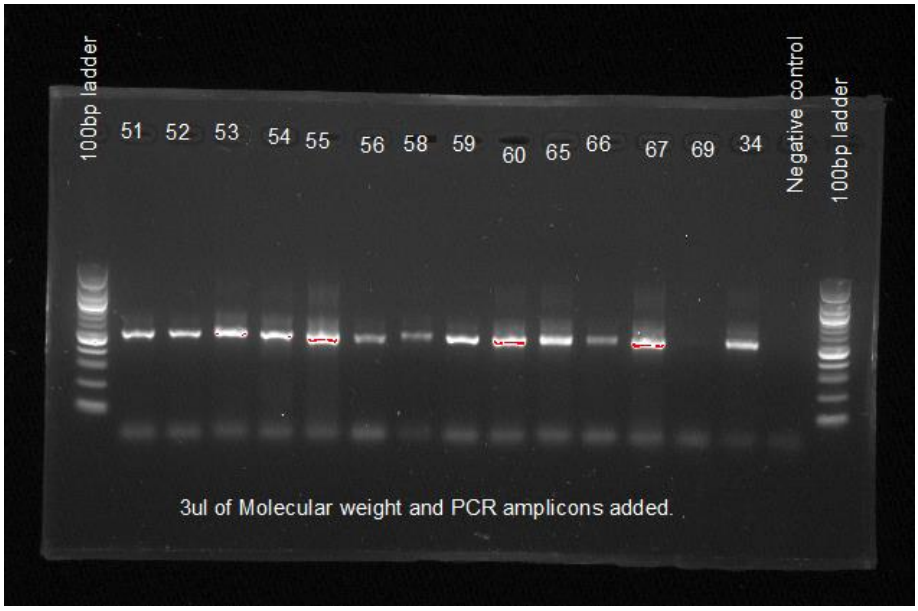

Figure 3.1 Amplified Samples (represented in various numbers) run by agarose gel electrophoresis gel and examined on BioRad GelDoc XR+ image viewer. A 1000bp molecular weight marker (NBS Biologicals) was run alongside the samples.

3.2.3 NGS Sequencing results – Read Quality

Assessment of the overall quality of data from NGS sequencing is necessary to ensure accurate 16S taxonomic profiling. The EzbioCloud pipeline filters out low quality data on the following basis; an average quality control value of <25, sequences that are either longer than 2,000 bp or less than 100 bp, sequences not identified as a 16S gene in reference to the Hidden Markov Model (HMM) based search, sequences that do not match the reference database with at least 97% similarity (EZbioCloud, 2019). Chimeric amplicons are artefacts formed during the PCR amplification by bonding of two or more DNA sequences and falsely influence the microbial diversity as a novel organism (Haas *et al*., 2011). These hybrid products are unpreventable during amplicon sequencing libraries preparation for NGS. As a result, before any microbiome analyses are performed, it is paramount to detect and filter out any chimeric products (EZbioCloud, 2019). With the use of UCHIME, chimera-free data is generated by EZbioCloud's 16S-based MTP application.

Table 3.1a shows a total average of 92490.20 reads after pre-filter (pre-processing steps) were obtained and the total average total valid reads (the number of reads valid for further analysis after passing quality control and are considered) is 80.25 % which indicates that a substantial portion of the sequencing reads passed the quality and *can* be considered good for many NGS applications. Gupta *et al*., (2019) demonstrated that 75.70 % of the distinct bacterial species cultivated in each sample were bacteria identified by NGS. Low-quality reads can introduce noise into the data, and a low percentage might suggest that the data quality control measures are effective. The average total for low amplicons is 2.57 % which is relatively low. Low-quality amplicons, if not removed from the analysis, could introduce erratic and possibly random sequences into the dataset which could pose a significant issue for any downstream analysis process and result in inaccurate data interpretations (Del Fabbro *et al*., 2013). Non-target amplicon is typically considered contaminants (Bedarf *et al*., 2021) a percentage of 0.46 % indicates that most amplicon were on target. The average percentage of chimeric amplicons is 16.31%. While there is not a set proportion that is generally agreed upon, the objective is to limit the influence of chimeric readings on downstream analysis and guarantee data accuracy by keeping them as low as feasible.

Table 3.1a Showing a summarised NGS data using the curated from EzbioCloud using the FASTQ data. (Full table found in appendix 4, table A4.1)

Samples	Total Reads After Pre-Filter	Total Valid Reads	Low Quality Amplicon	Non-Target Amplicons	Chimeric Amplicons
Mean ± SD	92490.20 ± 16755.71	74469.74 ± 21470.24	2372.68 ± 10439.33	422.03 ± 1104.65	15082.94 ± 16084.46
% of total reads after filter		80.52	2.57	0.46	16.31

3.2.3.1 NGS Sequencing results – Controls

The controls results presented in Table 3.1b suggests potential for some level of contamination in the extraction control and the PCR control as both controls possess some reasonable number of valid reads. The PCR Negative control seems to have a cleaner profile with lower numbers of non-target and chimeric amplicons, which might imply possible contamination of the negative samples during the gDNA extraction. Contamination in negative controls is a legitimate concern in NGS microbial sequencing studies, especially since bacteria are ubiquitous in nature. In this study, a robust sequencing technique and depth was utilised to adequately capture the true microbial diversity and abundance in the samples (This can help in distinguishing between true microbial signals and contaminants by identifying consistent patterns across multiple sequencing reads) The implications of this controls results are discussed in chapter 8, section 8.8.

Table 3.1b demonstrates the quality of PCR data for the controls.

Samples	Total Reads After Pre-Filter	Total Valid Reads	Low Quality Amplicon	Non-Target Amplicons	Chimeric Amplicons
Mean read data for decomposition samples	92,490	74,470	2373	422	15,083
gDNA Extraction Negative Control	100,000	54,693	263	33,876	11,168
PCR Negative Control	21,527	21,094	82	335	16

3.2.4 NGS Sequencing results – Read Identification

Good coverage of library measures how closely the species population in the sample matches the amount of sequencing reads used for analysis when aligned to a reference database (EzbioCloud 2020; illumina, 2022). The NGS sequencing coverage indicates all samples had an average of 99.63% with a small standard deviation of 0.45% percent, suggesting a good capture high proportion of the true species diversity in your community (sample). The number of reads identified at species level characterises the species per and the mean number of for all sample is 64029.03 ± 25013.07. The average number of species are 811.78 indicating that the samples exhibit a diverse microbial composition, and the large standard deviation of 839.88, however, indicates a considerable degree of variation within samples, and certain samples may have a significantly higher or lower level of species diversity. The *OTUs* which are frequently employed in microbial communities as proxies for species diversity are found to be 1542.14 ± 1540.1, additionally, the standard deviation shows that the number of OTUs varies throughout samples. The overall numerical value of the number of reads, species identified, operational taxonomic units (OTUs), and Good's coverage percentage for all individual sample collected at respective different time points, and curated from the EZbioCloud 16S-based MTP application are displayed on appendix 4, table A4.2.

3.3 CONCLUSION

Assessment of the overall quality of data was carried. The nanodrop drop data confirmed the gDNA extracts were good enough for PCR amplification. Also, images from agarose gel electrophoresis observed on the BioRad GelDoc XR+ image viewer showed the samples generated good quality amplicons for the NGS procedure. The NGS data set suggests the NGS procedure on the different samples type from different sources selected for this study were successful, the NGS data was shown to have a high proportion of good quality reads, low levels on non-specific and chimeric reads. The EzbioCloud output quality is good with the Good's coverage of library values suggesting a high level of successful taxonomic assignment. The results are suitable for downstream analysis which will be carried out in subsequent chapters.

4.0 CHAPTER FOUR: BIODIVERSITY OF MICROBIAL COMMUNITIES – ALPHA DIVERSITY ANALYSIS

4.1 INTRODUCTION

This chapter looks at the microbial biodiversity of samples that accounts for the spatial (Day 0) and temporal changes (across the observed time interval) of microbial communities through measuring parameters such as species richness, species evenness, and phylogenetic diversity. Microbial diversity in the ecological sense is commonly considered to refer to microbiome complexity i.e., distinct bacterial species, according to their taxonomic classifications (Lozupone *et al*., 2012). Species richness can be described as the count of all the distinct taxa that have been seen in the area (sample), regardless of how frequently they occur (Wagner *et al*., 2018). Species evenness on the other hand, accounts for the frequencies at which those distinct taxa occur. Phylogenetic information is not limited to taxonomic richness but can offer a more insightful view on the diversity of traits and functions (O'Dwyer *et al*., 2012). Hence, the phylogenetic diversity metric accounts for the phylogenetic connections between species in a community (sample) contained in the same phylogenetic trees (Manson and Steel, 2023). The construction of a phylogenetic tree involves several key steps. First, multiple sequence alignment (MSA) is performed using tools like MUSCLE or MAFFT (Chang, Di Tommaso, and Notredame, 2014). Next, the tree building process occurs, employing methods such as Neighbour-Joining (NJ), Maximum Likelihood (ML), or Bayesian Inference (BI) (Kapli, Yang, and Telford, 2020). Once the phylogenetic tree is constructed, it is calculated using Faith's Phylogenetic Diversity (PD), a common metric that measures the total branch length of the tree covering all species within a community (Faith, 2006; Chao *et al*., 2014; Constantinos and Sandel, 2015). Additionally, other metrics, such as weighted and unweighted UniFrac, are used to assess the phylogenetic distance between different communities (Lozupone *et al*., 2010; Chang, Luan, and Sun, 2011).The alpha diversity are metrics which includes Jackknife, Chao1, and ACE can be used to evaluate the species richness and, NPShannon, Shannon, and Simpson to evaluate evenness (Yang *et al*., 2019; Tenzin *et al*., 2020) in microbial datasets, which in turn can equally assess the phylogenetic relationships in an OTUs. Bacteria are widely categorized using operational taxonomic units (OTUs), based on how similar their 16S marker gene sequences (Liu *et al*., 2021; He *et al*., 2015, Lladó Fernández, Větrovsky and Baldrian, 2019). As seen in chapter 3, the genetic similarity thresholds employed in this study to establish the OTUs is 97% similarity in the 16S rRNA gene sequence.

The Simpson diversity index measures the amount to which an assemblage is occupied by one or few members of a taxa: such that it evaluates a trait of assemblage that is the inverse of assemblage evenness (Magurran, 2021). Simpson index shows the likelihood that two sequences chosen at random belong to

the same species. Its values vary from zero to one, with lower values indicating greater diversity (Magurran, 2013). Shannon is a species evenness indicator that displays values higher than zero and higher values imply more diversity. The highest values are obtained when the members of the taxa identified are equal number (Magurran, 2013). NPShannon calculates richness when there are unseen species and abundance are unknown. Values are exceeding 0, with larger values indicating greater diversity (Magurran, 2013; EzbioCloud, 2020).

Jackknife, Chao1 and ACE are metrics used to observe the richness of a community in a sample and are sensitive to rare OTUs (singletons and doubletons) (Oh *et al*., 2021, Liu *et al*., 2020; EzbioCloud, 2020). The Jackknife can also be sensitive to abundant OTUs that occur three times (Tripletons) or beyond within a sample (Oh *et al*., 2021; EzbioCloud, 2020). For instance, during sample collection and other activites, rare species can be lost, and these richness indices can still assess the true richness of the community (Patuzzi, 2018; Patuzzi *et al*., 2019; Roswell, Dushoff and Winfree, 2021; Finotello, Mastrorilli and Di Camillo, 2018).

The importance of diversity is often understood by examining communities that exhibit distinct environmental characteristics (Martin, 2002). Applications of Jackknife, Chao1 and ACE as bacterial community richness estimators (Finotello *et al*., 2018; Chin-Hee Song *et al*., 2021; Choi, Kim and Cha, 2014), Shannon and NPShannon as evenness estimators (Kim *et al*., 2022; EzbioCloud, 2020), and the phylogenetic diversity would be utilised in this chapter to measure the community structure of the microbial community in each sample on day 0 and overtime. NPshannon and Jackknife were selected for statistical analyses of alpha diversity over time. Regression analysis was performed to see any statistical differences between the measures of diversity, and as cited in chapter 2, section 2.10 statical models would be employed to check the relationships with the alpha and phylogenetic diversity on the onset of decomposition and over the observed period.

4.2 RESULTS AND DISCUSSION

4.2.1 Alpha and Phylogenetic Diversity Composition Across all Communities on Day 0

On Day 0, an examination of alpha and phylogenetic diversity composition in each communities/samples provides a snapshot of the initial microbial landscape. Diversity analysis on day 0 can set the foundational platform for tracking temporal shifts and ecological dynamics as the communities evolve over time, contributing to a deeper understanding of the microbial ecosystems under investigation. Analysis of variance was used to test for differences in alpha diversity measures between the different sample types. Tukey's Honest Significant Differences test was used to assess pairwise comparisons for each of the pig samples.

4.2.1.1 Pig Samples (Body Sites and Internal Organs)

The corresponding p-value (0.00000067) for species richness across all pig samples is exceedingly low. This suggests that among the pig sample sites there are highly significant differences in species richness on the first sampling day. The Tukey multiple comparison from the ANOVA test suggests on the pig sample, the richness of microbial communities in the body sites are significantly different from the internal organs (Table 4.1). This could be due to the lung been exposed to regular extirpation of colonised microbes via immunity of host, and the process of mucociliary protection and movements, coughing. (O'Dwyer, Dickson and Moore, 2016; Mathieu *et al*., 2018) and the lungs host a unique microbiome whose constituent is influenced by distinct ecological principles (Huffnagle, Dickson and Lukacs, 2016; Natalini, Singh and Segal, 2022). The liver is recognized for harbouring more than half of the body's macrophage (Kuppfer cells) supply, which maintains liver functions and effectively annihilate any bacteria they encounter (Nguyen-Lefebvre and Horuzsko, 2015; British Liver Trust, 2022). The resemblance in species richness between the liver and lung, as opposed to the significant differences observed in other comparisons after death on day 0 could be the proximity or direct anatomical connections between the liver and lungs may facilitate exchange or colonization of microbial communities between the two organs (Reyman *et al*., 2021), the similarities of microenvironmental conditions (Temperature, oxygen levels and nutrient availability) might support the survival of only certain comparable microbial species (Belkaid and Hand, 2014) and the lung and liver are involved in the physiological function of immune response which might prompt their microbial compositions to reflect adaptations to support such function (Odom *et al*., 2021; Kubes and Jenne, 2018; Zheng, Liwinski and Elinav, 2020). The body site samples (belly, anus, and mouth) represent varying conditions, The oral cavity is exposed to external factors through ingestion, the belly may have a different nutrient environment, and the anus represents the endpoint of the digestive system with unique

conditions. These discrepancies might support the observed significant differences in species richness and phylogenetic diversity between these samples. The evenness for all pig sample site had similar ratio of bacteria on the first day of sampling as the ANOVA regression results for NPShannon (p= 0.582) all cross species had no significant differences between pig samples (body sites and internal organs). The Tukey multiple comparison test for evenness as revealed in Table 4.1 were all non-significant, indicating a comparable bacteria distribution level across all sample sites. The ANOVA results of Phylogenetic diversity (p=0.00678) imply statically significant differences across various body sites and internal organs of sampled on the pigs on the first day of decomposition. Although not all paired samples were significant, the sites responsible for this variety in phylogenetic diversity as revealed by the Tukey multiple test comparison is highlighted on Table 4.1. These sites were also had significant Jackknife values, indicating those sites had more distinct bacteria species present that may not be closely related.

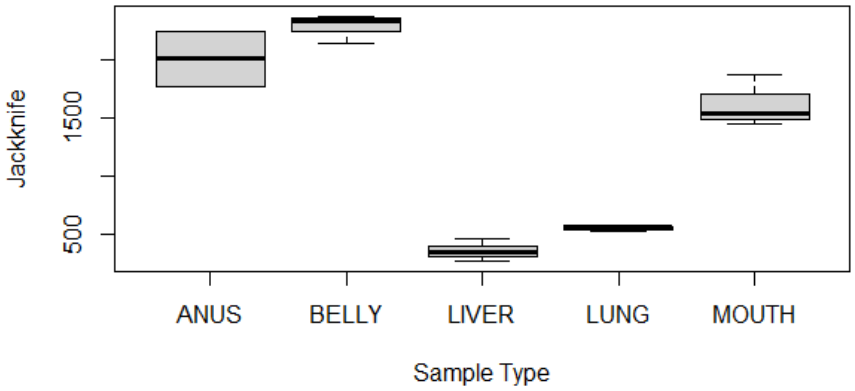

Figure 4.1 Average species richness (Jackknife) between the pig (internal and external) samples on Day 0. For all samples n= 3 (except anus where n=2)). The box represents the inter-quartile range with the thick bar representing the median value. The whiskers indicate the range of the data.

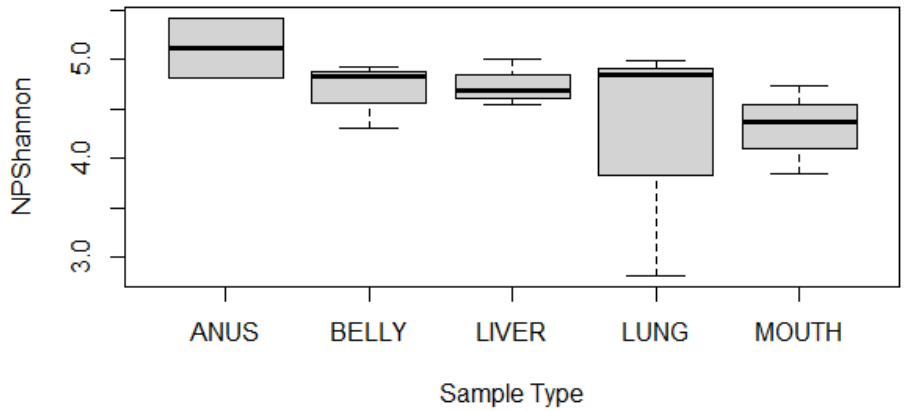

Figure 4.1 Average species richness (Jackknife) between the pig (internal and external) samples on Day 0. For all samples n= 3 (except anus where n=2). The box represents the inter-quartile range with the thick bar representing the median value. The whiskers indicate the range of the data.

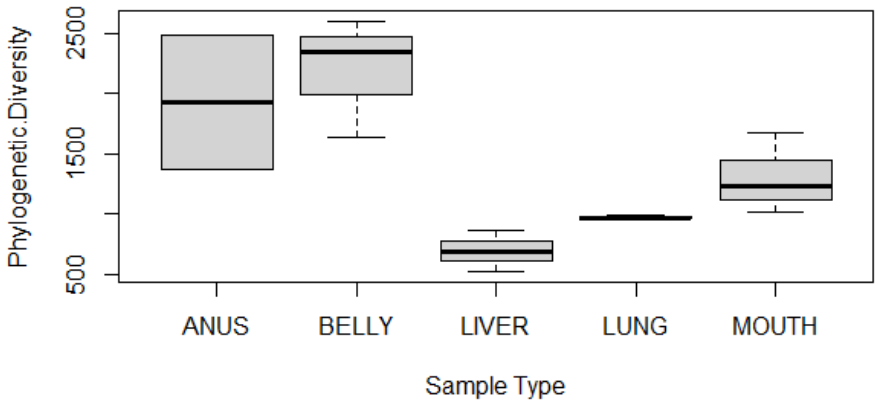

Figure 4.3 Average Phylogenetic Diversity between the pig (internal and external) samples on Day 0. For all samples n= 3 (except anus where n=2). The box represents the inter-quartile range with the thick bar representing the median value. The whiskers indicate the range of the data.

Table 4.1 Results of ANOVA analysis and Tukey multiple comparisons of species diversity (Jackknife, NPShannon, Phylogenetic Diversity) between of various pig samples (internal and external) on day 0. The precise sample duos that are significantly diverse are highlighted by the p-value. The non-significant pairs for Jackknife and Phylogenetic Diversity might suggest that the microbial richness levels of those sample sites are similar.

Tukey Multiple Comparison				**Anova Regression**
Samples	*Jackknife*	*NPShannon*	*Phylogenetic Diversity*	
Mouth - Lung	0.0002114	0.9996738	0.8372574	
Mouth -Liver	0.0000541	0.9256943	0.3832501	
Lung - Liver	0.6218904	0.8571724	0.9012182	
Mouth - Belly	0.0065483	0.9538436	0.1204861	
Lung - Belly	0.000004	0.8988433	0.0270198	
Liver - Belly	0.0000016	0.9999658	0.0079611	$F_{4,9}$=74.77, 0.00000067
Mouth - Anus	0.1734351	0.678052	0.4590228	(Richness); $F_{4,9}$=0.751,
Lung - Anus	0.0000435	0.5851885	0.1393659	0.582 (Evenness); $F_{4,9}$=
Liver - Anus	0.0000151	0.9671669	0.0450124	7.252 0.00678
Belly - Anus	0.4332284	0.9466562	0.9442946	(Phylogenetic diversity)

4.2.1.2 Environmental Samples (Soil and Aquatic Samples)

As initiated by the soil sample against the water sample, the general ANOVA Regression for the environmental sample were, p=0.0000036 (Richness), p=0.000536 (Evenness), and p=0.0000081 (Phylogenetic diversity). The Tukey multiple comparison for all diversity indices (Richness, evenness, phylogenetic diversity) regarded the soil microbial communities to be highly and positively significantly

different from the aquatic microbiome. The richness, evenness, phylogenetic diversity comparisons between the individual water samples on day 0 were not statistically significant may be due to similar inherent variability of the water sample since it was just the salt concentration that differed the water samples (see Chapter 2, *section 2.1.2.2.2.1* for the salt concentration of the water samples). The significance in phylogenetic diversity between soil and water samples suggests that there are huge differences in the evolutionary lineages of the microbial communities in the aquatic and the soil habitats. Evolutionary relationships of the species between the individual water samples were not statistically significant. Comparisons in water sample might not show statistical significance difference in phylogenetic diversity as the microbial communities might be impacted by specific biogeographical factors that result in regional similarities. In contrast, the soil samples, being more localised, may exhibit more significant variation to influence phylogenetic diversity. The soil is a major site for the decomposition of organic matter, including plant material and animal remains (Pérez-Valera, Goberna and Verdú, 2015; Weber 2002; European Commission, 2011). There might be possibilities of decaying residues from organic matter in the soil before the commencement of this study and the breakdown of those complex organic matter or compounds can support the richness of microbial communities in the soil, the water samples were artificially created to accommodate the pig carcasses and had no evidence of decaying organic matter before pig carcasses were deposited in it. Studies has revealed a greater impact of biodiversity in natural ecosystems than in controlled experiments (Schmidt *et al*., 2020).

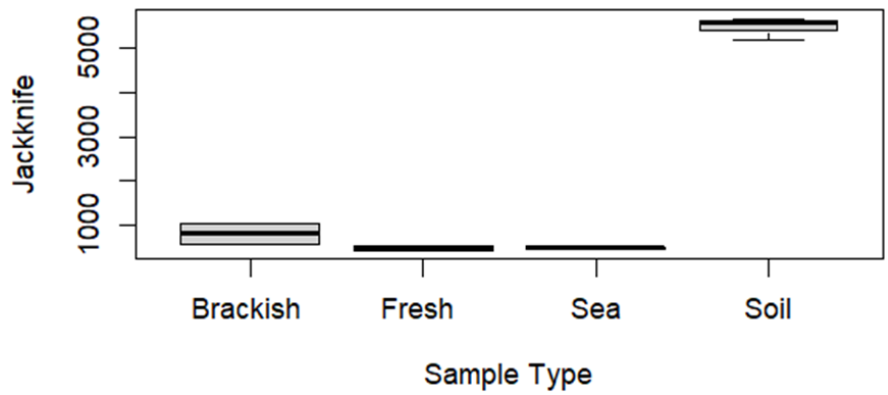

Figure 4.4 A graph displaying the Richness (Jackknife) correlation between the environmental samples on Day 0. For all samples n= 2 (except soil where n=3). The box represents the inter-quartile range with the thick bar representing the median value. The whiskers indicate the range of the data.

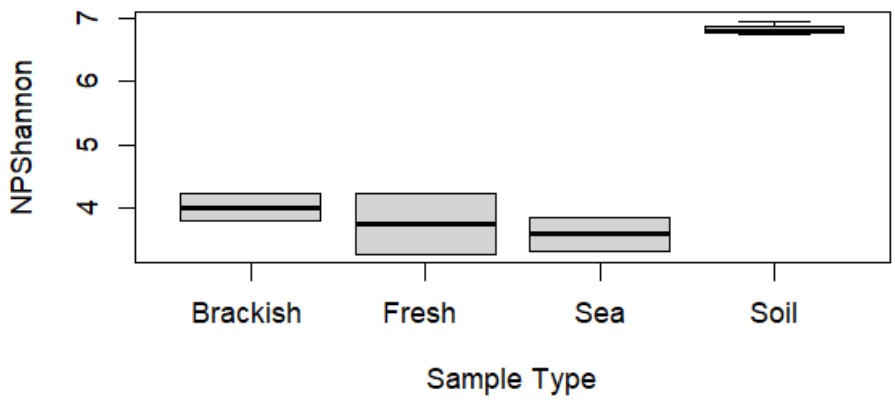

Figure 4.5 A graph displaying the Evenness (NPShannon) correlation between the environmental samples on Day 0. For all samples n= 2 (except soil where n=3). The box represents the inter-quartile range with the thick bar representing the median value. The whiskers indicate the range of the data.

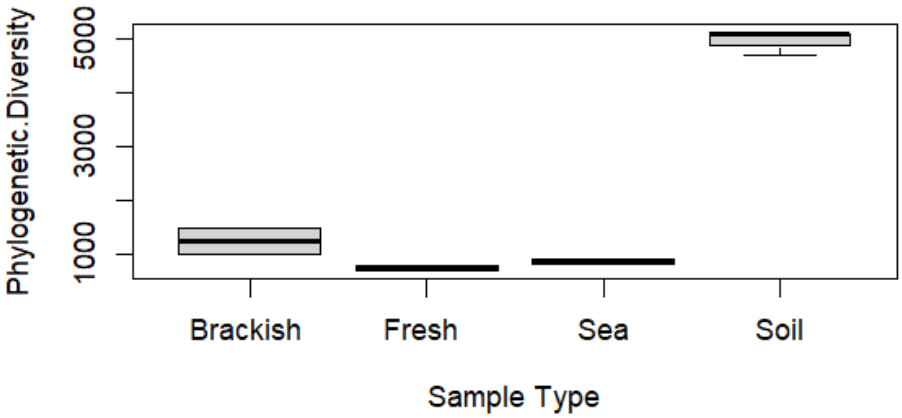

Figure 4.6 A graph displaying the Phylogenetic Diversity correlation between the environmental samples on Day 0. For all samples n= 2 (except soil where n=3). The box represents the inter-quartile range with the thick bar representing the median value. The whiskers indicate the range of the data.

Table 4.2 Expresses the p-values of regression analysis of Richness (Jackknife), Evenness (NPShannon), and Phylogenetic Diversity between the various environmental samples on day 0. The precise sample duos that are significantly diverse are highlighted.

Tukey Multiple Comparison				**ANOVA Regression**
Samples	*Jackknife*	*NPShannon*	*Phylogenetic Diversity*	$F_{4,9}$= 330.7, p=0.0000036 (Richness); $F_{4,9}$= 43.15, p=0.000536 (Evenness); $F_{4,9}$=238.9 p=0.0000081 (Phylogenetic diversity)
Fresh -Brackish water	0.508441	0.9027521	0.2166434	
Sea-Brackish water	0.5037388	0.6998921	0.3657393	
Soil-Brackish water	0.0000137	0.0017649	0.0000277	
Sea-Freshwater	0.9999996	0.9695748	0.9585900	
Soil-Freshwater	0.000011	0.0011749	0.0000173	
Soil-Seawater	0.000011	0.0009170	0.0000189	

4.2.2 Changes in Alpha diversity over time

Over the observed period, the exploration of alpha and phylogenetic diversity composition across all communities unveils the dynamic nature of microbial ecosystems. Alpha diversity, capturing the richness of species within individual communities, and phylogenetic diversity, illustrating the evolutionary relationships among these species, collectively depict the intricate patterns of microbial community changes over time. Ecosystem resilience refers to an ecosystem's ability to cope with or recover from disturbances, adapt to alterations, and sustain its functions and structure over time (Dakos & Kéfi, 2022). High diversity can be instrumental to increased stability and adaptability amid environmental changes (García-García *et al*., 2019, Wagg *et al*., 2021). The longitudinal analysis in this chapter allows for the identification of trends, fluctuations, or stability in diversity metrics, contributing valuable insights into the temporal dynamics and ecological resilience of the studied communities. Such an approach enhances our understanding of how microbial diversity evolves and adapts within these ecosystems across the observed timeframe. All three measures of species richness/evenness have been plotted but as all measures are highly correlated (Section 4.2.1) only Jackknife and NPShannon have been used for the statistical analysis. A positive or negative significant relationship in regression analysis of any diversity metrics over time suggests an incline or a decline of that metric the community.

4.2.2.1 Pigs (Body Sites and Internal Organs)

4.2.2.1.1 Belly

The microbial community richness in the belly samples achieved the greatest rise on Day 0 with the mean Jackknife value showing 2290.13±123.10. The lowest in richness was on day 23 is which exhibited the value of 6652±79.38. Regression analysis of Jackknife showed a negative significant relationship between species richness in the belly community over time ($F_{4,9}$ = 4.767, p=0.02428). The NPShannon metrics indicated that microbial community evenness was the highest on day 0 with values of 4.68±0.31 respectively. The lowest community evenness was noticed on day 2 with values of 3.13±1.22. Regression analysis of NPShannon showed no significant relationship between species evenness in the community over time ($F_{4,9}$=1.491, p=0.2834). Phylogenetic diversity shows the highest rise on day 0 with the value on 2192.67±500.22 and the lowest drop on day 23 with the value of 614±165.62. Regression analysis of phylogenetic diversity showed a negative significant relationship between species in the community over time ($F_{4,9}$=14.68, p= 0.0005576). The negative significant relationship of the phylogenetic diversity and richness exhibited might indicate a decrease functional redundant species as decomposition progresses, meaning the ecosystem loses species, especially those that are performing similar roles. However, the evenness of belly microbiome was not significant over time, suggesting there might be a decreasing

number of species without a significant change in the distribution of abundance among the species as decomposition advances and these changes do not necessarily lead to a shift in dominance of one or a few species overtime.

4.2.2.1.2 Anus

The average Jackknife measures indicated the highest richness of microbial community on Day 0 of decomposition with a value of 2012±329.60. The richness decreased to its lowest on day 4 with a value of 1311.65±228.19. Regression analysis of Jackknife showed no significant relationship between species richness in the anus community over time ($F_{1,7}$ = 0.168, p= 0.6937). The greatest rise in community evenness was noticed on day 0 of decomposition with an NPShannon value of 5.15±0.43. The lowest drop in community evenness was noticed on day 4 with a value of 3.75±0.40. Regression analysis of NPShannon showed no significant relationship between species evenness in the community over time ($F_{3,5}$=1.384, p= 0.3439). A clear pattern was seen in the phylogenetic diversity and alpha diversity dropped as days progressed, the highest was seen on day 0 and the lowest was on day 23 with values of 1930.5±782.77 and 913.67±92.31 respectively. Regression analysis of phylogenetic diversity showed no significant relationship between species in the community over time ($F_{3,5}$= 2.803, p= 0.1479). The anus sample displayed a very slight decline in evenness, richness, and phylogenetic diversity over time as decomposition advanced. The decrease slight diversity could signify a reduction in microbial diversity but not a shift in the dominance of certain microbial species as the regression analyses for each of these diversity measures did not show a significant relationship between species diversity and time. The microbial community within the anus sample may have high intraspecific variation. This implies that individual organisms within the same species that exhibits considerable differences (Harding *et al*., 2019). The gut and rectal of various organisms is known to contain intraspecific variation of microbes (Lange *et al*., 2023; Pacheco-Sandoval *et al*., 2022) and the anus serves as the external terminal point of the rectal passage. These intraspecific varied organisms if present on the anus sample of the pig carcasses might contribute to the non-statistically significant differences in diversity over time.

4.2.2.1.3 Mouth

According to the richness metrics, day 7 of decomposition was noticed to have the highest rise in microbial community richness with value of 2101±1197.13. The lowest drop is on day 4 with value of 933±261.56. Regression analysis of Jackknife showed no significant relationship between species richness in the community over time ($F_{4,8}$ =2.2242, p= 0.1539). Evenness reached its rising peak on day 7 with metrics value of 4.87±0.90 and had its lowest drop on day 4 of decomposition with values of 3.80±0.75. Although, day 7 and 4 had close metrics values. Regression analysis of NPShannon showed no significant relationship

between species evenness in the community over time ($F_{4,8}$=1.281, p= 0.3536). The phylogenetic diversity had its highest rise on day 0 and the lowest fall was noticed on day 7 with the values of 1030.5±238.29 and 482.50±197.28. Regression analysis of phylogenetic diversity showed no significant relationship between species in the community over time ($F_{4,8}$=3.391, p= 0.06661). The microbial community in the mouth demonstrated fluctuations changes in phylogenetic and alpha diversity metrics as decomposition progressed, but do not reflect to be dynamic no shift in microbial community composition. Despite the observed change given by the days of decomposition, the regression model of the diversity measures revealed no statistically significant change over time. The absence of significant relationships in the regression analyses may highlight the complexity of microbial community dynamics in the mouth during decomposition.

4.2.2.1.4 Liver

The highest microbial community richness was the highest on day 0 of decomposition with and Jackknife of 262.31±95.05. The lowest in richness was noticed on day 4 with values of 264.33±43.29 respectively. Regression analysis of Jackknife showed a non-significant relationship in species richness in the community over time ($F_{2,6}$ = 1.307, p= 0.3378). The highest microbial community evenness in this set of samples was noticed on day 0 of decomposition with a NPShannon value of 4.74±0.23, while the lowest drop in evenness metrics was on day 2 of decomposition with value of 1.72±0.46. Both day 2 and 4 showed very close values for both evenness metrics. Regression analysis of NPShannon showed a negative significant relationship in species evenness in the community over time ($F_{2,6}$= 55.77, p= 0.000133). The phylogenetic diversity's highest and lowest values were noticed on day 0 and 4 which had a respective value of 695±172.03 and 476.33±88.90. Regression analysis of phylogenetic diversity showed a decline in diversity however there was no significant relationship between species in the community over time ($F_{2,6}$= 1.837, p= 0.2385). The results of the regression model suggest a decline in community evenness leading to a shift in the composition of the microbial structure without a significant change in the species diversity or the overall evolutionary relationships among species. The liver is an important organ before death and also after death as it serves as a potential host for microbial communities. The available resources or nutrients provide by the decaying liver might by utilised effectively by some certain group of bacteria. For instance, in the liver, post-mortem bacteria have been found to employ riboflavin (vitamin B2) as a carbon source (Liu *et al*., 2023). A reduction in the even distribution of bacterial across the community can occur if the group is colonised by the specialized decomposers. The liver was quickly degraded, implying its gradual inability to host post-mortem bacterial and transmigration of bacterial species to find better

ecological niche can occur. The transmigration of these bacterial species to find new niches could lead to specie evenness reduction.

4.2.2.1.5 Lungs

The microbial community richness in the lung samples achieved the greatest rise on Day 4 with the mean Jackknife value of 823.96±316.04. The lowest in richness was noticed on day 2 of decomposition with values of 312.99±34.40 respectively. The greatest rise in community evenness was noticed on day 0 of decomposition with the average NP Shannon value of 4.21±1.22 while lowest was on day 4 with values of 1.86±0.24 respectively. The phylogenetic diversity of the community was on its highest on day 4 of decomposition with value of 1056.33±189.51, and on its lowest on day 2 which value gave 590.33±51.32. Regression analysis of Jackknife showed a positive significant relationship between species richness in the community over time ($F_{2,6}$ =5.785, p= 0.03982). Regression analysis of NPShannon showed a negative significant relationship between species evenness in the community over time ($F_{2,6}$=7.778, p= 0.02156). Regression analysis of phylogenetic diversity showed significant varying relationship between species in the community over time ($F_{2,6}$=14.37, p= 0.005148). A significant reduction in the distribution of species could imply that the tissue might be colonised by post-mortem Interspecific competitors that compete for the same resources in an ecosystem. Over time, interspecific competition can drive evolutionary divergence among competing species (Huang *et al*., 2020a). The phylogenetic diversity had a significant relationship with days of decomposition. This might indicate a vast array the inhibition of opportunistic evolutionary related bacterial as a result of differences in resource utilisation, feeding strategies, or patterns, (Wandrag, Catford and Duncan, 2022) reducing the intensity of competition and promoting coexistence (Zhang, 2003; Petry *et al*., 2018; Sottas *et al*., 2018) which may have led to the significant increased species richness (Sottas *et al*., 2018) as indicated on the linear regression results. Some bacteria group can release a broad range of molecule within their surroundings to perform a wide variety of tasks, spanning from the exploring of biochemical building blocks to protective measures against possible predators and competitors (Christie *et al*., 2018). Studies have shown the metabolic at activities by bacterial decomposers in the lungs to release compounds like cholesterol-dependent toxins during autolysis (Mraheil *et al*., 2020) which can be harmful to other bacterial group and potentially reduce the distribution and increase the population of some bacterial species.

4.2.2.2 Environmental samples

4.2.2.2.1 Soils

The average Jackknife indicated the highest richness of microbial community in the soil sample was on Day 4 of decomposition with value of 5799.67±184.32. while the lowest were on day 14 with value of

14567±849.04. Regression analysis of Jackknife showed no significant relationship between species richness in the community over time ($F_{4,10}$ =2.002, p= 0.1702). The greatest rise in community evenness was noticed on day 4 of decomposition and mean NP Shannon and Shannon values were highest 6.92±0.07. The lowest drop in community evenness was noticed on day 4 with value of 6.31±0.62, 6.24±0.62. Regression analysis of NPShannon showed no significant relationship between species evenness in the community over time ($F_{4,10}$=1.364, p= 0.3136). The phylogenetic diversity of the community was on its highest on day 4 with value of 5121.00±233.69, and on its lowest on day 2 which value gave 4357.53±653.83. Regression analysis of phylogenetic diversity showed no significant relationship between species in the community over time ($F_{4,10}$= 1.699, p= 0.2262). The soil microbiome seems to be relative stable over the sampling days. Regression analysis of the alpha and phylogenetic diversity indicates non-significant changes relationships with time during the observed decomposition period, indicating a consistent microbiome despite the slight fluctuation of diversity values. The soil sample is a host to diverse group of bacterial that also contains functional redundant species (Chen *et al*., 2022; Yin *et al*., 2000; Nielsen, Wall and Six, 2015; Liu *et al*., 2019; Maron *et al*., 2018; Jia and Whalen, 2020) and with more redundant species in the community, functional redundancy would be encouraged which can support ecological resilience and stability (Biggs *et al*., 2020; Kang *et al*., 2015).

4.2.2.2.2 Seawater

The microbial community richness in the seawater samples achieved the greatest rise on Day 14 with the mean ACE, CHOA, and Jackknife values of 1373.10±713.20, 1294.19±668.25, and 1404.56 ±759.80. The lowest in richness was noticed on day 7 of decomposition with values of 753.09±21.00, 691.55±11.28, and 737.57±21.21 respectively. Regression analysis of Jackknife showed no significant relationship between species richness in the community over time ($F_{2,3}$ =3.528, p= 0.163). The greatest rise in community evenness was noticed on day 14 with the average NP Shannon and Shannon values value of 3.74±0.35, 3.72±0.33 while lowest was on day 7 with values of 3.14±0.42 and 3.12±0.42 respectively. Regression analysis of NPShannon showed no significant relationship between species evenness in the community over time ($F_{2,3}$= 3.894, p= 0.1466). The phylogenetic diversity of the community was on its highest on day 14 with value of 1630±788.02, and on its lowest on day 7 which value gave 559.50±61.52. Regression analysis showed no significant relationship in phylogenetic diversity over time ($F_{2,3}$=3.153, p= 0.1831). The ANOVA regression result suggests these changes do not seem to be systematically influenced by time of decomposition as no statistically significant relationships between days of decomposition and all diversity metrics was established. The seawater ecosystem has distinct characteristics that are influenced by its marine environment. While alpha diversity may be decreased, this is most likely due to adaptation

to the sea's peculiar ecological conditions. The absence of a strong relationship with days of decomposition expresses stability of microbial community.

4.2.2.2.3 Brackish water

The average ACE, CHAO, and Jackknife indicated the highest richness of microbial community on Day 14 of decomposition and the values were 1765.04±109.01, 1677.66±99.186, and 1836.17±82.12 respectively. The richness at its lowest value was on day 0 with values of 1444.24±399.34, 1364.71±320.92, 1482.74±339.94. Regression analysis of Jackknife showed no significant relationship between species richness in the community over time ($F_{2,3}$= 4.055, p= 0.1403), The greatest rise in community evenness was noticed on day 14 and mean NP Shannon and Shannon values were 3.96±0.11 and 3.94±0.11. The lowest drop in community evenness was noticed on day 0 with values of 3.86±0.30 and 3.84±0.32). Regression analysis of NPShannon showed significant declining relationship between species evenness in the community over time ($F_{2,3}$=14.94, p= 0.02756). A clear pattern was seen in the phylogenetic diversity and diversity varied as days progressed. The highest was seen on Day 14 and the lowest was on day 7 with values of 1257.5±20.51 and 629±22.63 respectively. Regression analysis of phylogenetic diversity showed no significant relationship between species in the community over time ($F_{2,3}$= 6.133, p= 0.08712). The community appears to have changed as decomposition progressed with a significant fluctuation in evenness. The brackish water sample represents a transitional environment (Shevah, 2014; Geyer 2019; Montemurno, 2022), offering both nutrients from fresh and seawater and fluctuations in evenness diversity might reflect the habitat's distinctive characteristics. Brackish water could harbour a vast array of bacterial due to its transitional features (Raina *et al.*, 2019) and this could lead to high competitions in the community that could affect and fluctuate the proportional representation of different species. The pig carcass in the brackish water might be a sub niche for microbes. Free floating bacteria can adhere to surfaces (Dunne, 2002; Zhao, Sun and Liu, 2023; Nandakumar *et al*., 2012) and the planktonic microbes in this community can have preference for the nutrient-rich carcass and can attach or reside on the carcass permanently or temporally which can contribute to community evenness fluctuations over the sampling days.

4.2.2.2.4 Freshwater

The highest microbial community richness was the highest on day 7 of decomposition with ACE, CHAO and Jackknife of 4795.42±2763.098, 4544.75±2638.463, and 5020±2949.243. The lowest in richness was noticed on day 14 with values of 689.16±1075.736, 693.5±956.5316, 753.52±1068.071 respectively. Regression analysis of Jackknife showed no significant relationship between species richness in the community over time ($F_{2,3}$=0.9252, p= 0.4864). The highest microbial community evenness in this set of

samples was noticed on day 7 of decomposition with a NPShannon and Shannon value of 5.85±1.05 and 5.78±5.75, while the lowest drop in evenness for both metrics was on day 0 with values of 2.99±0.68 and 3.28±2.97. Regression analysis of NPShannon showed no significant relationship between species evenness in the community over time ($F_{2,3}$= 0.4961, p= 0.6514). The phylogenetic diversity's highest and lowest values were noticed on day 0 and 4 which had a respective value of 1818.5±1112.28 and 749.5±60.10. Regression analysis of phylogenetic diversity showed no significant relationship between species in the community over time ($F_{2,3}$=0.8552, p= 0.5083). Species evenness, richness, and phylogenetic diversity of the freshwater sample had high changes over the observed time of decomposition, mostly on day 7 (figure 4.35-4.37). However, these changes in the community structure were not statically significant denoting that the bacteria in the freshwater ecosystems may exhibit transient responses or short-term variations in the bacterial community to maintain their diversity consistently. There were artificial disturbances of water samples during sample collection and bacterial communities might be resilient to perturbations or eliciting a short-term response in regard to the external disturbance.

Table 4.3 Summary of the significant values of linear regression between the alpha metrics and phylogenetic diversity of all samples over time. The samples with significant values are highlighted in blue.

Sample	**Region/Community**	**Richness (Jackknife)**	**Evenness (Npshannon)**	**Phylogenetic Diversity**
Pigs (External body part)	Anus	p-value: 0.5763	p-value: 0.3494	p-value: 0.1479
	Belly	p-value: 0.02428	p-value: 0.2834	p-value: 0.0005576
	Mouth	p-value: 0.1539	p-value: 0.3536	p-value: 0.06661
Pigs (Internal Organs)	Liver	p-value: 0.3378	p-value: 0.000133	p-value: 0.2385
	Lungs	p-value: 0.03982	p-value: 0.02156	p-value: 0.005148
Environmental samples	Soil	p-value: 0.1702	p-value: 0.3136	p-value: 0.2262
	Seawater	p-value: 0.163	p-value: 0.1466	p-value: 0.1831
	Brackish water	p-value: 0.1403	p-value: 0.02756	p-value: 0.08712
	Freshwater	p-value: 0.4864	p-value: 0.6514	p-value: 0.5083

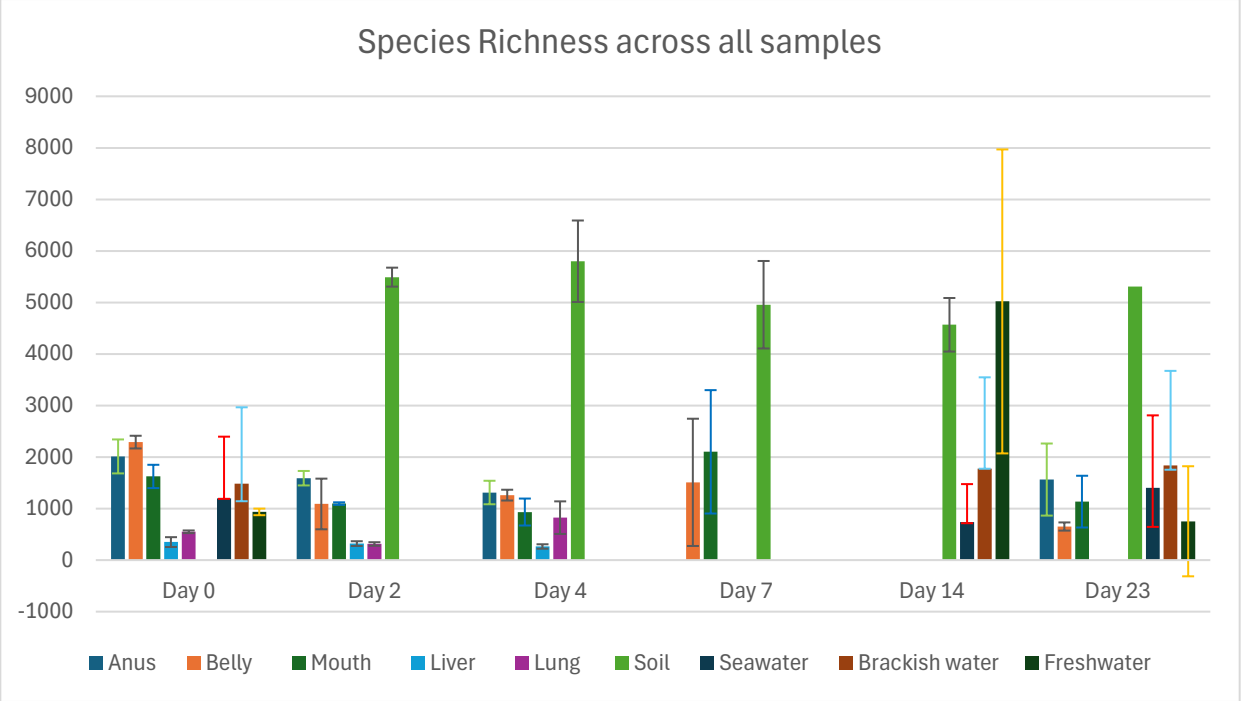

Figure 4.7 illustrates distinct variations in microbial richness diversity in different environmental and anatomical sites over a period of 23 days. The error bars indicate the variability (Standard deviation) in species richness. See table 2.1 for number of samples for each community used.

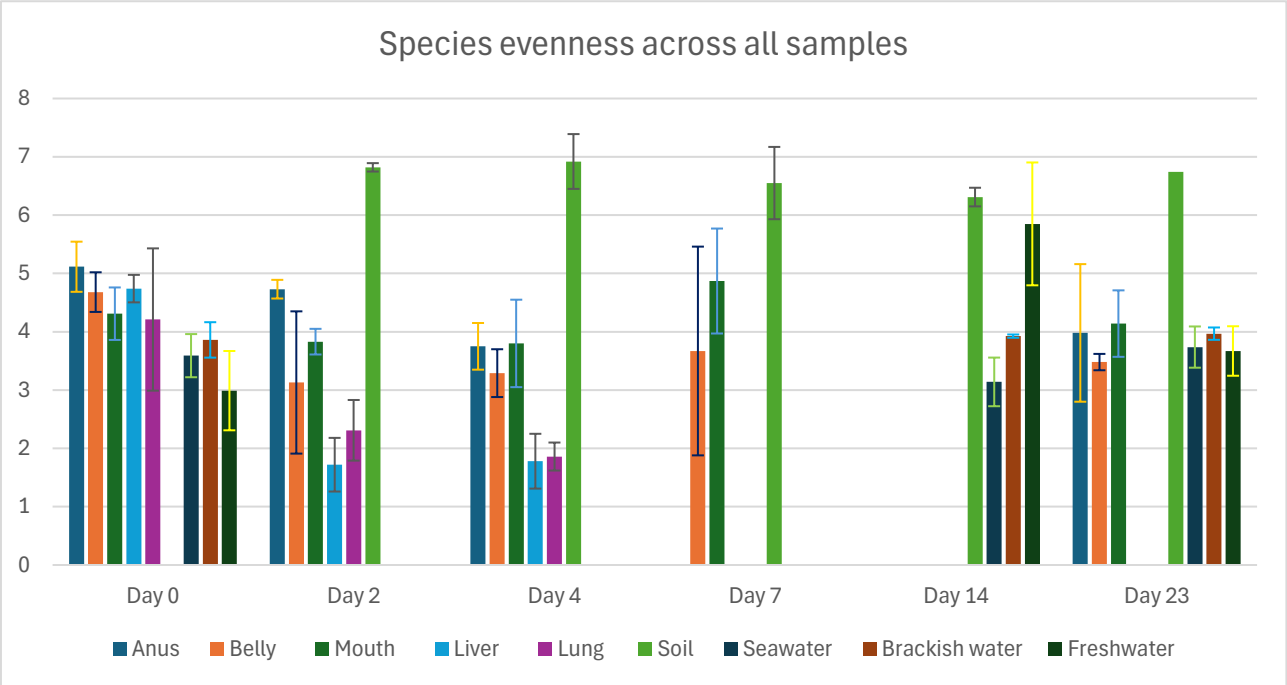

Figure 4.8 illustrates distinct variations in microbial evenness diversity in different environmental and anatomical sites over a period of 23 days. The error bars indicate the variability (Standard deviation) in species evenness. See table 2.1 for number of samples for each community used.

4.2.3 Inter-biodiversity between samples across decomposition days.

The level of evolutionary relatedness of species which is revealed by the Phylogenetic diversity also shows temporal changes across samples. The kinship of species in communities had dynamic trends over time, which tend to decrease when compared to day 0. Although microbial ecology has advanced quickly, the mechanisms that shape the organisation process of microbial communities are still poorly understood (O'Dwyer *et al*., 2012). Wagner *et al*., 2018, pointed out challenges regarding the concept of diversity and its application which are; there are a variety of widely used diversity indices that can produce different results, the nomenclature presently used to describe diversity is complex and unclear, the utility of breaking diversity down into components like richness and evenness varies depending on the diversity measure, and the application to sequence data is challenging (Wagner *et al*., 2018). The easiest way to quantify species diversity is species richness, which is either a count of the number of species or a list of all the species that may be found in a certain habitat or location (Kiester, 2013).

Soil sampling started on day 2 of decomposition with no pigs laid on the soil, and there was a consistent rise in the richness value of soil samples up until the final day of sample collection. Soil showed the highest value of species richness and evenness, and phylogenetic diversity compared to other samples. It has long been known that soil contain a high abundance and diversity of organisms, and several theories have been proposed to explain this phenomenon (Erktan *et al*., 2020). Although, the complex physical and chemical properties of soil make it a diverse niche for microorganism and the diversity of niches can increase the phylogenetic diversity. The richness of organic matter and nutrients, and the intricate interactions among microbial species in the soil before pig were laid, and the purging of nutrient (cells that have been broken down by enzymes) and microbes to soil resulting from the decomposition process can also contribute to why soil is more diverse than other samples. All sets of water samples were the next that showed higher values in microbial community richness after the soil samples. The water pigs were decomposed in tight containers which can impact microbial migration and pigs laid out on soil have more chances of microbes being lost to the environment. Samples used to examine microbial activities and succession on pig decomposition in water environment were equally used to conduct forensic anthropology, and there may be a chance of external microbial introduction during body scoring which can influence microbial ecology. This might be explained by the influence of salts (see material and methods chapter, section 2.1.2.2.2.1) present in the sample that possible inhibit or reduce microbial activities and biodiversity. Freshwater samples on day 7 gave a much higher richness on water samples. This can be characterised to the absence of salt compared to sea simulated samples on day 7 that showed the lowest in richness and evenness. The liver and lungs degraded quicker than other body parts and were not visible after day four. The mouth

samples were the third highest in richness followed by the belly samples and liver had the list richness value. The belly region was autopsied would make purging faster in that region so this might be the reason it is high in richness value. Belly, liver, and soil the lowest and highest days in community richness is the same as the phylogenetic diversity.

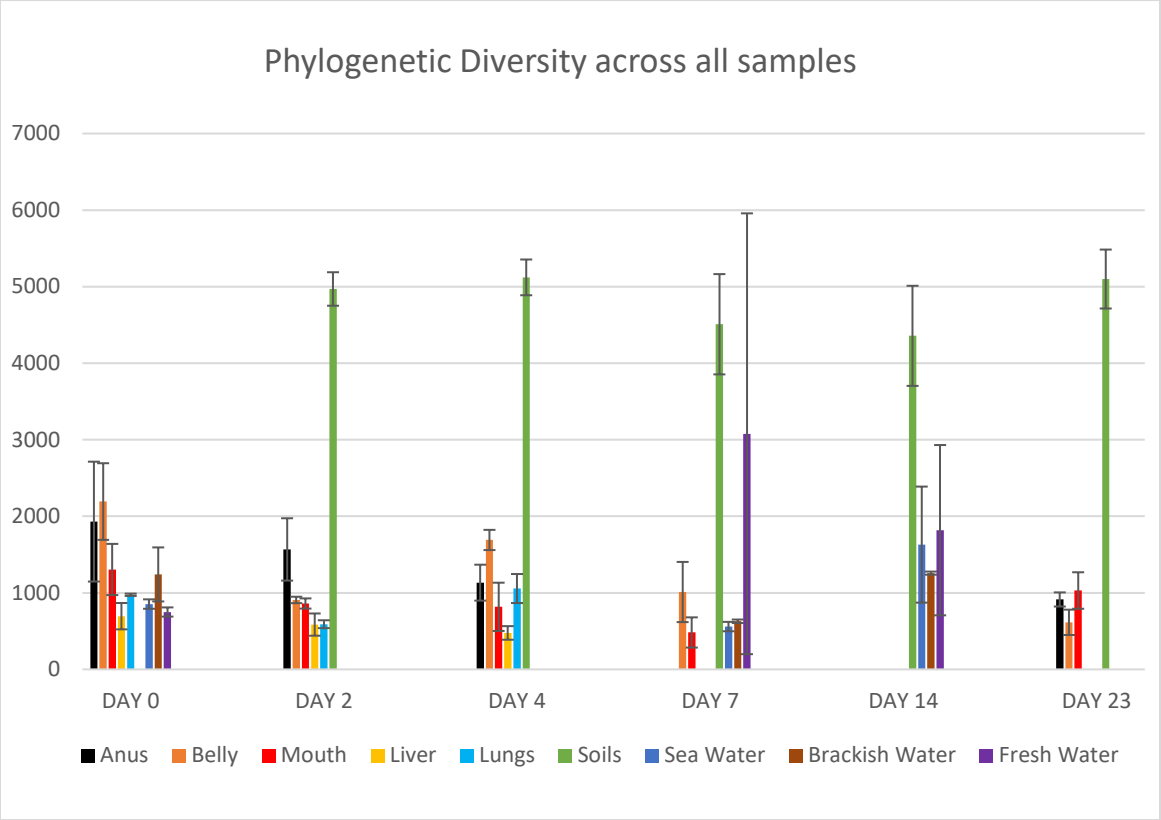

Figure 4.9 Phylogenetic Diversity showing soil to have the highest diversity. The error bars on the plot represents the standard deviation. See table 2.1 for number of samples of each community used.

4.3 CONCLUSION

The data indicates the spatial and temporal trends in biodiversity shown in the pig samples differ from the environmental samples. While the belly and anus samples had higher phylogenetic diversity values, the lung was the only sample type that showed significant changes in all 3 alpha diversity measurements over time displaying a dynamic temporal change having implications for the inter-biodiversity compared to other pig samples (internal organ and body sites) on different days. The environmental ecological niches as indicated by the behavioural pattern of the microbial communities were stable as decomposition advanced. Evenness can reflect the temporal richness patterns, and the evenness as presented in the internal organs (liver and lung) declined as decomposition advanced, suggesting that a few species are abundant.

The investigation revealed overall diversity measurements at the initial stages of decomposition (day 0), serving as a start point to assess post-mortem changes in alpha and phylogenetic diversity before the intricate activities and interference of post-mortem visiting bacteria on carcasses begins. Although, some significant difference between samples were revealed, the overall picture is complex and samples with no statistically significant difference may still be biologically relevant. As decomposition unfolds, the balance shifts, and certain species may seize dominance and could lead to temporal trends. Microbial interactions, availability of resources, and successional changes are ecological conditions that could be attributed to the temporal pattern. The interplay of these factors impacts the structure, ecological roles, and biodiversity of these communities over time. The dynamic interplay within communities highlights the fluidity of ecological niches and the adaptive strategies microorganisms employ to thrive. These findings underscore the spatial and temporal heterogeneity of microbial communities within the pig and its platform for decomposition.

Bacterial phylum and families responsible for the community richness, evenness, and phylogenetic diversity between samples of body parts collected from pigs across all days of decomposition are discussed in later chapters. Chapter 5, which will investigate the taxonomic composition of each sample type on day 0, and the differences observed over time will be investigated further in Chapters 6 and 7. The relationship between alpha and phylogenetic diversity is complex and varies across different the pig and environmental samples. The results from this chapter, contribute to understanding the bacterial community dynamics during decomposition, highlighting both significant changes and stability in diverse ecosystem.

5.0 CHAPTER 5: MICROBIAL COMPOSITION ON DAY 0

5.1 INTRODUCTION

In this chapter, focus will be drawn to the microbial compositions of each sample on day 0. Microbial composition on day zero is important to explore as it provides information about bacterial taxa existing in each body part or decomposition site before active and advanced decay progresses (Lauber *et al.*, 2014) and sets the scene for the succession of other microorganisms in the later stages of decomposition. Bacteria form symbiotic relationships with their hosts (humans, plants, and animals), and even after death, some bacteria continue to do so. The relationship that exists between bacterial communities and their hosts after death can also be described as symbiotic, as the host provides an ecological environment for bacteria to breed and interact, while the bacteria are also agents that contribute to the decomposition process of the host. Each sample representing various body parts comprises both majority and minority phyla, allowing for a direct insight into the dominating phyla. Microbes have been assessed according to the sample types, i.e., samples from various sites of the pig and the environmental platforms that enhance decay (water and soil samples). Post-mortem bacterial communities are part of a larger microbial taxon of organisms known as the "necrobiome" (Benbow *et al.*, 2013). According to Pechal *et al.* (2014), bacterial cells living on the surface of a body undergoing decomposition are referred to as “epinecrotic microbial communities." On the other hand, organisms found in the internal organs and orifices are referred to as “Thanatomicrobiome” (Can *et al.*, 2014). In this study, we may also refer to all organisms found within an internal ecological unit of a carcass or cadaver as a Thanatomicrobial community, which includes the environmental microbes, as they can interact with other varieties of microorganisms (epinecrotic and thanatomicrobiome) to influence decomposition.

Around the early 2000s, attempts were made by Arpad Vas to catalogue bacteria associated with human decomposition, but this was later abandoned because of the sheer number of species isolated from a cadaver undergoing the decay process. He concluded that every bacterium known is linked with some aspect of the human decomposition cycle, except for those from deep-sea vents (Vass, 2001; Hyde *et al.*, 2013). The diversity of microbial communities across every ecological system on Earth and their role in decomposition can be acknowledged. In some ecological niches, the bacterial species cultivable is less than one percent (Carter *et al.*, 2017) and therefore discoverable only through metagenomic approaches; this includes the candidate phylum radiation. The candidate phylum radiation (CPR) relates to phyla with species that rarely have a represented member cultured and can occur in ratios of less than one percent, depending on the environment (Ji *et al.*, 2022; Kadnikov *et al.*, 2020; Tsurumaki, 2020; Jaffe *et al.*, 2021;

Cornish *et al.*, 2022; Castelle & Banfield, 2018). Members of this group have joined the tree of life as a new branch (Maatouk *et al.*, 2021) and are generally considered to have extremely small cell sizes, streamlined genomes, and inadequate metabolic capabilities (Ji *et al.*, 2022; Moreira *et al.*, 2020) that have resulted from the evolutionary radiation of bacterial lineages, the majority of whose species have never been cultured and are only known through metagenomic sequencing (Ji *et al.*, 2022; Kadnikov *et al.*, 2020). They account for more than 26% of the microbiome (Maatouk *et al.*, 2021), and a minimum of 74 CPR candidate phyla have been identified. These bacteria are found in a variety of environments, including soil (Nicolas *et al.*, 2021; Tsurumaki, 2020), sediments, groundwater, freshwater, and the human oral cavity (Tsurumaki, 2020). These bacteria are typically thought to survive by parasitism or symbiosis (Ji *et al.*, 2022), as they have previously been identified to exist in decomposing matter.

The PVC superphylum groups (Planctomycetes, Verrucomicrobiae, and Chlamydiae) which are represented in most ecological niches, are groups of phyla (Rivas-Marín *et al.*, 2016; Dharamshi *et al.*, 2021) that have only been detected as a result of extensive 16S rRNA gene analysis (Wagner and Horn, 2006; Rivas-Marín and Devos, 2017). Currently, other phyla such as Lentisphaerae, Poribacteria, OP3, and WWE2 have been included in the PVC superphylum (Wagner and Horn, 2006; Pinos *et al.*, 2016). More recently, a few uncultured candidate phyla have also been added to this group of bacteria (Zheng *et al.*, 2021). These superphylum phyla are grouped together because of their common ancestry, but they also exhibit diverse biological and ecological traits (Lagkouvardos *et al.*, 2014). The PVC phyla share a unique multiplex cell plan, with an intracellular membrane enhancing the cytoplasm, which is compartmentalised into the paryphoplasm and pirellulosome regions (Pinos *et al.*, 2016). Some species within the PVC phylum possess more than two cell plans (Fuerst, 2012; Lee *et al.*, 2009; Santarella-Mellwig *et al.*, 2010).

5.1.1 The ICSP (The International Committee on Systematics of Prokaryotes) New System of Naming Prokaryotes

The ICSP (International Committee on Systematics of Prokaryotes) is in charge of naming cultured archaea and bacteria and represents microbiological societies worldwide. In February 2021, they implemented a new system of nomenclature for prokaryotes (Perinchery, 2022; Oren *et al.*, 2023; Oren and Garrity, 2020). The new method requires that the stem of the prokaryote's genus, which is the second-to-last taxonomic rank, must now end in "-ota" to create the names of each phylum (Perinchery, 2022; Oren *et al.*, 2023; Oren and Garrity, 2020). The names of prokaryotes belonging to 42 phyla were altered as a result (Perinchery, 2022; Oren and Garrity, 2020) and were also announced by the National Centre for Biotechnology Information (NCBI), a network of biological databases that acts as a resource for researchers (Robitzski, 2022). Details of the new nomenclature can be found in Appendix 2, Table A2.

Although some scientists have lambasted the altered names newly assigned to the affected phyla (Panda *et al.*, 2022; Lloyd & Tahon, 2022), making the matter a controversial one (Döring, 2022), the ICSP's decision applies only to names governed by the International Code of Nomenclature of Prokaryotes (Perinchery, 2022). As shown in Appendix 2, Table A2, the phylum of Firmicutes is now called Bacillota according to the new nomenclature, but this study utilises both old and new names interchangeably. One disadvantage of the new NCBI system is that scientists and microbiologists researching affected organisms will need to search existing literature for the same bacteria using several names (Perinchery, 2022). Only prokaryotes that have been grown, preserved, and researched in the laboratory will have their names used in the International Code of Nomenclature of Prokaryotes (Perinchery, 2022). Another way to put it is that the code does not recognise the prokaryote's genome or anything other than lab-cultured specimens as the type of material (Panda *et al.*, 2022). A few monophyletic groups have also recently undergone reclassification and renaming from their previous class/order names, despite the fact that the ICSP does not regulate classification. These groups include (i) phylum Bdellovibrionota, previously the order Bdellovibrionales; (ii) the phylum Campylobacterota, formerly the class Epsilonproteobacteria; and (iii) the phylum Myxococcales, initially known as order Myxococcales (Myxobacteria) (Panda *et al.*, 2022).

On Day 0, sampling was carried out on both the external and internal parts of the pig. The external part can reveal the epinecrotic bacterial community present on the skin surface, while the internal organs can also reveal the thanatomicrobial community present in the organs of the pig (Javan *et al.*, 2016). Sampling on Day 0 also provides access to evaluate bacterial groups responsible for the spatial differences in richness across all samples (Chapter 4). The 16S rRNA sequences were categorised at the phylum and family levels in order to recognise the spatial colonisation of the bacterial community structure on Day 0 and subsequent days. Guo *et al.* (2016) also categorised the evolution of bacterial colonisation at both the phylum and family levels, utilising 16S rRNA sequences. Guo *et al.*'s (2016) taxonomic level of bacterial identification was adopted for this study because, based on the research question or hypothesis being investigated, focusing on higher taxonomic levels was sufficient to meet the aims and objectives of this project, as the taxonomic levels (Phylum and Family) had sufficient distinctions to notice microbial interactions and trends across days of decomposition. Analysing data at the lower taxonomic level can also be less time-efficient and requires more computational resources, making it more computationally intensive compared to analysing at higher taxonomic levels. Findings regarding the community structure may shed light on the underlying microbial ecology of pig decomposition and help enhance our understanding in establishing a linear relationship for the prospective use of microorganisms as a forensic tool (Guo *et al.*, 2016). In addition to the body sites and organs of pigs, the bacterial taxa within the

microbial communities found in the environmental platforms of the swine carcass (in the soil and water) will also be assessed.

5.2 RESULTS AND DISCUSSION

In this section, there is a presentation of the analysis of the microbial community composition at the phylum and family levels across different samples collected on day 0 of the study. Table 5.1 highlights the three most abundant phyla and families, alongside their respective average percentages, within each sample. This initial data serves as a baseline for understanding the microbial landscape prior to the onset of decomposition processes, which will be further elaborated upon in subsequent chapters.

Table 5.1 Displays the top 3 phylum, families, and their respective dominion ratio in each sample on day 0, highlighting the dominance of Firmicutes in pig tissues and Proteobacteria in aquatic environments.

SAMPLE	TOP 3 RELATIVE AMBUDANT PHYLA	AVERAGE % OF PHYLUM	TOP 3 RELATIVE AMBUDANT FAMILIES	AVERAGE % OF FAMILY	PHYLUM BELONGING TO THE DOMINATING FAMILY
Belly	Firmicutes	57.6	Lactobacillaceae	25.7	Firmicutes
	Actinobacteria	20.8	Corynebacteriaceae	11.6	Actinobacteria
	Proteobacteria	13.5	Moraxellaceae	9.3	Proteobacteria
Anus	Firmicutes	45.7	Prevotellaceae	18.5	Bacteroidetes
	Bacteroidetes	35.0	Ruminococcaceae	15.5	Firmicutes
	Proteobacteria	12.6	Lachnospiraceae	13.3	Firmicutes
Mouth	Bacteroidetes	35.0	Moraxellaceae	18.9	Proteobacteria
	Proteobacteria/Firmicutes	26.6/26.3	Prevotellaceae	15.8	Bacteroidetes
	Fusobacteria	8.1	Porphyromonadaceae	12.2	Firmicutes
Liver	Firmicutes	50.0	Planococcaceae	10.1	Firmicutes
	Proteobacteria	24.0	Moraxellaceae	8.3	Proteobacteria
	Actinobacteria	13.0	Propionibacteriaceae	6.5	Actinobacteria
Lungs	Firmicutes	70.9	Peptostreptococcaceae	21.6	Firmicutes
	Proteobacteria	13.3	Lactobacillaceae	14.0	Firmicutes
	Actinobacteria	8.0	Clostridiaceae	9.4	Firmicutes
soil	Proteobacteria	28.5	Bradyrhizobiaceae	9.0	Proteobacteria
	Acidobacteria	14.4	Bacillaceae	8.4	Firmicutes
	Firmicutes	12.3	Chthoniobacteraceae	5.6	Verrucomicrobia
Seawater	Proteobacteria	66.3	Pseudomonadaceae	23.8	Proteobacteria
	Firmicutes	18.3	Rickettsiaceae	16.2	Proteobacteria
	Actinobacteria	8.1	Ignatzschineria_f	7.7	Proteobacteria
Brackish water	Proteobacteria	58.2	Planococcaceae	9.3	Firmicutes
	Actinobacteria	18.0	Propionibacteriaceae/ Moraxellaceae	8.3	Actinobacteria/Proteobacteria
	Firmicutes	11.9	Sphingomonadaceae	7.5	Proteobacteria
Freshwater	Firmicutes	68.0	Planococcaceae	41.8	Firmicutes
	Proteobacteria	19.4	Tissierellaceae	8.8	Firmicutes
	Actinobacteria	8.5	Ignatzschineria_f	7.2	Proteobacteria

5.2.1 Overview of Bacterial Phyla Distribution

The bacterial composition of different sample types (internal organs and body sites of pigs, as well as environmental samples) was represented on pie charts (Figure 5.1 – 5.9) and analysed, focusing on the relative abundance of various bacterial phyla. The taxa with less than 1% average count were categorised as "other less than one percent." The most prominent phyla observed were Actinobacteria (High presence in the belly sample of pigs and significant presence in soil and brackish water among environmental samples), Bacteroidetes (dominant in the mouth sample of pigs and second most abundant in the anus sample), Firmicutes (most dominant phylum in the belly, anus, liver, and lungs of pigs and high presence in freshwater samples), and Proteobacteria (dominant in all environmental samples except for freshwater water, and second most abundant in the mouth sample), which have been frequently reported in post-mortem microbiology studies (Roy *et al*., 2021; Emmons *et al*., 2020; Tuccia *et al*., 2019).

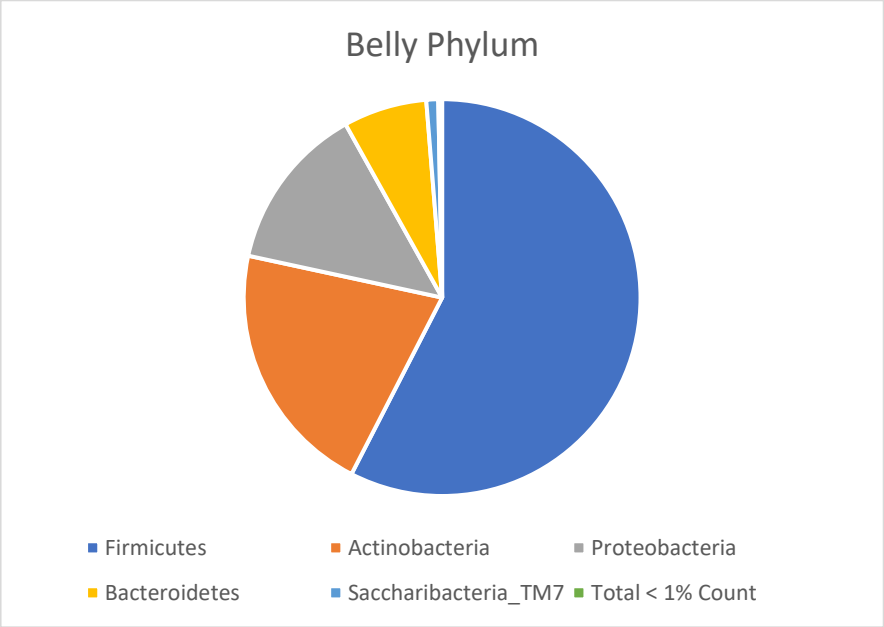

Figure 5.1 pie chart showing the average individual taxa of all pigs represented in the belly sample of all pigs. The respective ratios of the phyla are Firmicutes: 57.6%, Actinobacteria: 20.8%, Proteobacteria: 13.5%, Bacteroidetes: 6.8%, Saccharibacteria_TM7: 1%, Total <1% 0.3%

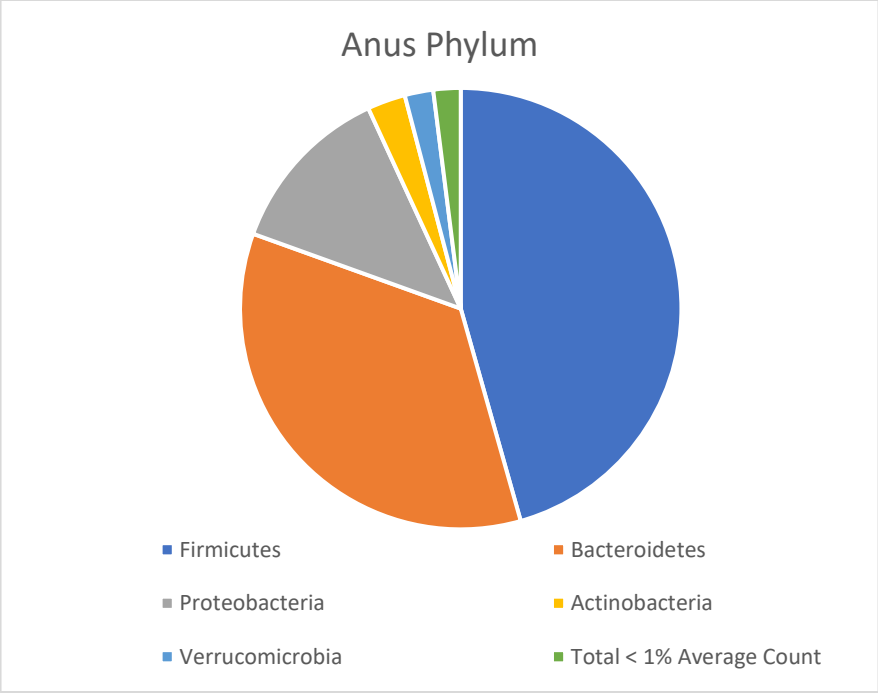

Figure 5.2 A pie chart showing the average individual taxa of all pigs represented in the anus sample of all pigs. The respective ratios of the phyla are Firmicutes: 45.7%, Bacteroidetes: 35.0% Proteobacteria: 12.6% Actinobacteria: 2.8% Verrucomicrobia: 2.1 %, Total < 1% Average Count: 2.0%.

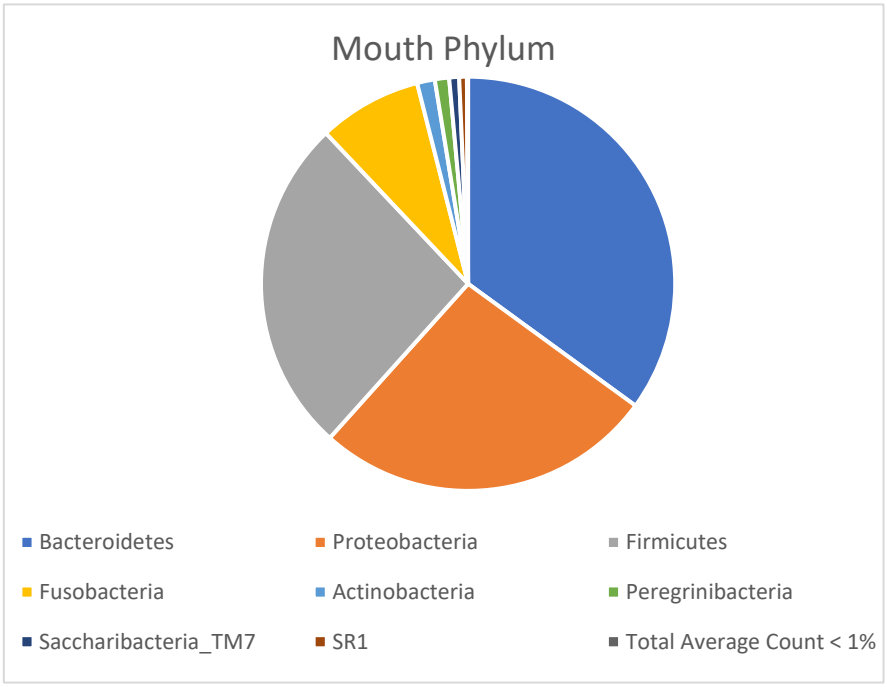

Figure 5.3 A pie chart showing the average individual taxa of all pigs represented in the mouth sample of all pigs. The respective ratios of the phyla are Bacteroidetes: 35.0%, Proteobacteria: 26.6%, Firmicutes: 26.3%, Fusobacteria: 8.1%, Actinobacteria: 1.4%, Peregrinibacteria: 1.1%, Saccharibacteria_TM7: 1%, SR1: 1%, Average total of other Count < 1%: 0.1%

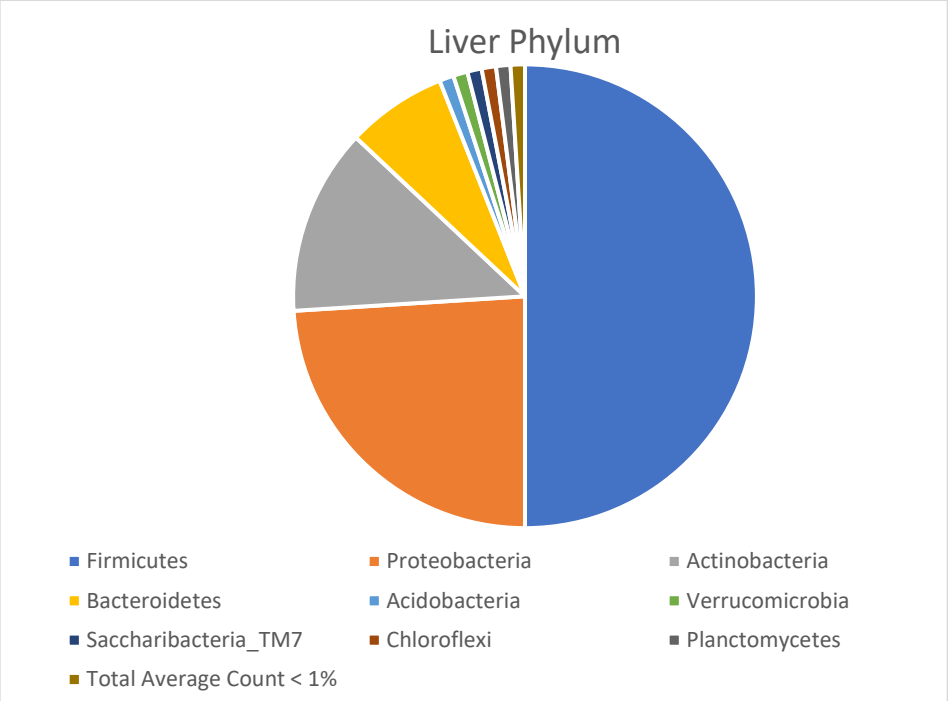

Figure 5.4 A pie chart showing the average individual taxa of all pigs represented in the Liver sample of all pigs. The respective ratios of the phyla are Bacteroidetes Firmicutes: 50.0%, Proteobacteria: 24.0%, Actinobacteria:13.0%, Bacteroidetes: 7.0%, Acidobacteria: 1.0%, Verrucomicrobia: 1.0%, Sacharibacteria_TM7: 1.0%, Chloroflexi: 1.0%, Planctomycetes: 1.0%, Total Average Count < 1%: 1.0%

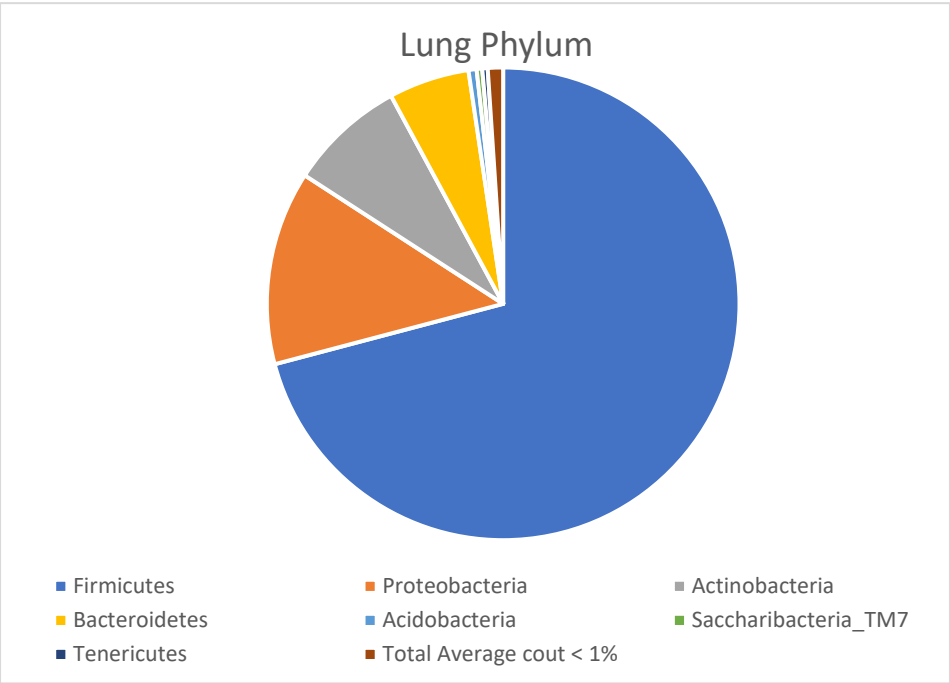

Figure 5.5 A pie chart showing the average individual taxa of all pigs represented in the Lung sample of all pigs. The respective ratios of the phyla are Firmicutes: 70.9%, Proteobacteria: 13.3%, Actinobacteria: 8.0%, Bacteroidetes: 5.5%, Acidobacteria: 0.6%, Saccharibacteria_TM7: 0.4%, Tenericutes: 0.4%, Total Average count < 1%: 1.0%

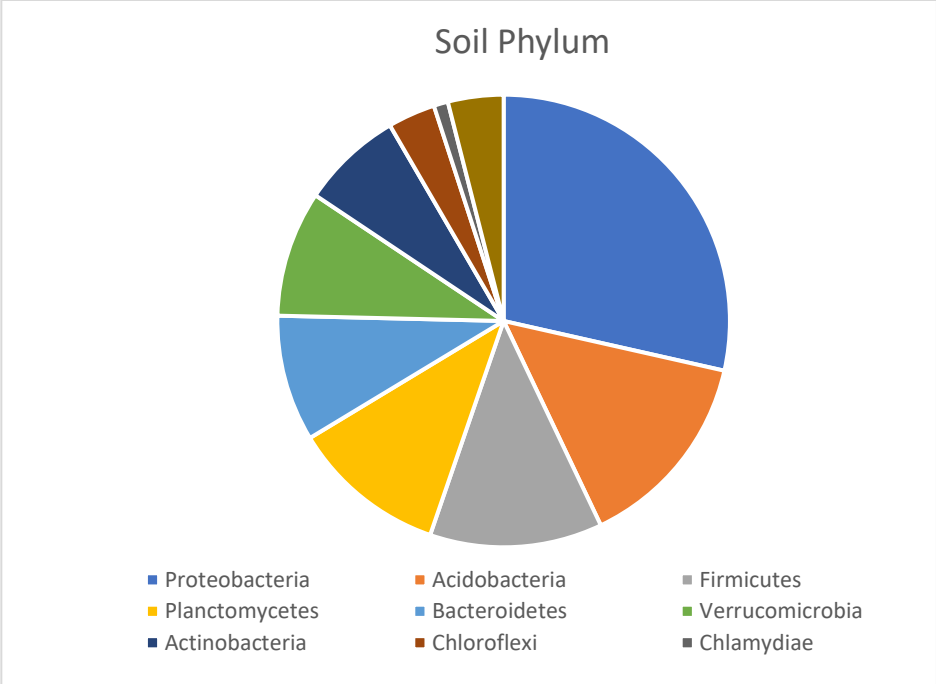

Figure 5.6 A pie chart showing the average individual taxa of all pigs represented in the Soil sample of all pigs. The respective ratios of the phyla Proteobacteria: 28.5%, Acidobacteria: 14.4%, Firmicutes: 12.3%, Planctomycetes: 11.1%, Bacteroidetes:9.0%, Verrucomicrobia: 9.0%, Actinobacteria: 7.2%, Chloroflexi: 3.4%, Chlamydiae: 1.0%, Total Average count < 1%: 4.0%

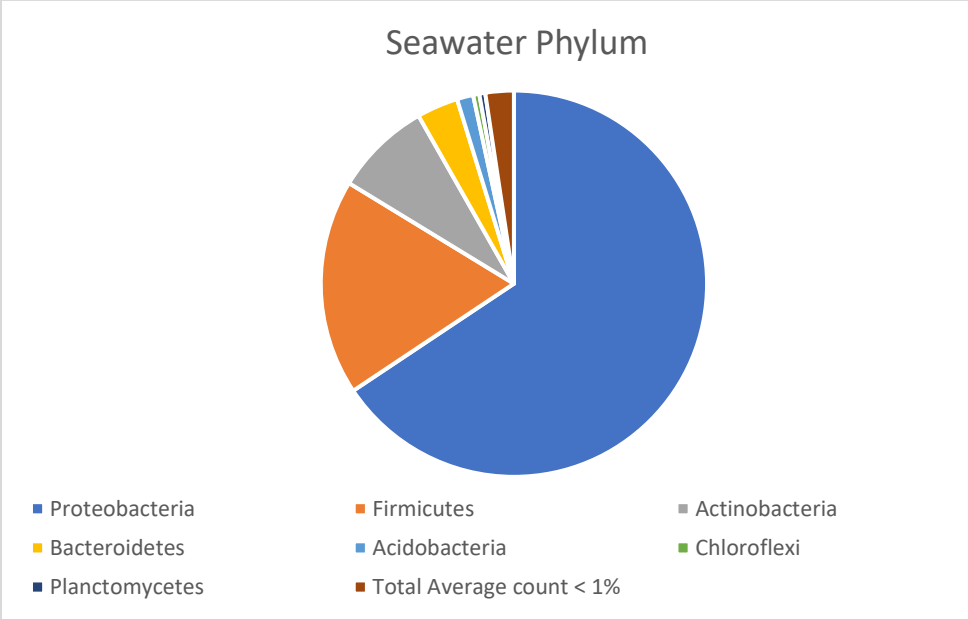

Figure 5.7 A pie chart showing the average individual taxa of all pigs represented in the seawater sample of all pigs. The respective ratios of the phyla are Proteobacteria: 66.3%, Firmicutes: 18.3%, Actinobacteria: 8.1%, Bacteroidetes: 3.5%, Acidobacteria: 1.4%, Planctomycetes: 1% Total Average count < 1%: 2.4%

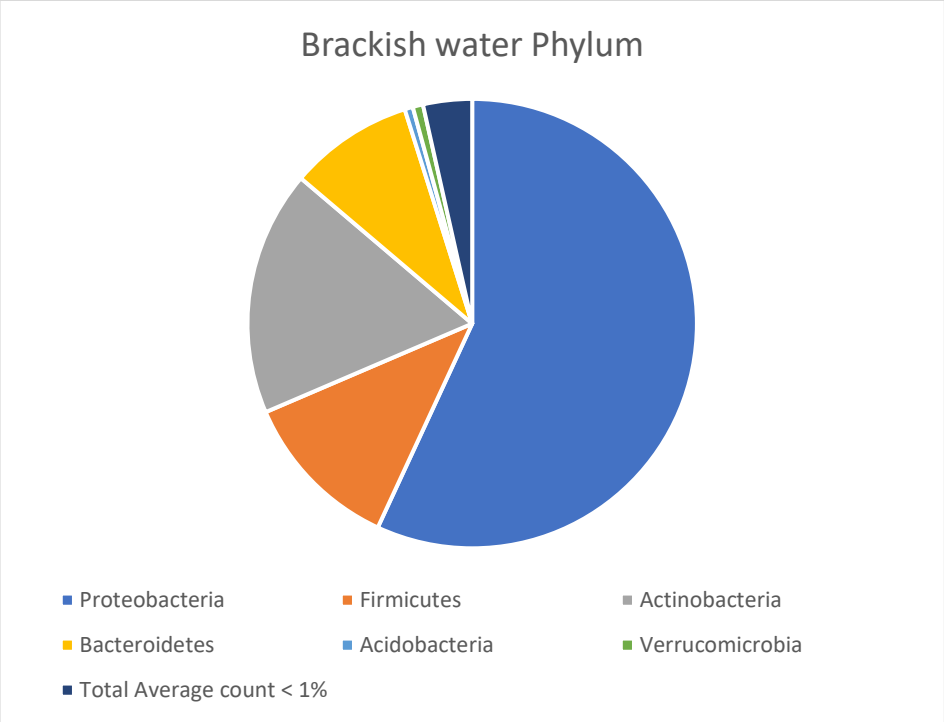

Figure 5.8 A pie chart showing the average individual taxa of all pigs represented in the Brackish water sample of all pigs. The respective ratios of the phyla are Proteobacteria: 58.2%, Firmicutes: 11.9%, Actinobacteria: 18.0%, Bacteroidetes:9.1%, Acidobacteria: 1%, Verrucomicrobia:1%, Total Average count < 1%: 3.6%

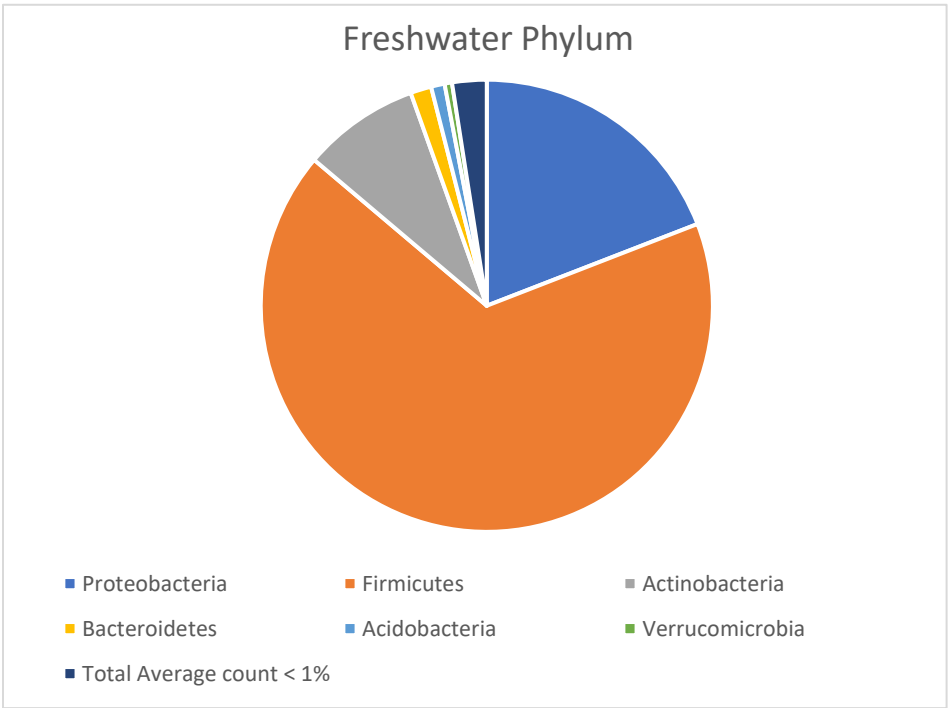

Figure 5.9 A pie chart showing the average individual taxa of all pigs represented in the freshwater sample of all pigs. The respective ratios of the phyla are Proteobacteria: 19.4%, Firmicutes: 68.0%, Actinobacteria: 8.5%, Bacteroidetes: 1.5%, Acidobacteria: 1.0%, Verrucomicrobia:1%, Total Average count < 1%: 2.5%

5.2.1.1 Relationship between Biodiversity and Bacterial Phyla on Day 0

According to chapter four (Table 4.5), no significant differences in NPShannon were observed between the pig samples suggesting that the changes in phyla abundance primarily affected richness and phylogenetic diversity rather than evenness. On day 0, Bacteroidetes were reduced in the belly and liver compared to the anus and were increased in the mouth compared to the belly and internal organs. The differences in Bacteroidetes abundance could influence phylogenetic diversity, particularly in the internal organs compared to the belly as the observed reduction of Bacteroidetes in the belly may lower its phylogenetic diversity compared to other samples. Actinobacteria were significantly reduced in the mouth and liver compared to the belly, contributing to the observed lower microbial richness in the liver compared to the belly. The decreased abundance of Actinobacteria in the liver compared to the belly may contribute to a lower phylogenetic diversity in the liver. Cyanobacteria were significantly minimal in the mouth compared to the anus, although in chapter four (Table 4.5), the relationship between the mouth and anus were did not possess a significant value, its reduced presence in the mouth may also donate to a trend of lower richness compared to the anus. Similar to richness, no significant impact on phylogenetic diversity, but the reduction in Cyanobacteria might influence overall diversity trends. Peregrinibacteria were increased in the mouth compared to the belly and internal organs. The increased abundance of Peregrinibacteria in the mouth tend not to affect the phylogenetic diversity but likely contributes to higher richness compared to the belly and liver.

The Tukey multiple comparison of Jackknife, NPShannon, and Phylogenetic Diversity between the aquatic samples indicated no statically significant value (Chapter four, Table 4.2). The lack of significant differences in all diversity metrics suggests that the microbial communities in freshwater, brackish water, and seawater are not only similar in number but also have similar evolutionary backgrounds and comparable species distribution patterns. This might be due to the microbial communities been subject to similar ecological pressures or share environmental characteristics, despite the varying salinity and other chemical properties of the water types. Nevertheless, in all biodiversity metrics, the soil gesticulated statically significant difference in respect to the aquatic samples. Verrucomicrobia, Chlamydiae, Planctomycetes, Chloroflexi, Acidobacteria, and Tenericutes were significantly increased in soil compared to brackish and freshwater environments and these taxa tend to be responsible for the increased biodiversity metrics. The soil showing an increased and significant differences in all biodiversity metrics suggests that the environments differ profoundly in their microbial communities: soil supports a larger number of different species compared to aquatic environments (higher richness), soil has a more balanced distribution of species, with no single species overwhelmingly dominant (higher evenness), soil contains

a broader range of evolutionary lineages, indicating a more diverse set of evolutionary histories (higher Phylogenetic Diversity).

Bacterial taxa (Proteobacteria, Firmicutes, Fusobacteria, Saccharibacteria_TM7, SR1) that were present in pig and environmental sample type, and signified no significant difference in their abundance can still influence the community's biodiversity depending on the ecological structure and function. Some of the taxa that were significantly different in the environmental sample was driven by the soil and water samples being combined (to make the environmental sample) for the comparison. This shows that the adaptability prowess of these phyla is not restricted to sample type and can be distributed within the body sites and environment. Although the relationship between microorganisms that influence diversity within an ecosystem can be complex. Some of these microorganisms can contribute to recycling nutrients, and making resources available for other microbes, which can lead to an increase species richness within that ecosystem. As species richness increases, dominate of individual taxa are likely to reduce in the community since there are more species sharing the available resources. In some cases, microbes that have more adaptive features within communities can prey on other microbes leading to a specie reduction and this can lead to a more even community.

Table 5.2 Showing summary of ANOVA test used to examine the variation in abundance of various phyla across different sample types. The significant values are highlighted.

Individual Phyla	**Pig Samples**	**Site**	**Environmental Samples**	**Site**
Proteobacteria	$F_{4,9}$= 2.698, p= 0.0996		$F_{3,5}$=1.135, p= 0.419	
Actinobacteria	$F_{4,9}$=4.76, p= 0.0244	Reduced in mouth and liver compared to belly	$F_{3,5}$=0.669, p= 0.607	
Firmicutes	$F_{4,9}$=1.558, p= 0.2661		$F_{3,5}$=1.337, p= 0.361	
Bacteroidetes	$F_{4,9}$=19.28, p=0.0001941	Reduced in belly and liver compared to anus; increased in mouth compared to belly & internal organs	$F_{3,5}$=2.892, p=0.141	
Verrucomicrobia	$F_{4,9}$=2.51, p= 0.116		$F_{3,5}$=109.8, p= 0.000055	Increased in the soil compared to the aquatic samples

Chlamydiae	$F_{4,9}$=0.656, p= 0.638		$F_{3,5}$=575.6, p= 0.00000091	Increased in the soil compared to the aquatic samples
Fusobacteria	$F_{4,9}$=3.431, p= 0.0576		$F_{3,5}$=1.234, p= 0.39	
Planctomycetes	$F_{4,9}$=1.66, p= 0.242		$F_{3,5}$= 198.8, p= 0.000013	Increased in the soil compared to the aquatic samples
Saccharibacteria_TM7	$F_{4,9}$= 1.923, p= 0.191		$F_{3,5}$= 1.725, p= 0.277	
SR1	$F_{4,9}$= 3.319, p=0.0623		$F_{3,5}$=0.556, p= 0.667	
Chloroflexi	$F_{4,9}$= 2.237, p=0.145		$F_{3,5}$= 88.02, p= 0.000093	Increased in the soil compared to the aquatic samples
Cyanobacteria	$F_{4,9}$= 4.773, p= 0.0242	Reduced in the mouth compared to the anus	$F_{3,5}$= 1.215, p= 0.395	
Acidobacteria	$F_{4,9}$= 2.744, p=0.0961		$F_{3,5}$=88.33, p= 0.000094	Increased in the soil compared to the aquatic samples
Tenericutes	$F_{4,9}$= 1.523, p= 0.275		$F_{3,5}$= 154.2, p=0.000024	Highly Increased in the soil compared to the aquatic samples
Peregrinibacteria	$F_{4,9}$=5.448, p=0.0165	Increased in the mouth compared to the belly and internal organs	$F_{3,5}$=1.296, p= 0.372	

5.2.2 Overview of Bacterial Family Distribution

The microbial of individual samples were composed of several varying bacterial family taxa and most abundance community was primarily seen in phyla such as Firmicutes, Actinobacteria, Bacteroidetes, Proteobacteria. The ranked position of families was estimated with some variation in their exact position observed when compared to the data analysis a phyla level. This is because multiple families could make exact or similar proportions on the community ratio. For instance, whilst at the phyla level the most abundant group in the anus are the Firmicutes, at the family level in the same sample type the Prevotellaceae (Phyla: Bacteriodetes) have the highest abundance. In this chapter, some bacterial families were found to only be present in a particular community (appendix 3, Table A3.1 – A3.4), showcasing their adaptability to a specific environment which could be related to their ecological function, this can lead to an increase of phylogenetic diversity within that community, for instance, the high significant levels of phylogenetic diversity in the soil as revealed in chapter 4 correlates to the microbial composition of samples in this chapter as soil has the highest number of peculiar taxa that are not detected in other samples, suggesting that the soil microbial community reflect non-random ecological processes such as mutualism.

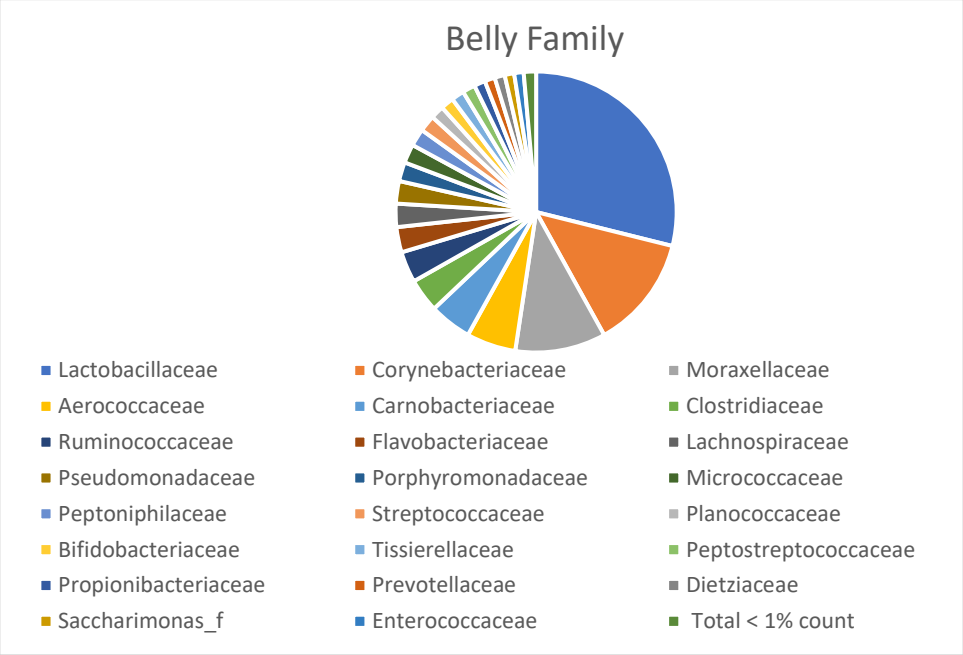

Figure 5.10 A pie chart showing the average proportion of family subdivision in the bacterial taxon found in the belly sample of pigs. The families are Lactobacillaceae: 25.7%, Corynebacteriaceae: 11.6%, Moraxellaceae: 9.3%, Aerococcaceae: 5.1%, Carnobacteriaceae: 4.3%, Clostridiaceae: 3.4 %, Ruminococcaceae: 3.2 %, Flavobacteriaceae: 2.6 %, Lachnospiraceae:2.4 %, Pseudomonadaceae: 2.3 %, Porphyromonadaceae: 2.0 %, Micrococcaceae: 1.9 %, Peptoniphilaceae :1.8 %, Streptococcaceae: 1.7 %, Planococcaceae: 1.4 %, Bifidobacteriaceae: 1.3 %, Tissierellaceae : 1.3 %, Peptostreptococcaceae :1.3 %, Propionibacteriaceae: 1.1 %, Prevotellaceae: 1.1 %, Dietziaceae:1.0 %, Saccharimonas_f:1.0 %, Enterococcaceae:1.0 %, Total of others < 1% count: 13.0 %

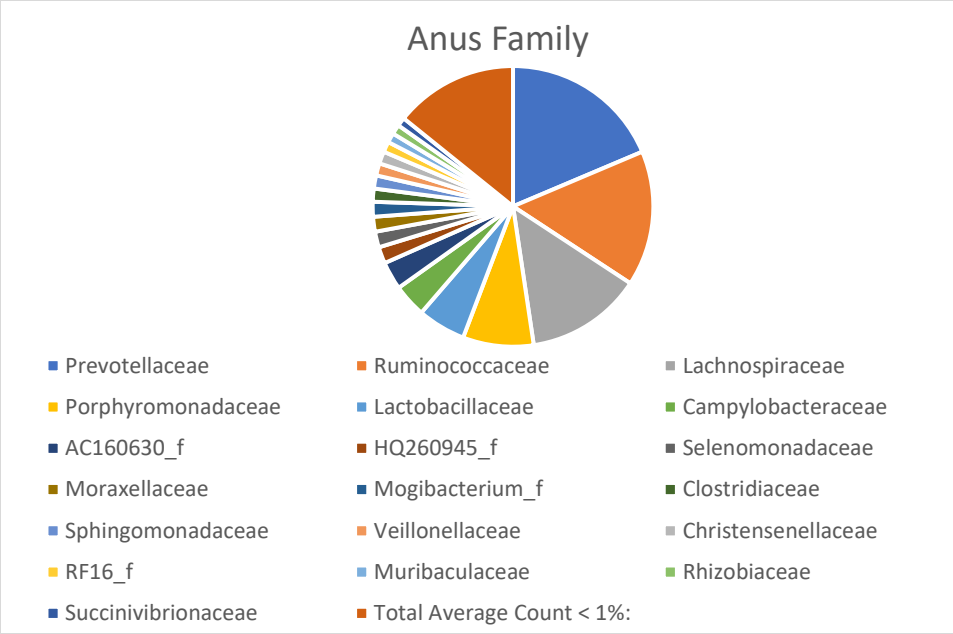

Figure 5.11 A pie chart showing the average proportion of family subdivision in the bacterial taxon found in the anus of pigs. The families are Prevotellaceae: 18.5%, Ruminococcaceae: 15.5%, Lachnospiraceae: 13.3%, Porphyromonadaceae: 8.1%, Lactobacillaceae: 5.5%, Campylobacteraceae 3.8%, AC160630_f: 3.2%, HQ260945_f:1.9%, Selenomonadaceae:1.8%, Moraxellaceae, 1.7%, Mogibacterium_f: 1.7% ,Clostridiaceae: 1.5%, Sphingomonadaceae: 1.5%, Veillonellaceae: 1.4%, Christensenellaceae: 1.4%, RF16_f: 1.2%, Muribaculaceae: 1.1%, Rhizobiaceae: 1.1%, Succinivibrionaceae: 1.0%, , Total of average of < 1%: 14.1%

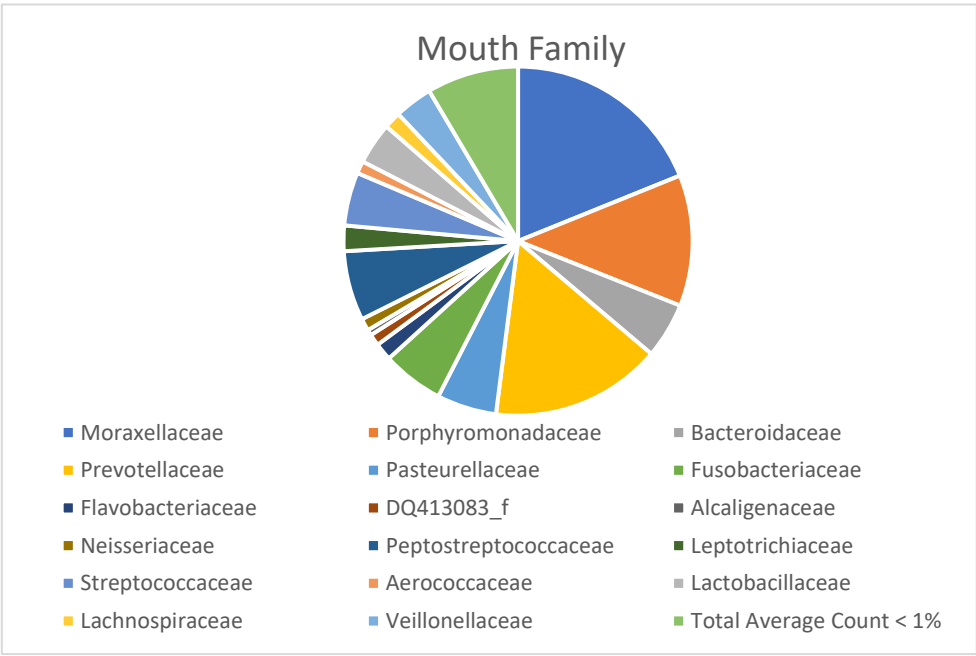

Figure 5.12 A pie chart showing the average proportion of family subdivision in the bacterial taxon found in the mouth of pigs. The families are Moraxellaceae:18.9%, Porphyromonadaceae: 12.2%, Bacteroidaceae: 5.1%, Prevotellaceae: 15.8%, Pasteurellaceae: 5.5%, Fusobacteriaceae: 5.7%, Flavobacteriaceae: 1.6%, DQ413083_f: 1.1%, Alcaligenaceae:1%, Neisseriaceae: 1.1%, Peptostreptococcaceae: 6.4%, Leptotrichiaceae: 2.4%, Streptococcaceae: 4.9%, Aerococcaceae: 1.2%, Lactobacillaceae: 3.9%, Lachnospiraceae: 1.6%, Veillonellaceae: 3.5%, Total Average Count < 1%: 8.5%

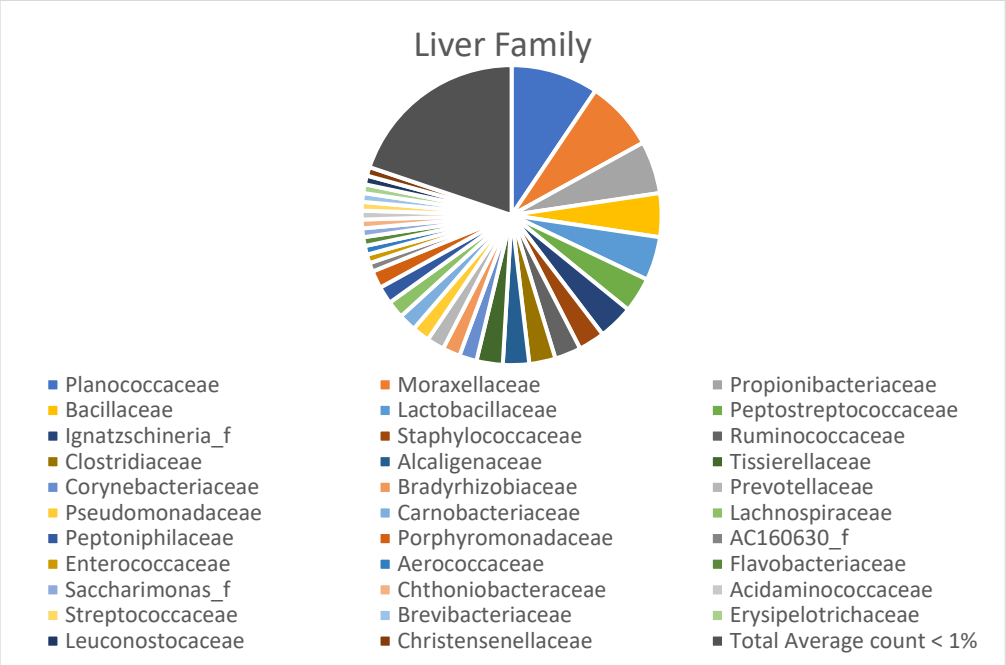

Figure 5.13 A pie chart showing the average proportion of family subdivision in the bacterial taxon found in the liver of pigs. The families are: Planococcaceae: 10.1%, Moraxellaceae:8.3%, Propionibacteriaceae:6.5%, Bacillaceae: 5.3%, Lactobacillaceae: 5.3%, Peptostreptococcaceae:4.5%, Ignatzschineria_f: 3.5%, Staphylococcaceae: 3.5%, Ruminococcaceae: 3.2%, Clostridiaceae: 3.2%, Alcaligenaceae: 3.0% Tissierellaceae: 2.8% Corynebacteriaceae: 2.3% Bradyrhizobiaceae: 2.2%, Prevotellaceae: 2.1%, Pseudomonadaceae: 1.8%, Carnobacteriaceae: 1.8%, Lachnospiraceae: 1.6%, Peptoniphilaceae: 1.6%, Porphyromonadaceae: 1.6%, AC160630_f: 1.3%, Enterococcaceae: 1.3%, Aerococcaceae: 1.3%, Flavobacteriaceae: 1.0%, Total Average count < 1%: 21%

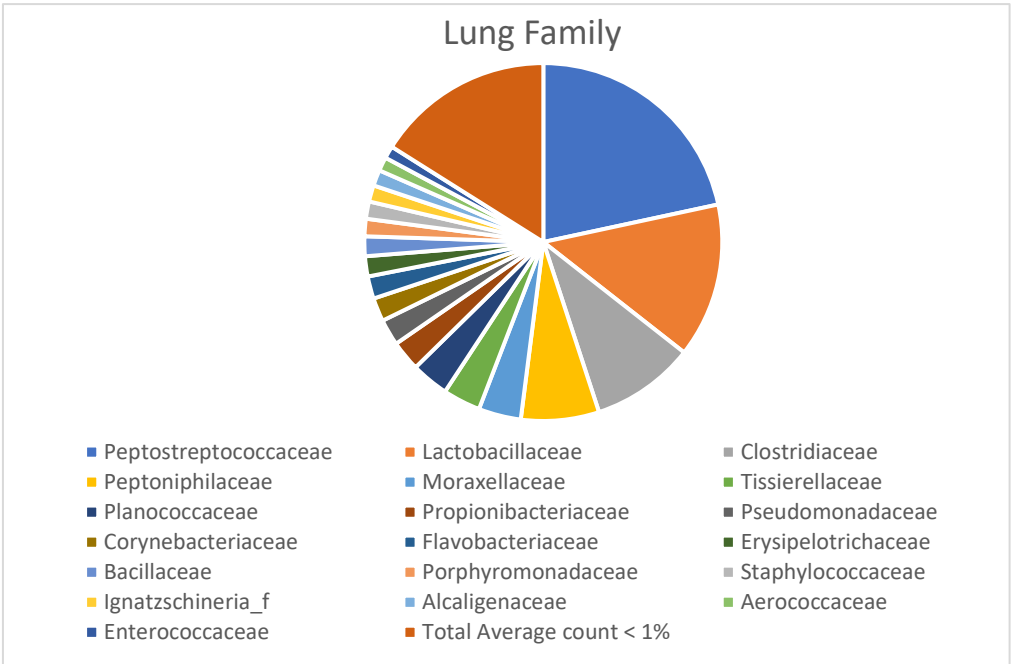

Figure 5.14 A pie chart showing the average proportion of family subdivision in the bacterial taxon found in the lung of pigs. The families are: Peptostreptococcaceae: 21.6%, Lactobacillaceae: 14.0%, Clostridiaceae: 9.4%, Peptoniphilaceae: 7.1%, Moraxellaceae: 3.8%, Tissierellaceae: 3.4%, Planococcaceae: 3.4%, Propionibacteriaceae: 2.7%, Pseudomonadaceae: 2.4%, Corynebacteriaceae: 2.1%, Erysipelotrichaceae: 1.8%, Bacillaceae: 1.8%, Porphyromonadaceae: 1.6%, Staphylococcaceae: 1.6%, Ignatzschineria_f: 1.5%, Alcaligenaceae: 1.4%, Aerococcaceae: 1.2%, Enterococcaceae: 1.1%, Total Average count < 1%: 16.1%

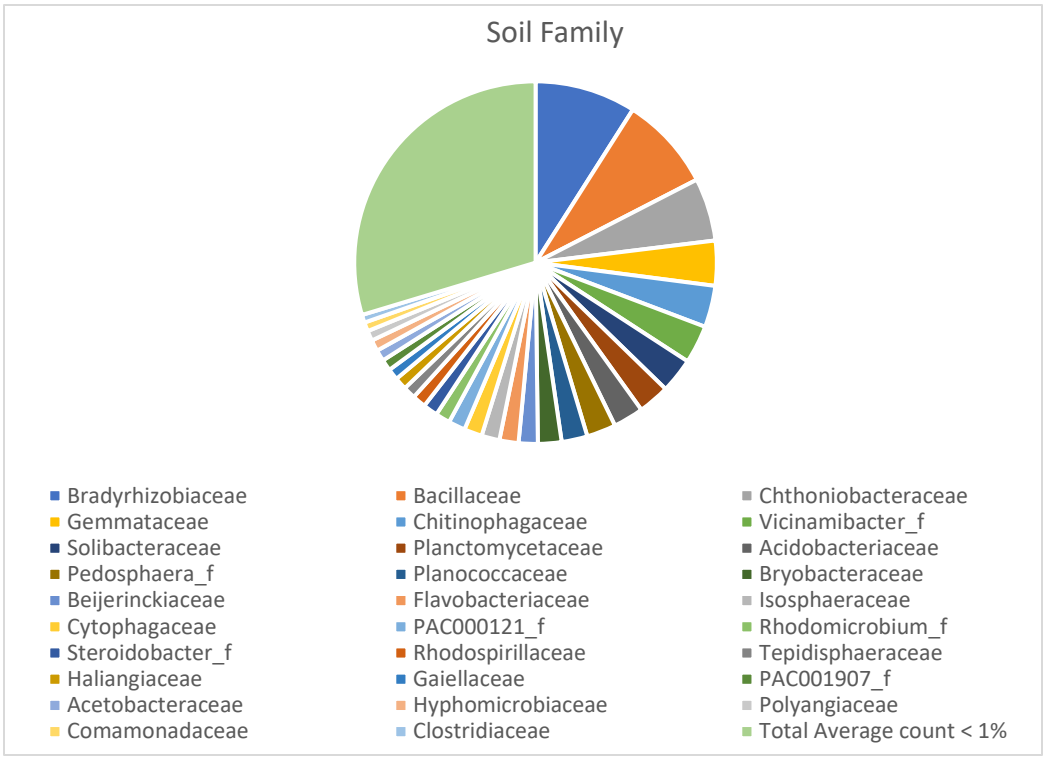

Figure 5.15 A Pie chart of average family subdivision ratios in bacterial taxa from soil sample. The families are: Bradyrhizobiaceae:9.0%, Bacillaceae: 8.4%, Chthoniobacteraceae 5.6%, Gemmataceae: 4.0%, Chitinophagaceae: 3.7%, Vicinamibacter_f: 3.4%, Solibacteraceae:3.1%, Planctomycetaceae:2.8%, Acidobacteriaceae: 2.7%, Pedosphaera_f: 2.6%, Planococcaceae: 2.3%, Bryobacteraceae: 2.1%, Beijerinckiaceae: 1.7%, Flavobacteriaceae: 1.7%, Isosphaeraceae: 1.6%, Cytophagaceae:1.6%, PAC000121_f:1.5%, Rhodomicrobium_f:1.3%, Steroidobacter_f 1.3%, Rhodospirillaceae 1.2%, Tepidisphaeraceae 1.1%, Haliangiaceae:1.1%, Gaiellaceae:1.0%, PAC001907_f:1.0%, Acetobacteraceae: 1.0%, Hyphomicrobiaceae: 1.0%, Polyangiaceae: 1.0%, Comamonadaceae: 1.0%, Clostridiaceae: 1.0%, Total Average count < 1%: 30%

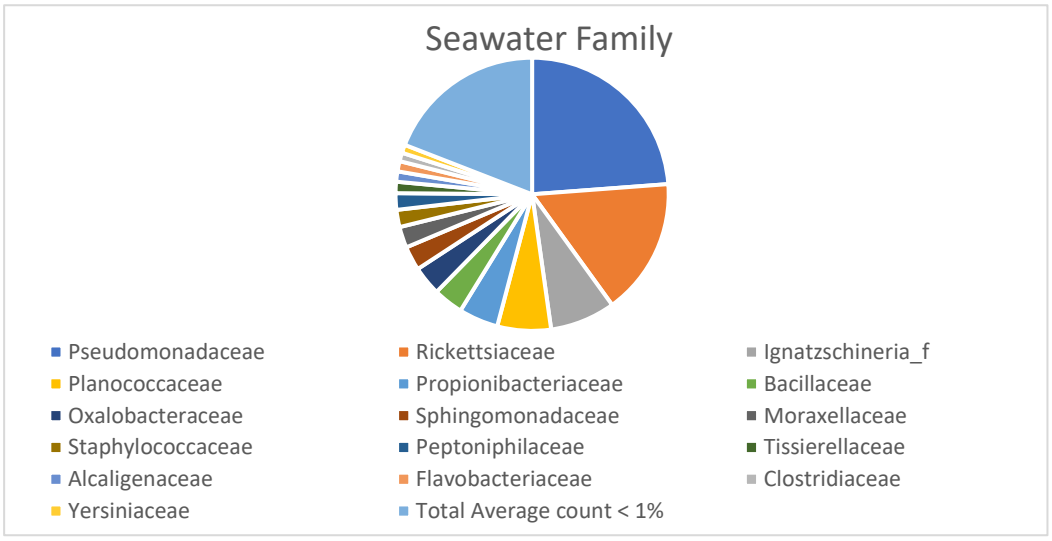

Figure 5.16 A pie chart showing the average proportion of family subdivision in the bacterial taxon found in the seawater sample. The families are: Pseudomonadaceae: 23.8%, Rickettsiaceae: 16.2%, Ignatzschineria_f: 7.7%, Planococcaceae: 6.3%, Propionibacteriaceae: 4.7%, Bacillaceae: 3.5%, Oxalobacteraceae: 3.5%, Sphingomonadaceae: 2.9%, Moraxellaceae: 2.5%, Staphylococcaceae: 2.0%, Peptoniphilaceae: 2.0%, Tissierellaceae: 1.3%, Alcaligenaceae: 1.2%, Flavobacteriaceae: 1.2%, Clostridiaceae: 1.0%, Yersiniaceae: 1.0%, Total Average count < 1%: 19.1%

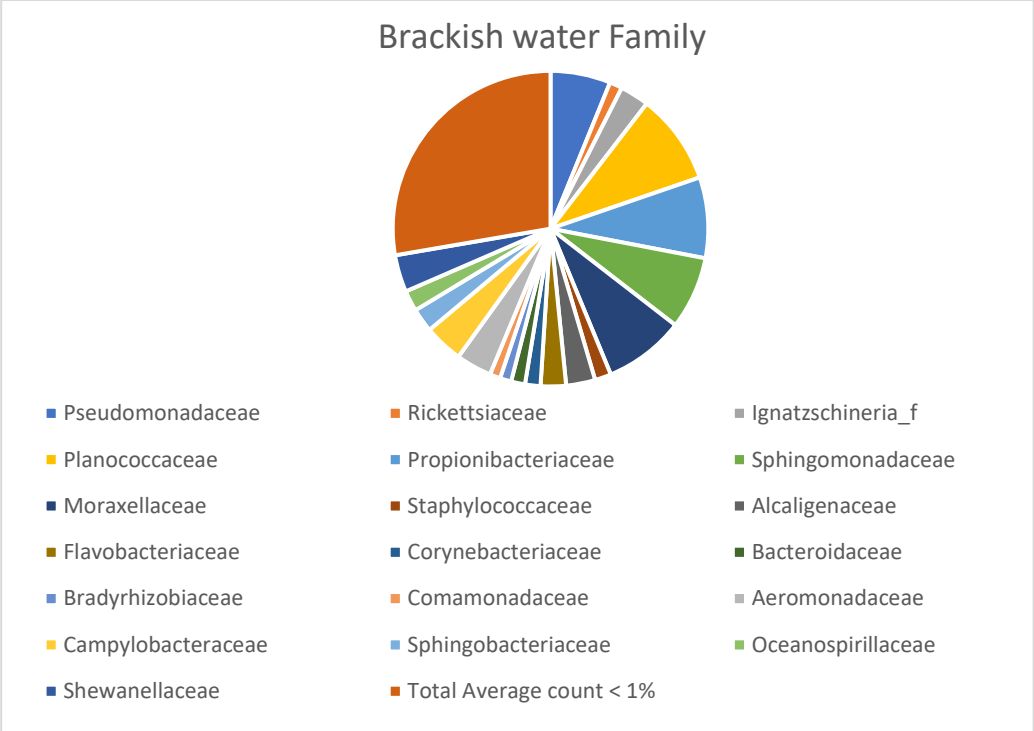

Figure 5.17 A pie chart showing the average proportion of family subdivision in the bacterial taxon found in the brackish water sample. The families are: Pseudomonadaceae: 6.2%, Rickettsiaceae: 1.3%, Ignatzschineria_f: 3.0%, Planococcaceae: 9.3%, Propionibacteriaceae: 8.3%, Sphingomonadaceae: 7.5%, Moraxellaceae: 8.3%, Staphylococcaceae: 1.7%, Alcaligenaceae: 3.0%, Flavobacteriaceae: 2.6%, Corynebacteriaceae: 1.6%, Bacteroidaceae: 1.4%, Bradyrhizobiaceae: 1.2%, Comamonadaceae: 1.1%, Aeromonadaceae: 3.7%, Campylobacteraceae: 4.0%, Sphingobacteriaceae: 2.4%, Shewanellaceae: 3.8%, Total Average count < 1%: 27.7%

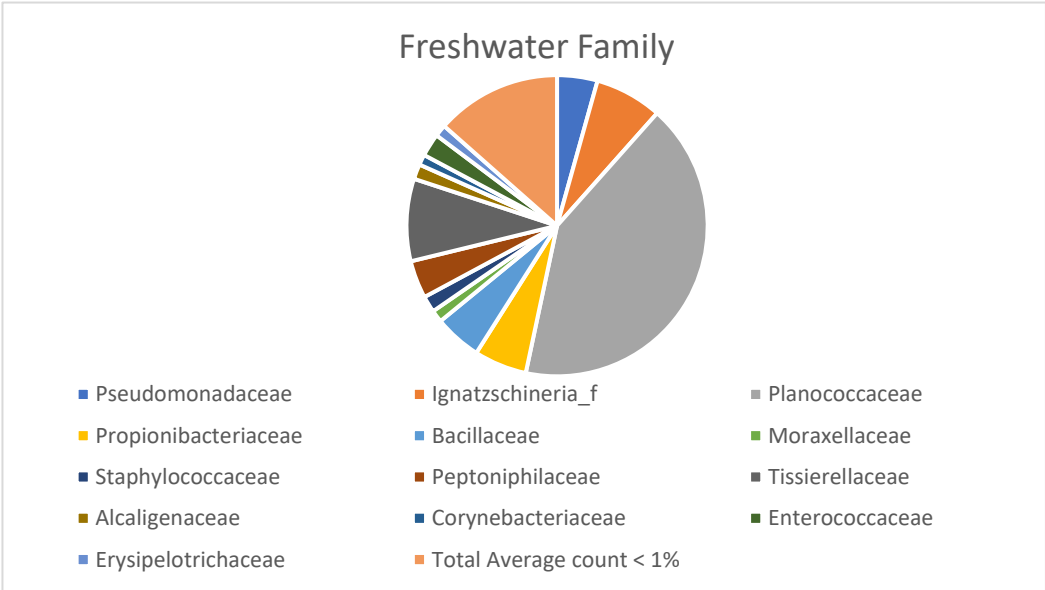

Figure 5.18 A pie chart showing the average proportion of family subdivision in the bacterial taxon found in the Freshwater sample. The families are: Pseudomonadaceae:4.3%, Ignatzschineria_f: 7.2%, Planococcaceae: 41.8%, Propionibacteriaceae: 5.7%, Bacillaceae: 5.1%, Sphingomonadaceae 0.6%, Moraxellaceae: 1.3%, Staphylococcaceae: 1.8%, Peptoniphilaceae: 4.1%, Tissierellaceae: 8.8%, Alcaligenaceae:1.6%, Corynebacteriaceae: 1.1%, Enterococcaceae: 2.5%, Campylobacteraceae, Erysipelotrichaceae: 1.3%, Total Average count < 1%: 13.5%

5.2.2.1 Bacterial families with Significant Differences

This section presents the distribution of bacterial families across various sample types with highlights to taxa that exhibited significant differences in abundance, as indicated by an ANOVA test results (summarised in Table 5.3).

Table 5.3 Showing summary of ANOVA test used to examine the variation in abundance of various families across different sample types. The significant values are highlighted. Bifidobacteriaceae, Lachnospiraceae, Aerococcaceae Flavobacteriaceae were significant in both sample types.

Families	**Pig**	**Sites**	**Environmental**	**Sites**
Lactobacillaceae	$F_{4,9}$=3.508, p=0.0545		$F_{3,5}$=5.911, p= 0.0424	Reduced in the soil compared to freshwater
Leuconostocaceae	$F_{4,9}$= 1.695, p=0.234		$F_{3,5}$=0.667, p= 0.607	
Enterococcaceae	$F_{4,9}$=5.108, p=0.0199	Reduced in the mouth compared to the belly and lungs;	$F_{3,5}$=1.966, p= 0.238	
Carnobacteriaceae	$F_{4,9}$=12.74, p=0.000948	Increased in the belly compared to the anus; Reduced in the mouth and internal organs compared to the belly	$F_{3,5}$=1.054, p= 0.446	
Aerococcaceae	$F_{4,9}$=1.112, p=0.00315	Increased in the belly compared to the anus; Reduced in the mouth and internal organs compared to the belly	$F_{3,5}$= 5.777, p= 0.0443	Reduced in the soil compared to brackish water
Streptococcaceae	$F_{4,9}$=2.527, p=0.114		$F_{3,5}$=6.609, p= 0.0343	Reduced in the soil compared to brackish water
Corynebacteriaceae	$F_{4,9}$=5.574, p= 0.0154	Increased in the belly compared to the anus; Reduced in the mouth and internal organs compared to the belly	$F_{3,5}$=2.873, p= 0.143	
Moraxellaceae	$F_{4,9}$= 7.375 p= 0.00642	Increased in the mouth compared to the anus and internal organs	$F_{3,5}$=1.809, p= 0.262	
Clostridiaceae	$F_{4,9}$=1.996 p= 0.179		$F_{3,5}$=1.635, p= 0.294	
Ruminococcaceae	$F_{4,9}$= 18.48, p=0.000229	Reduced in the belly, mouth and internal organs compared to the anus	$F_{3,5}$=16.17, p= 0.00525	Reduced in the seawater compared to brackish water; Reduced in the soil compared to freshwater
Lachnospiraceae	$F_{4,9}$=6.924, p=0.00788	Reduced in the belly, mouth and internal organs	$F_{3,5}$=9.624, p= 0.0161	Reduced in the freshwater compared to brackish water

		compared to the anus		
Flavobacteriaceae	$F_{4,9}$=1.167, p=0.387		$F_{3,5}$=1.147, p= 0.416	
Pseudomonadaceae	$F_{4,9}$=2.654 p=0.103		$F_{3,5}$=2.532, p= 0.171	
Porphyromonadaceae	$F_{4,9}$=4.741, p=0.0247	Increased in the mouth compared to the internal organs	$F_{3,5}$=2.07, p= 0.223	
Micrococcaceae	$F_{4,9}$=5.378, p= 0.0172	Increased in the belly compared to the anus; Reduced in the mouth and liver compared to the belly	$F_{3,5}$=1.579, p= 0.305	
Peptoniphilaceae	$F_{4,9}$=1.084, p=0.42		$F_{3,5}$=1.587, p= 0.304	
Planococcaceae	$F_{4,9}$=1.532 p=0.273		$F_{3,5}$=1.536, p= 0.314	
Bifidobacteriaceae	$F_{4,9}$=5.45, p= 0.0165	Reduced in the internal organs compared to the belly	$F_{3,5}$=8.679, p= 0.02	Reduced in the sea and soil compared to brackish water
Tissierellaceae	$F_{4,9}$=4.24, p= 0.0335	Reduced in the mouth compared to the lungs	$F_{3,5}$=1.548, p= 0.312	
Peptostreptococcaceae	$F_{4,9}$= 0.733, p= 0.592		$F_{3,5}$=0.322, p= 0.81	
Propionibacteriaceae	$F_{4,9}$=3.146, p=0.0707		$F_{3,5}$=1.254, p= 0.384	
Prevotellaceae	$F_{4,9}$= 4.638, p= 0.0262	No significant pair found	$F_{3,5}$=0.999, p= 0.465	
Bacteroidaceae	$F_{4,9}$= 1.323, p=0.333		$F_{3,5}$=2.218, p= 0.204	
Ignatzschineria_f	$F_{4,9}$= 3.35, p=0.061		$F_{3,5}$=2.287, p= 0.196	
Comamonadaceae	$F_{4,9}$=0.647 p=0.643		$F_{3,5}$=2.216, p= 0.204	
Campylobacteraceae	$F_{4,9}$= 2.499, p=0.117		$F_{3,5}$=1.48, p= 0.327	
Sphingomonadaceae	$F_{4,9}$=1.599 p= 0.256		$F_{3,5}$=3.521, p= 0.105	
AC160630_f	$F_{4,9}$= p= 0.000326	Reduced in the belly, mouth and internal organs compared to the anus	not found at all	
Selenomonadaceae	$F_{4,9}$=1.975 p= 0.182		$F_{3,5}$= 1.785, p=0.266	
Mogibacterium_f	$F_{4,9}$=1.939 p= 0.188		$F_{3,5}$=2.347, p= 0.19	
Saccharimonas_f	$F_{4,9}$=2.04, p=0.172		$F_{3,5}$=0.958, p= 0.48	
Alcaligenaceae	$F_{4,9}$=1.033 p=0.441		$F_{3,5}$=16.14, p= 0.00527	Reduced in the soil compared to aquatic samples
Bradyrhizobiaceae	$F_{4,9}$=2.301 p=0.138		$F_{3,5}$=975.9, p= 0.00000024	Increased in the soil compared to aquatic samples
Enterobacteriaceae	$F_{4,9}$=2.301 p=0.138		$F_{3,5}$=1.45, p= 0.334	
Erysipelotrichaceae	$F_{4,9}$=1.621 p=0.251		$F_{3,5}$=1.351, p= 0.358	
Staphylococcaceae	$F_{4,9}$= 2.061 p=0.169		$F_{3,5}$=1.176, p= 0.407	
Chthoniobacteraceae	$F_{4,9}$=2.163 p=0.155		$F_{3,5}$= 56.08, p= 0.000285	Increased in the soil compared to aquatic samples

Bacillaceae	$F_{4,9}$=2.456 p=0.121		$F_{3,5}$=7.66, p= 0.0257	Reduced in the soil compared to brackish water

Significant differences in family distribution are shown in table 5.3. Enterococcaceae showed a negative significant difference observed across pig sample types, with mouth and belly, lung and anus being the closest to significance. Enterococcaceae are facultative anaerobes, and their abundance might still be influenced by variations in oxygen levels across different anatomical sites. Carnobacteriaceae, Corynebacteriaceae and Aerococcaceae been had significantly positive presence in the belly against the anus and significantly negative population against the mouth and internal organs. Carnobacteriaceae, Corynebacteriaceae and Aerococcaceae in are part of the LAB and can ferment cellulose, their presence in the anus (the orifice of the gastrointestinal tract) may indicate their specific roles associated with fermenting undigested cellulose found in faecal matter. Moraxellaceae possessed a positively significant occupancy in the mouth compared to the internal organs and anus samples. Members of the Moraxellaceae are known to colonise mucus membrane (Teixeira and Merquior, 2014) and have been found among bacteria to dominate the salivary microbiome (Hattab *et al*., 2021) and oral cavities (Crielaard *et al*., 2011). The abundance of Lachnospiraceae was negatively significantly in the anus compared to other pig samples. Lachnospiraceae thrive in environments with low oxygen levels. The location of the anus makes it exposed to oxygen and it may not be conducive for the growth of certain anaerobic bacteria, leading to lower abundance of Lachnospiraceae.

Porphyromonadaceae was significantly more abundant in the mouth compared to the internal organs, its members are strictly anaerobic have been noticed to reside in the oral cavity (Morrison *et al*., 2023 Berman, 2019). Micrococcaceae was significantly more abundant in the Belly when compared to the anus, liver, and mouth. Micrococcaceae members mostly prefers oxygen-rich environments and that is why they may be more abundant on the belly sample (Skin swab). The internal organs and mouth against the anus had a negative significant abundance of AC160630_f. Tissierellaceae occupied a negative significant presence in the mouth compared to the lung samples set. This is an indication of Tissierellaceae's aerotolerant ability since the lungs is an environment with higher oxygen levels. Bifidobacteriaceae had negative relationships in the pig (Belly against internal organs) and environmental sample (freshwater against seawater and soil). Bifidobacteriaceae can survive in conditions with lower pH levels (Wang *et al*., 2022), If the pH is different in the various environment, it could affect the abundance of Bifidobacteriaceae. Prevotellaceae Ignatzschineria_f had significant p values, but the Tukey HSD test results had no statistically significant values less than 0.05.

Negative significant differences in Lactobacillaceae were also detected in the environmental samples with significantly negative abundance in the soil compared to freshwater. Ruminococcaceae were also found to be negatively significant among pig sample types, with the mouth and internal organs being the most significant compared to the anus, this might be an indication of the metabolic activities of Ruminococcaceae as discussed initially. The environmental samples also had the presence of Ruminococcaceae with negative significant in seawater sample compared to brackish water, and positive difference in the soil sample compared to the freshwater. Compared to other environmental samples, the soil microbiome furthermore hosted significant negative abundance of Aerococcaceae, Streptococcaceae, Bifidobacteriaceae, Alcaligenaceae, which are usually associated with tissues and body sites and a positive abundance of Bradyrhizobiaceae, Chthoniobacteraceae, and Bacillaceae which are linked to contribute to soil microbial ecological process as previously mentioned. Different bacteria families such as Candidate Bacteria that show their ubiquitous nature were noticed on day 0 although they were not found among dominate taxa. Other bacteria family that can be categorised into other groups such as, the LAB, fermentative bacteria, nitrogen-fixing bacteria, cellulose-degrading bacteria, sulfate-reducing bacteria.

5.3 CONCLUSION

The results for Day 0 (the fresh stage) revealed the community of resident bacteria in the various samples at both phyla and family levels. Bacterial taxa responsible for the evenness, richness, and phylogenetic diversity of phyla and families within each community were presented in this chapter. For instance, Bacteroidetes, Actinobacteria, Cyanobacteria, and Peregrinibacteria exhibited significant variations in abundance across pig sample sites, directly influencing the microbial richness and phylogenetic diversity within these environments. In the environmental samples, Chlamydiae, Planctomycetes, Chloroflexi, Acidobacteria, and Tenericutes were particularly abundant in soil, contributing to its higher biodiversity compared to the aquatic samples. All three aquatic environments harbour sets of microbial communities that were significantly different from terrestrial environments. Family-level microbial analysis provided a more detailed understanding of the environment than phylum-level observations alone. The variation in bacterial phyla and families found on Day 0 could serve as a reference point for forensic experts to link specific bacterial taxa to anatomical sites or environmental conditions based on the microbial signature.

Carnobacteriaceae, Corynebacteriaceae, and Aerococcaceae, which are from the phylum Firmicutes and are part of the lactic acid bacteria (LAB) group, were detected on Day 0 and have the potential to reveal intricate details about microbial activity related to changes in nutrient availability, which could be valuable in forensic investigations. The distribution of Bifidobacteriaceae (phylum: Actinobacteria) across the

diverse sites might be influenced by the pH levels of the samples and could indicate environments with specific pH conditions. Micrococcaceae, another family within Actinobacteria, prefers oxygen-rich environments; their distribution on the belly (a skin swab site) suggests a correlation between environmental oxygen levels and microbial abundance, which could be instrumental in determining the environmental conditions of the skin or external body sites during decomposition. The distribution of Porphyromonadaceae (Bacteroidetes) could serve as an indicator of the anaerobic conditions prevalent in specific body sites, contributing to the understanding of microbial succession during decomposition.

Early decay is a period of decomposition where microbial succession is relatively quick, making this the time to produce the most reliable estimations of PMI (Tozzo *et al.*, 2022). A significant amount of data gathered from repeated samples taken over time would be utilised (Tozzo *et al.*, 2022) and explored in Chapters 6 and 7 by leveraging these microbial signatures from Day 0 that may change over time. Forensic scientists can utilise the data from these microbial indicators to improve the accuracy of investigations, leading to more reliable and insightful forensic conclusions.

6.0 CHAPTER SIX: MICROBIAL COMPOSITION IN PIG SAMPLES OVER TIME

6.1 INTRODUCTION

This chapter highlights the succession patterns from day 0 to the final sampling day of the pig samples (external body parts and internal organs). A large, sophisticated ecosystem from physical and biological changes exhibited throughout the decomposition process could give important details regarding the time since death (Roy *et al*., 2021). Therefore, it would be of interest in establishing the connections between the carcass microbiome, and its succession patterns, as potential markers which will fill the gap in bio forensic and medicolegal applications. The use of microorganisms as physical evidence for forensic science is promising due to their ubiquity and constructible ecologies (Roy *et al*., 2021). The aim below is targeted to address the bacterial succession patterns and ecological roles of the pig carcass used in this study as potential markers for post-mortem intervals (PMI).

To achieve this, multivariate dispersion analysis was employed investigate potential differences in the bacterial taxa, which reflect the structural fluctuation of these bacterial communities throughout the days of decomposition. Specifically, the *betadisper* function of the R package VEGAN was employed to compute multivariate dispersion, ANOVA, and Tukey's post-hoc test was also conducted to assess differences in multivariate dispersion among groups which are the days of decomposition. Based on the relative abundance, regression was also performed to evaluate the relationships between the most abundant phyla and families across the days of decomposition.

6.2 RESULTS AND DISCUSSION

6.2.1 Phylum

Based on the relative abundance, below are the phylum taxa for each pig sample (belly, anus, mouth, liver and lung), and the selected phyla to be tested for statically significant relationship across the observed time point in the respective samples. All phyla represented on the graph existed in the respectively community in 1% and above while the ones below 1% were grouped together.

6.2.1.1 Belly

On Day 0 of the decomposition process, Firmicutes was the most dominant phylum in the belly microbiome (58%). By Day 2, Firmicutes increased in dominance to 71% and further rose to 78% on Day 4, maintaining its dominant status. However, Day 7 noted the substantial drop in the relative abundance of Firmicutes (34%) and it further declined to 30% by Day 23. Actinobacteria was the second most dominant phylum on Day 0, accounting for 21% of the community. However, its proportion dropped drastically to 2% on Day 2. Actinobacteria continued to struggle and remained at a low level throughout the decomposition process, with only 3% of the community on Day 23. Proteobacteria, which initially occupied 17% of the microbiome on Day 0, maintained its proportion on Day 2 (17%). Remarkably, by Day 4, Proteobacteria severely increased to 78%, becoming the most dominant phylum at that stage. Although their dominance decreased on Day 7 (61%), Proteobacteria remained the most abundant phylum. By Day 23, their proportion had reduced further to 34%, sharing dominance with Bacteroidetes. Bacteroidetes, initially comprising 7% of the community on Day 0, showed a gradual increase in relative abundance as decomposition progressed. On Day 2, Bacteroidetes became the third most abundant phylum (11%), decreased slightly on Day 4 (7%), but regained its size to 11% by Day 7. By Day 23, Bacteroidetes had increased further to 34%, sharing the position of the most dominant phylum with Proteobacteria. Saccharibacteria_TM7 was present in 1% of the community on Day 0, and other bacterial phyla lower than 1% were observed but did not collectively exceed 1% of the belly community. As shown in Table 6.1, the dispersion analysis over time indicated no significant relationship in the belly community. However, the regression analysis revealed statistically significant trends for specific bacterial phyla across the days of decomposition. Bacteroidetes exhibited a significant positive trend, while Actinobacteria showed a significant negative trend, likely due to its higher initial proportion on Day 0. In contrast, the trends observed for Firmicutes and Proteobacteria were not statistically significant.

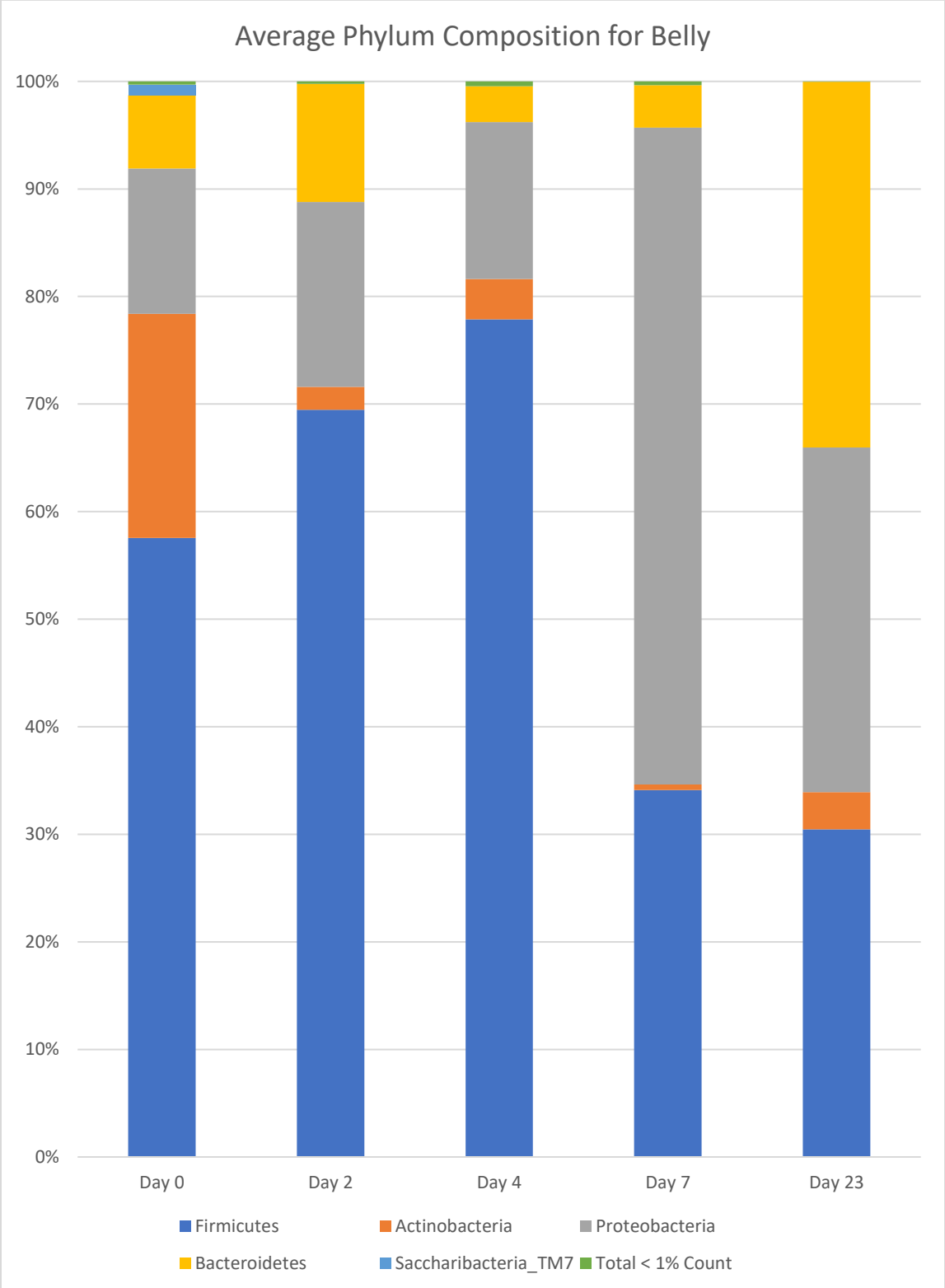

Figure 6.1 Displaying the average phylum composition for the belly sample in respect to the decomposition days.

6.2.1.2 Anus

Several bacterial phyla including Firmicutes, Bacteroidetes, Proteobacteria, Actinobacteria, Verrucomicrobia competed for phylum succession in the anus community. Firmicutes started on day 0 as the dominant phylum with 40% community occupancy. On day 2, they continued to prevail, reaching 49% occupancy, maintaining dominance. Firmicutes on day 4, remained relatively stable, increasing by 2% from the previous sampling day. The dominance of Firmicutes declined on day 23, but still played a significant role in the community. Bacteroidetes on day 0 comprised 31% of the community, making them the second most abundant phylum in the anus community. They experienced a decrease to 23% on day 2 and recovered slightly on day 4, reaching 25%. On Day 23, Bacteroidetes experienced a significant drop, making up only 13% of the anus community. Proteobacteria accounted for 11% of the community on day 0, maintained the same proportion (11%) on day 2, and experienced no notable change on day 4. A late-stage surge was noticed on day 23, Proteobacteria's relative abundance greatly increased on day 23, making up 46% of the community. Actinobacteria had a minor presence (2%) in the community on day 0 and saw a relative increase to 9% on day 2. On day 4, they decreased in ratio and on day 23, they constituted 1% of the community. As displayed in Table 6.1, the Regression and multivariate dispersion analysis over time revealed no significant relationship shown in this community. Additionally, the results of the regression analysis for the bacterial phyla Bacteroidetes, Proteobacteria, and Firmicutes in the anus samples across the days of decomposition were not statistically significant.

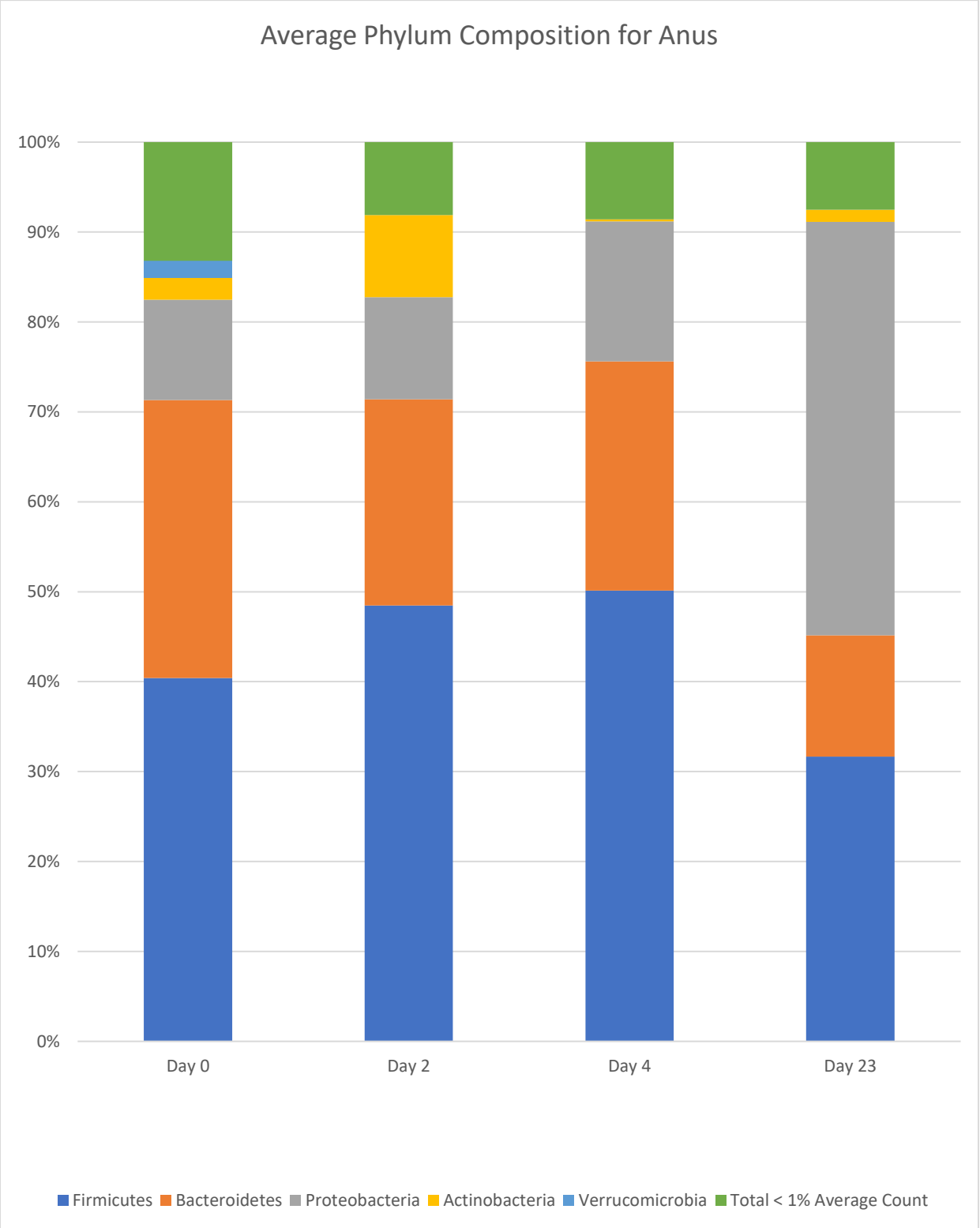

Figure 6.2 Displaying the average phylum composition for the Anus sample in respect to the decomposition days.

6.2.1.3 Mouth

In the oral microbial community, Bacteroidetes initially constituted a major portion, representing 35% of the total bacterial population on Day 0, making it the dominant phylum. By Day 2, the relative abundance of Bacteroidetes increased to 42%, maintaining their dominance. Although a slight decline to 39% was observed on Day 4, Bacteroidetes continued to be a major component of the community. However, by Day 7, their abundance dramatically decreased (7%). Despite this decline, Bacteroidetes regained by Day 23, comprising 27% of the community, thus remaining a prominent phylum as depicted in Figure 6.3. Proteobacteria initially accounted for 27% of the microbial community on Day 0. By Day 2, they surged to 43%, becoming the most dominant phylum at that stage. A marked reduction in their relative abundance was noted on Day 4 (24%) and Day 7 (12%). However, by Day 23, Proteobacteria showed a resurgence, increasing to 34% of the community, indicating a dynamic shift in the microbial succession. Firmicutes were also prominent on Day 0, comprising 26% of the microbial population. A significant decline was observed on Day 2, with their relative abundance dropping to 12%. However, by Day 4, Firmicutes exhibited a resurgence, rising to 27%, and further to an overwhelming 81% on Day 7, making them the dominant phylum at that point. By Day 23, their abundance decreased to 21%. Fusobacteria inhibited 8% on Day 0 but declined greatly to 1% by Day 2, subsequently becoming part of the <1% category in the following days of decomposition. Other phyla such as Actinobacteria, Peregrinibacteria, Saccharibacteria_TM7, and SR1, which initially represented about 1% of the community, were not detected as decomposition progressed. As seen in Table 6.1, the dispersion analysis over time revealed no significant relationship shown in the mouth community. Furthermore, the results of the regression analysis for Proteobacteria, Bacteroidetes, Fusobacteria, Actinobacteria across the days of decomposition were non-significant statistically. However, Firmicutes were highly statistically significant with the coefficients on day 7 showing a positive indication.

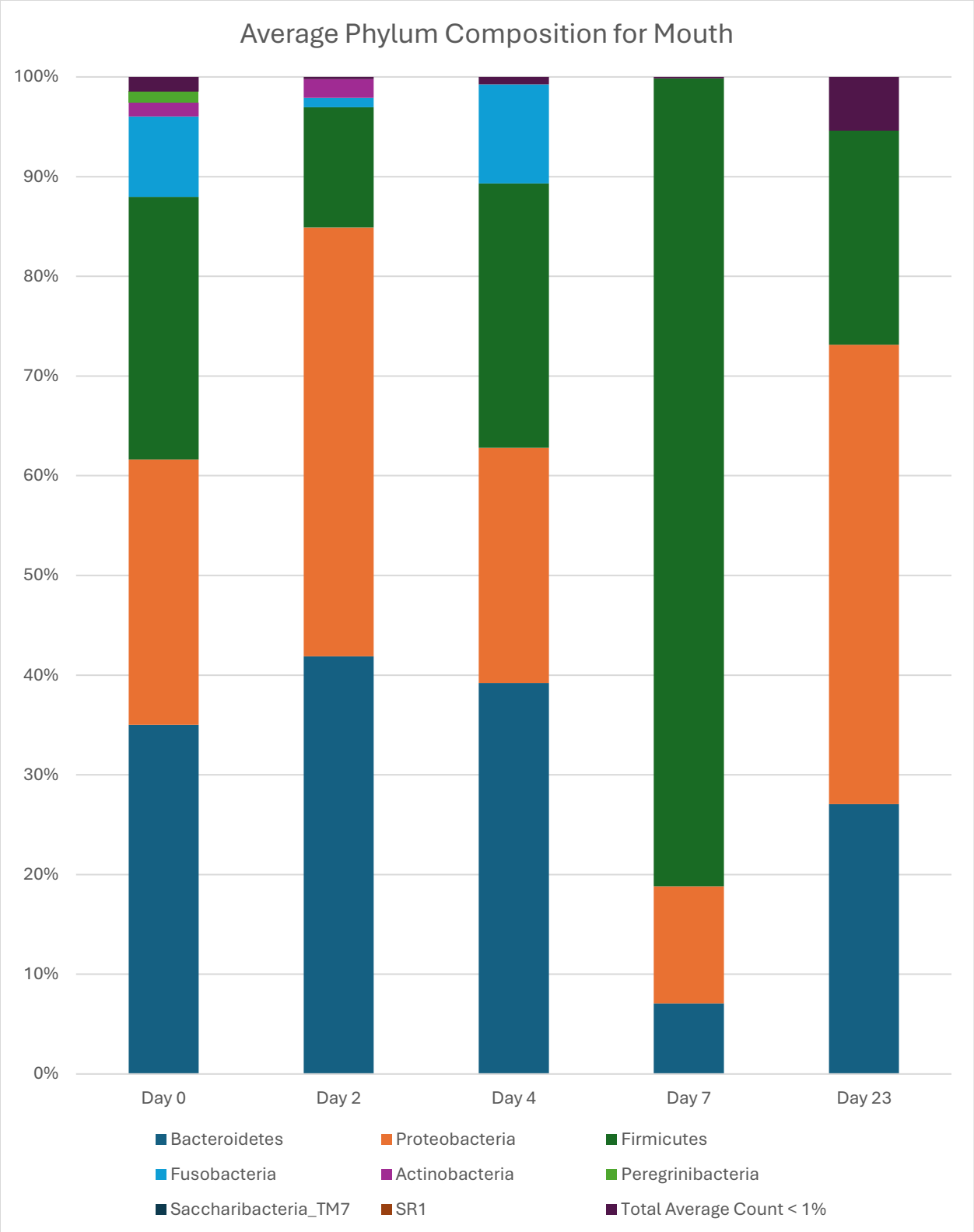

Figure 6.3 Displaying the average phylum composition for the Mouth sample in respect to the decomposition days.

6.2.1.4 Liver

Firmicutes on day 0 was the most dominant phyla, occupying 50% of the community's microbial population. On day 2, they Increased significantly to 95%, showing a substantial rise in dominance. On day 4, Firmicutes tremendously claimed 99% occupancy. Proteobacteria on day 0 was the second highest dominant phyla on day 0 with 28% community occupancy. Proteobacteria Remains present but decreases to 3% and 1% of the community's space on day 2 and 4 respectively. Acidobacteria, Verrucomicrobia, Saccharibacteria_TM7, Chloroflexi, and Planctomycetes inhabited 1% of the community's space on day 0 while Actinobacteria (13%) and Bacteroidetes (7%) were also noticed on same day. On day 2, there were reduction of Actinobacteria and Bacteroidetes to 1%. The Regression and multivariate dispersion analysis over time revealed no significant relationship shown in the liver community. As revealed in Table 6.1, The results of the regression analysis showed Proteobacteria, Bacteroidetes, Actinobacteria across the days of decomposition were non-significant statistically. However, Firmicutes were highly and positively statistically significant and the coefficients of Tukey post-hoc test suggest day 2 and 4 made the increment.

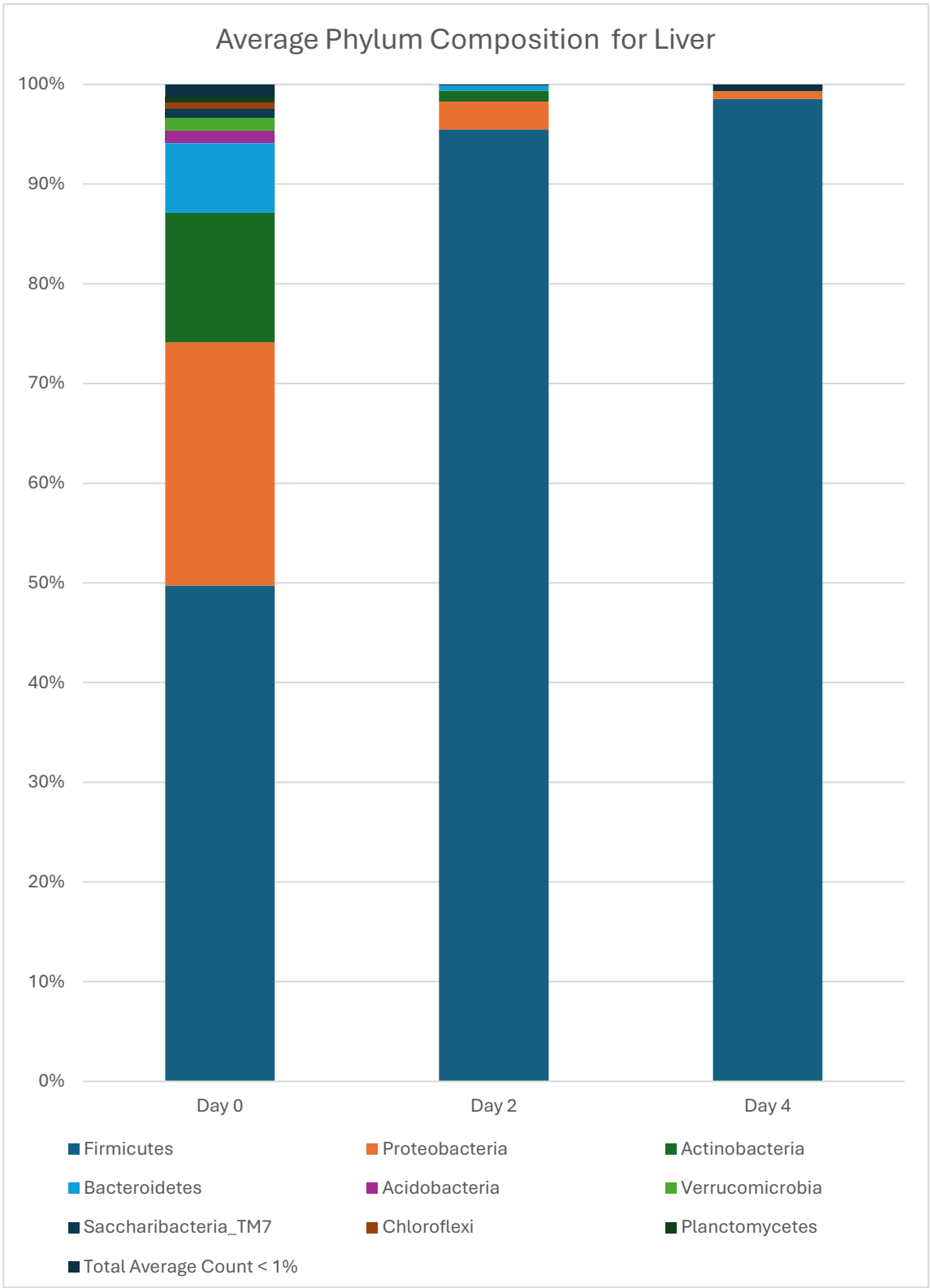

Figure 6.4 Displaying the average phylum composition for the Liver sample in respect to the decomposition days.

6.2.1.5 Lung

Firmicutes on day 0 and 2 emerged the highest dominator of the community, respectively inhibiting 71% and 85% of the bacterial population. On day 4 Firmicutes increased greatly and occupied 97% of the microbial community. Proteobacteria was noticed the second highest ratio with 13% on day 0 and declined to 12% on day 2 and made up 1.6% of the phylum presence in the lungs on day 4. Actinobacteria was third on the domination spot with 8% occupancy followed by Bacteroidetes (6%) and Acidobacteria (1%). Actinobacteria and Bacteroidetes declined to 1% in proportion on day and joined the group that were <1% on day 4. As presented in Table 6.1, the Regression and multivariate dispersion analysis over time revealed no significant relationship shown in the lung community. Additionally, the results of the regression analysis for the bacterial phyla Proteobacteria across the days of decomposition were non-significant statistically. However, Bacteroidetes and Actinobacteria were statistically significant showing a decrease in relative abundance on day 2 and 4 (Table 6.1).

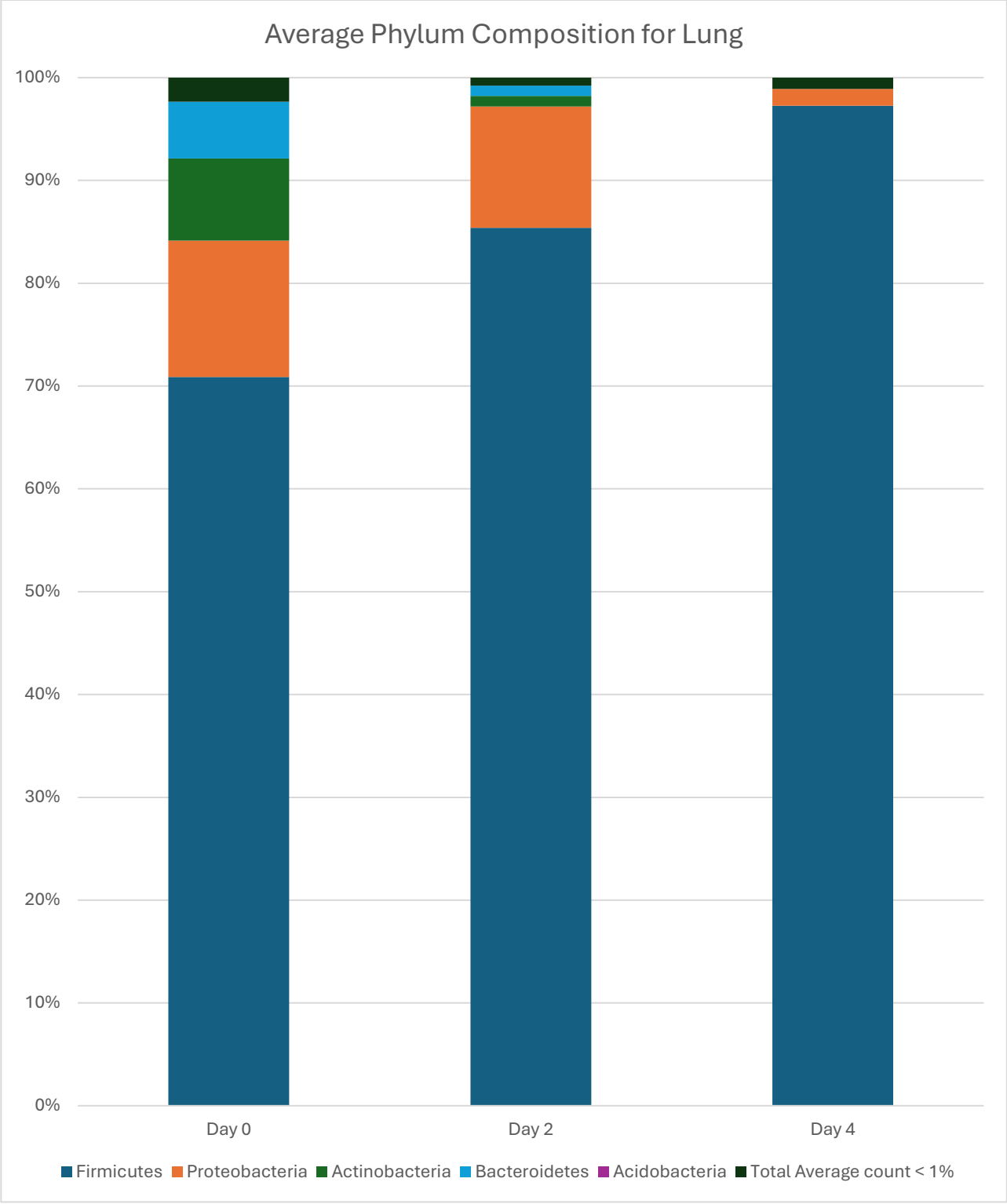

Figure 6.5 Displaying the average phylum composition for the Lung sample in respect to the decomposition days.

6.2.1.6 *Phyla with significant changes over time*

The bacterial community in the belly samples exhibited dynamic changes over time, with Bacteroidetes significantly increasing in number, while Actinobacteria struggled to maintain prominence in the belly microbial community and experienced a significant decline across the observed period of decomposition. On day 23, the pig reached its skeletonization stage, and Bacteroidetes' metabolic properties might be responsible for its significance. Studies have previously suggested that members of the Bacteroidetes (Bacteroides genus) are involved in bone metabolism (Yan, Cai and Guo, 2022; Ozaki *et al.*, 2020). Actinobacteria in the belly sample were more prominent on day 0, probably utilising resources available during the fresh stage of decomposition. As decomposition advanced, the fluctuating decline of Actinobacteria (figure 6.1) might have been prompted by factors such as changes in nutrient availability or competition with other microbial groups. In the mouth microbial community, Firmicutes became a dominant phylum during the putrefaction/active decay stages, particularly on day 7. Firmicutes again had a highly statistically significant relationship with the sampling days in the liver sample, which is reflected in their steady increase as decomposition progressed. Firmicutes, in other research on pig carcasses, have equally experienced a shift that led to a dominating presence in the later stage of decomposition (day 5) (Pechal *et al.*, 2013). The significant impact of Firmicutes during the bloat and putrefaction/active decay stages may be facilitated by their fermentative metabolic strategy. They include members responsible for gas production (H_2 and CO_2) (Mutuyemungu *et al.*, 2023), which contributes to the bloat stage of carcasses. Based on the increased nutrients (organic compounds) present as the pig carcass undergoes rapid decomposition, bacteria in the Firmicutes phylum may thrive by utilising available substrates after the bloat stage, leading to active decay through fermentative processes and contributing to their increased abundance.

Bacteroidetes and Actinobacteria in the lung sample exhibited a significant relationship as they consistently decreased over the observed period. These bacterial phyla may have declined due to the continuous dominance of Firmicutes (figure 6.5). The lung community saw Bacteroidetes succeed Firmicutes throughout decomposition, probably because Bacteroidetes are also known to produce gas (H_2 and CO_2) (Mutuyemungu *et al.*, 2023), which can enhance the bloat stage. The effect of these gases can serve as an avenue to enhance the growth of Firmicutes, with a preference for Bacteroidetes' metabolic activities. There is a possibility that Bacteroidetes and Actinobacteria responded to changes in nutrient availability in the lung sample during the observed period. In the anus sample, the taxa statistically tested did not establish any statistically significant relationships over time. The non-significant statistical relationships of any phylum in the sample in correlation with the time of decomposition may imply that

they respond to factors influencing the bacterial ecosystem without necessarily showing a consistent directional trend over time. These trends (whether consistent or not) provide insights into the complex microbial interactions during the decomposition process. Bacteroidetes and Actinobacteria are prospective contributors to nutrient cycling processes, and their ecological role may be important in providing and maintaining nutrients for other bacteria in the ecosystem.

Table 6.1 Summary of betadisper Multiple dispersion and Individual ANOVA analysis of bacterial phylum over time on pig sample (Belly, Anus, Mouth, liver, and Lung). Significant values are highlighted.

Sample	**Multiple Dispersion Analysis Over Time**	**Phylum**	**Individual ANOVA Results**	**Significant Day**
Belly	$F_{4,9}$=1.6186, p= 0.2516	Firmicutes	$F_{4,9}$= 3.051, p= 0.07593	
		Proteobacteria	$F_{4,9}$= 1.297, p= 0.3412	
		Actinobacteria	$F_{4,9}$= 5.233, p= 0.01859	Decrease on Day 2, 4, and 7
		Bacteroidetes	$F_{4,9}$= 4.499, p= 0.02853	Increase on Day 23
Anus	$F_{3,5}$= 0.2119, p= 0.8842	Firmicutes	$F_{3,5}$= 0.6415, p= 0.6205	
		Bacteroidetes	$F_{3,5}$= 1.444, p= 0.3349	
		Proteobacteria	$F_{3,5}$= 0.5585, p= 0.665	
Mouth	$F_{4,8}$= 0.4425, p= 0.7753	Fusobacteria	$F_{4,8}$=1.105, p=0.417	
		Firmicutes	$F_{4,8}$= 11.41, p=0.002177	Increase on Day 7
		Proteobacteria	$F_{4,8}$= 1.626, p= 0.2586	
		Bacteroidetes	$F_{4,8}$= 1.367, p=0.3268	
		Actinobacteria	$F_{4,8}$= 1.524, p=0.2831	
Liver	$F_{2,6}$=2.236, p= 0.1881	Firmicutes	$F_{2,6}$=89.91, p=0.00003366	Increase on Day 2 and 4
		Proteobacteria	$F_{2,6}$=1.396, p=0.3178	
		Actinobacteria	$F_{2,6}$=0.9882, p= 0.4256	
		Bacteroidetes	$F_{2,6}$=1.235, p=0.3554	
Lungs	$F_{2,6}$= 1.5298, p= 0.2905	Firmicutes	$F_{2,6}$=3.615, p=0.09329	
		Proteobacteria	$F_{2,6}$=1.11, p=0.389	
		Actinobacteria	$F_{2,6}$=7.096, p=0.02624	Decrease on Day 2 and 4
		Bacteroidetes	$F_{2,6}$=9.477, p=0.0139	Decrease on Day 2 and 4

6.2.2 Families

Based on relative abundance, below are the families for each sample that were selected and tested for statically significant relationship across the various time points. The families on the graph were inhabited the community from 1% and above.

6.2.2.1 Belly

On day 0, Lactobacillaceae exhibited strong dominance at 26%, suggesting its role as an early coloniser with high initial abundance. However, its decline to 17% by day 4, 8% by day 7, and eventual disappearance by day 23 indicates competitive exclusion or resource depletion as decomposition progressed. Corynebacteriaceae also showed an early presence at 12% but experienced a significant reduction to 1% by day 2, reflecting its limited competitive ability in the shifting microbial landscape. Conversely, Leuconostocaceae rapidly became dominant at 30% on day 2, likely capitalising on specific substrates or environmental conditions, before undergoing a sharp decline to 9% on day 4, possibly due to competitive displacement by other taxa. Planococcaceae and Tissierellaceae displayed fluctuating abundances, with Planococcaceae peaking at 13% on day 2 and 21% on day 23, and Tissierellaceae peaking at 6% on days 2, 7, and 23, suggesting their roles as transient or opportunistic taxa in the microbial community. Clostridiaceae and Peptostreptococcaceae both demonstrated substantial increases to 20% during mid-decomposition, particularly on day 4, although Clostridiaceae is significantly impactful which may reflect a niche partitioning strategy during this phase, facilitated by the availability of anaerobic conditions or specific nutrients. The substantial increase in Ignatzschineria_f to 60% on day 7, aligning with insect activity, suggests a symbiotic or opportunistic relationship with decomposer fauna. Overall, while some individual bacterial families showed significant successional patterns, the broader microbial community did not exhibit a significant directional change, as indicated by the general PERMANOVA analysis (Table 6.2) implying that the community's compositional shifts are driven by complex, context-dependent interactions rather than a linear successional process. This highlights the importance of species interactions, resource availability, and external factors such as insect activity in shaping the microbial community dynamics during decomposition.

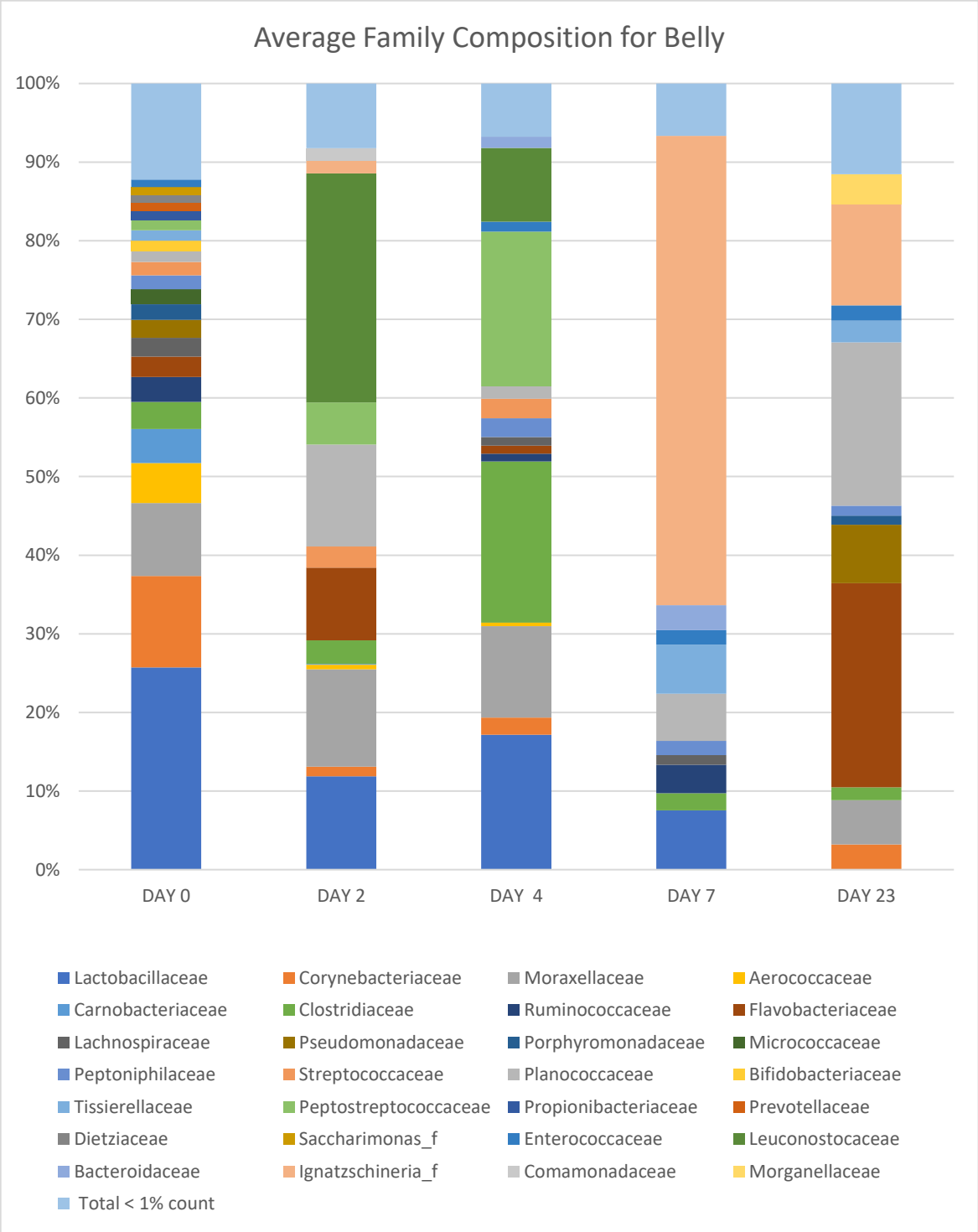

Figure 6.6 Displaying the average family composition for the Belly sample in respect to the decomposition days.

6.2.2.2 Anus

Within the pig anus microbiome, Prevotellaceae initially dominated at 19% on day 0 but steadily declined to 16% on day 2 and 5% on day 4, eventually disappearing by day 23, with no significant trend observed. Ruminococcaceae rose to prominence on day 2 with 21%, surpassing Prevotellaceae, but declined to 5% by day 4 and was absent by day 23, showing a significant effect of decomposition stages. Clostridiaceae emerged as the dominant family on day 4 with 31% but had minimal presence before and after, while Bacteroidaceae became the second most dominant on day 4 with 18% and decreased to 2% by day 23, with a significant increase noted on day 4. Lachnospiraceae, starting at 13% on day 0, gradually declined to 9% by day 2 and 1% by day 4, disappearing by day 23, with no significant relationship found. Pseudomonadaceae and Planococcaceae both appeared late in the decomposition process (day 23), with Pseudomonadaceae reaching 27% as the most dominant and Planococcaceae (22%) emerging as the second most dominant family, though without significant trends over time. Flavobacteriaceae and Moraxellaceae followed similar late-stage patterns, peaking at 12% and 11% on day 23, respectively, despite earlier minimal presence in the decomposition stage. Ignatzschineria_f and Tissierellaceae both surged to 6% after only being detected on day 23, with no significant changes across decomposition stages. Generally, certain individual bacterial families (Ruminococcaceae, Bacteroidaceae) exhibited significant changes, the broader microbial community in the anus site did not show a significant pattern of succession, indicating complex, context-dependent interactions rather than linear progression during decomposition.

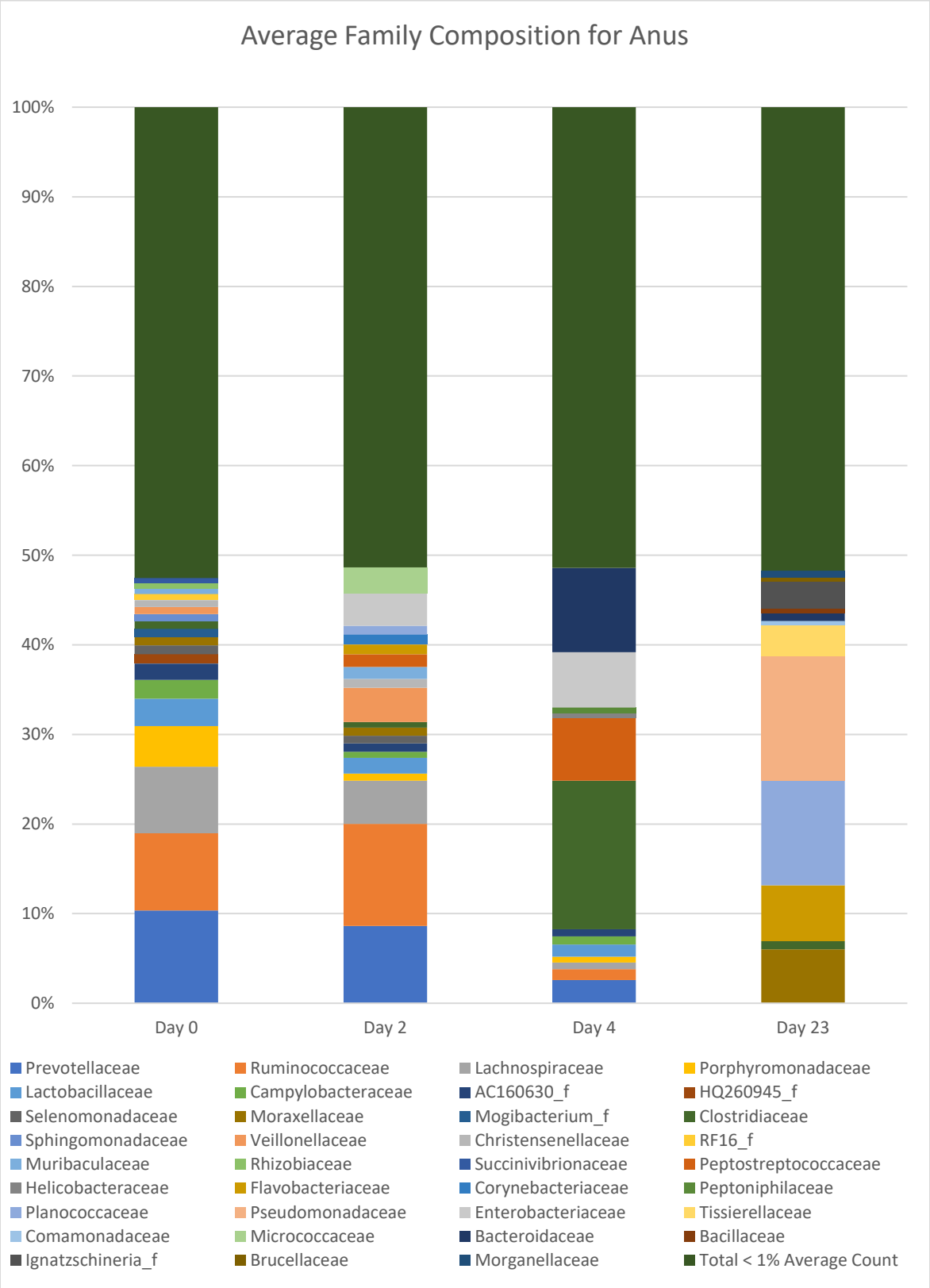

Figure 6.7 Displaying the average family composition for the anus sample in respect to the decomposition days.

6.2.2.3 Mouth

In the mouth of decomposing pigs, the microbial community experienced dynamic shifts with various bacterial families demonstrating different ecological patterns throughout decomposition. Moraxellaceae initially dominated, comprising 19% on Day 0 and increasing to 30% on Day 2, but then showed a substantial but non-significant decline, reducing to 1% on Day 7 and 17% on Day 23, reflecting temporal changes in community composition. Porphyromonadaceae exhibited a decline from 12% on Day 0 to 1% on Day 2, with further decreases and absence on Days 7 and 23, the lack of a significant correlation over time suggests Porphyromonadaceae role was transient or influenced by early decomposition stages. Bacteroidaceae demonstrated a fluctuating dynamic with no significant trend, starting at 5% on Day 0, decreasing to 3% by Day 2, then increasing on Day 4, and stabilising at 5% on Day 7 before falling to 0% on Day 23. The absence of a significant temporal relationship of Prevotellaceae began at 16% on Day 0, dropped to 1% on Day 2, rose to 16% again on Day 4, and became undetectable as decomposition advanced. Flavobacteriaceae experienced substantial fluctuations, increasing from 2% on Day 0 to 35% on Day 2, then decreasing to 13% on Day 4 and 2% on Day 7, before gaining dominance again at 21% on Day 23. Despite these variations of Flavobacteriaceae, the overall abundance pattern was not statistically significant. Planococcaceae, initially absent on the onset of decomposition, increased to 8% on Day 2, decreased to 5% and 3% on Days 4 and 7, respectively, and then rose to 11% on Day 23. Despite these fluctuations, the lack of a significant temporal relationship indicates a relatively stable presence with occasional increases. Ignatzschineria_f showed a non-significant minor presence, rising from 1% on Day 2 to 6% on Day 4 and fluctuating slightly thereafter. Tissierellaceae were absent on Days 0, 2, and 4, but became dominant on Day 7 with 70% of the community, before dropping to 1% on Day 23. The highly significant relationship and peak on Day 7 indicate a marked of dominance linked to specific mid-decomposition conditions. Pasteurellaceae decreased steadily from 6% on Day 0 to nearly undetectable levels by Day 7. Pseudomonadaceae experienced a highly significant and late-stage dominance as they were absent initially but increased to 2% on Day 2, dropped to 0% on Days 4 and 7, and then emerged as the third most dominant family at 27% on Day 23. Despite Tissierellaceae and Pseudomonadaceae demonstrating significant variations, just like the other body sites, the overall microbial community in the mouth exhibited a non-significant pattern of succession. This indicates a complex interplay of microbial interactions and environmental conditions rather than a linear progression in community structure during decomposition.

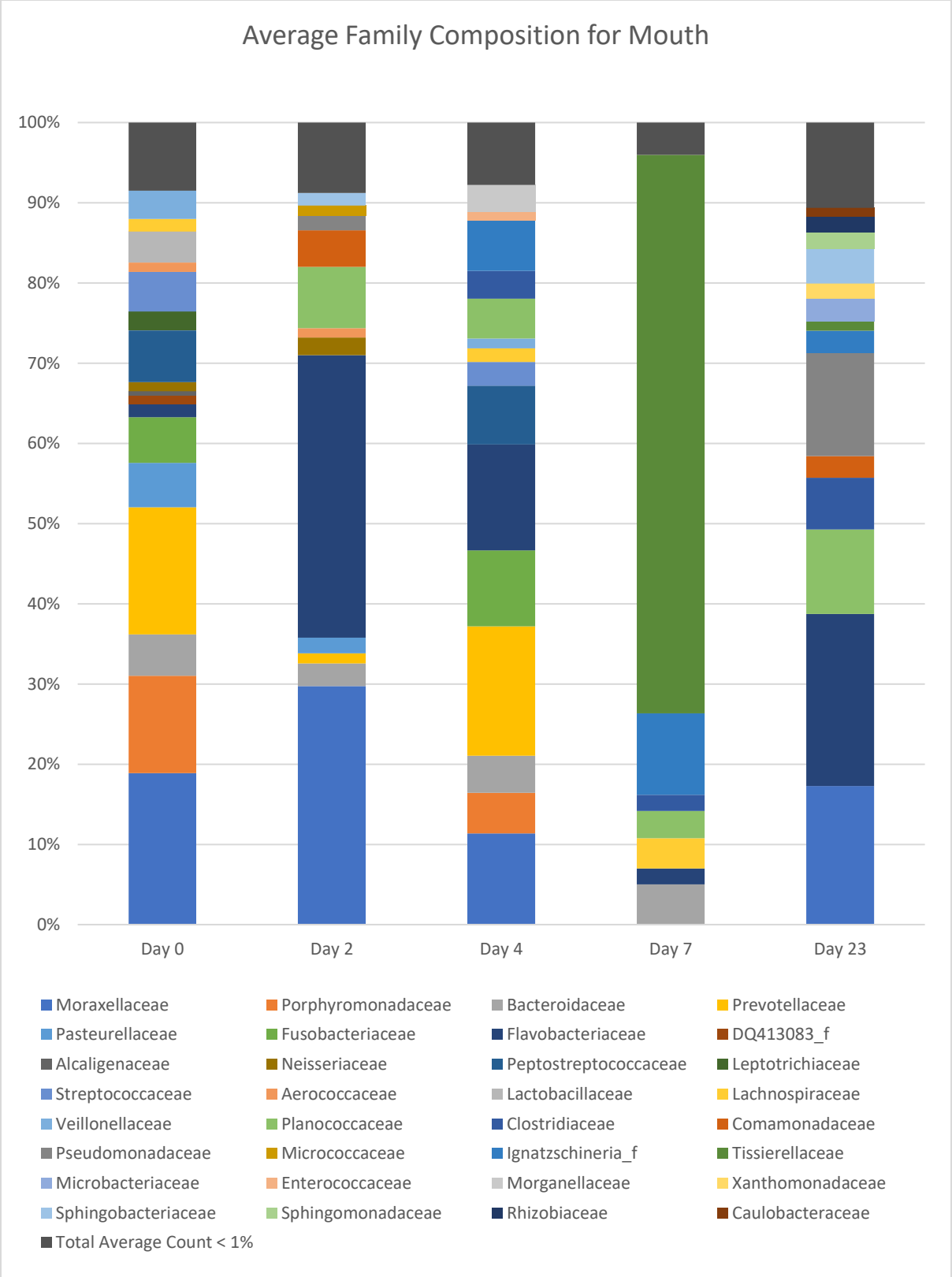

Figure 6.8 Displaying the average family composition for the mouth sample in respect to the decomposition days.

6.2.2.4 Liver

Planococcaceae a constituent of the liver microbiome started as the dominant family, constituting 10% of the community on Day 0 but was not detected on Day 2, with no significant change across decomposition days. Similarly, Moraxellaceae, which initially made up 8% of the community, dropped to 1% on Day 2 and then disappeared by Day 4, without showing any significant temporal correlation. Propionibacteriaceae and Bacillaceae were relatively prominent on Day 0, with 6% and 5% abundance respectively, but both were also not found by Day 2, following a nonsignificant trend of decline. In contrast, Lactobacillaceae showed a significant increase, rising from 5% on Day 0 to 46% on Day 2, and further to 59% by Day 4, becoming the most dominant family during these later stages. This growth was statistically significant, with positive effects on Days 2 and 4. Clostridiaceae increased from 3% on Day 0 to 32% on Day 2 and slightly decreased to 29% by Day 4, ranking third by the end, though the change was not statistically significant. Peptostreptococcaceae also showed a steady rise, starting at 4% on Day 0 and reaching 21% by Day 4, emerging as the third most abundant family by the end, although this increase did not have a significant relationship over time. While Lactobacillaceae saw significant changes, and as displayed on Table 6.2, the general PERMANOVA analysis did not reveal a significant pattern of microbial shifts in the liver microbiome over time during decomposition.

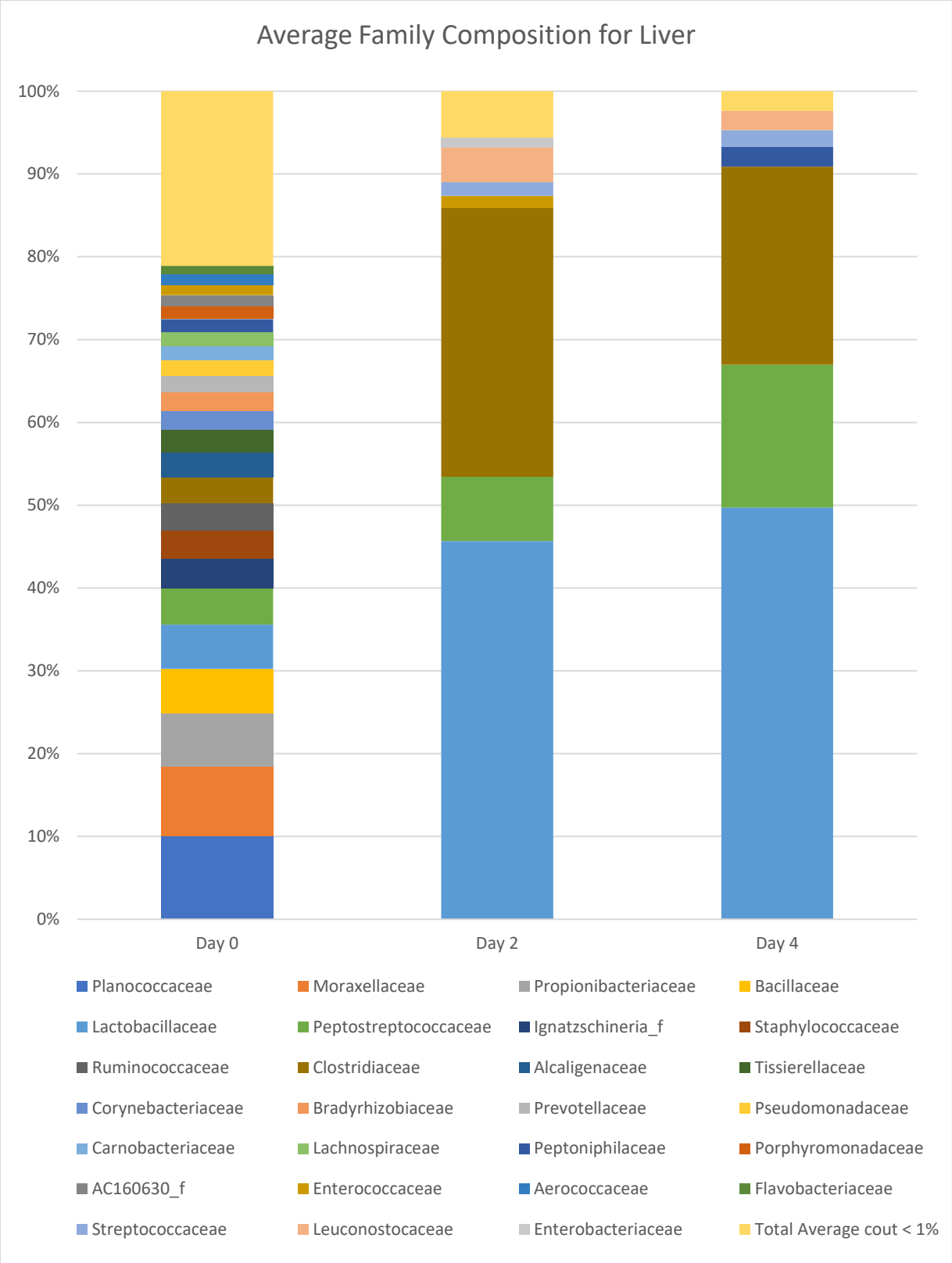

Figure 6.9 Displaying the average family composition for the liver sample in respect to the decomposition days.

6.2.2.5 Lung

Peptostreptococcaceae in the lung microbiome during decomposition initially dominated with 22% on Day 0, then decreased to 8.17% on Day 2 before rebounding to 19.8% on Day 4. Despite these fluctuations, the changes were not statistically significant over time. Lactobacillaceae began at 14%, increasing to 29% on Day 2 and reaching 30% on Day 4, maintaining a consistently high presence throughout decomposition, though this increase was not significant. Clostridiaceae showed a strong increase from 9% on Day 0 to 28% on Day 2 and 41.61% on Day 4, becoming the most dominant family by Day 4, yet without a statistically significant trend. Moraxellaceae started with a lower presence, at 4% on Day 0, and gradually declined to 1% by Day 4, reflecting a steady but insignificant decrease. Despite these shifts in microbial families, the general PERMANOVA analysis found no significant patterns in the lung microbial community during decomposition (Table 6.2).

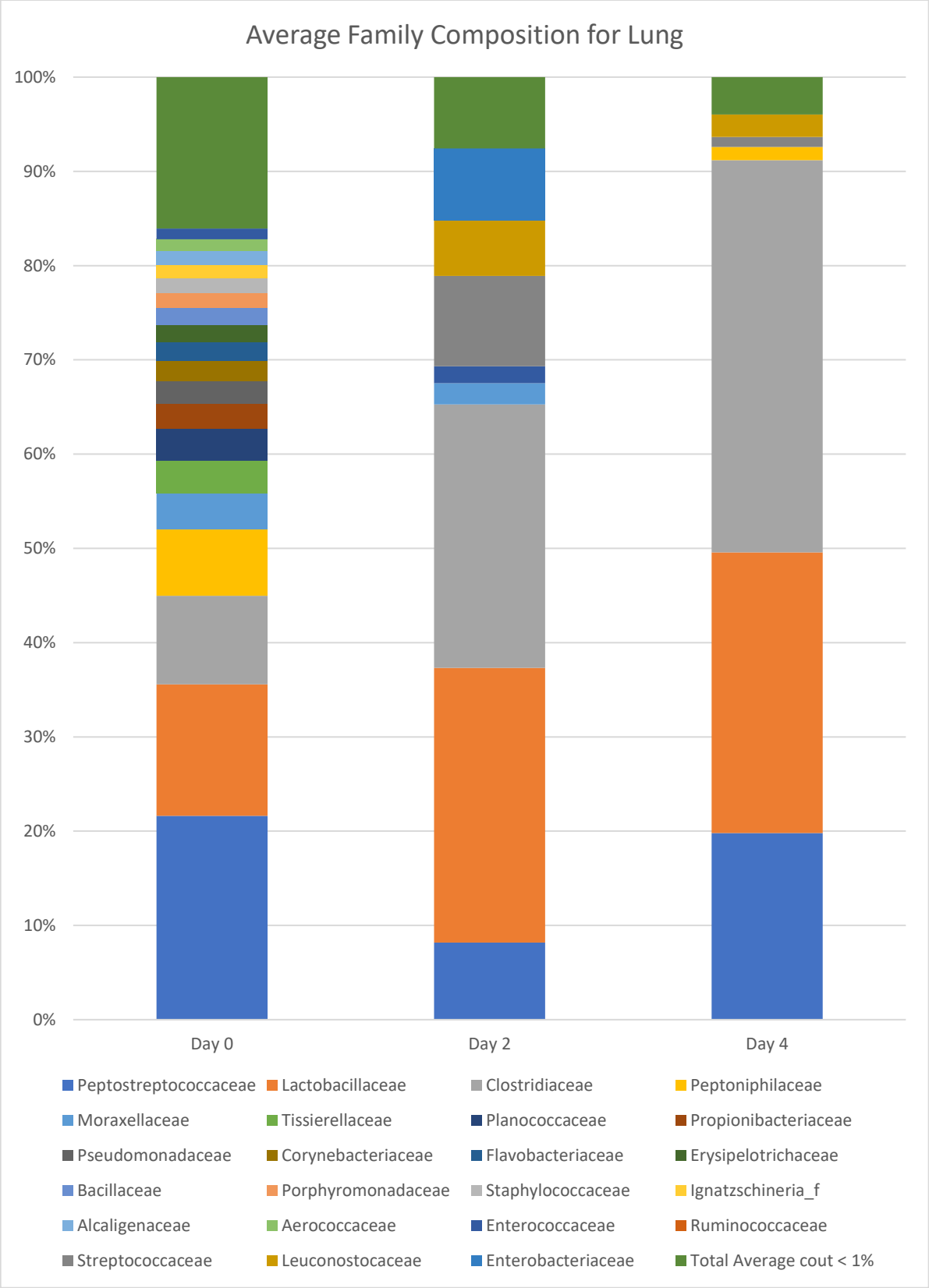

Figure 6.10 Displaying the average family composition for the lung sample in respect to the decomposition days.

6.2.2.6 Families with significant changes over time

This section displays the distribution of bacterial families across various sample types with highlights to taxa that demonstrated significant differences in abundance, as revealed by an ANOVA test (summarised in Table 6.2).

Table 6.2 Summary of betadisper Multiple dispersion and Individual ANOVA analysis of bacterial family over time on pig sample (belly, anus, mouth, liver, and lung). Significant values are highlighted.

Sample	**Multiple Dispersion Analysis Over Time**	**Families**	**Individual ANOVA Results**	**Significant Day**
belly	$F_{4,9}$=0.7622, p= 0.5754	Lactobacillaceae	$F_{4,9}$= 2.885, p= 0.08608	
		Moraxellaceae	$F_{4,9}$=1.204, p= 0.3732	
		Corynebacteriaceae	$F_{4,9}$= 3.815, p= 0.04419	Decrease on Day 2, Day 4, Day 7, and Day 23
		Leuconostocaceae	$F_{4,9}$=1.86, p= 0.3449	
		Planococcaceae	$F_{4,9}$= 2.486, p-value = 0.1181	
		Clostridiaceae	$F_{4,9}$=23.34, p= 0.00009049	Increase on day 4
		Planococcaceae	$F_{4,9}$=2.486, p= 0.1181	
		Peptostreptococcaceae	$F_{4,9}$=1.473, p= 0.2884	
		Morganellaceae	$F_{4,9}$=1.182, p= 0.3814	
		Tissierellaceae	$F_{4,9}$=11.95, p= 0.001202	Increase on day 7
		Ignatzschineria_f	$F_{4,9}$=2.336, p= 0.1336	
		Pseudomonadaceae	$F_{4,9}$=3.578, p= 0.05194	
Anus	$F_{3,5}$=0.3362, p= 0.8007	Prevotellaceae	$F_{3,5}$= 1.425, p=0.3394	
		Clostridiaceae	$F_{3,5}$=1.962, p= 0.2381	
		Lachnospiraceae	$F_{3,5}$= 5.185, p=0.05401	
		Ruminococcaceae	$F_{3,5}$= 7.736, p=0.02518	Decrease on day 23
		Bacteroidaceae	$F_{3,5}$=8.198, p=0.01888	Increase on day 4
		Pseudomonadaceae	$F_{3,5}$=0.8081, p=0.5413	
		Planococcaceae	$F_{3,5}$=2.837, p= 0.1454	
		Flavobacteriaceae	$F_{3,5}$=1.075, p=0.4387	

		Moraxellaceae	$F_{3,5}$=1.967, p=0.2374	
		Ignatzschineria_f	$F_{3,5}$=1.267, p=0.3802	
		Tissierellaceae	$F_{3,5}$=4.206 p=0.078	
Mouth	$F_{4,8}$= 1.0096, p= 0.4567	Moraxellaceae	$F_{4,8}$=3.743, p=0.05304	
		Porphyromonadaceae	$F_{4,8}$=3.773 p=0.05206	
		Prevotellaceae	F4,8=2.535 p= 0.1224,	
		Pasteurellaceae	$F_{4,8}$=3.526 p= 0.06097,	
		Bacteroidaceae	$F_{4,8}$=0.4829 p= 0.7485,	
		Flavobacteriaceae	$F_{4,8}$=1.797, p= 0.2227	
		Tissierellaceae	$F_{4,8}$=240.7, p=0.00000002289	Increase on day 7
		Pseudomonadaceae	$F_{4,8}$=202.9, p= 0.000000045	Increase on day 2 and 23
		Ignatzschineria_f	$F_{4,8}$=1.95, p=0.1955	
		Planococcaceae	$F_{4,8}$= 0.6053, p=0.67	
Liver	$F_{2,6}$= 1.5298, p= 0.2905	Planococcaceae	$F_{2,6}$=1.242, p=0.3538	
		Moraxellaceae	$F_{2,6}$=1.568, p=0.2833	
		Bacillaceae	$F_{2,6}$=2.334, p=0.178	
		Propionibacteriaceae	$F_{2,6}$=1.818, p=0.2414	
		Lactobacillaceae	$F_{2,6}$=7.436, p=0.02376	Increase on day 2 and 4.
		Clostridiaceae	$F_{2,6}$=5.083, p=0.05112	
		Peptostreptococcaceae	$F_{2,6}$=1.407, p=0.3155	
Lungs	$F_{2,6}$= 0.0453, p= 0.956	Peptostreptococcaceae	$F_{2,6}$=0.3564, p=0.7141	
		Lactobacillaceae	$F_{2,6}$=0.5646, p=0.5961	
		Clostridiaceae	$F_{2,6}$=2.832, p=0.1361	
		Moraxellaceae	$F_{2,6}$=0.6382, p=0.5607	

There was a significant decrease in species richness and phylogenetic diversity (PD) in the belly over time (Chapter 4, section 4.2.3.1.1). The reduction in the overall number of species and evolutionary diversity as decomposition progresses is reflected in the phylum and family analysis. In the belly community, the Bacteroidetes and families from Firmicutes (Clostridiaceae, Tissierellaceae) increased significantly, began to dominate the community, and outcompeted other taxa such as Actinobacteria (Corynebacteriaceae),

which were noted to have significantly decreased. This could be due to Clostridiaceae and Tissierellaceae's ability to produce fermentation by-products such as organic acids (e.g., butyric acid, acetic acid) and gases (e.g., hydrogen, carbon dioxide) (Atasoy, Eyice and Cetecioglu, 2020; Peña-Carrillo *et al.*, 2023). The accumulation of these by-products can lower the pH and create an environment that is inhospitable for other bacteria, particularly aerobes (Ratzke and Gore, 2018), like Corynebacteria. Despite the lack of significant trends in diversity metrics of the mouth community (Table 4.6), the fluctuations in richness and phylogenetic diversity of the mouth community might reflect the significant shifts in Firmicutes (Tissierellaceae) populations, which tend to dominate during the active decay stages (day 7). Additionally, Pseudomonadaceae thrive on day 2 (early stages), when oxygen is less utilised in the mouth, while Tissierellaceae increase in the later stages (day 7) under anaerobic and acidic conditions. By day 23, the unique metabolic ability of Pseudomonadaceae (utilising alternative electron acceptors under anaerobic or microaerophilic conditions [Kumar *et al.*, 2021]) might have allowed them to re-establish dominance in anaerobic or microaerophilic environments. Regardless of the dynamic trends of microbes in the mouth sample, the overall species diversity and evolutionary relationships remain relatively stable. In the anus community, an inclined trend in Bacteroidaceae abundance on day 4 and a decrease in Ruminococcaceae on day 23 was observed. This pattern might be due to the dominance of Bacteroidaceae in decomposition, given their ability to ferment complex carbohydrates in anaerobic conditions (Yao, Chen and Lindemann, 2020), which are associated with early decomposition, while Ruminococcaceae are less competitive in environments with lower nutrient availability or changing pH. Hence, they declined at the later stage of decomposition as substrates (mostly fibrous proteins [Biddle *et al.*, 2013]) became limited, and the environment became more acidic and less favourable for fibre-degrading microbes. The liver undergoes significant physiological post-mortem changes, including reduced blood flow and oxygen depletion, creating anaerobic conditions that favour the growth of anaerobic bacteria like Lactobacillaceae, which increased on day 2 (early bloat stage) and day 4 (end of bloat stage). In addition, the increase of Lactobacillaceae in the liver sample can be attributed to their role in fermenting carbohydrates to produce lactic acid; the anaerobic conditions in decomposing liver during decomposition possibly offer opportunities for lactic acid fermentation, contributing to the growth of lactic acid bacteria. Species evenness in the liver sample was highly negatively significant (Chapter 4, section 4.2.3.1.4) and may have been facilitated by the significant increase of Firmicutes (Lactobacillaceae), disrupting the balance of the microbiota. Table 4.6 indicates the significant decline in evenness and variation in phylogenetic diversity in the lung microbial community. The observation in the lung might be impacted by the significant

reduction of Actinobacteria and Bacteroidetes (noted at just the phyla level), which, in turn, might be responsible for the increased species richness observed over time.

6.3 CONCLUSION

The study reveals that both at the phylum and family levels, the overall microbial communities across different body sites (belly, mouth, liver, lungs, and anus) do not demonstrate a statistically significant linear progression. This makes it challenging to use the entire community for reliable postmortem interval (PMI) estimation. However, certain individual bacterial taxa within these body sites exhibit significant changes over time and may serve as useful indicators for PMI estimation. Specifically, in the belly, Corynebacteriaceae and Clostridiaceae exhibited significant changes, with the former decreasing over time and the latter increasing. The anus showed significant results for Ruminococcaceae and Bacteroidaceae, with notable decreases and increases, respectively, on specific days. The mouth revealed significant increases in Tissierellaceae and Pseudomonadaceae, while the liver exhibited significant increases in Lactobacillaceae. Therefore, these findings suggest that, while the body site as a whole might not be reliable for PMI analysis, as indicated by the multiple dispersion analysis over time, specific microbial taxa within these sites could provide valuable forensic insights. This chapter makes evident the importance of targeted microbial analysis in body sites, where tracking changes in key bacterial families could enhance the accuracy of PMI estimation in forensic investigations. Chapter 7 focuses on the trends of bacterial populations in the decomposing environment.

7.0 CHAPTER SEVEN: MICROBIAL COMPOSITION IN THE ENVIRONMENTAL SAMPLES OVER TIME.

7.1 INTRODUCTION

Swine often are considered suitable models for examining human decomposition because of the analogous features they possess when compared to humans. Hence multiple researchers have employed swine proxies of decomposition to study numerous forensic questions. Terrestrial environments include habitats with soil components. Soil hosts rich and diverse microorganisms and are crucial in maintaining its ecological function (Danielsen *et al*., 2023). Plant litter, dead organisms, and other organic residues (Oades, 1988; Litterick, 2023; Benbow, Receveur and Lamberti, 2020; Department of Primary Industries, 2021) are receipts of ecological activities in terrestrial habitats that may be deposited on soil during a natural or artificial process are broken down by bacteria alongside other microorganisms. The microbial dynamics during the decomposition of organic matter in various environmental niches provide valuable insights into the ecological processes shaping bacterial community structures that are impacted by numerus environmental conditions and nutritional factors. The detection of corpses in aquatic settings may arise due to drownings or possible disposal of dead bodies (Bray *et al*., 2023). Nonetheless, surrounding aquatic microbiome lacks the ability to always reflect the bacterial communities of the sunken carcass (Sehnal *et al*., 2021).

In this chapter, exploration to the trends and abundance of planktonic (free-floating) bacterial phylum and families detected in aquatic settings (seawater, brackish water and freshwater), and in soil environments of pig carcasses over a defined observation period was made. The same statistical approach from chapter 6 was also adopted in this chapter. By analysing bacterial phyla and families in diverse environmental samples, we aim to unravel the intricate relationships responsible for their abundance and distribution during the course of pig decomposition in the respective niche. The information that will be revealed in this chapter might be relevance for environmental conservation, ecosystem management, and a deeper comprehension of the intricate web of interactions of bacteria that sustains post-mortem life in soil and water habitats.

7.2 RESULTS AND DISCUSSION

7.2.1 Phylum

Based on the relative abundance, below is the phylum for each environmental sample (soil, seawater, brackish water, freshwater) selected to be tested for statically significant relationship across the observed time point. All phyla characterised on the graph occurred inhabited the respectively community in 1% and above.

7.2.1.1 Soil

Proteobacteria appears to be the most prevailing microbial phyla throughout the observed period of decomposition. Proteobacteria were stable on day 2 and 4 with 29%, dropped a little in abundance to 27% and slightly rose with an increase ratio on Day 14 to 31% before experiencing another drop in population to 30%. Acidobacteria was the second most dominate phyla on day 2 and claimed 14% of the total population in the soil community and had had a decreasing trend, on day 4 (12%), day 7 (11%) to day 14 (8%) before a slight increment on day 23 (9%). Firmicutes emerged the third largest phyla at the inception of decomposition and started the community dominance with 12%, increased slightly on day 4(13%) and was stable on day 7 and 14 with 25% on each day before dropping to 18% on the final day of sampling (making them the second most abundant phyla on day 23). Planctomycetes were fourth on the microbial community hegemony ranking on day 2 with 11% occupancy, it remained so on day 4 and decline to 10% on day 7. Planctomycetes further decline to 8% on day 14 and remained so on day 23. Bacteroidetes, from the onset of decomposition occupied 9% of the total population is the microbial community of the soil. They marginally grew to 10% on day 4, dropped on day 7 (7%). Bacteroidetes, increased again on day 14 and to its highest value on day 23 (15%). Verrucomicrobia commenced decomposition on day 2 with 9% abundance and retained same proportion on day 4. Verrucomicrobia decreased on day 7 (7%) and further declined on day 14 (5%) before minorly elevating to 6% on day 23. Actinobacteria, on day 2 and 4 were 7% and marginally declined to 5% on day 7 before undergoing a slight increment on day 14 (7%) and day 23 (8%). Actinobacteria experienced similar variation pattern like other high and low abundant phyla that were stable on the first and second decomposition days (having same ratio). Chloroflexi (3%) Gemmatimonadetes (1%), Latescibacteria_WS3 (1%), Chlamydiae (1%) were relative stable with constant abundance over the observed period as they displayed exact values for all decomposition days. The Regression and multivariate dispersion analysis across the existing soil phylum over the observed period of decomposition revealed no significant relationship. This also confirms the

results of the ANOVA regression analysis for the individual bacterial phyla (Bacteroidetes, Acidobacteria, Firmicutes and Proteobacteria) that were not significant.

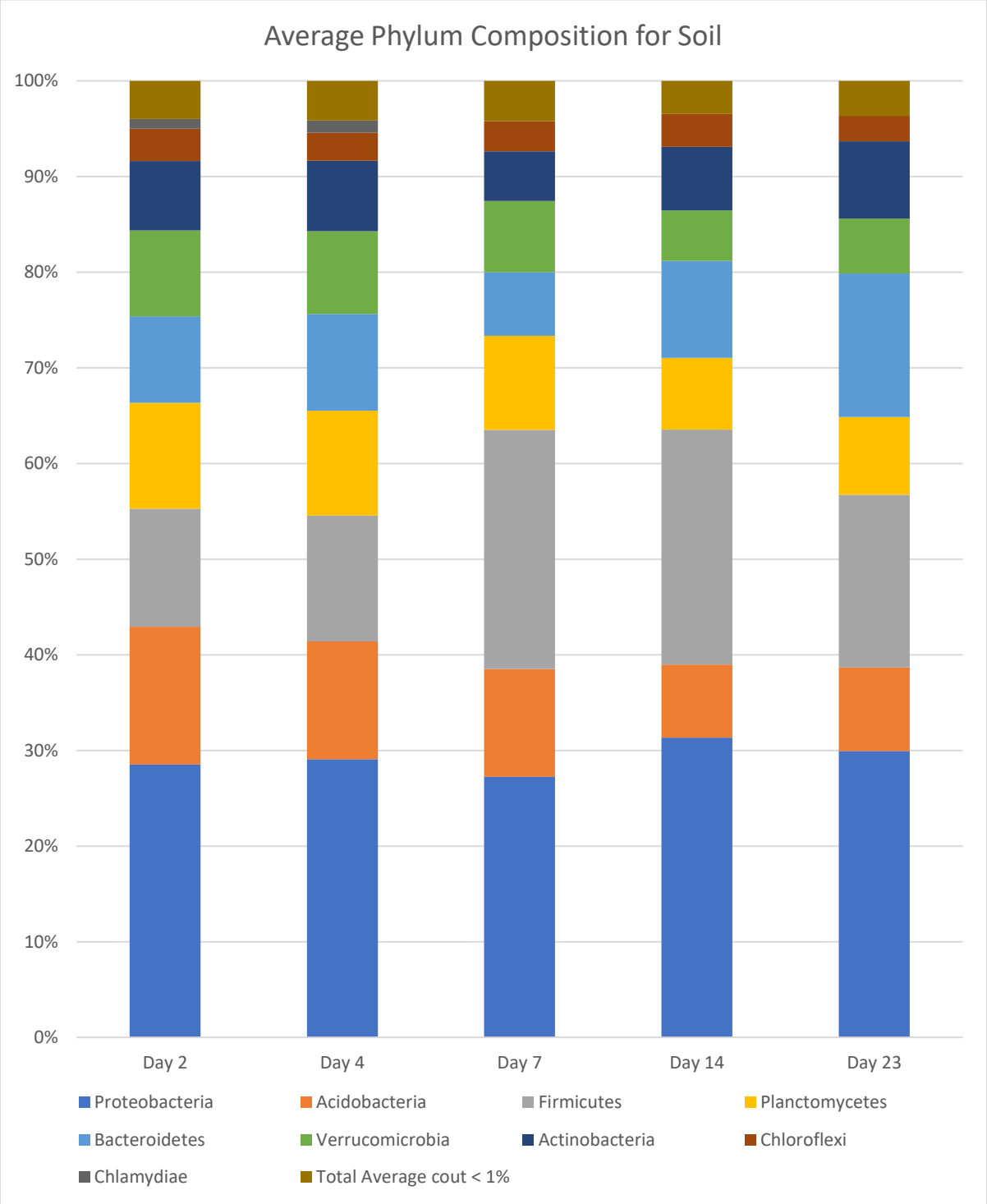

Figure 7.1 Displaying the average phylum composition for the soil sample in respect to the decomposition days.

7.2.1.2 Seawater

Proteobacteria, as seen on figure 7.2, made up 66% of the microbial community, making them the most abundant phylum on the onset of decomposition. A significant decrease to 16% was noticed on day 7, and further declined to 11% on Day 14 (Table 7.2). Firmicutes occupied 18% of the total population that contributes to the microbial community structure, increased to 29%, although the second most abundance phyla on day 14, Firmicutes slightly decreased to 27%. Actinobacteria were third in abundance hierarchy on day 0 as they were present with 8% and were not detected across the further days of decomposition. Bacteroidetes contributed an inclining trend to the diversity of the community as they were seen on day 0 (4%), day (34%) and amassed a high abundance on day 14 (44%). Acidobacteria, Chloroflexi, Planctomycetes were detected in 1% and were negligible as decomposition advanced. Fusobacteria, on day 0 were 0% and on Day 7 Increased to 21% and shifted slightly to 18% on day 23. The Regression and multivariate dispersion analysis across the existing seawater phylum over the observed period of decomposition revealed a highly significant relationship. However, the results of the regression analysis for the bacterial phyla Bacteroidetes, Actinobacteria, and Firmicutes across the days of decomposition were not statistically significant.

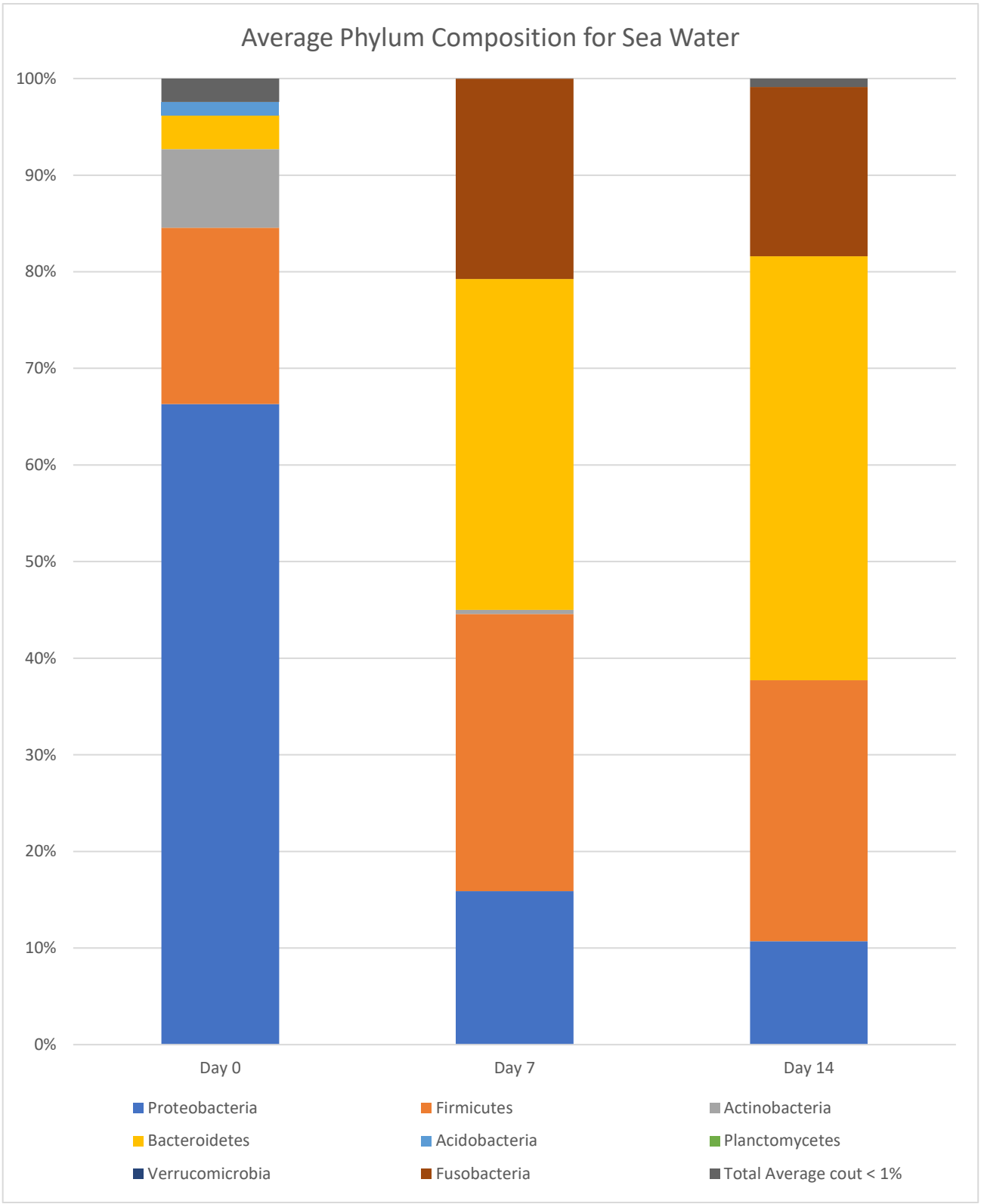

Figure 7.2 Displaying the average phylum composition for the seawater sample in respect to the decomposition days.

7.2.1.3 Brackish water

Proteobacteria made up 58% of microbes, establishing them the most abundant phylum on the commencement of decomposition. Although Proteobacteria declined to 41% on day 7 and 14, they were still the most dominant phyla across other days of decomposition. Firmicutes accumulated 12% of the community biomass, significantly increased to 23%, Firmicutes were the third most abundance phyla on day 14 even though they marginally reduced to 18%. Actinobacteria were third in community hegemony on day 0 inhibited 18% and were not detected onwards. Bacteroidetes displayed an elevating shift pattern as they were seen on day 0 (9%), day (31%) and minorly increased in abundance on day 14 (38%) to make a significant impact. Acidobacteria were spotted to make up 1% of the brackish water's biomass and were not found as decomposition progressed. Fusobacteria on day 0 were not discoverable but increased on day 7 (4%) and slightly depreciated to 2% on day 14. The regression and multivariate dispersion analysis across the existing brackish waters phylum over the observed period of decomposition revealed a highly significant relationship (Table 7.1). Actinobacteria and Proteobacteria were not statistically significant.

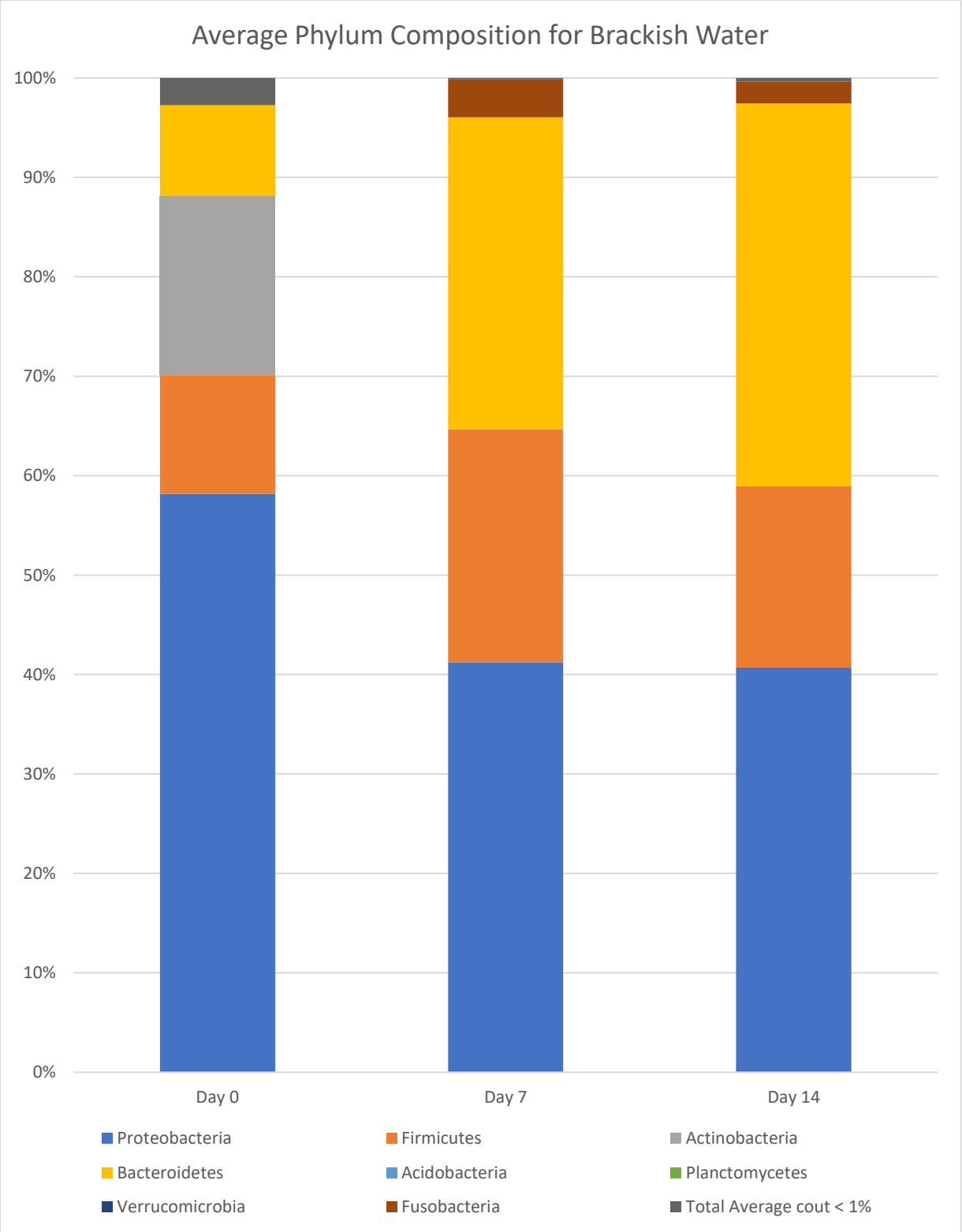

Figure 7.3 Displaying the average phylum composition for the Brackish water sample in respect to the decomposition days.

7.2.1.4 Freshwater

Proteobacteria on Day 0 was Present in the community at 19%, on day 7 significantly Increased to 43%, suggesting a great rise in relative abundance and claiming the 1st spot on the abundance hierarchy. Proteobacteria, day 14 declined to 2%. Firmicutes was the largest occupant of the community on day 0 and dominated with 68%, forming a substantial part of the initial community. On day 7, a substantial decline of Firmicutes to 31% was noticed but they bounced back on day 14 to dominate the community with 71%. Firmicutes's ratio on day 14 in the freshwater community is the highest ratio attained by any phyla in the entire water bacterial community. Actinobacteria contributed to the initial diversity at 8% was not detectable on day 7 and increased to 1% on day 14. Bacteroidetes inhibited the community with a 2% presence and on day 7 like Proteobacteria, they also significantly Increased (15%), which placed them third on the abundance hierarchy for day 7. On day 14, Bacteroidetes return to their initial lower abundance (2%) that was noticed on day 0. Acidobacteria's and Verrucomicrobia's contributing presence to the community on Day 0 was at 1%. Acidobacteria increased to 3% while Verrucomicrobia increased to 2% on day 7 and were not detectable on day 14. Chloroflexi and Fusobacteria were not noticed on day 0 (0%), rose to 1% on day 7 and was not detected on day 14(0.00%). Planctomycetes had a similar pattern to Chloroflexi and Fusobacteria that were not spotted on the inception of decomposition (0%) but minorly inclined on day 7 (2%) and was not found in the community on day 14. Acidobacteria, Chloroflexi, Fusobacteria, Planctomycetes, Verrucomicrobia showed variability but lingered in the community at a very low abundance and were not detected on the final sampling day. The regression and multivariate dispersion analysis across the existing freshwater phylum over the observed period of decomposition as displayed on table 7.1, revealed a highly significant relationship. Actinobacteria and Firmicutes were not statistically significant.

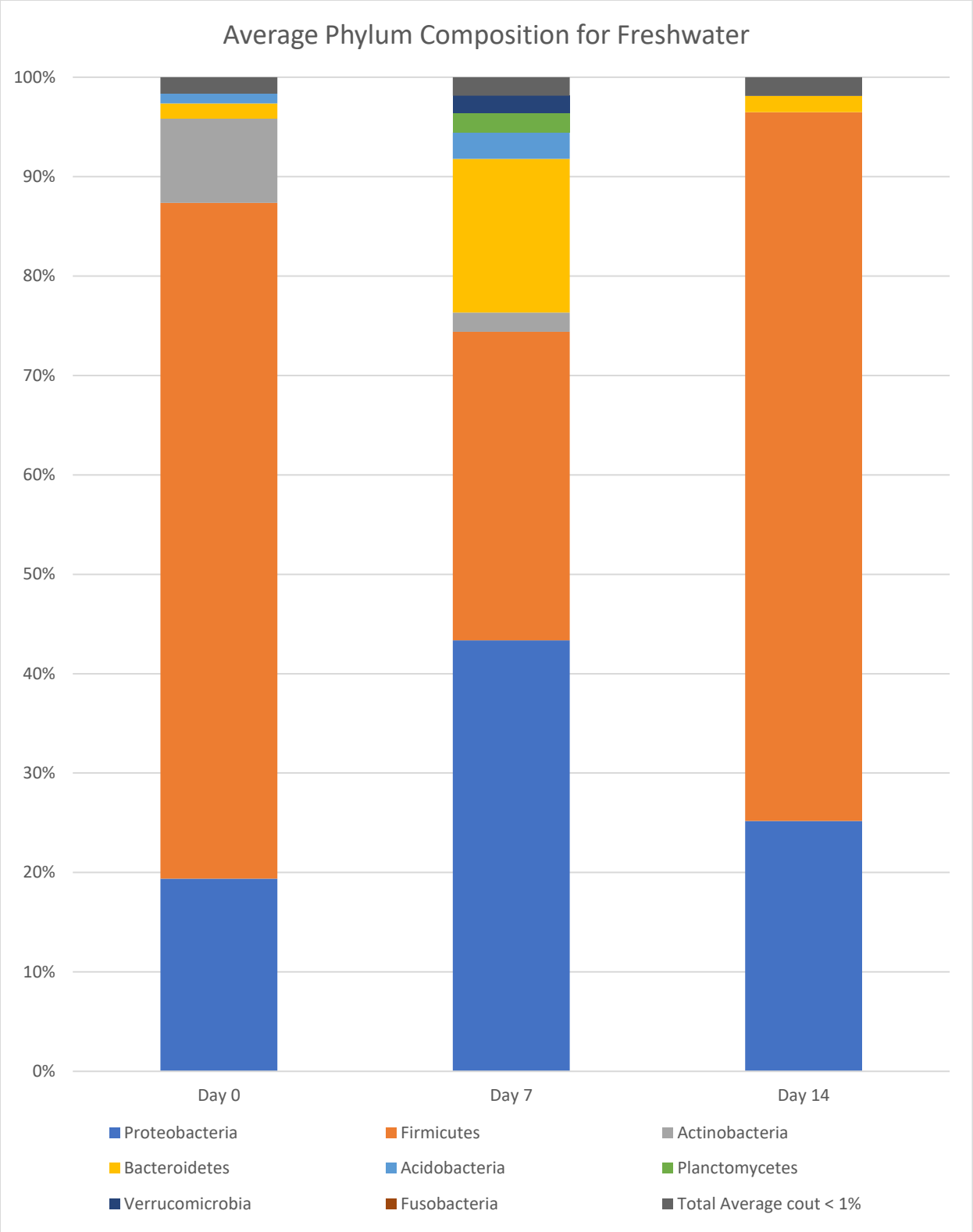

Figure 7.4 Displaying the average phylum composition for the freshwater sample in respect to the decomposition days.

7.2.1.*5 Phyla with Significant changes over time.*

Despite the diversity of the soil sample, as indicated in the previous chapters, none of the top competitors (tested phyla) for the community's abundance had a significant impact on the minor fluctuations observed in the soil sample. The microbial phylum in the soil can be described as being relatively stable, which suggests a potentially consistent ecological niche. In the water samples, significantly influential phyla were found. Proteobacteria in the seawater sample exhibited a constant declining trend in the mid-stages of decomposition, which might be among the reasons for the significant impact on the community's structure, as indicated by the regression results. Microbial communities break down organic material, consuming oxygen in the process, which can deplete oxygen levels, leading to hypoxic conditions (low oxygen concentrations in the water column, typically defined as oxygen levels below 2 mg/L [Baxa *et al.*, 2020]). Aerobic Proteobacteria, when exposed to hypoxic conditions, may initiate stress responses (Broman *et al.*, 2017), which can lead to cell death (Burton and Jauniaux, 2011) and a decline in population. The succession pattern of Bacteroidetes was significantly impactful in the brackish and freshwater. Firmicutes and Bacteroidetes in the aquatic samples also contributed significantly to the brackish water microbial structure by increasing in abundance on days 7 and 14. Firmicutes are often fermentative bacteria with the capability to break down organic matter in low-oxygen conditions that might be initiated in the mid-decomposition stage. Bacteroidetes are proficient in the hydrolysis of complex organic materials, leading to an increase in available nutrients that support their growth. As organic matter decomposes, simple sugars, amino acids, and fatty acids are released into the environment (Khatoon et al., 2017; Thomas, 1997; Gunina and Kuzyakov, 2022). This influx of nutrients during the mid-decomposition stage can drive the proliferation of Firmicutes and Bacteroidetes, as they are well adapted to utilise these substrates efficiently. Actinobacteria held the same position in the abundance hierarchy (third) in both sea and brackish water. Actinobacteria and Fusobacteria exhibited a similar shift pattern in all water, with both phyla rising on day 7 and dropping to undetectable levels on day 14.

Table 7.1 Summary of betadisper Multiple dispersion and Individual ANOVA analysis of bacterial phylum over time on Environmental sample (soil, seawater, brackish water, freshwater). Significant values are highlighted.

Sample	**Multiple Dispersion Analysis Over Time**	**Individual Phylum**	**ANOVA Results**	**Significant Day**
Soil	$F_{4,10}$=0.7585, p= 0.5752	Proteobacteria	$F_{4,10}$=0.5465, p= 0.7059	
		Acidobacteria	$F_{4,10}$=2.326, p= 0.1272	
		Firmicutes	$F_{4,10}$=1.229, p= 0.3586	
		Verrucomicrobia	$F_{4,10}$=3.386, p= 0.05359	
		Bacteroidetes	$F_{4,10}$=2.68, p=0.09394	
Seawater	$F_{2,3}$=3.0052e+30, p= 2.2e-16	Proteobacteria	$F_{2,3}$=13.47, p= 0.03171	Decrease on day 7 and 14
		Firmicutes	$F_{2,3}$=1.171, p= 0.4209	
		Actinobacteria	$F_{2,3}$=6.003, p= 0.08938	
		Bacteroidetes	$F_{2,3}$=4.997, p=0.1109	
		Fusobacteria	$F_{2,3}$=3.769, p=0.1519	
Brackish water	$F_{2,3}$=1.13e+31, p= < 2.2e-16	Proteobacteria	$F_{2,3}$=0.1576, p=0.8608	
		Actinobacteria	$F_{2,3}$=1.613, p= 0.3345	
		Firmicutes	$F_{2,3}$=35.45, p= 0.008179	Increase on day 7 and 14
		Bacteroidetes	$F_{2,3}$=12.52, p= 0.03499	Increase on day 7 and 14
Freshwater	$F_{2,3}$=5.84e+29, p= < 2.2e-16	Firmicutes	$F_{2,3}$=0.939, p= 0.4823	
		Actinobacteria	$F_{2,3}$=2.642, p= 0.218	
		Proteobacteria	$F_{2,3}$=10.94, p=0.04188	Increase on day 7
		Bacteroidetes	$F_{2,3}$=36.66, p= 0.007793	Increase on day 7

7.2.2 Families

Based on the relative abundance, below are the families for each environmental sample selected to be tested for statically significant relationship across the various time points. The families exhibited on the graph inhabited the community from 1% and above.

7.2.2.1 Soil

Bradyrhizobiaceae had a exhibited a minor but noticeable decline from its peak on day 2. Initially prominent, its presence decreased over time, stabilising at 8% on days 4 and 7, and further reducing to 6% by day 23. Bacillaceae from the onset of decomposition started with 8% abundance, fluctuated slightly, peaking at 11% on day 14 before decreasing to 9% by day 24. Chthoniobacteraceae occupied 6% of the microbial community on day 2 and demonstrated a declined on subsequent days of decomposition with day 14(4%) and 23(4%) significantly impacted. Chitinophagaceae was stable from the initial stage of decomposition (day 2: 4%, day4: 4%) and significantly decreased to 3% on day 7 and day 23. Gemmataceae remained constant at 4% through days 2, 4, and 7, and decreased slightly to 3% on days 14 and 23. Gemmataceae exhibited stability by acquiring 4% of community space on day 2 and 4, 7 and insignificantly decreased to 3%on day 14 and 23. Vicinamibacter_f, Solibacteraceae, Planctomycetaceae demonstrated consistency by gaining 3.00% of community space on day 2 and 4, 7 and negligibly decreased to 2% on day 14 and 23. Clostridiaceae on day 2 and 4 were 1%, which suggest their stability and rose to 3% and 4.00% on day 7. Clostridiaceae decreased to 2.00% on the final sampling day (day 23). Ktedonobacteraceae, CP011489_f, Polyangiaceae, Gaiellaceae, PAC001907_f, Acetobacteraceae, Hyphomicrobiaceae, Rhodospirillaceae, Tepidisphaeraceae, PAC000121_f, Rhodomicrobium_f all existed in the community at 1% across all observed period of decomposition. PAC000121_f, Rhodomicrobium_f, Steroidobacter_f, Rhodospirillaceae, Tepidisphaeraceae, Haliangiaceae, Gaiellaceae, PAC001907_f, Acetobacteraceae, Hyphomicrobiaceae, Polyangiaceae, Comamonadaceae, GQ396871_f, CP011489_f was 1% on day 2 and 4. Planococcaceae Beijerinckiaceae, Bryobacteraceae, Isosphaeraceae, Cytophagaceae were 2% on day 2 and 4. Overall, the PERMANOVA analysis indicates that the general microbial community structure did not show a consistent pattern of change, indicating that while specific taxa exhibited significant changes in abundance, the overall microbial community remained relatively stable throughout the decomposition process. This stability could be attributed to the resilience and adaptability of the microbial community as a whole, balancing changes in individual taxa across the decomposition stages.

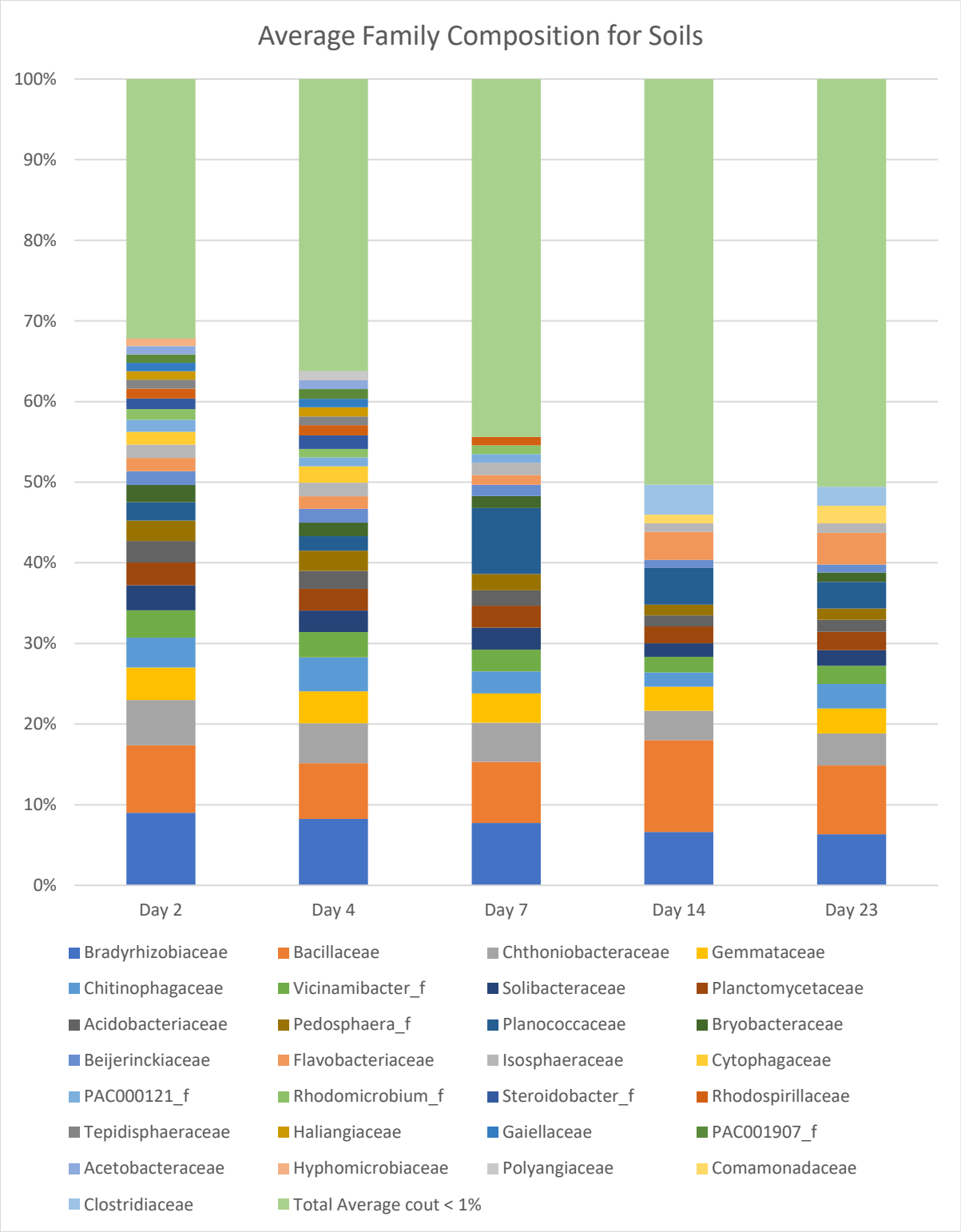

7.5 Displaying the average family composition for the soil sample in respect to the decomposition days.

7.2.2.2 Seawater

Pseudomonadaceae was seen to be the most abundant family possessing 24% on day 0 and decreased to 0% on both Day 7 and Day 14. Rickettsiaceae were detected to be the second most abundant family (16%) on Day 0, becoming undetectable (0%) on both Day 7 and Day 14. Ignatzschineria_f was the third in the abundance hierarchy and was discovered to decrease from 8% on Day 0 to 1% on day 7, and then maintaining at 1% on the final sampling day. Moraxellaceae occupied 3% of the community's space on day 0 and decreased to 5% on day 7, and then slightly decreasing to 4% on day 14. Peptostreptococcaceae were not detected in the community on day 0 but were found on 7% and 5% on day 7 and 14. Fusobacteriaceae were not detected on day 0. They turned out to be the second largest bacterial family with on day 7 and 14 with 21% and 18% respectively. Clostridiaceae inhabited 1% of the community space on day 0 and rose to 8.00% on day 7 (third largest on day 7) before declining to 3.00% on day 14. Bacteroidaceae showed steady increase over the observed period of decomposition as they were 1% on day 0, 31% on day 7 and 41% on day 14. Bacteroidaceae were the largest occupant of the community on day 14. Planococcaceae's abundance was noticed to be 6% on Day 0 and declined to 1% on Day 7, and then minorly inclined to 2% on Day 14. Other families were equally detected on the day the first sampling day were undetectable in subsequent days of decomposition [(Propionibacteriaceae (5%), Bacillaceae (4%), Oxalobacteraceae (4%), Sphingomonadaceae (3%), Staphylococcaceae (2%)]. Although the families' tested in this aquatic community were not significant, the general PERMANOVA analysis of microbial families in the seawater sample of decomposing pig overtime revealed a highly significant relationship existing in this community (Table 7.2). This indicates that the general microbial communities show an increasing pattern of change might have been influenced by patterns caused by taxa grouped together that are less than 1% and were not tested for significance.

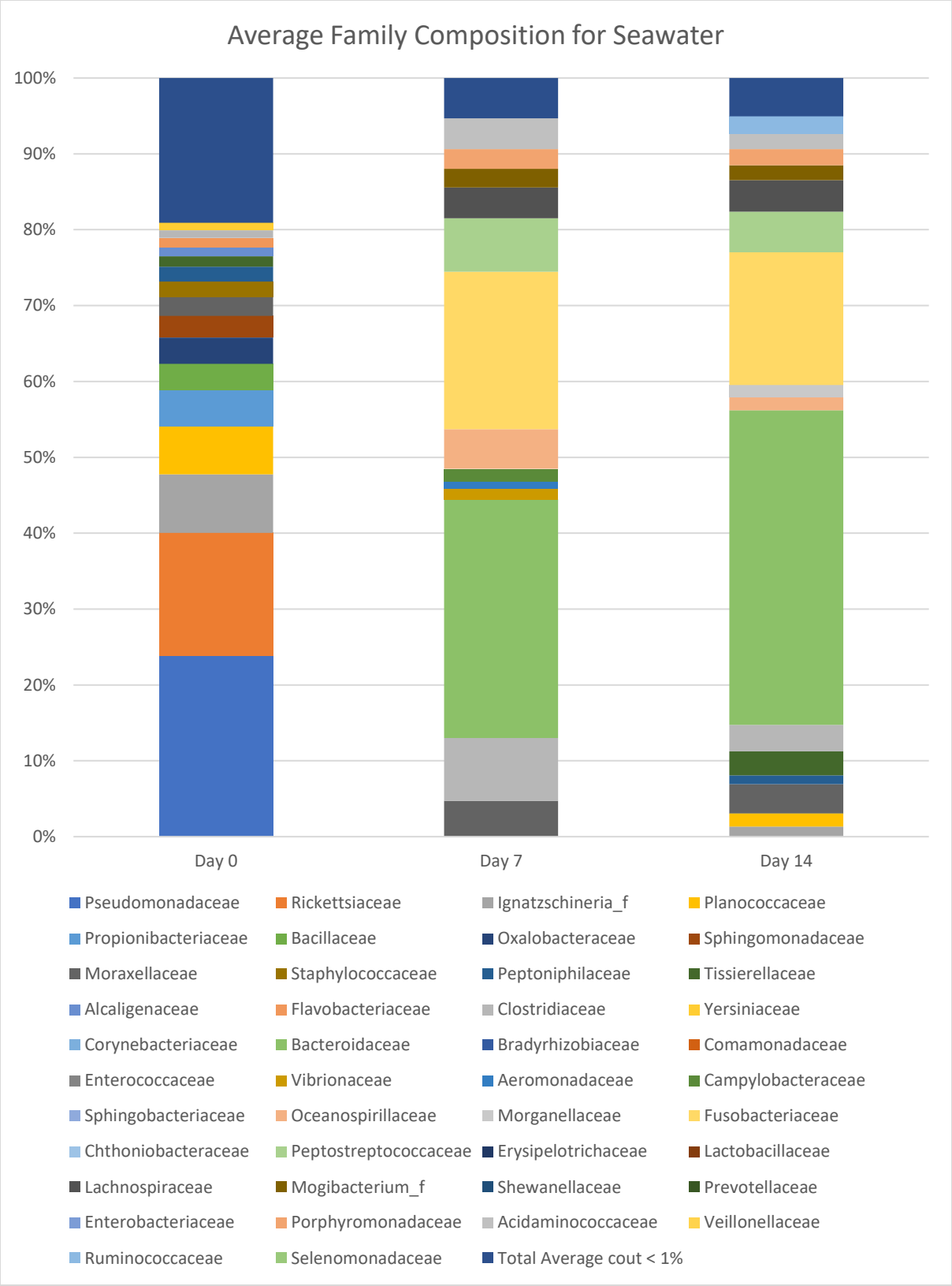

Figure 7.6 Displaying the average family composition for the seawater sample in respect to the decomposition day.

7.2.2.3 Brackish water

Pseudomonadaceae appeared to be the most dominant family in the community with an initial abundance on day 0 at 6%, decreased to 0.03% on Day 7, and not found on Day 14. Bacteroidaceae demonstrated steady increase in abundance, starting at 1% on day 0, a significantly rising to 28% by day 7 and reaching 37% on day 14, making them the dominant microbial family at this stage. This significant rise reflects Bacteroidaceae's role in later stages of decomposition, likely due to its ability to exploit the nutrient-rich environment created as decomposition progresses. Also, Moraxellaceae started with 8% on day 0, increased to 12% on day 7, and then insignificantly surged to 35% by day 14, becoming the second most dominant family. This indicates that their rise might be influenced by transient factors or competitive dynamics rather than a consistent ecological trend. Planococcaceae inhabited 9% on day 0, decreasing to 1.00% on Day 7 and 14. Propionibacteriaceae were noticed at % on Day 0 and were not detected on both Day 7 and Day 14. Campylobacteraceae were 4% on the onset of decomposition and elevated to be the third most abundant bacterial family on day 7 with 11%. Campylobacteraceae declined to 0% on day 14, indicating a fluctuating trend. Acidaminococcaceae displayed a consistent and significant increase over the observed sampling days. Acidaminococcaceae were not detected on day 0, but they were found to have significant increase be 1% and 4% on day 7 and 14. Rickettsiaceae (1%) and Staphylococcaceae (2%) appeared on day 0 but were not discovered in successive days of decomposition. Tissierellaceae exhibited a fluctuating pattern as the days of decomposition. On day 0, Tissierellaceae were 1%, they declined to 0% on day 7 and increased to 13% on day 14, making them the second largest residing bacterial family in the community on day 14. Ignatzschineria_f remained steady in the community at 3% on Day 0 and 7 and increased to 18% on Day 14, making them the second most populous bacterial family on day 14. Bacillaceae’s abundance in the community on day 0 started at 1.00% and increased to 2% on Day 7, and were not detected on day 14, indicating a varying pattern. Sphingomonadaceae (7%). The general PERMANOVA analysis of microbial families in the brackish water sample of decomposing pig overtime revealed a highly significant relationship shown in this community (Table 7.2), supporting the significantly discovered families.

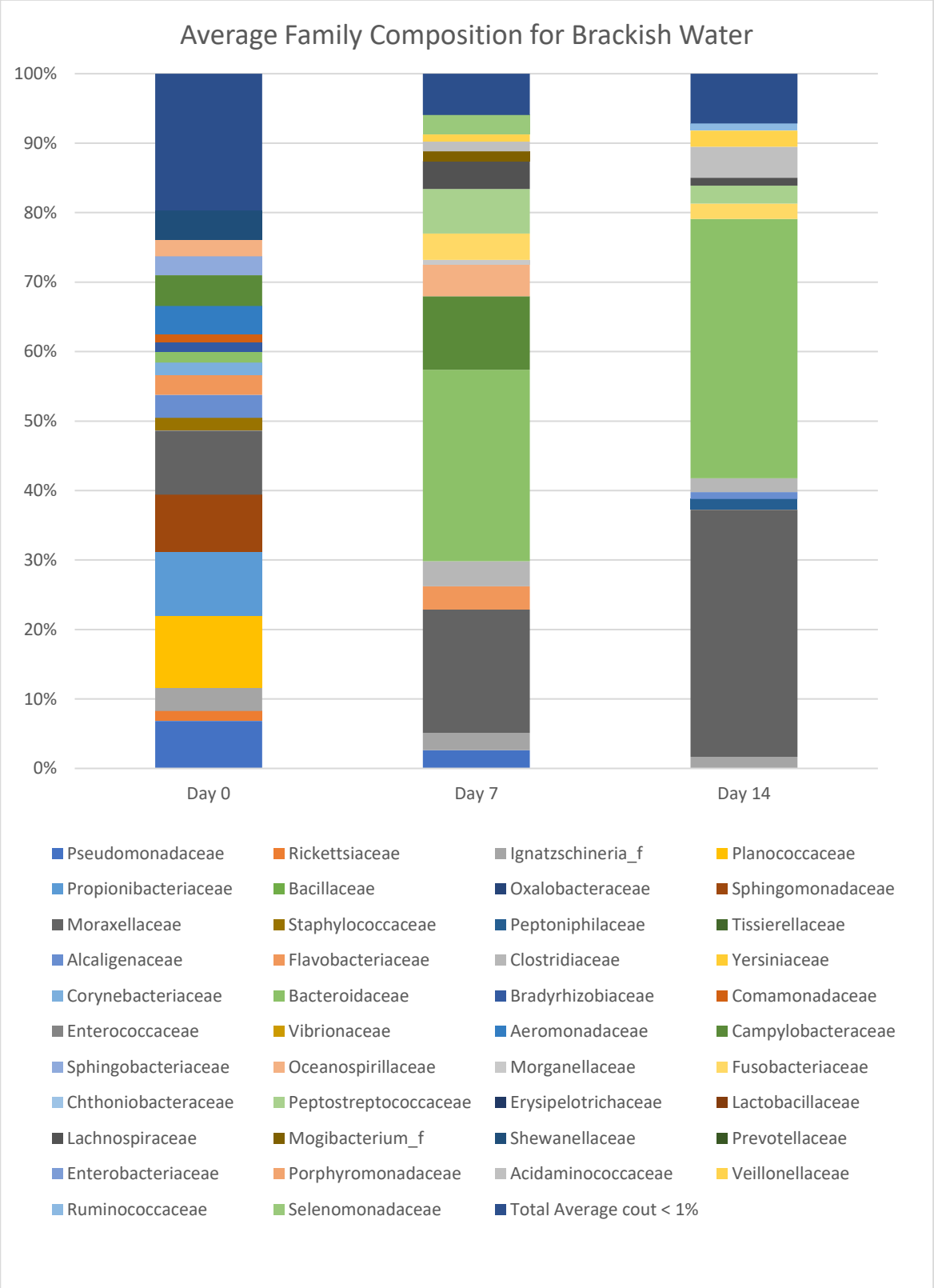

Figure 7.7 Displaying the average family composition for the brackish water sample in respect to the decomposition day.

7.2.2.4 Freshwater

In the freshwater decomposition environment, Pseudomonadaceae exhibited a significant increase in abundance, starting at 4% on day 0 and rising to 15% by day 7, where they became the dominant family. However, they disappeared by day 14. This significant increase highlights their early dominance in the decomposition process, likely due to their adaptability to the initial stages of nutrient release. Bacteroidaceae were not detected on day 0 but were discovered to be the third largest bacterial family on day 7 with 11.00% and reduced to 1% on day 14. Although the overall relationship was not significant, their notable rise on day 7 suggests a temporary ecological advantage during the intermediate stage. Ignatzschineria_f showed an initial presence of 7% on day 0, decreasing to 3% on day 7, but then became the most abundant family by day 14 at 18%. Despite these fluctuations, the lack of significant relationship implies that their dominance on day 14 might be due to their ability to exploit specific decomposition stage associated with rapid insect activities. Tissierellaceae and Peptoniphilaceae on day 0 were seen to be 9.00% and 4.00%, both dropped to 1.00% and increased to 13.00% and 14% respectively on day 14. Planococcaceae were the highest dominators of the community on day 0 with 42% and decreased to 10.00% on Day 7and 14. Propionibacteriaceae and Staphylococcaceae on day 0 were 6% and 2% respectively on day 0 and they were not found on Day 7 and Day 14. Bacillaceae initiated a 5% presence on Day 0, declined to 2% on Day 7, and was not sighted on day 14. Moraxellaceae amassed an abundance of 1% on Day 0, slightly increased to 0.02% on Day 7, and minorly decreased to 1% on day 14. Clostridiaceae and Peptostreptococcaceae displayed an increasing trend. They were noticed on day 0 to be 1% and 0%, then rose to 9% and 2% on day 7, with a further increase of 11% and 2% on day 14. The general PERMANOVA analysis of microbial families in the freshwater sample of decomposing pig overtime revealed a highly significant relationship shown in this community (Table 7.2), encouraging the significant rise of Pseudomonadaceae.

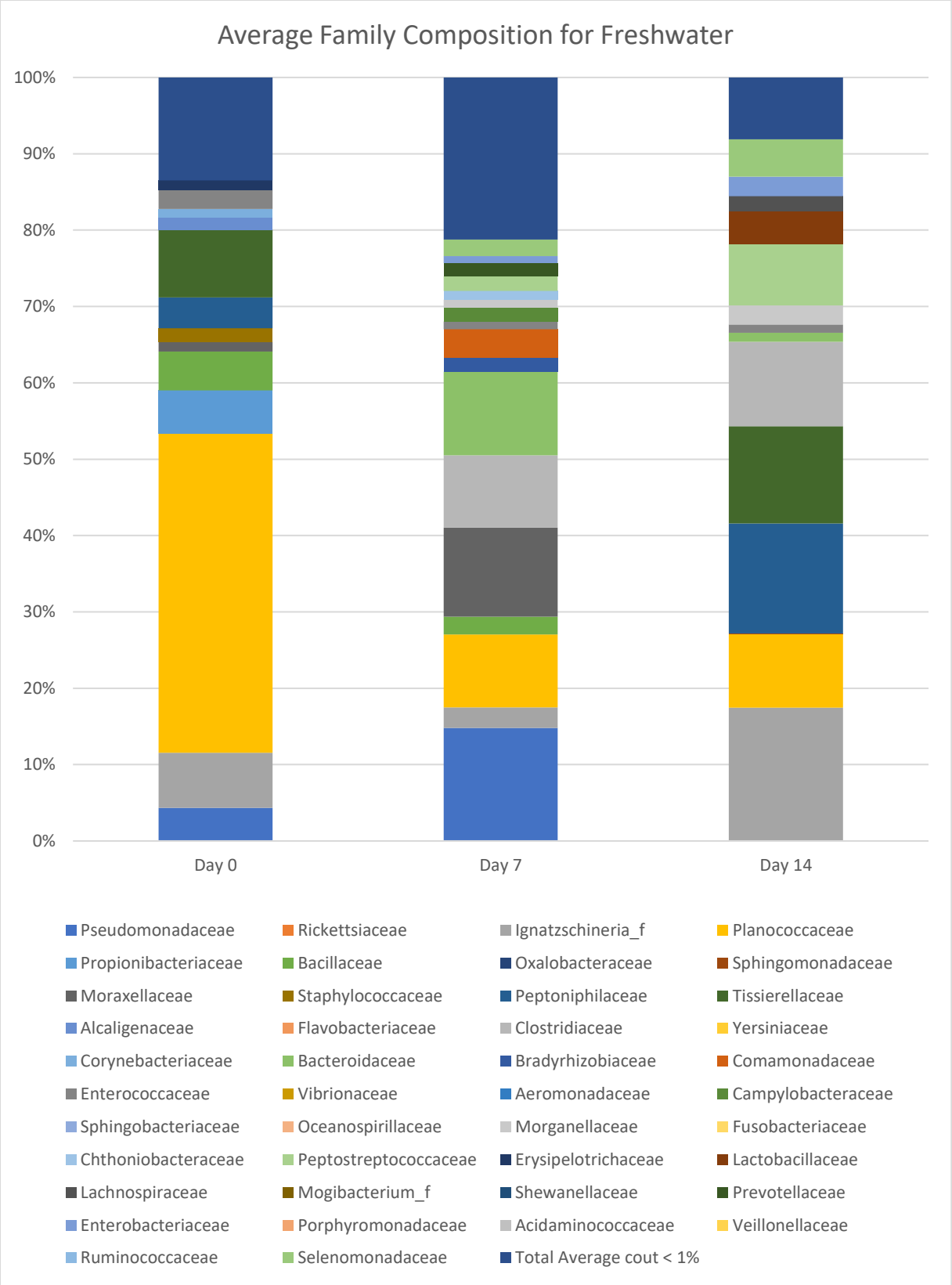

Figure 7.8 Displaying the average family composition for the freshwater sample in respect to the decomposition days.

7.2.3 *Families with Significant changes over time.*

This section presents the distribution of bacterial families across various sample types with highlights to taxa that exhibited significant differences in abundance, as indicated by an ANOVA test results (summarised in Table 5.3).

Table 7.2 Summary of betadisper Multiple dispersion and Individual ANOVA analysis of bacterial families over time on Environmental sample (soil, seawater, brackish water, freshwater). Significant values are highlighted.

Sample	**Multiple Dispersion Analysis Over Time**	**Individual Phylum**	**ANOVA Results**	**Significant Day**
Soil	$F_{4,10}$=0.8869, p= 0.506	Bradyrhizobiaceae	$F_{4,10}$= 2.816, p= 0.08391	
		Bacillaceae	$F_{4,10}$=1.05 p=0.4292	
		Chthoniobacteraceae	$F_{4,10}$=3.754 p=0.04083	Decrease on day 14 and 23
		Gemmataceae	$F_{4,10}$= 1.969, p= 0.1755.	
		Vicinamibacter_f	$F_{4,10}$=3.121 p=0.06574	
		Clostridiaceae	$F_{4,10}$= 2.351 p=0.1245	
		Chitinophagaceae	$F_{4,10}$ = 7.709, p = 0.004205	Decrease on day 14 and 23
		Solibacteraceae	$F_{4,10}$=1.541 p=0.2635	
		Planctomycetaceae	$F_{4,10}$=2.247, p =0.1365	
Seawater	$F_{2,3}$= 5.92e+29, p= < 2.2e-16	Pseudomonadaceae	$F_{2,3}$= 3.708, p= 0.1546	
		Rickettsiaceae	$F_{2,3}$=1.001, p= 0.4646	
		Ignatzschineria_f	$F_{2,3}$= 2.564 p=0.2242	
		Bacteroidaceae	$F_{2,3}$=4.548, p= 0.1235	
		Clostridiaceae	$F_{2,3}$=2.122, p= 0.2665	
		Moraxellaceae	$F_{2,3}$=1.379, p= 0.376	
		Fusobacteriaceae	$F_{2,3}$= 3.767, p= 0.152	
		Peptostreptococcaceae	$F_{2,3}$= 1.362, p= 0.3795	
		Planococcaceae	$F_{2,3}$=8.163 p= 0.06116	

Brackish water	$F_{2,3}$=1.13e+31, p= < 2.2e-16	Pseudomonadaceae	$F_{2,3}$=1.647, p= 0.329	
		Rickettsiaceae	$F_{2,3}$=0.5, p= 0.6495	
		Bacteroidaceae	$F_{2,3}$=97.45, p= 0.001866	Increase over time on day 7 and 14
		Moraxellaceae	$F_{2,3}$=2.451, p= 0.2339	
		Campylobacteraceae	$F_{2,3}$= 1.917, p= 0.2909	
		Propionibacteriaceae	$F_{2,3}$=1.285 p=0.3953	
		Acidaminococcaceae	$F_{2,3}$=20.4, p= 0.01793	Increase on day 14
Freshwater	$F_{2,3}$=5.84e+29, p= < 2.2e-16	Tissierellaceae	$F_{2,3}$=2.114 p= 0.2674	
		Propionibacteriaceae	$F_{2,3}$=3.054 p= 0.189	
		Peptoniphilaceae	$F_{2,3}$=2.946 p=0.1959	
		Ignatzschineria_f	$F_{2,3}$=6.132 p=0.08714	
		Pseudomonadaceae	$F_{2,3}$=46.48 p= 0.005461	Increase on day 7
		Moraxellaceae	$F_{2,3}$=7.401 p= 0.06917	
		Clostridiaceae	$F_{2,3}$=1.578, p=0.3402	
		Bacillaceae	$F_{2,3}$=1.012 p= 0.4615	
		Peptoniphilaceae	$F_{2,3}$= 2.946, p=0.1959	
		Tissierellaceae	$F_{2,3}$=2.114, p= 0.2674	
		Peptostreptococcaceae	$F_{2,3}$=3.928 p= 0.1453	
		Planococcaceae	$F_{2,3}$=0.5898 p= 0.6081	
		Bacteroidaceae	$F_{2,3}$=7.069 p= 0.07324	

The soil sample displayed overall community stability and a balanced community structure across the observed decomposition period, as noted at the phylum level. The stability of the bacterial communities in the soil sample over time was also indicated by the alpha and PD outcomes (Chapter 4, section 4.2.3.2.1). Noppol Arunrat *et al.* (2023), using 16S rRNA gene-based metagenomic analysis, also discovered that the bacterial richness, diversity, and composition in undisturbed soil samples were stable over a given period. Families like Chthoniobacteraceae (Verrucomicrobia) and Chitinophagaceae (Bacteroidetes) exhibited significant declining patterns in the soil sample, but their non-adaptive actions

were not affected by richness, evenness, and PD in the soil microbiome. Members of Verrucomicrobia are often characterised by slow growth rates (Bünger *et al.*, 2020) and are seen to have a low frequency in soil (Bergmann *et al.*, 2011), making them unable to compete with faster-growing bacteria. Chitinophagaceae are involved in the degradation of chitin, a polymer found in the exoskeletons of arthropods and fungal cells. Due to the reduction of insects in the later stages of decomposition, chitin might have been unavailable, negatively affecting the growth of Chitinophagaceae. The stability of the soil's alpha and diversity measures is further established by the regression and multivariate dispersion analysis, which also showed no significant relationship during the observed period of decomposition. Therefore, the interplay of the bacterial taxa in the soil microbiome appeared relatively stable over the sampling days, as no phyla were significant when individually tested against the days of decomposition. Members of Pseudomonadaceae (Pseudomonas) have been discovered to be the most abundant in freshwater settings (Batrich *et al.*, 2019) and are represented in other aquatic settings, possibly acting as waterborne opportunistic pathogens (Alatraktchi, 2022). At the family level, Pseudomonadaceae (Proteobacteria) were the only family in freshwater that was significant, with a notable inclination, especially on day 7 (which was the highest day for richness in the freshwater sample, [Chapter 4, section 4.2.3.2.4]). Additionally, certain species of Pseudomonadaceae possess advanced quorum sensing systems, allowing them to regulate group behaviours such as biofilm formation and the manufacture of various antimicrobial compounds, such as pyocyanin and other secondary metabolites (DeBritto *et al.*, 2020; Abdelaziz *et al.*, 2023; Bastos *et al.*, 2022; Lin and Cheng, 2019; Tuon *et al.*, 2022; Bastos *et al.*, 2022), which can enable them to inhibit the growth of competing bacteria on day 7 (putrefaction/active decay). The regression and multivariate dispersion analysis across the existing freshwater phyla over days showed a highly significant relationship, supported by the testing of Proteobacteria and Bacteroidetes, whose fluctuations were significant. The significant decline in the distribution of bacteria (evenness) in the brackish water (Chapter 4, section 4.2.3.2.3) could be attributed to the continuous increase of Bacteroidaceae (Bacteroidetes) and Acidaminococcaceae (Firmicutes) on day 14, as an increase in different bacterial groups could lead to reduced evenness in the community. Some Bacteroidaceae (Kumawat *et al.*, 2022; Ng *et al.*, 2023) and Acidaminococcaceae (Spelberg, 2013; Tseng, Nguyen, and Lin, 2023) strains may possess osmoadaptive mechanisms, making them well adapted to brackish water and giving them a competitive advantage. The distribution of bacteria in this community is further indicated by the significant relationship expressed by the microbial communities across days, as shown by the regression and multivariate dispersion analysis. However, the alpha and PD metrics in the seawater were also not statistically significant across the observed time points (4.2.3.2.2), aligning with the overall

regression and multivariate dispersion analysis of microbial taxa in the seawater, as there was no significant trend for families tested which is reflected in the biodiversity in the seawater.

7.3 CONCLUSION

In the aquatic community, statistically significant shifts in microbial composition were observed during decomposition and the trend might be influenced by multifarious interactions of biotic and abiotic factors. Proteobacteria, Firmicutes and Bacteroidetes appeared as key players in the microbial community that influence the temporal dynamics in the aquatic environmental samples, although Proteobacteria and Bacteroidetes declining patterns could not impact the biodiversity within the aquatic microbial communities. In soil, the stability of microbial communities, despite fluctuations in specific taxa like Chthoniobacteraceae and Chitinophagaceae, highlights the resilience and adaptability of the soil microbiome. The stability of the soil microbial communities even in the later stages of decomposition might suggest providing consistent biomarkers over time to aid PMI estimation. The significant changes in microbial families in aquatic environments (the decline of Pseudomonadaceae in seawater and the rise of Bacteroidaceae in brackish water) indicate that these environments may offer more precise temporal markers for PMI estimation. For instance, the notable increase of Bacteroidaceae in brackish water by day 14 could serve as a critical indicator of mid-decomposition stage, while the early dominance and subsequent disappearance of Pseudomonadaceae in freshwater and seawater may mark the initial phases of decomposition. Significant changes in these taxa at specific time of decomposition hold promise as indicators in forensic investigations, enhancing PMI estimations, providing forensic investigators with more refined microbial indicators to determine the time of death in various environmental contexts.

8.0 CHAPTER 8: GENERAL DISCUSSION AND CONCLUSION

8.1 INTRODUCTION

In this thesis, swine carcasses were used as proxies to extensively examine the dynamics of microbial taxa compositions on observed time points. The robustness of microbial communities of various ecological niche have been explored in this research. The study spanned from investigations of different body sites and internal organs (liver, lung, mouth, belly, anus) of pigs to the surrounding environment (soil, seawater, freshwater, brackish water) of the carcasses. EzbioCloud (www.ezbiocloud.com), a web-based microbiome taxonomic profiling (MTP) was employed for sequence matching, taxonomic assigning, and removal of chimeric sequences. The sequencing technology, read length, and the diversity of the microbial community are varying elements that can influence the performance of the algorithms (Logsdon et el., 2020; Huson *et al*., 2018). Regardless of the pipeline used, the depth and accuracy of the database influences the pipeline's ability to precisely ascertain and categories microbial taxa (Smith *et al*., 2022; Park *et al*., 2023). The selection of bioinformatics tools and databases can influence the metrics used for diversity analysis (such as alpha diversity), also varied algorithms employed by different tools in estimating diversity metrics can result in variations in the results for downstream analysis (De Santiago *et al*., 2021; Petit-Marty, Casas and Saborido-Rey, 2023). PKSSU4.0 is the latest version of database in EzbioCloud, and it aligns with the sequenced region of interest. PKSSU4.0 is the database used by EzbioCloud for the taxonomic profiling (Lindefeldt, *et al*., 2019; Kim, Kim and Jang, 2022; Iwatsuki *et al*., 2021), which includes information on the hierarchy of the taxa based on the 16S rRNA gene sequences. A comprehensive data overview of the NGS sequences was highlighted, emphasising the importance of data quality control measures, and suggesting its suitability for downstream analysis (Chapter 3). The downstream analysis entailed an integration of alpha and phylogenetic diversity analyses, and statistical approaches to unravel patterns in microbial communities of the samples. In the field of forensic microbiology and decomposition ecology, signatures of sequential changes of bacterial structure and the distribution of bacteria have been explored as markers of the PMI (Burcham *et al*., 2019). Significant differences in bacterial composition of body sites, internal organs, and environmental niche of swine carcasses on the initial time of decomposition were revealed in chapter 5. Chapter 6 and 7 revealed the succession and domination patterns of the bacterial taxa, which highlighted the complex interplay found in the samples used for this investigation.

8.2 MICROBIAL ECOLOGY DURING DECOMPOSITION OF THE BODY SITES ON PIG SAMPLE

There was no significant adjustment in total bacterial abundances in the mouth, anus, and belly samples. Nevertheless, alterations in community taxon proportions were observed. The mouth is home to one of the most diverse microbial ecological communities (Dong *et al*., 2019). One of the main areas of study for the engineering of human microbial communities is the oral cavity. It is the second-largest human microbial complex after the colon and one of the most populated sites in the human microbial community (Dong *et al*., 2019; Hou *et al*., 2022; An *et al*., 2022). This might be due to the mouth being the initial point of digestion and its moist environment (Caselli *et al*., 2020; Hou *et al*., 2022), hosting other sub microbial habitats like the buccal mucosa, tooth surfaces, gums, tongue, saliva, palate, and plaques (Hou *et al*., 2022). The mouth is also constantly exposed to external factors like air that can introduce a wide range of nutrients and environmental conditions that influence microbial growth and diversity. In the saliva, Firmicutes (Li *et al*., 2022) and Bacteroidetes (Könönen and Gursoy, 2022) are more abundant compared Actinobacteria and Fusobacteria that have more dominance in dental plaque (Li *et al*., 2022) and in this investigation, Bacteroidetes, Proteobacteria and Firmicutes were relatively the most abundant phylum in the mouth sample throughout observed period of decomposition, which is similar with the top 2 phyla (Proteobacteria and Firmicutes) found in the oral cavity of mouse models by Dong *et al*., (2019) and in human palates by (Ashe *et al*., 2021). Hyde *et al*. (2014) collected samples from 2 cadavers every 2 days for four weeks. The microbial content in both cadavers showed similar microbial succession pattern at the phylum level, with a domination of Proteobacteria in the early stage of decomposition and Firmicutes in the later stages of decomposition of oral samples. Members of the Flavobacteriaceae were noticed to fluctuate in the mouth community from day 2 to 4 and were not seen on the remaining sampling day of this investigation, although no significant impact was made by Flavobacteriaceae overtime, on day 0, they were only hosted by the mouth bacterial community. Flavobacteriaceae family can be saprophytic (break down complex organic compounds, such as remnants of food particles) or commensal to the of humans and animals (Jean-François Bernardet and Nakagawa, 2006; Lee *et al*., 2023) and some strains have been found on the mucous membranes in the mouth (Lapage *et al*., 1973), and other mucosal environments (Gabriel Marchesan Almeida *et al*., 2019; Tuttle *et al*., 2023; Holmes, 2006). Some bacteria from the Proteobacteria, Firmicutes, and Bacteroidetes are attributed to grow in biofilms community generally in the oral cavity (Fang *et al*., 2017; An *et al*., 2022) mostly because of the wet condition of the mouth. Also, the anus (Rectal orifices) in this investigation were characterised by colonisation by Firmicutes, Bacteroidetes, Proteobacteria as reported by Radhakrishnan *et al*., (2023) in their study while Actinobacteria competed strongly for dominate with the trio (Firmicutes, Bacteroidetes, Proteobacteria)

the bacterial microbiota of belly (outer skin surface). Firmicutes (Lactobacillaceae, Ruminococcaceae and Lachnospiraceae) were the most dominated sample in the anus sample until they were overthrown by Proteobacteria on the final observation day. The dominance of Firmicutes in the anus samples used in this study could be ascribed to the metabolic activities of complex polysaccharides and other sugar to manufacture butyrate and other SCFAs via hydrolysis (Fusco *et al*., 2023; Parada Venegas *et al*., 2019). In the gut, Bacteroidetes and Firmicutes are part of normal flora taxa composition (Bray, 2021) and the rectal orifice might be able to reflect the gut microbiome since they are connected. It is important to note the incision made on the belly region of the carcass for autopsy (Chapter 2 section 2.1.2.1), can influence the bacterial composition of the region or entire carcass. The bacterial microbes found in the belly region of pig carcasses used in this study may also represent migrated thanatomicrobial members that could have been uncovered prematurely due to the autopsy. Microbial succession pattern in skin and body orifices (excluding rectum orifices) of eight cadavers samples detected by Iancu *et al*., (2023), Firmicutes declined slightly as decomposition advanced, which were like the pattern found in belly (skin) microbiome of this research. Firmicutes, as seen in figure 6.1 (chapter 6, section 6.2.1.1), were also the most abundant phyla at the start to the putrefaction stage and were second most dominating taxa to the final stage of decomposition (day 23).

8.3 MICROBIAL ECOLOGY OF INTERNAL ORGANS OF PIG SAMPLES DURING DECOMPOSITION

It might be crucial to examine the microorganisms within internal organs during corpse decomposition as it can reveal the existence or absence, as well as the population count of specific bacteria, which can offer valuable insights into estimating early post-mortem interval (Liu *et al*., 2023). There was no significant change in total bacterial abundances in all samples from internal organs (liver and lung), nonetheless, a distinct alteration in both community composition and function was observed. While the relative population of samples in the internal organs did not show a significant or consistent trend over time (maybe due to rapid degradation and had day 4 as a final sample day). Individual bacterial taxa were noticed to be significant over the observed period. Post-mortem microbiome among organ tissues from the same human cadaver (Can *et al*., 2014) and same mouse cadaver (Dell'Annunziata *et al*., 2021) have been reported to be similar. Can *et al*. (2014) found Firmicutes to be abundance in the liver sample, all other internal organs and blood samples also, Dell'Annunziata *et al*., (2021) detected the liver and spleen as the first organs colonised by Firmicutes. In this research, the liver and lung were dominated by Firmicutes during the observed period of decomposition and its presence over time was more significant in the liver. The decrease of Bacteroidetes was significant in the lung bacterial community. Despite the

differences in animal model and conditions used in various research (Javan *et al*., 2017, Liu *et al*., 2022, Wang *et al*., 2022), the family of Clostridiaceae has appeared as a dominant bacterial taxon. Although the liver samples in this research were conducted in a terrestrial environment, amongst other notable taxa connected to aquatic environment Wang *et al*., (2022) detected organisms linked to the family of Clostridiaceae in mouse liver on freshwater immersion for 0 to 14 days. Clostridiaceae in both organs was noticed to have an increased presence at the start and end bloat stage of decomposition in this research, although not significant, they were less dominate on day 0, but as decomposition advanced, they joined the most dominate up until day 4 when the liver sample degraded. The increment of Clostridiaceae may be a result of a fall in cell oxygen levels after death, were there is a rapid proliferation of anaerobic microorganisms belonging to the Clostridiaceae family, which are assumed to disintegrate lipids and complex carbohydrates that constitute the human tissues (García *et al*., 2020). Lactobacillaceae in the liver sample of this investigation was found to constitute 5% of the total bacterial community but had a tremendous increase to about half the size on day 2 and 4 (start and end bloat stage).

Although the lungs were once thought to be sterile, current research has revealed the presence of microbial communities in human lungs (Huang *et al*., 2018, Beck *et al*., 2012, Moffatt and Cookson 2017). Members from the Lactic acid bacteria (LAB) group of bacteria have been recovered from the lungs of humas (Stankovic *et al*., 2022), rats (Zhao *et al*., 2023), and swine (Huang *et al*., 2019) and ninety-six LAB strains have been discovered in commercial swine (Huang, *et al*. 2020b), although LAB play a crucial function in the health of a pig and are utilised as a probiotic in swine diets (Liao and Nyachoti, 2017; Yang *et al*., 2015; Zhu *et al*., 2022; Shim, 2005; Sirichokchatchawan *et al*., 2018). Probiotic lactic acid bacteria can inhibit or destroy victimised cells by pore formation, display antimicrobial function against other bacteria (Anjana and Tiwari, 2022; Lee, Chung and Seo, 2013; Adeniyi, Adetoye and Ayeni, 2015; Johansen, 2014). The lung microbiome is a diverse community of bacteria located in the lower respiratory tract, and some of these bacteria may play critical roles in maintaining body health of the host (Huang *et al*., 2018). There are clear distinctions in the microbial community structure of a healthy lung compared to disease-infected lungs of animals and humans (Huang *et al*., 2018). Flavobacteriaceae were noticed only on day 0 in the bacterial community of the lungs occupying 2%. Yoshizawa *et al*., (2022) discovered genera belonging to Lactobacillaceae and Streptococcaceae, which are facultative anaerobic bacteria and were dominant in the microbiota of six human cadavers. The result of this study showed the family of Streptococcaceae was among the dominant family on day 2 and occupied just about 1% of microbial taxa on day 4. Lactobacillaceae was not only evidently seen in the microbial taxa on decomposition days but had a rise from day 0 (14%) to day 2 (29%) and day 4 (30%). Lactobacillaceae were responsible for the

consistent and statistically significant increase of Firmicutes in the lung sample across the observed decomposition period of this research. Members belong to the Firmicutes phyla have previously been suggested as a potential indicator for PMI (Li *et al*., 2021; Tozzo *et al*., 2022). Burcham *et al*. (2019) tested lung sample and found.

8.4 MICROBIAL WATER ECOLOGY DURING DECOMPOSITION

Dickson *et al.* (2011) revealed microbial communities on submerged pig heads decomposing in the water system (Otago, Harbour, New Zealand). The group carried out their research in winter and summer and reported a succession-like colonisation pattern of microbial communities and discovered mostly Proteobacteria as the dominating phyla in both seasons (Dickson *et al.* 2011). Benbow *et al.*, 2015 used stillborn swine carcasses as models to examine freshwater decomposition during winter and summer seasons. They revealed epinecrotic communities (Proteobacteria and Firmicutes) as the most abundant phyla present on the swine carcass, which also conforms with the inverse relationship of both phyla seen in the aquatic samples of this study (Proteobacteria remained dominant during the observed period, while Firmicutes fluctuated in abundance). The relationship between Firmicutes and Proteobacteria can be seen in other investigations that account for pig carcasses in aquatic environments (Dmitrijs *et al.*, 2022; Diao *et al.*, 2017). Dmitrijs *et al.* (2022), in their research, examined drowned swine carcasses; Firmicutes and Proteobacteria emerged as the most abundant phyla before the carcasses were submerged. Wang *et al.* (2022) also found Proteobacteria, Firmicutes, and Bacteroidetes in high abundance throughout the decomposition process in carcasses in the water samples. Bacteroidetes, Proteobacteria, and Firmicutes played a major role in shaping microbial communities in all water samples of this research. Decomposition in marine environments can be different compared to other settings; moreover, the temperature, oxygen, and pressure levels in the deep sea are different from those in other niches such as soils (Wang *et al.*, 2020). Proteobacteria are recognised to tolerate high saline environments (Zheng *et al.*, 2017); also, inclined salinity can increase the interaction and prevalence of certain bacterial phyla such as Proteobacteria, Bacteroidetes, and Firmicutes (Yang *et al.*, 2023). But in the sea sample of this research, Proteobacteria declined substantially compared to the brackish water sample, which had reduced salinity levels. This could be as a result of families of Betaproteobacteria (Pseudomonadaceae and Moraxellaceae) that do not tolerate high salinity (Ji, Yu, and Guo, 2023). Heterophilic bacteria utilise carbon for their energy source and were also present in all water types due to the organic matter in the water samples (Matti *et al.*, 2023).

8.5 MICROBIAL SOIL ECOLOGY DURING DECOMPOSITION

According to studies, each gramme of soil contains about eight million different types of bacteria (Olakanye & Ralebitso-Senior, 2022). As decomposition progresses, microbial communities are likely to interact with grave soil throughout decomposition process and affect the overall microbial ecology of the associated soil (carter *et al*., 2015). Biotic stress brought on by climate change can alter the variety and functioning of soil microbes (Dutta & Dutta, 2016). Results from this study indicated that bacterial soil ecology was stable in the summer compared to Carter *et al*. (2015) that particularly demonstrated how the microbial communities found in gravesoil of pigs (*Sus scrofa domesticus*) were more stable in the winter than they were in the summer. Enzymatic digestion, microbial activity, and appropriate environmental factors all work together to mediate the complicated process of decomposition, which eventually results in nutrient transfer from the cadaver to the immediate ecosystem (Olakanye & Ralebitso-Senior, 2022), therefore, it might a surprise to see that in this research bacteria communities detected throughout decomposition on the pig carcass laid on the soil did not significantly alter the microbial community in the soil. The order of succession in the microbial community in the soil did not change as much. The dominating taxa from day 0 was still dominating till the end of sample collection. Nevertheless, the pigs were laid on soil on day 2 (which is the onset of decomposition) of decomposition and some nutrient may have been purged out of the pig carcass before they were transported to the soil. The absence of these key microbial communities from pig carcasses the bloat stage might be responsible for the stable microbial soil communities through decomposition. Studies have examined bacterial communities and succession on other vertebrates such as rat for example Metcalf *et al* (2013) studied the necrobiome of decomposing murine in soil in a controlled laboratory setting. They discovered that microbiomes varied across different body sites but changes in a successive fashion as decomposition carried on. The results of this study revealed by the bacterial communities on the pig carcass, as compared to reports from other studies that soil bacterial comm similar findings reported in Metcalf *et al*., (2013); Cobaugh *et al*., (2015), that showed the decrease of Acidobacteria in the soil sample, which might be caused by an increase in soil pH after the breakage of the carcass and release of ammonia-rich fluids (Metcalf *et al*., 2013). Members from the Proteobacteria phyla were noticed to inclined throughout the observed time and emerged the most abundant decay (putrefaction and carnivores) to the dry (skeletonization) stage soil samples. This also conforms to the results of Metcalf *et al*., (2013) that showed an increase in the members of the Proteobacteria phyla after post-Rupture stage to dry remains of their investigation (Metcalf *et al*., 2013; Deel *et al*., 2021; Cobaugh *et al*., 2015), suggesting that Proteobacteria are characterised by comparatively higher nutrient availability and can outperform Acidobacteria (Metcalf

et al., 2013). Putrefaction as explain in the introductory chapter is the known process that promotes bacterial proliferation on carcass or cadavers when death occurs and results in gas build up and tissue breakdown. The soil was not influenced much by the bacterial communities on the pig carcass as compared to reports of other studies that soil bacterial communities changed significantly when purging of nutrient from the gut invaded the soil underneath the carcasses (Ewald, 2021). This might be due to loss of nutrients that could have contained bacterial communities during and after autopsy performed on the pig carcasses. The pig carcasses were left to decompose on a surface with the sackcloth before being deposited on the soil on day 2 of decomposition and this might have encouraged further loss of post-mortem bacterial communities because microbes may have transmitted to the initial decay platform.

8.6 MICROBIAL ECOLOGY ASSOCIATED WITH INSECTS DURING DECOMPOSITION.

Another noteworthy attribute connected with post-mortem microbial investigations is the impact of insects invading the microbiome on corpses (Speruda et al., 2022). According to Hyde et al. (2014), after purge (visibly seen when the bloated carcass is ruptured), there was an increase in the members of Ignatzschineria bacteria. This is not surprising, as members of this group are associated with adult flies and larvae (DiFranza et al., 2021; DeBruyn and Hauther, 2017; Deguenon et al., 2019; Muse et al., 2017; Iancu, Necula-Petrareanu, and Purcarea, 2020) and insect activities, which proliferated after purge. The family that is strongly linked with fly larvae and mature insects was detected on the pig carcass as decomposition progressed. On day 4, the pigs had reached the bloat stage, and in the mouth sample, Ignatzschineria_f was detected, occupying 6% of the bacterial community, which increased on day 7 as decomposition advanced. In the freshwater sample, they were the most populous family on day 14. The partial skeletonisation of pigs (day 14) did not keep the presence of Ignatzschineria_f reduced because decomposition is slow in aquatic environments, and there will be much nutrient for insect activities as decomposition occurred in a tightly covered container. In the belly sample on day 7 (advanced decay), Ignatzschineria_f composed 60%, representing the high interaction between insects and pig carrion (voracious feeding on the host and possible reproduction of insects on the host). Harrison et al. (2020) also performed experiments using pig analogues and discovered Ignatzschineria in the advanced phase of decay. Ignatzschineria is a group of bacteria that fall into the aerobic, gram-negative category, belonging to the class of Gammaproteobacteria; they are usually non-spore-forming, non-haemolytic, and rod-shaped in nature. It might not be out of place to say that insects colonising the decomposing carrion might introduce bacteria to the carrion and can affect the dynamics of the microbial community structure and function (Pachal et al., 2013). From the initial stage of decomposition, insects form a component of primary colonisers and can impact the initiation of bacterial communities specific to the carcass, which

might influence the integrity of the microbial community as decomposition advances (Harrison, 2018). Lactobacillaceae, Pseudomonadaceae, and Enterobacteriaceae have been associated with the gut of insect larvae (Magagnoli et al., 2022; Paniagua Voirol et al., 2018; Gu et al., 2023; Wang, Liu, and Yin X, 2022). The study by Iancu, Necula-Petrareanu, and Purcarea (2020) on the transfer of Ignatzschineria and Wohlfahrtiimonas chitiniclastica from Lucilia illustris (Diptera: Calliphoridae) immature stages to the colonised tissues showed that bacterial species increased as the insect life stages progressed. Although the impact of these microbes can be multifaceted, the general increase of Lactobacillaceae in the internal organs across the observed period (liver sample; 5% - 59%; lungs 14% - 30%) might also indicate the targeted feeding on the internal organs by insect larvae, as these were the first samples to be degraded by decomposers. The decline of Pseudomonadaceae in brackish water (6% - 0%) and seawater (24% - 0%) from the onset to the final sample day may be impacted by the changes in water quality, including salinity and the chemical composition present in brackish water and seawater, which can reduce insect and microbial activities. Enterobacteriaceae had their highest presence in the anus sample on day 4 (12%), which is the end of the bloat stage. The metabolic by-products produced by Enterobacteriaceae, Lactobacillaceae, and Pseudomonadaceae during decomposition may emit chemical signals that attract insects.

8.7 TEMPORAL CHANGES IN BACTERIAL COMMUNITIES AS A TOOL FOR POST-MORTEM INTERVAL INVESTIGATION

To successfully admit microbial evidence for validation in forensic investigations, Metcalf (2019) proposed the identification of needs, primary research, the development of prototypes, validation and acceptance, ultimately resulting in integration. The processes proposed by Metcalf (2019) might involve the utilisation of microbial technologies, which can be more effective through collaboration and communication between researchers and the medicolegal community (Roy *et al.*, 2021). PMI examination can be a challenging task (Guo *et al.*, 2016). However, how to correctly predict the PMI, or the time since death of an organism, individual, or group of individuals, is an important question in a medicolegal death investigation procedure (Bala and Sharma, 2016; Shedge *et al.*, 2020). Utilising the microbial taxa appearing on a corpse and in soil throughout the course of decomposition might be a valuable technique for advancing PMI evaluations (Procopio *et al.*, 2019). The data from this investigation offer further evidence to contribute to establishing a linear relationship for using bacterial taxa as a potential instrument for forensic objectives (Guo *et al.*, 2016). A fundamental approach to understanding the temporal changes in microbial communities during decomposition involves collecting time-series samples (Chitra Jangid and Dalal, 2023), which can establish the linear relationships in the examined microbial

communities. This study highlights the potential of microbial taxa and their temporal and spatial variations, which may have been influenced by biotic and abiotic factors, as indicators for PMI estimation. Specific communities harboured distinct microbial populations that might indicate forensic relevance. There were bacterial families found on the initial day of decomposition that were peculiar to the sample type (anus, mouth, soil, and water samples), i.e., they were found existing on day 0 in just the respective communities (Appendix 3, Table A3.1 – A3.4). This could be due to the unique nutrient and environmental conditions (such as salinity, pH, and temperature) of these ecological niches.

The internal organs (lungs) showed dynamic changes in species richness over time, whereas environmental samples (soil) were more resilient to external influences and remained stable. The decline in microbial evenness over time (internal organs) suggests that dominant bacterial species can serve as markers of later decomposition stages. In Chapters 6 and 7, in the pig, (liver: Lactobacillaceae; mouth: Tissierellaceae, Pseudomonadaceae; anus: Bacteroidaceae, Ruminococcaceae; belly: Tissierellaceae, Clostridiaceae, Corynebacteriaceae) and environmental samples (soil: Chitinophagaceae, Chthoniobacteraceae; freshwater: Pseudomonadaceae; brackish water: Acidaminococcaceae, Bacteroidaceae) were detected to have a significant impact on their communities, supporting the idea that specific bacterial taxa, rather than entire microbial communities, is more reliable for PMI estimation. The microbial signatures in the belly indicated high levels of Corynebacteriaceae on day 0, which decreased over time, while Clostridiaceae increased over time (mid-stage decomposition to advanced stage decomposition), indicating a reliable temporal shift that correlates with the decomposition timeline. Similarly, in aquatic environments, the rise of Bacteroidaceae in brackish water around day 14 serves as a potential marker for the mid-decomposition stage. These taxa' temporal variations in abundance across different body sites and environments can establish a baseline for tracking decomposition progress. Iancu *et al.* (2023) noted Firmicutes as a constant marker between different body areas, and in this research, at the phylum level, they were found to be significant markers in the mouth and liver samples. Actinobacteria and Bacteroidetes were also important markers in the belly and lung, while in the environmental samples, Protobacteria (seawater, freshwater) and Bacteroidetes (freshwater and brackish water) were significant. The Multiple Dispersion Analysis Over Time results from chapters 5 to 7 suggest that while the overall microbial community (belly, anus, mouth, liver, lungs, soil) diversity may not always provide a straightforward linear progression for PMI estimation, targeted analysis of specific bacterial taxa within body sites and environmental samples can offer a more precise temporal marker. The significant taxa responsible for temporal dynamics in the pig and body site (Chapter 6) and the environmental samples (Chapter 7) were identified, and those taxa can be significant indicators of PMI based on their linear

relationship with days. This can be subject to further checks, as the basis and limitations of this research discussed in the sections below can be crucial parameters to consider. Additional research is needed to assess the overall applicability of the predictive model (Zhou and Bian, 2018).

8.8 BIASES IN THIS STUDY

Pig carcasses were autopsied (Chapter 2, section 2.2.2.1). There is a possibility that the carcass may not be completely sealed off from the outside environment even after the incisions are sewn up following the internal organ sampling. This can introduce bacteria from the surrounding environment into the body cavity and contaminate the sampled organs. This contamination might potentially alter the microbial diversity and composition, which may then yield inaccurate results. The rate of the natural decomposition process of the pig carcasses may also be affected after sampling the organs; for instance, as the organs are dissected, microbial communities that can be regarded as primary decomposers are altered, which could lead to false findings. The efficiency of the sewing process in minimising external contamination and ensuring consistency in organ dissection across different time points or carcasses varied. Variability in the efficacy of stitching up the pig carcasses may introduce inconsistencies in the samples gathered from different pigs, affecting the reliability and comparability of the results. The competence in extracting DNA can be subject to the experimental protocol (which might depend on sample type) and may vary among different microbial taxa (Nayfach and Pollard, 2016; Flint *et al.*, 2022). The variation in the recovery of DNA from different microbial taxa could be influenced by the type of environmental sample, such as soil samples, that may possess compounds such as polysaccharides, humic acids, and phenolic compounds that could inhibit downstream PCR amplification. In this study, the soil had a different extraction protocol and was tested for inhibition (Lim *et al.*, 2017; Hu *et al.*, 2015; Wydro, 2022). Bacterial cells, particularly Gram-positive bacteria that can possess tough cell walls, may experience challenging cell lysis during DNA extraction, leading to reduced DNA yield (Roopnarain *et al.*, 2017). Some Gram-negative bacteria may have an outer membrane or form endospores, like Firmicutes, which possess highly resistant structures that might be difficult to break during DNA extraction (Knüpfer *et al.*, 2020). These factors mentioned as possible influences during extraction can potentially affect the relative abundance of bacterial populations in downstream analyses.

Bacterial species are ubiquitous in nature and in every ecological niche on earth, and cross-contamination between samples can easily occur. To prevent inconsistent results brought about by contamination or modification of the microbiomes, it would be practical to strengthen standardisation in the sample collection, storage, and analysis processes (García *et al.*, 2020). This would aid the outcomes of

investigations to be more widely accepted, primarily regarding forensics or clinical affairs (García *et al.*, 2020). It is not surprising that the negative controls (extraction and PCR blanks) have some level of contamination. Other studies have reported the ubiquitous nature of contaminating DNA from widely used DNA extraction kits and laboratory reagents, as well as the significant negative effects on data analysis in downstream experiments such as PCR-based 16S rRNA gene surveys and shotgun metagenomics (Salter *et al.*, 2014; Glassing *et al.*, 2016). Additionally, the PCR sample used by Glassing *et al.* (2016), which contained only water and no DNA template, was found, using Illumina MiSeq 16S rRNA gene microbiota sequencing, to have a plethora of bacterial contaminants.

Although primers for the pre-NGS PCR amplification are specifically recommended for this type of metagenomic analysis and can capture the target region, there were differences in amplification success. The environmental samples produced better amplicons in the pre-NGS PCR amplification step. The environmental samples yielded amplicons for all sampling days, whereas samples from days 7 and 14 for the mouth, belly, and anus barely produced amplicons for NGS. This might be because either the gDNA extractions on those sampling days were not successful (regardless of the high amount of DNA indicated by the Nanodrop results, appendix 1, table A1) or the intense interplay of all agents of decomposition on those days produced substances that could inhibit pre-NGS PCR amplification. The mouth, belly, and anus that did not produce amplicons were reamplified with adjusted annealing temperatures and extension times, but they still did not produce results. The soil samples were selective of the master mix and only amplified using a different master mix from the other samples.

8.9 LIMITATIONS OF THIS RESEARCH

In this study, swine carcasses were utilised as non-human models, as mentioned in the introduction chapter. The findings from this experiment might not be directly comparable to human carcasses, as the rate of decomposition is different in pigs and human carcasses (DeBruyn *et al.*, 2021; Knobel *et al.*, 2018), which might be due to interspecies differences. As shown in Chapter 2, section 2.1, the number of proxies, however, in both the pilot and main studies was limited. The generalisability of the findings may be impacted by the limited sample size (body sample sites not equally represented, number of swine carcasses) (Fox *et al.*, 2009; Lakens, 2022). Additionally, replication of the experimental procedure will enhance accurate statistical analysis and the trustworthiness of observed patterns in the samples (Filazzola and Cahill, 2021; Nosek *et al.*, 2022). This research was conducted in a single location (Chapter 2, section 2.1); microbial communities are influenced by geographic factors (such as soil composition and climate) that differ in various locations (Kozjek *et al.*, 2022; Fillinger, Hug, and Griebler, 2019). These

variations might not be fully captured in this single location. During the course of decomposition, uncontrolled external variables, such as weather conditions, could introduce confounding factors. The DNA-based technique for microbial analysis accounts for both living and dead microbial cells (Emerson *et al.*, 2017; Rogers *et al.*, 2010), which might affect the reliability of microbial populations and trends associated with decomposition.

8.10 FUTURE RESEARCH

Longitudinal studies on repeated samples over an extensive period for more accurate PMI predictions should be considered. Functional metagenomic analyses of the specific roles of bacterial members in various communities can be carried out to understand their contributions to the ecosystem. Environmental variations can impact bacterial communities responsible for decomposition in a predictive manner with respect to the post-mortem interval (Burcham *et al.*, 2019). Unfortunately, this research did not cover examinations of these environmental variations, insect activity, or pig carcass body temperature, all of which can improve the quality of PMI investigations. Investigating external factors, such as weather conditions, that may influence the observed trends in microbial communities during decomposition would be ideal. Microbial evidence for PMI investigations remains a contentious issue regarding evidence admissibility in the courtroom. These issues may arise from the rules and regulations of the criminal justice system in a country (Roy *et al.*, 2021). Validation of the robustness of the statistical methods that should reflect parameters shaping microbiome composition might still be an issue (Clarke *et al.*, 2017; Gouello *et al.*, 2021), as it can potentially be perplexing for the jury to consider the different factors impacting the statistical interpretation (Roy *et al.*, 2021). Further examination of the applicability of these detected microbial communities for accurate PMI estimations in forensic analyses, as well as a defined legal framework for microbial evidence admissibility in court, should be considered since the judiciary systems in every country are different. For the past few decades, post-mortem microbial communities have been making waves in forensic research. Scientists are working round the clock to understand how the cause of death plays a crucial role in the dynamics of decomposition. This is influenced by varying factors such as time, season, and site of decomposition. Adult pigs were employed for this study as proxies for human cadavers, so in contrast to studies involving children, the results can offer microbial data useful for investigations concerning crimes involving adults. Additionally, the results from the current research can provide information on aquatic microbiomes in the event of an investigation that might involve water submersion. Future studies on bacterial succession patterns in decaying plants, humans, and animal carcasses can improve the existing protocols in forensic microbiology.

8.11 CONCLUSION

In this post-mortem study, the pattern of relative abundance and the succession pattern among bacterial decomposers varied across sample types. The aquatic sample can be suggested to the community of forensic microbiologists as having potential for PMI investigation in the case of drowning or crime that involves aquatic decomposition, as all water types showed significant changes over time and contained identifiable taxa responsible for those significant temporal changes. The decomposition of pig carcasses gave bacterial species from different lineage an opportunity to create an organic environment that played a crucial role in microbial interactions and activities on host and neighbouring environment. The complexity of the microbiome and the dynamic changes observed during decomposition of the pig carcasses demonstrate the challenges of this type of analysis; and no significant changes over time were demonstrated at the community level. However, the abundance of specific taxa did vary significantly suggesting an approach targeting specific indicator species may prove useful. This study can add to the body of work already established in finding post-mortem bacterial trends for PMI predictions. The specific taxa and the mechanisms through which internal and external factors exert influence on the bacterial communities their abundance should further be examined.

REFERENCE LIST

Abdelaziz, A., Abo, A.M., Al-Monofy, K.B. and Al-Madboly, L.A. (2023). Pseudomonas aeruginosa's greenish-blue pigment pyocyanin: its production and biological activities. *Microbial Cell Factories*, 22(1). doi:https://doi.org/10.1186/s12934-023-02122-1.

Acharya, K., Khanal, S., Pantha, K., Amatya, N., Davenport, R.J. and Werner, D. (2019). A comparative assessment of conventional and molecular methods, including MinION nanopore sequencing, for surveying water quality. Scientific Reports, [online] 9(1). doi:https://doi.org/10.1038/s41598-019-51997-x.

Adeniyi, B., Adetoye, A. and Ayeni, F. (2015). Antibacterial activities of lactic acid bacteria isolated from cow faeces against potential enteric pathogens. African Health Sciences, 15(3), p.888. doi:https://doi.org/10.4314/ahs.v15i3.24.

Adserias-Garriga, J., Quijada, N.M., Hernandez, M., Rodríguez Lázaro, D., Steadman, D. and Garcia-Gil, L.J. (2017). Dynamics of the oral microbiota as a tool to estimate time since death. Molecular Oral Microbiology. doi:https://doi.org/10.1111/omi.12191.

Alatraktchi, F.A. (2022). Rapid measurement of the waterborne pathogen Pseudomonas aeruginosa in different spiked water sources using electrochemical sensing: Towards on-site applications. Measurement, [online] 195, p.111124. doi:https://doi.org/10.1016/j.measurement.2022.111124.

Al-Awadhi, H., Dashti, N., Khanafer, M., Al-Mailem, D., Ali, N. and Radwan, S. (2013). Bias problems in culture-independent analysis of environmental bacterial communities: a representative study on hydrocarbonoclastic bacteria. SpringerPlus, [online] 2(1), p.369. doi:https://doi.org/10.1186/2193-1801-2-369.

Albuquerque, L., da Costa, M.S. (2014). The Family Gaiellaceae . In: Rosenberg, E., DeLong, E.F., Lory, S., Stackebrandt, E., Thompson, F. (eds) The Prokaryotes. Springer, Berlin, Heidelberg. https://doi.org/10.1007/978-3-642-30138-4_394

Almulhim, A.M. and Menezes, R.G. (2020). Evaluation of Post-mortem Changes. [online] PubMed. Available at: https://www.ncbi.nlm.nih.gov/books/NBK554464/.

Anjana and Tiwari, S.K. (2022). Bacteriocin-Producing Probiotic Lactic Acid Bacteria in Controlling Dysbiosis of the Gut Microbiota. Frontiers in Cellular and Infection Microbiology, 12. doi:https://doi.org/10.3389/fcimb.2022.851140.

Apprill, A., McNally, S., Parsons, R. and Weber, L. (2015). Minor revision to V4 region SSU rRNA 806R gene primer greatly increases detection of SAR11 bacterioplankton. Aquatic Microbial Ecology, 75(2), pp.129-137.

Arenas, M., Pereira, F., Oliveira, M., Pinto, N., Lopes, A.M., Gomes, V., Carracedo, A. and Amorim, A. (2017). Forensic genetics and genomics: Much more than just a human affair. PLOS Genetics, [online] 13(9), p.e1006960. doi:https://doi.org/10.1371/journal.pgen.1006960.

Ashe, E.C., Comeau, A.M., Zejdlik, K. and O'Connell, S.P. (2021). Characterization of Bacterial Community Dynamics of the Human Mouth Throughout Decomposition via Metagenomic, Metatranscriptomic, and Culturing Techniques. Frontiers in Microbiology, 12. doi:https://doi.org/10.3389/fmicb.2021.689493.

Atasoy, M., Eyice, Ö. and Cetecioglu, Z. (2020). Volatile fatty acid production from semi-synthetic milk processing wastewater under alkali pH: The pearls and pitfalls of microbial culture. *Bioresource Technology*, 297, p.122415. doi:https://doi.org/10.1016/j.biortech.2019.122415.

Bala, M. and Sharma, A. (2016). Post-mortem Interval Estimation of Mummified Body Using Accumulated Degree Hours (ADH) Method: A Case Study from Punjab (India). Journal of Forensic Sciences & Criminal Investigation, 1(1). doi:https://doi.org/10.19080/jfsci.2016.01.555552.

Baldani, J.I., Videira, S.S., Teixeira, K.R.D.S., Reis, V.M., de Oliveira, A.L.M., Schwab, S., Maltempi de Souza, E., Pedraza, R.O., Divan Baldani, V.L. & Hartmann, A. (2014). The Family Rhodospirillaceae. In: Rosenberg, E., DeLong, E.F., Lory, S., Stackebrandt, E., Thompson, F. (eds) The Prokaryotes. Springer, Berlin, Heidelberg. https://doi.org/10.1007/978-3-642-30197-1_300

Bastos, R.W., Akiyama, D., dos Reis, T.F., Colabardini, A.C., Luperini, R.S., de Castro, P.A., Baldini, R.L., Fill, T. and Goldman, G.H. (2022). Secondary Metabolites Produced during Aspergillus fumigatus and Pseudomonas aeruginosa Biofilm Formation. *mBio*, 13(4). doi:https://doi.org/10.1128/mbio.01850-22.

Batrich, M., Maskeri, L., Schubert, R., Ho, B., Kohout, M., Abdeljaber, M., Abuhasna, A., Kholoki, M., Psihogios, P., Razzaq, T., Sawhney, S., Siddiqui, S., Xoubi, E., Cooper, A., Hatzopoulos, T. and Putonti, C. (2019). Pseudomonas Diversity Within Urban Freshwaters. Frontiers in Microbiology, [online] 10. doi:https://doi.org/10.3389/fmicb.2019.00195.

Baxa, M., Musil, M., Kummel, M., Hanzlík, P., Tesařová, B. and Pechar, L. (2020). Dissolved oxygen deficits in a shallow eutrophic aquatic ecosystem (fishpond) – Sediment oxygen demand and water column respiration alternately drive the oxygen regime. *Science of The Total Environment*, p.142647. doi:https://doi.org/10.1016/j.scitotenv.2020.142647.

Bedarf, J.R., Beraza, N., Khazneh, H., Ezgi Özkurt, Baker, D., Borger, V., Ullrich Wüllner and Hildebrand, F. (2021). Much ado about nothing? Off-target amplification can lead to false-positive bacterial brain microbiome detection in healthy and Parkinson's disease individuals. Microbiome, 9(1). doi:https://doi.org/10.1186/s40168-021-01012-1.

Belkaid, Y. and Hand, Timothy W. (2014). Role of the Microbiota in Immunity and Inflammation. Cell, [online] 157(1), pp.121–141. doi:https://doi.org/10.1016/j.cell.2014.03.011.

Benbow, M.E., Lewis, A.J., Tomberlin, J.K. and Pechal, J.L. (2013). Seasonal Necrophagous Insect Community Assembly During Vertebrate Carrion Decomposition. *Journal of Medical Entomology*, 50(2), pp.440–450. doi:https://doi.org/10.1603/me12194.

Benbow, M.E., Pechal, J.L., Lang, J.M., Erb, R. and Wallace, J.R. (2015). The Potential of High-throughput Metagenomic Sequencing of Aquatic Bacterial Communities to Estimate the Post-mortem Submersion Interval. Journal of Forensic Sciences, 60(6), pp.1500–1510. doi:https://doi.org/10.1111/1556-4029.12859.

Benbow, M.E., Receveur, J.P. and Lamberti, G.A. (2020). Death and Decomposition in Aquatic Ecosystems. Frontiers in Ecology and Evolution, 8. doi:https://doi.org/10.3389/fevo.2020.00017.

Bergmann, G.T., Bates, S.T., Eilers, K.G., Lauber, C.L., Caporaso, J.G., Walters, W.A., Knight, R. and Fierer, N. (2011). The under-recognized dominance of Verrucomicrobia in soil bacterial communities. *Soil Biology and Biochemistry*, [online] 43(7), pp.1450–1455. doi:https://doi.org/10.1016/j.soilbio.2011.03.012.

Berman, J.J. (2019). Bacteria. Taxonomic Guide to Infectious Diseases, pp.39–119. doi:https://doi.org/10.1016/b978-0-12-817576-7.00003-1.

Besser, J., Carleton, H.A., Gerner-Smidt, P., Lindsey, R.L. and Trees, E. (2018). Next-generation sequencing technologies and their application to the study and control of bacterial infections. Clinical Microbiology and Infection, [online] 24(4), pp.335–341. doi:https://doi.org/10.1016/j.cmi.2017.10.013.

Biddle, A., Stewart, L., Blanchard, J. and Leschine, S. (2013). Untangling the Genetic Basis of Fibrolytic Specialization by Lachnospiraceae and Ruminococcaceae in Diverse Gut Communities. *Diversity*, 5(3), pp.627–640. doi:https://doi.org/10.3390/d5030627.

Biggs, C.R., Yeager, L.A., Bolser, D.G., Bonsell, C., Dichiera, A.M., Hou, Z., Keyser, S.R., Khursigara, A.J., Lu, K., Muth, A.F., Negrete, B. and Erisman, B.E. (2020). Does functional redundancy affect ecological stability and resilience? A review and meta-analysis. Ecosphere, 11(7). doi:https://doi.org/10.1002/ecs2.3184.

Bishop, A.H. (2019). The signatures of microorganisms and of human and environmental biomes can now be used to provide evidence in legal cases. FEMS Microbiology Letters, 366(3). doi:https://doi.org/10.1093/femsle/fnz021.

Boers, S.A., Jansen, R. and Hays, J.P. (2019). Understanding and overcoming the pitfalls and biases of next-generation sequencing (NGS) methods for use in the routine clinical microbiological diagnostic laboratory. European Journal of Clinical Microbiology & Infectious Diseases, 38(6), pp.1059–1070. doi:https://doi.org/10.1007/s10096-019-03520-3.

Bray, S., Conlan, X.A. and Harvey, M. (2023). Decomposition in an artificial lentic environment: approaches to post-mortem interval estimation. Australian Journal of Forensic Sciences, pp.1–17. doi:https://doi.org/10.1080/00450618.2023.2231984.

Brenner, D. J. & Farmer III, J. J. (2005). Family I. Enterobacteriaceae. In Bergey's Manual of Systematic Bacteriology, 2nd edn, vol. 2, pp. 587–607. Edited by D. J. Brenner, N. R. Krieg, J. T. Staley, G. M. Garrity, D. R. Boone, P. Vos, M. Goodfellow, F. A. Rainey & K.-H. Schleifer. NewYork, NY: Springer.

British Liver Trust (2022). About the liver. [online] British Liver Trust. Available at: https://britishlivertrust.org.uk/information-and-support/liver-health-2/aboutheliver/ [Accessed 5 Dec. 2023].

Broman, E., Sachpazidou, V., Pinhassi, J. and Dopson, M. (2017). Oxygenation of Hypoxic Coastal Baltic Sea Sediments Impacts on Chemistry, Microbial Community Composition, and Metabolism. *Frontiers in Microbiology*, 8. doi:https://doi.org/10.3389/fmicb.2017.02453.

Brooks, J.W. (2016). Post-mortem Changes in Animal Carcasses and Estimation of the Post-mortem Interval. Veterinary Pathology, 53(5), pp.929–940. doi:https://doi.org/10.1177/0300985816629720.

Budowle, B., Murch, R. and Chakraborty, R. (2005). Microbial forensics: the next forensic challenge. International Journal of Legal Medicine, 119(6), pp.317–330. doi:https://doi.org/10.1007/s00414-005-0535-y.

Budowle, B., Schutzer, S.E., Burans, J.P., Beecher, D.J., Cebula, T.A., Chakraborty, R., Cobb, W.T., Fletcher, J., Hale, M.L., Harris, R.B., Heitkamp, M.A., Keller, F.P., Kuske, C., LeClerc, J.E., Marrone, B.L., McKenna, T.S., Morse, S.A., Rodriguez, L.L., Valentine, N.B. and Yadev, J. (2006). Quality Sample Collection, Handling, and Preservation for an Effective Microbial Forensics Program. Applied and Environmental Microbiology, 72(10), pp.6431–6438. doi:https://doi.org/10.1128/aem.01165-06.

Bugelli, V., Gherardi, M., Focardi, M., Pinchi, V., Vanin, S. and Campobasso, C. (2018). Decomposition pattern and insect colonization in two cases of suicide by hanging. Forensic Sciences Research, 3(1), pp.94-102.

Bukin, Y., Galachyants, Y., Morozov, I., Bukin, S., Zakharenko, A. and Zemskaya, T. (2019). The effect of 16S rRNA region choice on bacterial community metabarcoding results. Scientific Data, 6(1).

Bünger, W., Jiang, X., Müller, J., Hurek, T. and Reinhold-Hurek, B. (2020). Novel cultivated endophytic Verrucomicrobia reveal deep-rooting traits of bacteria to associate with plants. *Scientific Reports*, 10(1). doi:https://doi.org/10.1038/s41598-020-65277-6.

Burcham, Z.M., Pechal, J.L., Schmidt, C.J., Bose, J.L., Rosch, J.W., Benbow, M.E. and Jordan, H.R. (2019). Bacterial Community Succession, Transmigration, and Differential Gene Transcription in a Controlled Vertebrate Decomposition Model. Frontiers in Microbiology, 10. doi:https://doi.org/10.3389/fmicb.2019.00745.

Burton, G.J. and Jauniaux, E. (2011). Oxidative stress. *Best Practice & Research Clinical Obstetrics & Gynaecology*, [online] 25(3), pp.287–299. doi:https://doi.org/10.1016/j.bpobgyn.2010.10.016.

Cameron, E.S., Schmidt, P.J., Tremblay, B.J.-M. ., Emelko, M.B. and Müller, K.M. (2021). Enhancing diversity analysis by repeatedly rarefying next generation sequencing data describing microbial communities. Scientific Reports, [online] 11(1), p.22302. doi:https://doi.org/10.1038/s41598-021-01636-1.

Can, I., Javan, G.T., Pozhitkov, A.E. and Noble, P.A. (2014). Distinctive thanatomicrobiome signatures found in the blood and internal organs of humans. Journal of Microbiological Methods, 106, pp.1–7. doi:https://doi.org/10.1016/j.mimet.2014.07.026.

Can, I., Javan, G.T., Pozhitkov, A.E. and Noble, P.A. (2014). Distinctive thanatomicrobiome signatures found in the blood and internal organs of humans. Journal of Microbiological Methods, 106, pp.1–7. doi:https://doi.org/10.1016/j.mimet.2014.07.026.

Caporaso, J. G., Kuczynski, J., Stombaugh, J., Bittinger, K., Bushman, F. D., Costello, E. K., ... & Knight, R. (2010). QIIME allows analysis of high-throughput community sequencing data. Nature methods, 7(5), 335-336.

Caporaso, J.G., Lauber, C.L., Walters, W.A., Berg-Lyons, D., Huntley, J., Fierer, N., Owens, S.M., Betley, J., Fraser, L., Bauer, M., Gormley, N., Gilbert, J.A., Smith, G. and Knight, R. (2012). Ultra-high-throughput microbial community analysis on the Illumina HiSeq and MiSeq platforms. The ISME Journal, 6(8), pp.1621–1624. doi:https://doi.org/10.1038/ismej.2012.8.

Carareto Alves, L.M., de Souza, J.A.M., Varani, A. de M. and Lemos, E.G. de M. (2014). The Family Rhizobiaceae. The Prokaryotes, pp.419–437. doi:https://doi.org/10.1007/978-3-642-30197-1_297.

Carraro, L., Maifreni, M., Bartolomeoli, I., Martino, M.E., Novelli, E., Frigo, F., Marino, M. and Cardazzo, B. (2011). Comparison of culture-dependent and -independent methods for bacterial community monitoring during Montasio cheese manufacturing. Research in Microbiology, [online] 162(3), pp.231–239. doi:https://doi.org/10.1016/j.resmic.2011.01.002.

Carter, D.O., Yellowlees, D. and Tibbett, M. (2006). Cadaver decomposition in terrestrial ecosystems. Naturwissenschaften, 94(1), pp.12–24. doi:https://doi.org/10.1007/s00114-006-0159-1.

Carter, J.L., Resh, V.H. and Hannaford, M.J. (2017). Macroinvertebrates as Biotic Indicators of Environmental Quality. Methods in Stream Ecology, [online] pp.293–318. doi:https://doi.org/10.1016/b978-0-12-813047-6.00016-4.

Caselli, E., Fabbri, C., D'Accolti, M., Soffritti, I., Bassi, C., Mazzacane, S. and Franchi, M. (2020). Defining the oral microbiome by whole-genome sequencing and resistome analysis: the complexity of the healthy picture. BMC Microbiology, 20(1). doi:https://doi.org/10.1186/s12866-020-01801-y.

Castelle, C.J. and Banfield, J.F. (2018). Major New Microbial Groups Expand Diversity and Alter our Understanding of the Tree of Life. Cell, [online] 172(6), pp.1181–1197. doi:https://doi.org/10.1016/j.cell.2018.02.016.

Cendron, F., Niero, G., Carlino, G., Penasa, M. and Cassandro, M. (2020). Characterizing the fecal bacteria and archaea community of heifers and lactating cows through 16S rRNA next-generation sequencing. Journal of Applied Genetics, 61(4), pp.593–605. doi:https://doi.org/10.1007/s13353-020-00575-3.

Chakravorty, S., Helb, D., Burday, M., Connell, N. and Alland, D. (2007). A detailed analysis of 16S ribosomal RNA gene segments for the diagnosis of pathogenic bacteria. Journal of Microbiological Methods, 69(2), pp.330-339.

Chang, J.-M., Di Tommaso, P. and Notredame, C. (2014). TCS: A New Multiple Sequence Alignment Reliability Measure to Estimate Alignment Accuracy and Improve Phylogenetic Tree Reconstruction. Molecular Biology and Evolution, 31(6), pp.1625–1637. doi:https://doi.org/10.1093/molbev/msu117.

Chang, Q., Luan, Y. and Sun, F. (2011). Variance adjusted weighted UniFrac: a powerful beta diversity measure for comparing communities based on phylogeny. BMC Bioinformatics, 12(1), p.118. doi:https://doi.org/10.1186/1471-2105-12-118.

Chao, A., Chiu, C.-H., Hsieh, T.C., Davis, T., Nipperess, D.A. and Faith, D.P. (2014). Rarefaction and extrapolation of phylogenetic diversity. Methods in Ecology and Evolution, [online] 6(4), pp.380–388. doi:https://doi.org/10.1111/2041-210x.12247.

Chen, H., Ma, K., Lu, C., Fu, Q., Qiu, Y., Zhao, J., Huang, Y., Yang, Y., Schadt, C.W. and Chen, H. (2022). Functional Redundancy in Soil Microbial Community Based on Metagenomics Across the Globe. Frontiers in Microbiology, 13. doi:https://doi.org/10.3389/fmicb.2022.878978.

Chisiu, I. (2018). Estimating the Time of Death. Algor Mortis. [online] www.lawyr.it. Available at: https://www.lawyr.it/index.php/articles/reflections/1272-estimating-the-time-of-death-algor-mortis [Accessed 2 Dec. 2023].

Chitra Jangid and Dalal, J. (2023). Exploring the Potential of Microbial Communities: Understanding their Role in PMI estimation. IntechOpen eBooks. doi:https://doi.org/10.5772/intechopen.1002055.

Choi, J.H., Kim, G.B. and Cha, C.J. (2014). Spatial heterogeneity and stability of bacterial community in the gastrointestinal tracts of broiler chickens. Poultry Science, 93(8), pp.1942–1950. doi:https://doi.org/10.3382/ps.2014-03974.

Cholewa, M., Bonar, M. and Kadej, M. (2022). Can plants indicate where a corpse is buried? Effects of buried animal tissues on plant chemistry: Preliminary study. Forensic Science International, 333, p.111208. doi:https://doi.org/10.1016/j.forsciint.2022.111208.

Christie, M.P., Johnstone, B.A., Tweten, R.K., Parker, M.W. and Morton, C.J. (2018). Cholesterol-dependent cytolysins: from water-soluble state to membrane pore. Biophysical Reviews, 10(5), pp.1337–1348. doi:https://doi.org/10.1007/s12551-018-0448-x.

Ciuffreda, L., Rodríguez-Pérez, H. and Flores, C. (2021). Nanopore sequencing and its application to the study of microbial communities. Computational and Structural Biotechnology Journal, 19, pp.1497–1511. doi:https://doi.org/10.1016/j.csbj.2021.02.020.

Claassen, S., du Toit, E., Kaba, M., Moodley, C., Zar, H.J. and Nicol, M.P. (2013). A comparison of the efficiency of five different commercial DNA extraction kits for extraction of DNA from faecal samples. Journal of microbiological methods, 94(2), pp.103-110.

Clark, M.A., Worrell, M.B. and Pless, J.E., (1997). Post-mortem changes in soft tissues. Forensic taphonomy: the post-mortem fate of human remains, pp.151-164

Clarke, T.H., Gomez, A., Singh, H., Nelson, K.E. and Brinkac, L.M. (2017). Integrating the microbiome as a resource in the forensics toolkit. Forensic Science International: Genetics, [online] 30, pp.141–147. doi:https://doi.org/10.1016/j.fsigen.2017.06.008.

Cláudia-Ferreira, A., Daniel José Barbosa, Veroniek Saegeman, Fernández-Rodríguez, A., Ricardo Jorge Dinis-Oliveira and Freitas, A.R. (2023). The Future Is Now: Unraveling the Expanding Potential of Human (Necro)Microbiome in Forensic Investigations. Microorganisms, 11(10), pp.2509–2509. doi:https://doi.org/10.3390/microorganisms11102509.

Cobaugh, K.L., Schaeffer, S.M. and DeBruyn, J.M. (2015). Functional and Structural Succession of Soil Microbial Communities below Decomposing Human Cadavers. PLOS ONE, 10(6), p.e0130201. doi:https://doi.org/10.1371/journal.pone.0130201.

Constantinos Tsirogiannis and Sandel, B. (2015). PhyloMeasures: a package for computing phylogenetic biodiversity measures and their statistical moments. Ecography, 39(7), pp.709–714. doi:https://doi.org/10.1111/ecog.01814.

Cornish, K.A.S., Lange, J., Arnthór Aevarsson and Pohl, E. (2022). CPR-C4 is a highly conserved novel protease from the Candidate Phyla Radiation with remote structural homology to human vasohibins. Journal of Biological Chemistry, 298(5), pp.101919–101919. doi:https://doi.org/10.1016/j.jbc.2022.101919.

Costello, E.K., Lauber, C.L., Hamady, M., Fierer, N., Gordon, J.I. and Knight, R. (2009). Bacterial community variation in human body habitats across space and time. Science (New York, N.Y.), [online] 326(5960), pp.1694–7. doi:https://doi.org/10.1126/science.1177486.

Crielaard, W., Zaura, E., Schuller, A.A., Huse, S.M., Montijn, R.C. and Keijser, B.J. (2011). Exploring the oral microbiota of children at various developmental stages of their dentition in the relation to their oral health. BMC Medical Genomics, 4(1). doi:https://doi.org/10.1186/1755-8794-4-22.

Cristina, J., Hess, M., Bilton, T.P., Henry, H.M., Dodds, K.G., Janssen, P.H., McEwan, J.C. and Rowe, S. (2022). Low-cost sample preservation methods for high-throughput processing of rumen microbiomes. Animal Microbiome, 4(1). doi:https://doi.org/10.1186/s42523-022-00190-z.

Cryan, J.F., O'Riordan, K.J., Cowan, C.S.M., Sandhu, K.V., Bastiaanssen, T.F.S., Boehme, M., Codagnone, M.G., Cussotto, S., Fulling, C., Golubeva, A.V., Guzzetta, K.E., Jaggar, M., Long-Smith, C.M., Lyte, J.M., Martin, J.A., Molinero-Perez, A., Moloney, G., Morelli, E., Morillas, E. and O'Connor, R. (2019). The Microbiota-Gut-Brain Axis. *Physiological Reviews*, [online] 99(4), pp.1877–2013. doi:https://doi.org/10.1152/physrev.00018.2018.

D'Agostino, M. and Cook, N. (2016). Foodborne Pathogens. www.sciencedirect.com, [online] pp.83–86. doi:https://doi.org/10.1016/B978-0-12-384947-2.00326-3.

Dairawan, M. and Shetty, P. (2020). The Evolution of DNA Extraction Methods. The Evolution of DNA Extraction Methods, 8(1).

Dakos, V. and Kéfi, S. (2022). Ecological resilience: what to measure and how. Environmental Research Letters, 17(4), p.043003. doi:https://doi.org/10.1088/1748-9326/ac5767.

Danielsen, A.-C.S., Nielsen, P.H., Hermansen, C., Weber, P.L., de Jonge, L.W., Jørgensen, V.R., Corcoran, D., Bruhn, D., Greve, M.H. and Dueholm, M.K.D. (2023). Improved description of terrestrial habitat types by including microbial communities as indicators. Journal of Environmental Management, 344, pp.118677–118677. doi:https://doi.org/10.1016/j.jenvman.2023.118677.

Das, H.K. (2019). Azotobacters as biofertilizer. Advances in Applied Microbiology, 108, pp.1–43. doi:https://doi.org/10.1016/bs.aambs.2019.07.001.

Dash, H. and Das, S. (2020). Thanatomicrobiome and epinecrotic community signatures for estimation of post-mortem time interval in human cadaver. Applied Microbiology and Biotechnology, 104(22), pp.9497-9512.

de Carvalho, C.C.C.R. (2018). Marine Biofilms: A Successful Microbial Strategy With Economic Implications. Frontiers in Marine Science, 5. doi:https://doi.org/10.3389/fmars.2018.00126.

De Luca E., Sonsiray Álvarez-Narváez, Grazieli Maboni, Baptista, R.P., Nemeth, N.M., Niedringhaus, K.D., Ladner, J.T., Lorch, J.M., Koroleva, G.I., Lovett, S., Palacios, G. and Sánchez, S. (2021). Comparative Genomics Analyses Support the Reclassification of Bisgaard Taxon 40 as Mergibacter gen. nov., With Mergibacter septicus sp. nov. as Type Species: Novel Insights Into the Phylogeny and Virulence Factors of a Pasteurellaceae Family Member Associated With Mortality Events in Seabirds. Frontiers in Microbiology, 12. doi:https://doi.org/10.3389/fmicb.2021.667356.

De Santiago, A., Pereira, T.J., Mincks, S.L. and Bik, H.M. (2021). Dataset complexity impacts both MOTU delimitation and biodiversity estimates in eukaryotic 18S rRNA metabarcoding studies. Environmental DNA. doi:https://doi.org/10.1002/edn3.255.

DeBritto, S., Gajbar, T.D., Satapute, P., Sundaram, L., Lakshmikantha, R.Y., Jogaiah, S. and Ito, S. (2020). Isolation and characterization of nutrient dependent pyocyanin from Pseudomonas aeruginosa and its dye and agrochemical properties. *Scientific Reports*, 10(1). doi:https://doi.org/10.1038/s41598-020-58335-6.

DeBruyn, J.M. and Hauther, K.A. (2017). Post-mortem succession of gut microbial communities in deceased human subjects. PeerJ, 5, p.e3437. doi:https://doi.org/10.7717/peerj.3437.

DeBruyn, J.M., Hoeland, K.M., Taylor, L.S., Stevens, J.D., Moats, M.A., Bandopadhyay, S., Dearth, S.P., Castro, H.F., Hewitt, K.K., Campagna, S.R., Dautartas, A.M., Vidoli, G.M., Mundorff, A.Z. and Steadman, D.W. (2021). Comparative Decomposition of Humans and Pigs: Soil Biogeochemistry, Microbial Activity and Metabolomic Profiles. Frontiers in Microbiology, [online] 11. doi:https://doi.org/10.3389/fmicb.2020.608856.

Dedysh, S.N. (2019). B ryobacteraceae . Bergey's Manual of Systematics of Archaea and Bacteria, pp.1–4. doi:https://doi.org/10.1002/9781118960608.fbm00317.

Deel, H., Emmons, A.L., Kiely, J., Damann, F.E., Carter, D.O., Lynne, A., Knight, R., Xu, Z.Z., Bucheli, S. and Metcalf, J.L. (2021). A Pilot Study of Microbial Succession in Human Rib Skeletal Remains during Terrestrial Decomposition. mSphere, 6(4). doi:https://doi.org/10.1128/msphere.00455-21.

Deguenon, J.M., Travanty, N., Zhu, J., Carr, A., Denning, S., Reiskind, M.H., Watson, D.W., Michael Roe, R. and Ponnusamy, L. (2019). Exogenous and endogenous microbiomes of wild-caught Phormia regina (Diptera: Calliphoridae) flies from a suburban farm by 16S rRNA gene sequencing. Scientific Reports, 9(1). doi:https://doi.org/10.1038/s41598-019-56733-z.

Del Fabbro, C., Scalabrin, S., Morgante, M. and Giorgi, F.M. (2013). An Extensive Evaluation of Read Trimming Effects on Illumina NGS Data Analysis. PLoS ONE, 8(12), p.e85024. doi:https://doi.org/10.1371/journal.pone.0085024.

Dell'Annunziata, F., Martora, F., Pepa, M.E.D., Folliero, V., Luongo, L., Bocelli, S., Guida, F., Mascolo, P., Campobasso, C.P., Maione, S., Franci, G. and Galdiero, M. (2021). Post-mortem interval assessment by

MALDI-TOF mass spectrometry analysis in murine cadavers. Journal of Applied Microbiology, 132(1), pp.707–714. doi:https://doi.org/10.1111/jam.15210.

Demanèche, S., Schauser, L., Dawson, L., Franqueville, L. and Simonet, P. (2017). Microbial soil community analyses for forensic science: Application to a blind test. Forensic Science International, 270, pp.153–158. doi:https://doi.org/10.1016/j.forsciint.2016.12.004.

Department of Primary Industries (2021). Soil organic matter. [online] www.dpi.nsw.gov.au. Available at: https://www.dpi.nsw.gov.au/agriculture/soils/guides/soil-carbon/organic-matter [Accessed 20 Dec. 2023].

Dharamshi, J. E. (2021). Expanding the Chlamydiae tree. Insights into genome diversity and evolution. Digital Comprehensive Summaries of Uppsala Dissertations from the Faculty of Science and Technology 2040. 87 pp. Uppsala: Acta Universitatis Upsaliensis. ISBN 978-91-513-1203-3.

Diao, M., Sinnige, R., Kalbitz, K., Huisman, J. and Muyzer, G. (2017). Succession of Bacterial Communities in a Seasonally Stratified Lake with an Anoxic and Sulfidic Hypolimnion. Frontiers in Microbiology, 8. doi:https://doi.org/10.3389/fmicb.2017.02511.

Díez López, C., Vidaki, A., Ralf, A., Montiel González, D., Radjabzadeh, D., Kraaij, R., Uitterlinden, A.G., Haas, C., Lao, O. and Kayser, M. (2019). Novel taxonomy-independent deep learning microbiome approach allows for accurate classification of different forensically relevant human epithelial materials. Forensic Science International: Genetics, 41, pp.72–82. doi:https://doi.org/10.1016/j.fsigen.2019.03.015.

DiFranza, L.T., Annavajhala, M.K., Anne-Catrin Uhlemann and Green, D.A. (2021). The Brief Case: A Maggot Mystery—Ignatzschineria larvae Sepsis Secondary to an Infested Wound. Journal of Clinical Microbiology, 59(3). doi:https://doi.org/10.1128/jcm.02279-20.

Dillon, S. (2019). Death and Kinetics. [online] Fsu.edu. Available at: https://www.chem.fsu.edu/chemlab/chm1020c/Lecture%208/02.php [Accessed 2 Dec. 2023].

Dmitrijs, F., Guo, J., Huang, Y., Liu, Y., Fang, X., Jiang, K., Zha, L., Cai, J. and Fu, X. (2022). Bacterial Succession in Microbial Biofilm as a Potential Indicator for Post-mortem Submersion Interval Estimation. Frontiers in Microbiology, 13. doi:https://doi.org/10.3389/fmicb.2022.951707.

Dong, K., Xin, Y., Cao, F., Huang, Z., Sun, J., Peng, M., Liu, W. and Shi, P. (2019). Succession of oral microbiota community as a tool to estimate post-mortem interval. Scientific Reports, [online] 9(1). doi:https://doi.org/10.1038/s41598-019-49338-z.

Dousse, F., Thomann, A., Brodard, I., Korczak, B., Schlatter, Y., Kuhnert, P., R. Miserez and Frey, J. (2008). Routine Phenotypic Identification of Bacterial Species of the Family Pasteurellaceae Isolated from Animals. Journal of Veterinary Diagnostic Investigation, 20(6), pp.716–724. doi:https://doi.org/10.1177/104063870802000602.

Driscoll, T.P., Verhoeve, V.I., Beier-Sexton, M., Azad, A.F. and Gillespie, J.J., 2021. The Family Rickettsiaceae. In Practical Handbook of Microbiology (pp. 511-526). CRC Press.

Dunne, W.M. (2002). Bacterial Adhesion: Seen Any Good Biofilms Lately? Clinical Microbiology Reviews, 15(2), pp.155–166. doi:https://doi.org/10.1128/cmr.15.2.155-166.2002.

Dwiyanto, J., Hussain, M.H., Reidpath, D., Ong, K.S., Qasim, A., Lee, S.W.H., Lee, S.M., Foo, S.C., Chong, C.W. and Rahman, S. (2021). Ethnicity influences the gut microbiota of individuals sharing a geographical location: a cross-sectional study from a middle-income country. Scientific Reports, 11(1). doi:https://doi.org/10.1038/s41598-021-82311-3.

Ehrenfellner, B., Zissler, A., Steinbacher, P., Monticelli, F. and Pittner, S. (2017). Are animal models predictive for human post-mortem muscle protein degradation? International Journal of Legal Medicine, 131(6), pp.1615-1621.

Eisenberg, T., Fawzy, A., Nicklas, W., Semmler, T. and Ewers, C. (2016). Phylogenetic and comparative genomics of the family Leptotrichiaceae and introduction of a novel fingerprinting MLVA for Streptobacillus moniliformis. BMC Genomics, 17(1). doi:https://doi.org/10.1186/s12864-016-3206-0.

Elshafei, A.M. (2020). Forensic Microbiology, an Important Tool in Crime Investigation. South Asian Journal of Research in Microbiology, pp.33–38. doi:https://doi.org/10.9734/sajrm/2020/v6i230147.

Emerson, J.B., Adams, R.I., Román, C.M.B., Brooks, B., Coil, D.A., Dahlhausen, K., Ganz, H.H., Hartmann, E.M., Hsu, T., Justice, N.B., Paulino-Lima, I.G., Luongo, J.C., Lymperopoulou, D.S., Gomez-Silvan, C., Rothschild-Mancinelli, B., Balk, M., Huttenhower, C., Nocker, A., Vaishampayan, P. and Rothschild, L.J. (2017). Schrödinger's microbes: Tools for distinguishing the living from the dead in microbial ecosystems. Microbiome, 5(1). doi:https://doi.org/10.1186/s40168-017-0285-3.

Estaki, M., Jiang, L., Bokulich, N.A., McDonald, D., González, A., Kosciolek, T., Martino, C., Zhu, Q., Birmingham, A., Vázquez-Baeza, Y., Dillon, M.R., Bolyen, E., Caporaso, J.G. and Knight, R. (2020). QIIME 2 Enables Comprehensive End-to-End Analysis of Diverse Microbiome Data and Comparative Studies with Publicly Available Data. Current Protocols in Bioinformatics, 70(1). doi:https://doi.org/10.1002/cpbi.100.

EzBioCloud (2019). MTP-Primary analysis – EzBioCloud Help center. [online] Available at: https://help.ezbiocloud.net/mtp-pipeline/ [Accessed 5 Dec. 2023].

EzbioCloud (2020). Microbiome Taxonomic Profile (MTP) Documentation & Glossary – EzBioCloud Help center. [online] Available at: https://help.ezbiocloud.net/mtp-documentation/ [Accessed 5 Dec. 2023].

Faith, D.P. (2006). The Role of the Phylogenetic Diversity Measure, PD, in Bio-Informatics: Getting the Definition Right. Evolutionary Bioinformatics, 2, p.117693430600200. doi:https://doi.org/10.1177/117693430600200008.

Fang, H., Chen, Y., Huang, L. and He, G. (2017). Analysis of biofilm bacterial communities under different shear stresses using size-fractionated sediment. Scientific Reports, 7(1). doi:https://doi.org/10.1038/s41598-017-01446-4.

Fang, H., Chen, Y., Huang, L. and He, G. (2017). Analysis of biofilm bacterial communities under different shear stresses using size-fractionated sediment. Scientific Reports, 7(1). doi:https://doi.org/10.1038/s41598-017-01446-4.

Farmer, J.J. and J. Michael Janda (2015). Vibrionaceae. Bergey's Manual of Systematics of Archaea and Bacteria, pp.1–7. doi:https://doi.org/10.1002/9781118960608.fbm00212.

Fasesan, D., Dawkins, K., Ramirez, R., Rasheed-Jada, H., Onilude, A., Nash, O. and Esiobu, N. (2020). Analysis of a Tropical Warm Spring Microbiota Using 16S rRNA Metabarcoding. Advances in Microbiology, 10(04), pp.145–165. doi:https://doi.org/10.4236/aim.2020.104012.

Fernande, C.C., Kishi, L.T., Lopes, E.M., Omori, W.P., de Souza, J.A.M., Alves, L.M.C. and Lemos, E.G. de M. (2018). Bacterial communities in mining soils and surrounding areas under regeneration process in a former ore mine. Brazilian Journal of Microbiology, [online] 49(3), pp.489–502. doi:https://doi.org/10.1016/j.bjm.2017.12.006.

Fierer, N., Lauber, C.L., Zhou, N., McDonald, D., Costello, E.K. and Knight, R. (2010). Forensic identification using skin bacterial communities. Proceedings of the National Academy of Sciences, 107(14), pp.6477–6481. doi:https://doi.org/10.1073/pnas.1000162107.

Figueiredo, G., Gomes, M., Covas, C., Mendo, S. and Caetano, T. (2021). The Unexplored Wealth of Microbial Secondary Metabolites: the Sphingobacteriaceae Case Study. Microbial Ecology, 83(2), pp.470–481. doi:https://doi.org/10.1007/s00248-021-01762-3.

Filazzola, A. and Cahill, J.F. (2021). Replication in field ecology: Identifying challenges and proposing solutions. Methods in Ecology and Evolution, 12(10), pp.1780–1792. doi:https://doi.org/10.1111/2041-210x.13657.

Fillinger, L., Hug, K. and Griebler, C. (2019). Selection imposed by local environmental conditions drives differences in microbial community composition across geographically distinct groundwater aquifers. FEMS Microbiology Ecology, 95(11). doi:https://doi.org/10.1093/femsec/fiz160.

Finotello, F., Mastrorilli, E. and Di Camillo, B. (2018). Measuring the diversity of the human microbiota with targeted next-generation sequencing. Briefings in Bioinformatics, [online] 19(4), pp.679–692. doi:https://doi.org/10.1093/bib/bbw119.

Flint, A., Laidlaw, A., Li, L., Raitt, C., Rao, M., Cooper, A.R., Weedmark, K., Carrillo, C.D. and Tamber, S. (2022). Choice of DNA extraction method affects detection of bacterial taxa from retail chicken breast. 22(1). doi:https://doi.org/10.1186/s12866-022-02650-7.

Fox, N., Hunn, A. and Mathers, N. (2009). Sampling and Sample Size Calculation Authors Nick Fox The NIHR Research Design Service for Yorkshire & the Humber. [online] Available at: https://www.bdct.nhs.uk/wp-content/uploads/2019/04/Sampling-and-Sample-Size-Calculation.pdf.

Franklin, R., & Mills, A. (2003). Multi-scale variation in spatial heterogeneity for microbial community structure in an eastern Virginia agricultural field.. FEMS microbiology ecology, 44 3, 335-46 . https://doi.org/10.1016/S0168-6496(03)00074-6.

Fuerst, J. (2012). Keys to eukaryality: Planctomycetes and ancestral evolution of cellular complexity. Frontiers in Microbiology, 3. doi:https://doi.org/10.3389/fmicb.2012.00167.

Fusco, W., Lorenzo, M.B., Cintoni, M., Porcari, S., Rinninella, E., Kaitsas, F., Lener, E., Mele, M.C., Gasbarrini, A., Collado, M.C., Cammarota, G. and Ianiro, G. (2023). Short-Chain Fatty-Acid-Producing Bacteria: Key Components of the Human Gut Microbiota. Nutrients, [online] 15(9), p.2211. doi:https://doi.org/10.3390/nu15092211.

Gabriel Marchesan Almeida, Laanto, E., Ashrafi, R. and Sundberg, L. (2019). Bacteriophage adherence to mucus mediates preventive protection against pathogenic bacteria. bioRxiv (Cold Spring Harbor Laboratory). doi:https://doi.org/10.1101/592097.

Gadiraju, S. and Oberle, J. (2021). Redefining Microbial Forensics: A Broader Scope of Applications Redefining Microbial Forensics: A Broader Scope of Applications. [online] Available at: https://rucore.libraries.rutgers.edu/rutgers-lib/67202/PDF/1/play/ [Accessed 20 Nov. 2023].

Gaël Toubon, Butel, M., Jean-Christophe Rozé, Ioannis Nicolis, Delannoy, J., Cécile Zaros, Ancel, P., Aires, J. and Charles, M. (2023). Early Life Factors Influencing Children Gut Microbiota at 3.5 Years from Two French Birth Cohorts. Microorganisms, 11(6), pp.1390–1390. doi:https://doi.org/10.3390/microorganisms11061390.

García, M.G., Pérez-Cárceles, M.D., Osuna, E. and Legaz, I. (2020). Impact of the Human Microbiome in Forensic Sciences: a Systematic Review. Applied and Environmental Microbiology, 86(22). doi:https://doi.org/10.1128/aem.01451-20.

Garcia, R. and Müller, R. (2018). Simulacricoccus ruber gen. nov., sp. nov., a microaerotolerant, non-fruiting, myxospore-forming soil myxobacterium and emended description of the family Myxococcaceae. International Journal of Systematic and Evolutionary Microbiology, 68(10), pp.3101–3110. doi:https://doi.org/10.1099/ijsem.0.002936.

García-Alegría, A.M., Anduro-Corona, I., Pérez-Martínez, C.J., Guadalupe Corella-Madueño, M.A., Rascón-Durán, M.L. and Astiazaran-Garcia, H. (2020). Quantification of DNA through the NanoDrop Spectrophotometer: Methodological Validation Using Standard Reference Material and Sprague Dawley Rat and Human DNA. International Journal of Analytical Chemistry, [online] 2020(8896738), pp.1–9. doi:https://doi.org/10.1155/2020/8896738.

García-García, N., Tamames, J., Linz, A.M., Pedrós-Alió, C. and Puente-Sánchez, F. (2019). Microdiversity ensures the maintenance of functional microbial communities under changing environmental conditions. The ISME Journal, [online] 13(12), pp.2969–2983. doi:https://doi.org/10.1038/s41396-019-0487-8.

García-López, R., Cornejo-Granados, F., Lopez-Zavala, A., Sánchez-López, F., Cota-Huízar, A., Sotelo-Mundo, R., Guerrero, A., Mendoza-Vargas, A., Gómez-Gil, B. and Ochoa-Leyva, A. (2020). Doing More with Less: A Comparison of 16S Hypervariable Regions in Search of Defining the Shrimp Microbiota. Microorganisms, 8(1), p.134.

Geng, J., Ni, Q., Sun, W., Li, L. and Feng, X. (2022). The links between gut microbiota and obesity and obesity related diseases. Biomedicine & Pharmacotherapy, 147, p.112678. doi:https://doi.org/10.1016/j.biopha.2022.112678.

Geyer, W.R. (2019). Brackish Water: Where Fresh Water Rivers Meet A Salt Water Sea. [online] Woods Hole Oceanographic Institution. Available at: https://www.whoi.edu/oceanus/feature/where-the-rivers-meet-the-sea/.

Gillespie, S.H. (1994). Gram-positive cocci. Medical Microbiology Illustrated, pp.12–29. doi:https://doi.org/10.1016/b978-0-7506-0187-0.50007-9.

Girard, L., Lood, C., De Mot, R., van Noort, V. and Baudart, J. (2023). Genomic diversity and metabolic potential of marine Pseudomonadaceae. Frontiers in Microbiology, 14. Doi:https://doi.org/10.3389/fmicb.2023.1071039.

Glassing, A., Dowd, S.E., Galandiuk, S., Davis, B. and Chiodini, R.J. (2016). Inherent bacterial DNA contamination of extraction and sequencing reagents may affect interpretation of microbiota in low bacterial biomass samples. Gut Pathogens, [online] 8(1). doi:https://doi.org/10.1186/s13099-016-0103-7.

Gouello, A., Dunyach-Remy, C., Siatka, C. and Lavigne, J.-P. (2021). Analysis of Microbial Communities: An Emerging Tool in Forensic Sciences. Diagnostics, [online] 12(1), p.1. doi:https://doi.org/10.3390/diagnostics12010001.

Gu, X., Xiang, J., Wei Lin Lee, Liang, C., Yvonne, Ega Danu Chang, Yii Ean Teh, Zhang, A., Armas, F., Chandra, F., Chen, H., Zhao, S., Lee, Z., Thompson, J.R., Eng Eong Ooi, Low, J.G., Alm, E.J. and Shirin Kalimuddin (2021). Low Gut Ruminococcaceae Levels are Associated with Occurrence of Antibiotic-associated Diarrhea. medRxiv (Cold Spring Harbor Laboratory). doi:https://doi.org/10.1101/2021.09.23.21263551.

Gu, Y.T., Wang, H., Wang, Y., Liang, D., Gao, J., Zhong, Y., Zhao, S. and Wang, S. (2023). Xylocopa caerulea and Xylocopa auripennis harbor a homologous gut microbiome related to that of eusocial bees. Frontiers in Microbiology, 14. doi:https://doi.org/10.3389/fmicb.2023.1124964.

Guinane, C.M. and Cotter, P.D. (2013). Role of the gut microbiota in health and chronic gastrointestinal disease: understanding a hidden metabolic organ. Therapeutic Advances in Gastroenterology, [online] 6(4), pp.295–308. doi:https://doi.org/10.1177/1756283x13482996.

Gunina, A. and Kuzyakov, Y. (2022). From energy to (soil organic) matter. *Global Change Biology*. doi:https://doi.org/10.1111/gcb.16071.

Guo, J., Fu, X., Liao, H., Hu, Z., Long, L., Yan, W., Ding, Y., Zha, L., Guo, Y., Yan, J., Chang, Y. and Cai, J. (2016). Potential use of bacterial community succession for estimating post-mortem interval as revealed by high-throughput sequencing. Scientific Reports, 6(1). doi:https://doi.org/10.1038/srep24197.

Gupta R. S. (2012). Molecular signatures for the PVC clade (Planctomycetes, Verrucomicrobia, Chlamydiae, and Lentisphaerae) of bacteria provide insights into their evolutionary relationships. Frontiers in Microbiology. doi:https://doi.org/10.3389/fmicb.2012.00327.

Gupta R. S. (2014). Identification of conserved indels that are useful for classification and evolutionary studies, in Methods in Microbiology: New Approaches to Prokaryotic Systematics, eds Goodfellow M., Sutcliffe I., Chun J. (Oxford: Academic Press;), 153–182.

Gupta, A.K., Dharne, M.S., Rangrez, A.Y., Verma, P., Ghate, H.V., Rohde, M., Patole, M.S. and Shouche, Y.S. (2011). Ignatzschineria indica sp. nov. and Ignatzschineria ureiclastica sp. nov., isolated from adult flesh flies (Diptera: Sarcophagidae). International Journal of Systematic and Evolutionary Microbiology, 61(6), pp.1360–1369. doi:https://doi.org/10.1099/ijs.0.018622-0.

Gupta, N. and Verma, V.K. (2019). Next-Generation Sequencing and Its Application: Empowering in Public Health Beyond Reality. Microorganisms for Sustainability, [online] 17, pp.313–341. doi:https://doi.org/10.1007/978-981-13-8844-6_15.

Gupta, R.S. and Patel, S., (2020). Robust demarcation of the family Caryophanaceae (Planococcaceae) and its different genera including three novel genera based on phylogenomics and highly specific molecular signatures. Frontiers in microbiology, 10, p.2821.

Gupta, R.S., Chander, P. and George, S. (2012). Phylogenetic framework and molecular signatures for the class Chloroflexi and its different clades; proposal for division of the class Chloroflexi class. nov. into the suborder Chloroflexineae subord. nov., consisting of the emended family Oscillochloridaceae and the family Chloroflexaceae fam. nov., and the suborder Roseiflexineae subord. nov., containing the family Roseiflexaceae fam. nov. Antonie van Leeuwenhoek, 103(1), pp.99–119. doi:https://doi.org/10.1007/s10482-012-9790-3.

Gupta, S., Mortensen, M.S., Schjørring, S., Trivedi, U., Vestergaard, G., Stokholm, J., Bisgaard, H., Krogfelt, K.A. and Sørensen, S.J. (2019). Amplicon sequencing provides more accurate microbiome information in healthy children compared to culturing. Communications Biology, 2(1). doi:https://doi.org/10.1038/s42003-019-0540-1.

Haas, B.J., Gevers, D., Earl, A.M., Feldgarden, M., Ward, D.V., Giannoukos, G., Ciulla, D., Tabbaa, D., Highlander, S.K., Sodergren, E., Methe, B., DeSantis, T.Z., Petrosino, J.F., Knight, R. and Birren, B.W. (2011). Chimeric 16S rRNA sequence formation and detection in Sanger and 454-pyrosequenced PCR amplicons. Genome Research, 21(3), pp.494–504. doi:https://doi.org/10.1101/gr.112730.110.

Halkman, H.B.D. and Halkman, A.K. (2014). Indicator Organisms. Encyclopedia of Food Microbiology, (978-0-12-384733-1), pp.358–363. doi:https://doi.org/10.1016/b978-0-12-384730-0.00396-7.

Harding, H.R., Timothy, G., Eastcott, E., Simpson, S.D. and Radford, A.N. (2019). Causes and consequences of intraspecific variation in animal responses to anthropogenic noise. Behavioral Ecology, [online] 30(6), pp.1501–1511. doi:https://doi.org/10.1093/beheco/arz114.

Harrison, L., Kooienga, E., Speights, C., Tomberlin, J., Lashley, M., Barton, B. and Jordan, H. (2020). Microbial succession from a subsequent secondary death event following mass mortality. BMC Microbiology, 20(1). doi:https://doi.org/10.1186/s12866-020-01969-3.

Harrison, Lindsay K., "Microbial Succession from a Controlled Death Event following Simulated Mass Mortality" (2018). Theses and Dissertations. 3081. https://scholarsjunction.msstate.edu/td/3081

Hassan, A., Usman, J., Kaleem, F., Omair, M., Khalid, A. and Iqbal, M. (2011). Evaluation of different detection methods of biofilm formation in the clinical isolates. Brazilian Journal of Infectious Diseases, [online] 15(4), pp.305–311. doi:https://doi.org/10.1590/s1413-86702011000400002.

Hattab, J., Marruchella, G., Pallavicini, A., Fabrizia Gionechetti, Mosca, F., Abigail Rose Trachtman, Lanci, L., Gabrielli, L. and Pietro Giorgio Tiscar (2021). Insights into the Oral Bacterial Microbiota of Sows. Microorganisms, 9(11), pp.2314–2314. doi:https://doi.org/10.3390/microorganisms9112314.

Hau, T.C., Hamzah, N.H., Hing, H.L. and Amir Hamzah, S.P.A. (2014). Decomposition Process and Post Mortem Changes: Review. Sains Malaysiana, 43(12), pp.1873–1882. doi:https://doi.org/10.17576/jsm-2014-4312-08.

Hauther, K., Cobaugh, K., Jantz, L., Sparer, T. and DeBruyn, J. (2015). Estimating Time Since Death from Post-mortem Human Gut Microbial Communities. Journal of Forensic Sciences, 60(5), pp.1234-1240.

He, J., Guo, J., Fu, X. and Cai, J. (2019). Potential use of high-throughput sequencing of bacterial communities for post-mortem submersion interval estimation. Brazilian Journal of Microbiology, 50(4), pp.999–1010. doi:https://doi.org/10.1007/s42770-019-00119-w.

He, Y., Caporaso, J.G., Jiang, X.-T., Sheng, H.-F., Huse, S.M., Rideout, J.R., Edgar, R.C., Kopylova, E., Walters, W.A., Knight, R. and Zhou, H.-W. (2015). Stability of operational taxonomic units: an important but neglected property for analyzing microbial diversity. Microbiome, 3(1). doi:https://doi.org/10.1186/s40168-015-0081-x.

Heather, J.M. and Chain, B. (2016). The Sequence of sequencers: the History of Sequencing DNA. Genomics, [online] 107(1), pp.1–8. doi:https://doi.org/10.1016/j.ygeno.2015.11.003.

Hegde, V. and Dhurandhar, N.V. (2013). Microbes and obesity—interrelationship between infection, adipose tissue and the immune system. Clinical Microbiology and Infection, 19(4), pp.314–320. doi:https://doi.org/10.1111/1469-0691.12157.

Holmes, B. (2006). The Genera Flavobacterium, Sphingobacterium and Weeksella. Springer eBooks, pp.539–548. doi:https://doi.org/10.1007/0-387-30747-8_19.

Hommel, R.K. (2014). Acetobacter. Encyclopedia of Food Microbiology, pp.3–10. doi:https://doi.org/10.1016/b978-0-12-384730-0.00001-x.

Hosoda, S., Nishijima, S., Fukunaga, T., Hattori, M. and Hamada, M. (2020). Revealing the microbial assemblage structure in the human gut microbiome using latent Dirichlet allocation. Microbiome, 8(1). doi:https://doi.org/10.1186/s40168-020-00864-3.

Hou, K., Wu, Z.-X., Chen, X.-Y., Wang, J.-Q., Zhang, D., Xiao, C., Zhu, D., Koya, J.B., Wei, L., Li, J. and Chen, Z.-S. (2022). Microbiota in Health and Diseases. Signal Transduction and Targeted Therapy, 7(1). doi:https://doi.org/10.1038/s41392-022-00974-4.

Huang, J., Zhang, W., Hu, Z., Liu, Z., Du, T., Dai, Y. and Xiong, T. (2020b). Isolation, characterization and selection of potential probiotic lactic acid bacteria from feces of wild boar, native pig and commercial pig. Livestock Science, 237, p.104036. doi:https://doi.org/10.1016/j.livsci.2020.104036.

Huang, Y., Wang, X., Yang, X., Jiang, J. and Hu, J. (2020a). Unveiling the roles of interspecific competition and local adaptation in phenotypic differentiation of parapatric frogs. Current Zoology, 66(4), pp.383–392. doi:https://doi.org/10.1093/cz/zoaa001.

Huber, K.J. and Overmann, J. (2018). Vicinamibacteraceae fam. nov., the first described family within the subdivision 6 Acidobacteria. International Journal of Systematic and Evolutionary Microbiology, 68(7), pp.2331–2334. doi:https://doi.org/10.1099/ijsem.0.002841.

Huber, K.J., Pascual, J., Foesel, B.U. and Overmann, J. (2017). Acidobacteriaceae . Bergey's Manual of Systematics of Archaea and Bacteria, pp.1–5. doi:https://doi.org/10.1002/9781118960608.fbm00001.pub2.

Huffnagle, G.B., Dickson, R.P. and Lukacs, N.W. (2016). The respiratory tract microbiome and lung inflammation: a two-way street. Mucosal Immunology, [online] 10(2), pp.299–306. doi:https://doi.org/10.1038/mi.2016.108.

Huson, D.H., Albrecht, B., Caner Bağcı, Bessarab, I., Górska, A., Jolic, D. and Williams (2018). MEGAN-LR: new algorithms allow accurate binning and easy interactive exploration of metagenomic long reads and contigs. 13(1). doi:https://doi.org/10.1186/s13062-018-0208-7.

Hwang, C., Ling, F., Andersen, G.L., LeChevallier, M.W. and Liu, W.-T. (2012). Evaluation of Methods for the Extraction of DNA from Drinking Water Distribution System Biofilms. Microbes and Environments, [online] 27(1), pp.9–18. doi:https://doi.org/10.1264/jsme2.ME11132.

Hyde, E.R., Haarmann, D.P., Lynne, A.M., Bucheli, S.R. and Petrosino, J.F. (2013). The Living Dead: Bacterial Community Structure of a Cadaver at the Onset and End of the Bloat Stage of Decomposition. PLoS ONE, 8(10), p.e77733. doi:https://doi.org/10.1371/journal.pone.0077733.

Hyde, E.R., Haarmann, D.P., Petrosino, J.F., Lynne, A.M. and Bucheli, S.R. (2014). Initial insights into bacterial succession during human decomposition. International Journal of Legal Medicine, 129(3), pp.661–671. doi:https://doi.org/10.1007/s00414-014-1128-4.

Iancu, L., Muslim, A., Shafiq Aazmi and Jitaru, V. (2023). Post-mortem skin microbiome signatures associated with human cadavers within the first 12 h at the morgue. Frontiers in Microbiology, 14. doi:https://doi.org/10.3389/fmicb.2023.1234254.

Iancu, L., Necula-Petrareanu, G. and Purcarea, C. (2020). Potential bacterial biomarkers for insect colonization in forensic cases: preliminary quantitative data on Wohlfahrtiimonas chitiniclastica and Ignatzschineria indica dynamics. Scientific Reports, 10(1). doi:https://doi.org/10.1038/s41598-020-65471-6.

Ibal, J., Pham, H., Park, C. and Shin, J. (2019). Information about variations in multiple copies of bacterial 16S rRNA genes may aid in species identification. PLOS ONE, 14(2), p.e0212090.

illumina , (2022). Sequencing Coverage for NGS Experiments. [online] emea.illumina.com. Available at: https://emea.illumina.com/science/technology/next-generation-sequencing/plan-experiments/coverage.html [Accessed 4 Dec. 2023].

Iwatsuki, T., Kanazawa, T., Ogasawara, T., Hosotani, K., Tsuchiya, K., Watanabe, S., Suzuki, T., Moriuchi, R., Kanesaki, Y. and Dohra, H. (2021). 16S rRNA Gene Amplicon Sequencing of Gut Microbiota in Three Species of Deep-Sea Fish in Suruga Bay, Japan. Microbiology Resource Announcements, 10(1). doi:https://doi.org/10.1128/mra.01260-20.

Jaffe, A.L., Thomas, A.D., He, C., Keren, R., Valentin-Alvarado, L.E., Munk, P., Bouma-Gregson, K., Farag, I., Amano, Y., Sachdeva, R. and West, P.T. (2021). Patterns of Gene Content and Co-occurrence Constrain the Evolutionary Path toward Animal Association in Candidate Phyla Radiation Bacteria. MBio, 12(4). doi:https://doi.org/10.1128/mbio.00521-21.

Javan, G., Finley, S., Abidin, Z. and Mulle, J. (2016a). The Thanatomicrobiome: A Missing Piece of the Microbial Puzzle of Death. Frontiers in Microbiology, 7

Javan, G., Finley, S., Can, I., Wilkinson, J., Hanson, J. and Tarone, A. (2016b). Human Thanatomicrobiome Succession and Time Since Death. Scientific Reports, 6(1).

Javan, G.T., Finley, S.J., Moretti, M., Silvia Damiana Visoná, Mezzari, M.P. and Green, R.L. (2023). COVID-19 and brain-heart-lung microbial fingerprints in Italian cadavers. Frontiers in Molecular Biosciences, 10. doi:https://doi.org/10.3389/fmolb.2023.1196328.

Javan, G.T., Finley, S.J., Smith, T., Miller, J. and Wilkinson, J.E. (2017). Cadaver Thanatomicrobiome Signatures: The Ubiquitous Nature of Clostridium Species in Human Decomposition. Frontiers in Microbiology, [online] 8. doi:https://doi.org/10.3389/fmicb.2017.02096.

Jean-François Bernardet and Nakagawa, Y. (2006). An Introduction to the Family Flavobacteriaceae. pp.455–480. doi:https://doi.org/10.1007/0-387-30747-8_16.

Ji, L., Yu, X. and Guo, D. (2023). Soil Fungal Community Structure and Its Effect on CO_2 Emissions in the Yellow River Delta. International Journal of Environmental Research and Public Health, 20(5), pp.4190–4190. doi:https://doi.org/10.3390/ijerph20054190.

Ji, Y., Zhang, P., Zhou, S., Gao, P., Wang, B. and Jiang, J. (2022). Widespread but Poorly Understood Bacteria: Candidate Phyla Radiation. Microorganisms, 10(11), p.2232. doi:https://doi.org/10.3390/microorganisms10112232.

Jia, Y. and Whalen, J.K. (2020). A new perspective on functional redundancy and phylogenetic niche conservatism in soil microbial communities. Pedosphere, 30(1), pp.18–24. doi:https://doi.org/10.1016/s1002-0160(19)60826-x.

Johansen, E. (2014). Twelve reasons you need to read about lactic acid bacteria - On Biology. [online] On Biology. Available at: https://blogs.biomedcentral.com/on-biology/2014/08/29/twelve-reasons-you-need-to-read-about-lactic-acid-bacteria/ [Accessed 7 Dec. 2023].

Joseph, I., Mathew, D., Sathyan, P. and Vargheese, G. (2011). The Use of Insects in Forensic investigations: an Overview on the Scope of Forensic Entomology. Journal of Forensic Dental Sciences, [online] 3(2), p.89. doi:https://doi.org/10.4103/0975-1475.92154.

Kadnikov, V.V., Mardanov, A.V., Beletsky, A.V., Карначук, O.B. and Ravin, N.V. (2020). Complete Genome of a Member of a New Bacterial Lineage in the Microgenomates Group Reveals an Unusual Nucleotide Composition Disparity Between Two Strands of DNA and Limited Metabolic Potential. Microorganisms, 8(3), pp.320–320. doi:https://doi.org/10.3390/microorganisms8030320.

Kanani, P., Shukla, Y.M., Modi, A.R., Subhash, N. and Kumar, S. (2019). Standardization of an efficient protocol for isolation of RNA from Cuminum cyminum. Journal of King Saud University - Science, 31(4), pp.1202–1207. doi:https://doi.org/10.1016/j.jksus.2018.12.008.

Kang, S., Ma, W., Li, F.Y., Zhang, Q., Niu, J., Ding, Y., Han, F. and Sun, X. (2015). Functional Redundancy Instead of Species Redundancy Determines Community Stability in a Typical Steppe of Inner Mongolia. PLOS ONE, [online] 10(12), p.e0145605. doi:https://doi.org/10.1371/journal.pone.0145605.

Kant, R., van Passel, M.W.J., Sangwan, P., Palva, A., Lucas, S., Copeland, A., Lapidus, A., Glavina del Rio, T., Dalin, E., Tice, H., Bruce, D., Goodwin, L., Pitluck, S., Chertkov, O., Larimer, F.W., Land, M.L., Hauser, L., Brettin, T.S., Detter, J.C. and Han, S. (2011). Genome Sequence of 'Pedosphaera parvula' Ellin514, an Aerobic Verrucomicrobial Isolate from Pasture Soil. Journal of Bacteriology, 193(11), pp.2900–2901. doi:https://doi.org/10.1128/jb.00299-11.

Kapli, P., Yang, Z. and Telford, M.J. (2020). Phylogenetic tree building in the genomic age. Nature Reviews Genetics, [online] 21(7), pp.428–444. doi:https://doi.org/10.1038/s41576-020-0233-0.

Kaszubinski, S.F., Pechal, J.L., Schmidt, C.J., Jordan, H.R., Benbow, M.E. and Meek, M.H. (2019). Evaluating Bioinformatic Pipeline Performance for Forensic Microbiome Analysis *,†,‡. Journal of Forensic Sciences, 65(2), pp.513–525. doi:https://doi.org/10.1111/1556-4029.14213.

Khatoon, H., Solanki, P., Narayan, M., Tewari, L., Rai, J. and Hina Khatoon, C. (2017). Role of microbes in organic carbon decomposition and maintenance of soil ecosystem. *International Journal of Chemical Studies*, *5*(6), pp.1648-1656.

Khetan, D., Gupta, N., Chaudhary, R. and Shukla, J. (2019). Comparison of UV spectrometry and fluorometry-based methods for quantification of cell-free DNA in red cell components. Asian Journal of Transfusion Science, 13(2), p.95. doi:https://doi.org/10.4103/ajts.ajts_90_19.

Kiani, A.K. (2022). Ethical considerations regarding animal experimentation. Journal of preventive medicine and hygiene, [online] 63(2 Suppl 3), pp.E255–E266. doi:https://doi.org/10.15167/2421-4248/jpmh2022.63.2S3.2768.

Kim J. H., Seo, H., Kim, S., Asad Ul-Haq, Song, H. and Yun Seob Song (2023). Malignant Prostate Tissue Is Associated with Different Microbiome Gene Functions. Diagnostics, 13(2), pp.278–278. doi:https://doi.org/10.3390/diagnostics13020278.

Kim, J.-K., Choi, M.S., Kim, J.-Y., Yu, J.S., Seo, J.I., Yoo, H.H. and Kim, D.-H. (2021). Ginkgo biloba leaf extract suppresses intestinal human breast cancer resistance protein expression in mice: Correlation with gut microbiota. Biomedicine & Pharmacotherapy, [online] 140, p.111712. doi:https://doi.org/10.1016/j.biopha.2021.111712.

Kim, M.J., Lee, S., Kwon, M.Y. and Kim, M. (2022). Clinical Significance of Composition and Functional Diversity of the Vaginal Microbiome in Recurrent Vaginitis. Frontiers in Microbiology, 13. doi:https://doi.org/10.3389/fmicb.2022.851670.

Kim, S.-G., Kim, D.-W. and Jang, H. (2022). Effects of Antibiotics on the Uterine Microbial Community of Mice. Development & reproduction, [online] 26(4), pp.145–153. doi:https://doi.org/10.12717/dr.2022.26.4.145.

Kingsley, D.H. (2014). SHELLFISH (MOLLUSCS AND CRUSTACEA) | Shellfish Contamination and Spoilage. Elsevier eBooks, pp.389–396. doi:https://doi.org/10.1016/b978-0-12-384730-0.00306-2.

Kisand, V. and Wikner, J. (2003). Combining Culture-Dependent and -Independent Methodologies for Estimation of Richness of Estuarine Bacterioplankton Consuming Riverine Dissolved Organic Matter. Applied and Environmental Microbiology, [online] 69(6), pp.3607–3616. doi:https://doi.org/10.1128/AEM.69.6.3607-3616.2003.

Klindworth, A., Pruesse, E., Schweer, T., Peplies, J., Quast, C., Horn, M. and Glöckner, F.O. (2012). Evaluation of general 16S ribosomal RNA gene PCR primers for classical and next-generation sequencing-based diversity studies. Nucleic Acids Research, [online] 41(1), pp.e1–e1. doi:https://doi.org/10.1093/nar/gks808.

Knight, R., Metcalf, J., Gilbert, J. and Carter, D. (2018). Evaluating the Skin Microbiome as Trace Evidence. [online] Available at: https://www.ojp.gov/pdffiles1/nij/grants/251647.pdf.

Knobel, Z., Ueland, M., Nizio, K.D., Patel, D. and Forbes, S.L. (2018). A Comparison of Human and Pig Decomposition Rates and Odour Profiles in an Australian Environment. Australian Journal of Forensic Sciences, 51(5), pp.1–16. doi:https://doi.org/10.1080/00450618.2018.1439100.

Knüpfer, M., Braun, P., Baumann, K., Rehn, A., Antwerpen, M., Grass, G. and Wölfel, and R. (2020). Evaluation of a Highly Efficient DNA Extraction Method for Bacillus anthracis Endospores. Microorganisms, 8(5), p.763. doi:https://doi.org/10.3390/microorganisms8050763.

Koetsier, G. and Cantor, E. (2019). A Practical Guide to Analyzing Nucleic Acid Concentration and Purity with Microvolume Spectrophotometers. [online] New England Biolabs. Available at: https://www.neb.com/en-gb/-/media/nebus/files/application-notes/technote_mvs_analysis_of_nucleic_acid_concentration_and_purity.pdf?rev=c24cea043416420d84fb6bf7b554dbbb [Accessed 4 Dec. 2023].

Könönen, E. and Gursoy, U.K. (2022). Oral Prevotella Species and Their Connection to Events of Clinical Relevance in Gastrointestinal and Respiratory Tracts. Frontiers in Microbiology, 12. doi:https://doi.org/10.3389/fmicb.2021.798763.

Kovaleva, O.L., Elcheninov, A.G., Kublanov, I.V. and Bonch-Osmolovskaya, E.A. (2019). T epidisphaeraceae . Bergey's Manual of Systematics of Archaea and Bacteria, pp.1–3. doi:https://doi.org/10.1002/9781118960608.fbm00305.

Kowalski, K. (2014). Recycling the dead. ScienceNewsExplores . Available at: https://www.snexplores.org/article/recycling-dead [Accessed 20 Nov. 2022].

Kozich, J., Westcott, S., Baxter, N., Highlander, S. and Schloss, P. (2013). Development of a Dual-Index Sequencing Strategy and Curation Pipeline for Analyzing Amplicon Sequence Data on the MiSeq Illumina Sequencing Platform. Applied and Environmental Microbiology, 79(17), pp.5112-5120.

Kozjek, K., Manoharan, L., Ahrén, D. and Hedlund, K. (2022). Microbial functional genes influenced by short-term experimental drought across European agricultural fields. Soil Biology and Biochemistry, 168, p.108650. doi:https://doi.org/10.1016/j.soilbio.2022.108650.

Kuiper, I. (2016). Microbial forensics: next-generation sequencing as catalyst. EMBO reports, 17(8), pp.1085-1087.

Kumar, R., Yadav, G., Kuddus, M., Ghulam Md Ashraf and Singh, R. (2023). Unlocking the microbial studies through computational approaches: how far have we reached? Environmental Science and Pollution Research, 30(17), pp.48929–48947. doi:https://doi.org/10.1007/s11356-023-26220-0.

Kumawat, C., Kumar, A., Parshad, J., Sharma, S.S., Patra, A., Dogra, P., Yadav, G.K., Dadhich, S.K., Verma, R. and Kumawat, G.L. (2022). Microbial Diversity and Adaptation under Salt-Affected Soils: A Review. *Sustainability*, 14(15), p.9280. doi:https://doi.org/10.3390/su14159280.

Lagkouvardos I., Till Robin Lesker, Thomas, Eric, Smit, N., Neuhaus, K., Wang, J., Baines, J., Abt, B., Stecher, B., Overmann, J., Till Strowig and Clavel, T. (2019). Sequence and cultivation study of Muribaculaceae

reveals novel species, host preference, and functional potential of this yet undescribed family. Microbiome, 7(1). doi:https://doi.org/10.1186/s40168-019-0637-2.

Lagkouvardos, I., Jehl, M.-A., Rattei, T. and Horn, M. (2014). Signature Protein of the PVC Superphylum. Applied and Environmental Microbiology, 80(2), pp.440–445. doi:https://doi.org/10.1128/aem.02655-13.

Lakens, D. (2022). Sample size justification. Collabra: Psychology, [online] 8(1), p.33267. doi:https://doi.org/10.1525/collabra.33267.

Lang, J., Erb, R., Pechal, J., Wallace, J., McEwan, R. and Benbow, M. (2016). Microbial Biofilm Community Variation in Flowing Habitats: Potential Utility as Bioindicators of Post-mortem Submersion Intervals. Microorganisms, 4(1), p.1. doi:https://doi.org/10.3390/microorganisms4010001.

Lange, C., Boyer, S., Bezemer, T. M., Lefort, M. C., Dhami, M. K., Biggs, E., ... & Kaltenpoth, M. (2023). Impact of intraspecific variation in insect microbiomes on host phenotype and evolution. The ISME journal, 17(11), 1798-1807

Lapage, S.P. and Owen, R.J. (1973). Flavobacterium meningosepticum from cases' of meningitis in Botswana and England. Journal of Clinical Pathology, 26(10), pp.747–749. doi:https://doi.org/10.1136/jcp.26.10.747.

Lauber, C.L., Metcalf, J.L., Keepers, K., Ackermann, G., Carter, D.O. and Knight, R. (2014). Vertebrate Decomposition Is Accelerated by Soil Microbes. Applied and Environmental Microbiology, [online] 80(16), pp.4920–4929. doi:https://doi.org/10.1128/aem.00957-14.

Lax, S., Hampton-Marcell, J.T., Gibbons, S.M., Colares, G.B., Smith, D., Eisen, J.A. and Gilbert, J.A. (2015). Forensic analysis of the microbiome of phones and shoes. Microbiome, [online] 3(1). doi:https://doi.org/10.1186/s40168-015-0082-9.

Leake, S.L. (2013). Is human DNA enough?—potential for bacterial DNA. Frontiers in Genetics, 4. doi:https://doi.org/10.3389/fgene.2013.00282.

Lee So-Yeon, Seung-Kyun Woo, You-Jin Hong, Go-Woon Choi, and Bin Eom, Y. (2015). Microbial Forensic Analysis of Bacterial Fingerprint by Sequence Comparison of 16S rRNA Gene. Journal of Forensic Research, 06(05). doi:https://doi.org/10.4172/2157-7145.1000297.

Lee, B.-H., Nicolas, P., Izzet Burcin Saticioglu, Fradet, B., Jean-François Bernardet, Dimitri Rigaudeau, Rochat, T. and Duchaud, E. (2023). Investigation of the Genus Flavobacterium as a Reservoir for Fish-Pathogenic Bacterial Species: the Case of Flavobacterium collinsii. Applied and Environmental Microbiology. doi:https://doi.org/10.1128/aem.02162-22.

Lee, J.-S., Chung, M.-J. and Seo, J.-G. (2013). In Vitro Evaluation of Antimicrobial Activity of Lactic Acid Bacteria against Clostridium difficile. Toxicological Research, 29(2), pp.99–106. doi:https://doi.org/10.5487/tr.2013.29.2.099.

Lee, K.-C., Webb, R.I., Janssen, P.H., Sangwan, P., Romeo, T., Staley, J.T. and Fuerst, J.A. (2009). Phylum Verrucomicrobia representatives share a compartmentalized cell plan with members of bacterial phylum Planctomycetes. BMC Microbiology, [online] 9, p.5. doi:https://doi.org/10.1186/1471-2180-9-5.

Lever, M.A., Torti, A., Eickenbusch, P., Michaud, A.B., Å antl-Temkiv, T. and JÃ¸rgensen, B.B. (2015). A modular method for the extraction of DNA and RNA, and the separation of DNA pools from diverse environmental sample types. Frontiers in Microbiology, [online] 6. doi:https://doi.org/10.3389/fmicb.2015.00476.

Levy, S.E. and Boone, B.E. (2018). Next-Generation Sequencing Strategies. Cold Spring Harbor Perspectives in Medicine, 9(7), p.a025791. doi:https://doi.org/10.1101/cshperspect.a025791.

Li, F., Fu, D., Tao, D., Feng, X., May, Xu, W. and Lu, H. (2021). Dynamic Observation of the Effect of Maternal Caries on the Oral Microbiota of Infants Aged 12–24 Months. [online] 11. doi:https://doi.org/10.3389/fcimb.2021.637394.

Li, H., Zhang, S., Liu, R., Yuan, L., Wu, D., Yang, E., Yang, H., Ullah, S., Ishaq, H.M., Liu, H., Wang, Z. and Xu, J. (2021). Potential use of molecular and structural characterization of the gut bacterial community for post-mortem interval estimation in Sprague Dawley rats. Scientific Reports, 11(1). doi:https://doi.org/10.1038/s41598-020-80633-2.

Li, X., Liu, Y., Yang, X., Li, C. and Song, Z. (2022). The Oral Microbiota: Community Composition, Influencing Factors, Pathogenesis, and Interventions. Frontiers in Microbiology, 13. doi:https://doi.org/10.3389/fmicb.2022.895537.

Liao, S.F. and Nyachoti, M. (2017). Using probiotics to improve swine gut health and nutrient utilization. Animal Nutrition, 3(4), pp.331–343. doi:https://doi.org/10.1016/j.aninu.2017.06.007.

Lim, H.J., Choi, J.-H. and Son, A. (2017). Necessity of purification during bacterial DNA extraction with environmental soils. Environmental Health and Toxicology, 32, p.e2017013. doi:https://doi.org/10.5620/eht.e2017013.

Lin, J. and Cheng, J. (2019). Quorum Sensing in*Pseudomonas aeruginosa*and Its Relationship to Biofilm Development. *ACS Symposium Series*, pp.1–16. doi:https://doi.org/10.1021/bk-2019-1323.ch001.

Lindefeldt, M., Eng, A., Darban, H., Bjerkner, A., Zetterström, C.K., Allander, T., Andersson, B., Borenstein, E., Dahlin, M. and Prast-Nielsen, S. (2019). The ketogenic diet influences taxonomic and functional composition of the gut microbiota in children with severe epilepsy. npj Biofilms and Microbiomes, 5(1). doi:https://doi.org/10.1038/s41522-018-0073-2.

Litterick, A. (2023). Organic matter in soils -what forms does it take and how important is it? [online] Available at: https://www.fas.scot/downloads/roxburghshire-soil-nutrient-network-organic-matter-presentation-slides-audrey-litterick/ [Accessed 20 Dec. 2023].

Liu, B.-N., Liu, X.-T., Liang, Z.-H. and Wang, J.-H. (2021). World Journal of Gastroenterology Gut microbiota in obesity Manuscript source: Invited manuscript. World J Gastroenterol, [online] 27(25), pp.3837–3850. doi:https://doi.org/10.3748/wjg.v27.i25.3837.

Liu, C., Du, M.-X., Abuduaini, R., Yu, H.-Y., Li, D.-H., Wang, Y.-J., Zhou, N., Jiang, M.-Z., Niu, P.-X., Han, S.-S., Chen, H.-H., Shi, W.-Y., Wu, L., Xin, Y.-H., Ma, J., Zhou, Y., Jiang, C.-Y., Liu, H.-W. and Liu, S.-J. (2021). Enlightening the taxonomy darkness of human gut microbiomes with a cultured biobank. Microbiome, 9(1). doi:https://doi.org/10.1186/s40168-021-01064-3.

Liu, F., Hewezi, T., Lebeis, S.L., Pantalone, V., Grewal, P.S. and Staton, M.E. (2019). Soil indigenous microbiome and plant genotypes cooperatively modify soybean rhizosphere microbiome assembly. BMC Microbiology, 19(1). doi:https://doi.org/10.1186/s12866-019-1572-x.

Liu, Q., Liu, H.-C., Zhou, Y.-G. and Xin, Y.-H. (2019). Stenotrophobium rhamnosiphilum gen. nov., sp. nov., isolated from a glacier, proposal of Steroidobacteraceae fam. nov. in Nevskiales and emended description of the family Nevskiaceae. International Journal of Systematic and Evolutionary Microbiology, 69(5), pp.1404–1410. doi:https://doi.org/10.1099/ijsem.0.003327.

Liu, R., Zhang, K., Li, H., Sun, Q., Wei, X., Li, H., Zhang, S., Fan, S. and Wang, Z. (2023). Dissecting the microbial community structure of internal organs during the early post-mortem period in a murine corpse model. BMC Microbiology, 23(1). doi:https://doi.org/10.1186/s12866-023-02786-0.

Liu, Z., DeSantis, T.Z., Andersen, G.L. and Knight, R. (2008). Accurate taxonomy assignments from 16S rRNA sequences produced by highly parallel pyrosequencers. Nucleic Acids Research, 36(18), pp.e120–e120. doi:https://doi.org/10.1093/nar/gkn491.

Lladó Fernández, S., Větrovský, T. and Baldrian, P. (2019). The concept of operational taxonomic units revisited: genomes of bacteria that are regarded as closely related are often highly dissimilar. Folia Microbiologica, [online] 64(1), pp.19–23. doi:https://doi.org/10.1007/s12223-018-0627-y.

Lloyd, K.G. and Tahon, G. (2022). Science depends on nomenclature, but nomenclature is not science. Nature Reviews Microbiology, [online] 20(3), pp.123–124. doi:https://doi.org/10.1038/s41579-022-00684-2.

Logsdon, G.A., Vollger, M.R. and Eichler, E.E. (2020). Long-read human genome sequencing and its applications. Nature Reviews Genetics, 21(10), pp.597–614. doi:https://doi.org/10.1038/s41576-020-0236-x.

López-García, A., Pineda-Quiroga, C., Atxaerandio, R., Pérez, A., Hernández, I., García-Rodríguez, A. and González-Recio, O. (2018). Comparison of Mothur and QIIME for the Analysis of Rumen Microbiota Composition Based on 16S rRNA Amplicon Sequences. Frontiers in Microbiology, 9. doi:https://doi.org/10.3389/fmicb.2018.03010.

Lozupone, C., Lladser, M.E., Knights, D., Stombaugh, J. and Knight, R. (2010). UniFrac: an effective distance metric for microbial community comparison. The ISME Journal, 5(2), pp.169–172. doi:https://doi.org/10.1038/ismej.2010.133.

Lozupone, C.A., Stombaugh, J.I., Gordon, J.I., Jansson, J.K. and Knight, R. (2012). Diversity, stability and resilience of the human gut microbiota. Nature, [online] 489(7415), pp.220–230. doi:https://doi.org/10.1038/nature11550.

Lucena-Aguilar, G., Sánchez-López, A.M., Barberán-Aceituno, C., Carrillo-Ávila, J.A., López-Guerrero, J.A. and Aguilar-Quesada, R. (2016). DNA Source Selection for Downstream Applications Based on DNA Quality Indicators Analysis. Biopreservation and Biobanking, [online] 14(4), pp.264–270. doi:https://doi.org/10.1089/bio.2015.0064.

Ma, X., Kim, J.-K., Shin, Y.-J., Son, Y.-H., Lee, D.-Y., Park, H.-S. and Kim, D.-H. (2023). Alleviation of Cognitive Impairment-like Behaviors, Neuroinflammation, Colitis, and Gut Dysbiosis in 5xFAD Transgenic and Aged Mice by Lactobacillus mucosae and Bifidobacterium longum. Nutrients, 15(15), pp.3381–3381. doi:https://doi.org/10.3390/nu15153381.

Maatouk Mohamad, Ibrahim, A., Rolain, J., Merhej, V. and Bittar, F. (2021). Small and Equipped: the Rich Repertoire of Antibiotic Resistance Genes in Candidate Phyla Radiation Genomes. MSystems, 6(6). doi:https://doi.org/10.1128/msystems.00898-21.

Magagnoli, S., Alberoni, D., Baffoni, L., Martini, A., Marini, F., Di Gioia, D., Mazzon, M., Marzadori, C., Campanelli, G. and Burgio, G. (2022). The ground beetle Pseudoophonus rufipes gut microbiome is influenced by the farm management system. Scientific Reports, [online] 12(1), p.22638. doi:https://doi.org/10.1038/s41598-022-25408-7.

Magurran, A.E. (2013). Measuring Biological Diversity. John Wiley & Sons.

Magurran, A.E. (2021). Measuring biological diversity. Current Biology, 31(19), pp.R1174–R1177. doi:https://doi.org/10.1016/j.cub.2021.07.049.

Majaneva, M., Diserud, O.H., Eagle, S.H.C., Boström, E., Hajibabaei, M. and Ekrem, T. (2018). Environmental DNA filtration techniques affect recovered biodiversity. Scientific Reports, 8(1). doi:https://doi.org/10.1038/s41598-018-23052-8.

Manson, K. and Steel, M. (2023). Spaces of Phylogenetic Diversity Indices: Combinatorial and Geometric Properties. Bulletin of Mathematical Biology, [online] 85(8). doi:https://doi.org/10.1007/s11538-023-01183-y.

Marín, I., Arahal, D.R. (2014). The Family Beijerinckiaceae. In: Rosenberg, E., DeLong, E.F., Lory, S., Stackebrandt, E., Thompson, F. (eds) The Prokaryotes. Springer, Berlin, Heidelberg. https://doi.org/10.1007/978-3-642-30197-1_255

Maron, P.-A., Sarr, A., Kaisermann, A., Lévêque, J., Mathieu, O., Guigue, J., Karimi, B., Bernard, L., Dequiedt, S., Terrat, S., Chabbi, A. and Ranjard, L. (2018). High Microbial Diversity Promotes Soil Ecosystem Functioning. Applied and Environmental Microbiology, 84(9). doi:https://doi.org/10.1128/aem.02738-17.

Martin, A.P. (2002). Phylogenetic Approaches for Describing and Comparing the Diversity of Microbial Communities. Applied and Environmental Microbiology, 68(8), pp.3673–3682. doi:https://doi.org/10.1128/aem.68.8.3673-3682.2002.

Mathieu, E., Escribano-Vazquez, U., Descamps, D., Cherbuy, C., Langella, P., Riffault, S., Remot, A. and Thomas, M. (2018). Paradigms of Lung Microbiota Functions in Health and Disease, Particularly, in Asthma. Frontiers in Physiology, 9. doi:https://doi.org/10.3389/fphys.2018.01168.

Matti Gralka, Pollak, S. and Cordero, O.X. (2023). Genome content predicts the carbon catabolic preferences of heterotrophic bacteria. Nature Microbiology, 8(10), pp.1799–1808. doi:https://doi.org/10.1038/s41564-023-01458-z.

Matuszewski, S., Hall, M.J.R., Moreau, G., Schoenly, K.G., Tarone, A.M. and Villet, M.H. (2019). Pigs vs people: the use of pigs as analogues for humans in forensic entomology and taphonomy research. International Journal of Legal Medicine, 134(2). doi:https://doi.org/10.1007/s00414-019-02074-5.

McBride, Z., Chen, D., Reick, C., Xie, J. and Szymanski, D.B. (2017). Global Analysis of Membrane-associated Protein Oligomerization Using Protein Correlation Profiling. Molecular & Cellular Proteomics, 16(11), pp.1972–1989. doi:https://doi.org/10.1074/mcp.ra117.000276.

McGuire, A.L., Colgrove, J., Whitney, S.N., Diaz, C.M., Bustillos, D. and Versalovic, J. (2008). Ethical, legal, and social considerations in conducting the Human Microbiome Project. Genome Research, 18(12), pp.1861–1864. doi:https://doi.org/10.1101/gr.081653.108.

Meadow, J.F., Altrichter, A.E. and Green, J.L. (2014). Mobile phones carry the personal microbiome of their owners. PeerJ, [online] 2, p.e447. doi:https://doi.org/10.7717/peerj.447.

Medina, D., Walke, J.B., Gajewski, Z., Becker, M.H., Swartwout, M.C. and Belden, L.K. (2017). Culture Media and Individual Hosts Affect the Recovery of Culturable Bacterial Diversity from Amphibian Skin. Frontiers in Microbiology, 8. doi:https://doi.org/10.3389/fmicb.2017.01574.

Melo, V.F., Testoni, S.A., Dawson, L., de Lara, A.G. and da Silva Salvador, F.A. (2019). Can analysis of a small clod of soil help to solve a murder case? Science & Justice, 59(6), pp.667–677. doi:https://doi.org/10.1016/j.scijus.2019.06.008.

Metcalf, J.L. (2019). Estimating the post-mortem interval using microbes: Knowledge gaps and a path to technology adoption. Forensic Science International: Genetics, 38, pp.211–218. doi:https://doi.org/10.1016/j.fsigen.2018.11.004.

Metcalf, J.L., Wegener Parfrey, L., Gonzalez, A., Lauber, C.L., Knights, D., Ackermann, G., Humphrey, G.C., Gebert, M.J., Van Treuren, W., Berg-Lyons, D., Keepers, K., Guo, Y., Bullard, J., Fierer, N., Carter, D.O. and Knight, R. (2013). A microbial clock provides an accurate estimate of the post-mortem interval in a mouse model system. eLife, [online] 2, p.e01104. doi:https://doi.org/10.7554/eLife.01104.

Mir, T. ul G., Wani, A.K., Akhtar, N., Sena, S. and Singh, J. (2022). Microbial forensics: A potential tool for investigation and response to bioterrorism. *Health Sciences Review*, [online] 5, p.100068. doi:https://doi.org/10.1016/j.hsr.2022.100068.

Mohammad Towsif Hossain (2023). Synthetic biology and metabolic engineering for improvement of lactic acid bacteria as cell factories. Elsevier eBooks, pp.17–28. doi:https://doi.org/10.1016/b978-0-323-91930-2.00006-7.

Montemurno, M. (2022). What are Brackish Water Environments? [online] Ocean Conservancy. Available at: https://oceanconservancy.org/blog/2022/06/30/brackish-water-environments/ [Accessed 7 Dec. 2023].

Moreira, D., Zivanovic, Y., López-Archilla, A.I., Iniesto, M. and López-García, P. (2021). Reductive evolution and unique predatory mode in the CPR bacterium Vampirococcus lugosii. Nature Communications, 12(1). doi:https://doi.org/10.1038/s41467-021-22762-4.

Morrison, A.G., Sarkar, S., Umar, S., Lee, S.T.M. and Thomas, S.M. (2023). The Contribution of the Human Oral Microbiome to Oral Disease: A Review. Microorganisms, [online] 11(2), p.318. doi:https://doi.org/10.3390/microorganisms11020318.

Muse, H., Jenkins, R.L., Oliver, M.B., Kim, S., Grantier, R.L., Malhotra, B.K., Parham, J.J. and Stover, K.R. (2017). A Case of Ignatzschineria indica Bacteremia following Maggot Colonization. Case Reports in Infectious Diseases, [online] 2017, p.3698124. doi:https://doi.org/10.1155/2017/3698124.

Mutuyemungu, E., Singh, M., Liu, S. and Rose, D.J. (2023). Intestinal gas production by the gut microbiota: A review. Journal of Functional Foods, [online] 100, p.105367. doi:https://doi.org/10.1016/j.jff.2022.105367.

Nandakumar, V., Chittaranjan, S., Kurian, V.M. and Doble, M. (2012). Characteristics of bacterial biofilm associated with implant material in clinical practice. Polymer Journal, 45(2), pp.137–152. doi:https://doi.org/10.1038/pj.2012.130.

Natalini, J.G., Singh, S. and Segal, L.N. (2022). The dynamic lung microbiome in health and disease. Nature Reviews Microbiology. doi:https://doi.org/10.1038/s41579-022-00821-x.

Naushad, S., Adeolu, M., Goel, N., Khadka, B., Al-Dahwi, A. and Gupta, R.S. (2015). Phylogenomic and Molecular Demarcation of the Core Members of the PolyphyleticPasteurellaceaeGeneraActinobacillus,Haemophilus, andPasteurella. International Journal of Genomics, [online] 2015, pp.1–15. doi:https://doi.org/10.1155/2015/198560.

Newton, R.J., Jones, S.E., Eiler, A., McMahon, K.D. and Bertilsson, S. (2011). A Guide to the Natural History of Freshwater Lake Bacteria. Microbiology and Molecular Biology Reviews, [online] 75(1), pp.14–49. doi:https://doi.org/10.1128/mmbr.00028-10.

Ng, K.M., Pannu, S., Liu, S., Burckhardt, J.C., Hughes, T., Will Van Treuren, Nguyen, J., Naqvi, K., Nguyen, B., Clayton, C.A., Pepin, D.M., Collins, S.R. and Tropini, C. (2023). Single-strain behavior predicts responses to environmental pH and osmolality in the gut microbiota. *mBio*. doi:https://doi.org/10.1128/mbio.00753-23.

Nguyen-Lefebvre, A.T. and Horuzsko, A. (2015). Kupffer Cell Metabolism and Function. Journal of enzymology and metabolism, [online] 1(1). Available at: https://www.ncbi.nlm.nih.gov/pmc/articles/PMC4771376/#.

Nicolas, A.M., Jaffe, A.L., Nuccio, E., Taga, M.E. and Firestone, M.K. (2021). Soil Candidate Phyla Radiation Bacteria Encode Components of Aerobic Metabolism and Co-occur with Nanoarchaea in the Rare Biosphere of Rhizosphere Grassland Communities. MSystems, 6(4). doi:https://doi.org/10.1128/msystems.01205-20.

Nielsen, U.N., Wall, D.H. and Six, J. (2015). Soil Biodiversity and the Environment. Annual Review of Environment and Resources, 40(1), pp.63–90. doi:https://doi.org/10.1146/annurev-environ-102014-021257.

Nieves Delgado, A. and Baedke, J. (2021). Does the human microbiome tell us something about race? Humanities and Social Sciences Communications, [online] 8(1), pp.1–12. doi:https://doi.org/10.1057/s41599-021-00772-3.

Noppol Arunrat, Chakriya Sansupa, Sukanya Sereenonchai and Hatano, R. (2023). Stability of soil bacteria in undisturbed soil and continuous maize cultivation in Northern Thailand. Frontiers in Microbiology, 14. doi:https://doi.org/10.3389/fmicb.2023.1285445.

Nosek, B.A., Hardwicke, T.E., Moshontz, H., Allard, A., Corker, K.S., Dreber, A., Fidler, F., Hilgard, J., Kline Struhl, M., Nuijten, M.B., Rohrer, J.M., Romero, F., Scheel, A.M., Scherer, L.D., Schönbrodt, F.D. and Vazire, S. (2022). Replicability, Robustness, and Reproducibility in Psychological Science. Annual Review of Psychology, 73(1), pp.719–748. doi:https://doi.org/10.1146/annurev-psych-020821-114157.

Nyongesa, S., Weber, P.M., Bernet, È., Pulido, F., Nieves, C., Nieckarz, M., Delaby, M., Viehboeck, T., Krause, N., Rivera-Millot, A., Nakamura, A., Vischer, N.O.E., vanNieuwenhze, M., Brun, Y.V., Cava, F., Bulgheresi, S. and Veyrier, F.J. (2022). Evolution of longitudinal division in multicellular bacteria of the Neisseriaceae family. Nature Communications, 13(1). doi:https://doi.org/10.1038/s41467-022-32260-w.

O'Dwyer, D.N., Dickson, R.P. and Moore, B.B. (2016). The Lung Microbiome, Immunity, and the Pathogenesis of Chronic Lung Disease. The Journal of Immunology, [online] 196(12), pp.4839–4847. doi:https://doi.org/10.4049/jimmunol.1600279.

O'Dwyer, J.P., Kembel, S.W. and Green, J.L. (2012). Phylogenetic Diversity Theory Sheds Light on the Structure of Microbial Communities. PLoS Computational Biology, 8(12), p.e1002832. doi:https://doi.org/10.1371/journal.pcbi.1002832.

Oades, J.M. (1988). The retention of organic matter in soils. Biogeochemistry, 5(1), pp.35–70. doi:https://doi.org/10.1007/bf02180317.

Odom, C., Kim, Y., Burgess, C.L., Baird, L.C., Korkmaz, F., Elim Na, Shenoy, A.T., Arafa, E.I., Lam, T.T., Jones, M.R., Mizgerd, J.P., Traber, K. and Quinton, L.J. (2021). Liver-Dependent Lung Remodeling during Systemic Inflammation Shapes Responses to Secondary Infection. Journal of Immunology, 207(7), pp.1891–1902. doi:https://doi.org/10.4049/jimmunol.2100254.

Ogunrinola, G.A., Oyewale, J.O., Oshamika, O.O. and Olasehinde, G.I. (2020). The Human Microbiome and Its Impacts on Health. International Journal of Microbiology, [online] 2020, pp.1–7. doi:https://doi.org/10.1155/2020/8045646.

Olakanye, A.O. and T. Komang Ralebitso-Senior (2018). Assessing Subsurface Decomposition and Potential Impacts on Forensic Investigations. Elsevier eBooks, (978-0-12-809360-3), pp.145–176. doi:https://doi.org/10.1016/b978-0-12-809360-3.00007-2.

Oldham, A.L., Drilling, H.S., Stamps, B.W., Stevenson, B.S. and Duncan, K.E. (2012). Automated DNA extraction platforms offer solutions to challenges of assessing microbial biofouling in oil production facilities. AMB Express, 2(1), p.60. doi:https://doi.org/10.1186/2191-0855-2-60.

Oliveira, M. and Amorim, A. (2018). Microbial forensics: new breakthroughs and future prospects. Applied Microbiology and Biotechnology, [online] 102(24), pp.10377–10391. doi:https://doi.org/10.1007/s00253-018-9414-6.

Oliveira, M., Mason-Buck, G., Ballard, D., Branicki, W. and Amorim, A. (2020). Biowarfare, bioterrorism and biocrime: A historical overview on microbial harmful applications. Forensic Science International, 314, p.110366. doi:https://doi.org/10.1016/j.forsciint.2020.110366.

Olsen, I. (2014). The Family Fusobacteriaceae . In: Rosenberg, E., DeLong, E.F., Lory, S., Stackebrandt, E., Thompson, F. (eds) The Prokaryotes. Springer, Berlin, Heidelberg. https://doi.org/10.1007/978-3-642-30120-9_213

Olson, N.D. and Morrow, J.B. (2012). DNA extract characterization process for microbial detection methods development and validation. BMC Research Notes, [online] 5(1). doi:https://doi.org/10.1186/1756-0500-5-668.

Oren, A. and Garrity, G. (2020). List of new names and new combinations previously effectively, but not validly, published. International Journal of Systematic and Evolutionary Microbiology, 70(7), pp.4043–4049. doi:https://doi.org/10.1099/ijsem.0.004244.

Oren, A., Arahal, D.R., Göker, M., Edward, Rosselló-Móra, R. and Sutcliffe, I.C. (2023). International Code of Nomenclature of Prokaryotes. Prokaryotic Code (2022 Revision). International Journal of Systematic and Evolutionary Microbiology, 73(5a). doi:https://doi.org/10.1099/ijsem.0.005585.

Oren, A., Xu, XW. (2014). The Family Hyphomicrobiaceae. In: Rosenberg, E., DeLong, E.F., Lory, S., Stackebrandt, E., Thompson, F. (eds) The Prokaryotes. Springer, Berlin, Heidelberg. https://doi.org/10.1007/978-3-642-30197-1_257

Osman, M., Neoh, H., Ab Mutalib, N., Chin, S. and Jamal, R. (2018). 16S rRNA Gene Sequencing for Deciphering the Colorectal Cancer Gut Microbiome: Current Protocols and Workflows. Frontiers in Microbiology, 9.

Ozaki, D., Kubota, R., Maeno, T., Abdelhakim, M. and Hitosugi, N. (2020). Association between gut microbiota, bone metabolism, and fracture risk in postmenopausal Japanese women. Osteoporosis International, 32(1), pp.145–156. doi:https://doi.org/10.1007/s00198-020-05728-y.

Pacheco-Sandoval, A., Lago-Lestón, A., Abadía-Cardoso, A., Solana-Arellano, E. and Schramm, Y. (2022). Age as a primary driver of the gut microbial composition and function in wild harbor seals. Scientific Reports, [online] 12(1), p.14641. doi:https://doi.org/10.1038/s41598-022-18565-2.

Panda, A., Islam, S.T. and Sharma, G. (2022). Harmonizing Prokaryotic Nomenclature: Fixing the Fuss over Phylum Name Flipping. mBio, 13(3). doi:https://doi.org/10.1128/mbio.00970-22.

Paniagua Voirol, L.R., Frago, E., Kaltenpoth, M., Hilker, M. and Fatouros, N.E. (2018). Bacterial Symbionts in Lepidoptera: Their Diversity, Transmission, and Impact on the Host. Frontiers in Microbiology, 9. doi:https://doi.org/10.3389/fmicb.2018.00556.

Parada Venegas, D., De la Fuente, M.K., Landskron, G., González, M.J., Quera, R., Dijkstra, G., Harmsen, H.J.M., Faber, K.N. and Hermoso, M.A. (2019). Short Chain Fatty Acids (SCFAs)-Mediated Gut Epithelial and Immune Regulation and Its Relevance for Inflammatory Bowel Diseases. Frontiers in Immunology, [online] 10(277). doi:https://doi.org/10.3389/fimmu.2019.00277.

Park, H., Shen Jean Lim, Cosme, J., O'Connell, K.A., J. Sai Sandeep, F.C. Gayanilo, Cutter, G.R., Montes, E., Chotinan Nitikitpaiboon, Fisher, S.S., Moustahfid, H. and Thompson, L.R. (2023). Investigation of machine learning algorithms for taxonomic classification of marine metagenomes. Microbiology spectrum, 11(5). doi:https://doi.org/10.1128/spectrum.05237-22.

Patuzzi, I. (2018). 16S rRNA gene sequencing sparse count matrices: a count data simulator and optimal pre-processing pipelines. [Thesis] p.109. Available at: https://www.research.unipd.it/handle/11577/3426369 [Accessed 5 Dec. 2023].

Patuzzi, I., Baruzzo, G., Losasso, C., Ricci, A. and Di Camillo, B. (2019). metaSPARSim: a 16S rRNA gene sequencing count data simulator. BMC Bioinformatics, 20(S9). doi:https://doi.org/10.1186/s12859-019-2882-6.

Pechal, J.L., Crippen, T.L., Benbow, M.E., Tarone, A.M., Dowd, S. and Tomberlin, J.K. (2014). The potential use of bacterial community succession in forensics as described by high throughput metagenomic sequencing. International Journal of Legal Medicine, 128(1), pp.193–205. doi:https://doi.org/10.1007/s00414-013-0872-1.

Pechal, J.L., Crippen, T.L., Tarone, A.M., Lewis, A.J., Tomberlin, J.K. and Benbow, M.E. (2013). Microbial Community Functional Change during Vertebrate Carrion Decomposition. PLoS ONE, 8(11), p.e79035. doi:https://doi.org/10.1371/journal.pone.0079035.

Peña-Carrillo, D., Díez-Antolínez, R., Rubén González, González, R. and Gómez, X. (2023). Anaerobic microbial communities for bioenergy production. *CRC Press eBooks*, (9781003394600), pp.165–206. doi:https://doi.org/10.1201/9781003394600-8.

Pérez-Valera, E., Goberna, M. and Verdú, M. (2015). Phylogenetic structure of soil bacterial communities predicts ecosystem functioning. FEMS Microbiology Ecology, 91(5). doi:https://doi.org/10.1093/femsec/fiv031.

Perito, B. and Cavalieri, D. (2018). Innovative metagenomic approaches for detection of microbial communities involved in biodeteriorattion of cultural heritage. IOP Conference Series: Materials Science and Engineering, 364, p.012074. doi:https://doi.org/10.1088/1757-899x/364/1/012074.

Petit-Marty, N., Casas, L. and Saborido-Rey, F. (2023). State-of-the-art of data analyses in environmental DNA approaches towards its applicability to sustainable fisheries management. Frontiers in Marine Science, 10. doi:https://doi.org/10.3389/fmars.2023.1061530.

Petry, W.K., Kandlikar, G.S., Kraft, N.J.B., Godoy, O. and Levine, J.M. (2018). A competition–defence trade-off both promotes and weakens coexistence in an annual plant community. Journal of Ecology, 106(5), pp.1806–1818. doi:https://doi.org/10.1111/1365-2745.13028.

Petters, S., Groß, V., Söllinger, A., Pichler, M., Reinhard, A., Bengtsson, M.M. and Urich, T. (2021). The soil microbial food web revisited: Predatory myxobacteria as keystone taxa? The ISME Journal, 15(9), pp.2665–2675. doi:https://doi.org/10.1038/s41396-021-00958-2.

Pinheiro, J.0., (2006). Decay process of a cadaver. Forensic anthropology and medicine: complementary sciences from recovery to cause of death, pp.85-116.

Pinos, S., Pontarotti, P., Didier Raoult, Baudoin, J.-P. and Pagnier, I. (2016). Compartmentalization in PVC super-phylum: evolution and impact. Biology Direct, 11(1). doi:https://doi.org/10.1186/s13062-016-0144-3.

Pope, M.A., (2010). Differential decomposition patterns of human remains in variable environments of the Midwest (Doctoral dissertation).

Procopio, N., Ghignone, S., Williams, A., Chamberlain, A., Mello, A. and Buckley, M. (2019). Metabarcoding to investigate changes in soil microbial communities within forensic burial contexts. Forensic Science International: Genetics, 39, pp.73–85. doi:https://doi.org/10.1016/j.fsigen.2018.12.002.

Radhakrishnan, S.T., Gallagher, K., Mullish, B.H., José Iván Serrano-Contreras, Alexander, J.L., Blanco, J., Danckert, N.P., Valdivia-Garcia, M., Hopkins, B.J., Ghai, A., Ayub, A., Li, J.V., Marchesi, J.R. and Williams, H.D. (2023). Rectal swabs as a viable alternative to faecal sampling for the analysis of gut microbiota functionality and composition. Scientific Reports, 13(1). doi:https://doi.org/10.1038/s41598-022-27131-9.

Raina, V., Ananta Narayan Panda, Mishra, S.R., Nayak, T. and Mrutyunjay Suar (2019). Microbial Biodiversity Study of a Brackish Water Ecosystem in Eastern India. pp.47–63. doi:https://doi.org/10.1016/b978-0-12-814849-5.00004-6.

Ralebitso-Senior, T.K., Thompson, T.J.U. and Carney, H.E. (2016). Microbial ecogenomics and forensic archaeology: new methods for investigating clandestine gravesites. Human Remains and Violence: An Interdisciplinary Journal, 2(1), pp.41–57. doi:https://doi.org/10.7227/hrv.2.1.4.

Ratzke, C. and Gore, J. (2018). Modifying and reacting to the environmental pH can drive bacterial interactions. *PLOS Biology*, [online] 16(3), p.e2004248. doi:https://doi.org/10.1371/journal.pbio.2004248.

Reyman, M., Clerc, M., van Houten, M.A., Arp, K., Chu, M.L.J.N., Hasrat, R., Sanders, E.A.M. and Bogaert, D. (2021). Microbial community networks across body sites are associated with susceptibility to respiratory infections in infants. Communications Biology, 4(1). doi:https://doi.org/10.1038/s42003-021-02755-1.

Ritz, K., Dawson, L., Miller, D. and Springerlink (Online Service (2009). Criminal and Environmental Soil Forensics. Dordrecht: Springer Netherlands.

Rivas-Marín, E. and Devos, D.P. (2017). The Paradigms They Are a-Changin': past, present and future of PVC bacteria research. Antonie van Leeuwenhoek, 111(6), pp.785–799. doi:https://doi.org/10.1007/s10482-017-0962-z.

Rivas-Marín, E., Canosa, I. and Devos, D.P. (2016). Evolutionary Cell Biology of Division Mode in the Bacterial Planctomycetes-Verrucomicrobia- Chlamydiae Superphylum. Frontiers in Microbiology, 7. doi:https://doi.org/10.3389/fmicb.2016.01964.

Robitzski, D. (2022). Newly Renamed Prokaryote Phyla Cause Uproar. [online] The Scientist Magazine®. Available at: https://www.the-scientist.com/news-opinion/newly-renamed-prokaryote-phyla-cause-uproar-69578 [Accessed 31 Jan. 2022].

Rogers, G.B., Marsh, P., Stressmann, A.F., Allen, C.E., Daniels, T.V.W., Carroll, M.P. and Bruce, K.D. (2010). The exclusion of dead bacterial cells is essential for accurate molecular analysis of clinical samples. Clinical Microbiology and Infection, [online] 16(11), pp.1656–1658. doi:https://doi.org/10.1111/j.1469-0691.2010.03189.x.

Roopnarain, A., Mukhuba, M., Adeleke, R. and Moeletsi, M. (2017). Biases during DNA extraction affect bacterial and archaeal community profile of anaerobic digestion samples. 3 Biotech, 7(6). doi:https://doi.org/10.1007/s13205-017-1009-x.

Roswell, M., Dushoff, J. and Winfree, R. (2021). A conceptual guide to measuring species diversity. Oikos, [online] 130(3), pp.321–338. doi:https://doi.org/10.1111/oik.07202.

Roy, D., Tomo, S., Purohit, P. and Setia, P. (2021). Microbiome in Death and Beyond: Current Vistas and Future Trends. Frontiers in Ecology and Evolution, 9. doi:https://doi.org/10.3389/fevo.2021.630397.

Rubenstein, M., Crowther, T., Maynard, D., Schilling, J., & Bradford, M. (2017). Decoupling direct and indirect effects of temperature on decomposition. Soil Biology & Biochemistry, 112, pp. 110-116. https://doi.org/10.1016/J.SOILBIO.2017.05.005.

Salter, S.J., Cox, M.J., Turek, E.M., Calus, S.T., Cookson, W.O., Moffatt, M.F., Turner, P., Parkhill, J., Loman, N.J. and Walker, A.W. (2014). Reagent and laboratory contamination can critically impact sequence-based microbiome analyses. BMC Biology, [online] 12(1). doi:https://doi.org/10.1186/s12915-014-0087-z.

Santarella-Mellwig, R., Franke, J., Jaedicke, A., Gorjanacz, M., Bauer, U., Budd, A., Mattaj, I.W. and Devos, D.P. (2010). The Compartmentalized Bacteria of the Planctomycetes-Verrucomicrobia-Chlamydiae Superphylum Have Membrane Coat-Like Proteins. PLoS Biology, 8(1), p.e1000281. doi:https://doi.org/10.1371/journal.pbio.1000281.

Santiago-Rodriguez, T.M. and Cano, R.J. (2016). Soil Microbial Forensics. Microbiology Spectrum, 4(4). doi:https://doi.org/10.1128/microbiolspec.emf-0007-2015.

Santos, E.d.O., Thompson, F. (2014). The Family Succinivibrionaceae . In: Rosenberg, E., DeLong, E.F., Lory, S., Stackebrandt, E., Thompson, F. (eds) The Prokaryotes. Springer, Berlin, Heidelberg. https://doi.org/10.1007/978-3-642-38922-1_368

Saraswat, P.K., Nirwan, P.S., Saraswat, S. and Mathur, P., (2008). Biodegradation of dead bodies including human cadavers and their safe disposal with reference to mortuary practice. J Indian Acad Forensic Med, 30, pp.273-80.

Satomi, M. (2014). The Family Shewanellaceae . In: Rosenberg, E., DeLong, E.F., Lory, S., Stackebrandt, E., Thompson, F. (eds) The Prokaryotes. Springer, Berlin, Heidelberg. https://doi.org/10.1007/978-3-642-38922-1_226

Schloss, P. D., Westcott, S. L., Ryabin, T., Hall, J. R., Hartmann, M., Hollister, E. B., ... & Weber, C. F. (2009). Introducing mothur: open-source, platform-independent, community-supported software for describing and comparing microbial communities. Applied and Environmental Microbiology, 75(23), 7537-7541.

Schmedes, S., Sajantila, A. and Budowle, B. (2016). Expansion of Microbial Forensics. Journal of Clinical Microbiology, 54(8), pp.1964-1974.

Schmidt, M.L., Biddanda, B.A., Weinke, A.D., Chiang, E., Januska, F., Props, R. and Denef, V.J. (2020). Microhabitats are associated with diversity–productivity relationships in freshwater bacterial communities. FEMS Microbiology Ecology, [online] 96(fiaa029). doi:https://doi.org/10.1093/femsec/fiaa029.

Schrader, C., Schielke, A., Ellerbroek, L. and Johne, R. (2012). PCR inhibitors - occurrence, properties and removal. Journal of Applied Microbiology, 113(5), pp.1014–1026. doi:https://doi.org/10.1111/j.1365-2672.2012.05384.x.

Sedlackova, T., Repiska, G., Celec, P., Szemes, T. and Minarik, G. (2013). Fragmentation of DNA affects the accuracy of the DNA quantitation by the commonly used methods. Biological Procedures Online, 15(1). doi:https://doi.org/10.1186/1480-9222-15-5.

Sehnal, L., Brammer-Robbins, E., Wormington, A.M., Blaha, L., Bisesi, J., Larkin, I., Martyniuk, C.J., Simonin, M. and Adamovsky, O. (2021). Microbiome Composition and Function in Aquatic Vertebrates: Small Organisms Making Big Impacts on Aquatic Animal Health. Frontiers in Microbiology, 12. doi:https://doi.org/10.3389/fmicb.2021.567408.

Shedge, R., Krishan, K., Warrier, V. and Kanchan, T. (2020). Post-mortem Changes. [online] PubMed. Available at: https://www.ncbi.nlm.nih.gov/books/NBK539741/ [Accessed 22 Dec. 2023].

Shevah, Y. (2014). 1.4 - Adaptation to Water Scarcity and Regional Cooperation in the Middle East. [online] ScienceDirect. Available at: https://www.sciencedirect.com/science/article/pii/B9780123821829000049.

Shim, S.B. (2005). Effects of prebiotics, probiotics and synbiotics in the diet of young pigs. [online] Available at: https://edepot.wur.nl/121655 [Accessed 7 Dec. 2023].

Sibulesky, L. (2013). Normal liver anatomy. Clinical Liver Disease, 2(S1), pp.S1-S3.

Singh, B., Minick, K.J., Strickland, M.S., Wickings, K.G., Crippen, T.L., Tarone, A.M., Benbow, M.E., Sufrin, N., Tomberlin, J.K. and Pechal, J.L. (2018). Temporal and Spatial Impact of Human Cadaver Decomposition on Soil Bacterial and Arthropod Community Structure and Function. Frontiers in Microbiology, 8. doi:https://doi.org/10.3389/fmicb.2017.02616.

Sirichokchatchawan, W., Pupa, P., Praechansri, P., Am-in, N., Tanasupawat, S., Sonthayanon, P. and Prapasarakul, N. (2018). Autochthonous lactic acid bacteria isolated from pig faeces in Thailand show probiotic properties and antibacterial activity against enteric pathogenic bacteria. Microbial Pathogenesis, 119, pp.208–215. doi:https://doi.org/10.1016/j.micpath.2018.04.031.

Smith, B.J., Miller, R.A. and Schmidt, T.M. (2021). Muribaculaceae Genomes Assembled from Metagenomes Suggest Genetic Drivers of Differential Response to Acarbose Treatment in Mice. mSphere, 6(6). doi:https://doi.org/10.1128/msphere.00851-21.

Smith, R.H., Glendinning, L., Walker, A.W. and Watson, M. (2022). Investigating the impact of database choice on the accuracy of metagenomic read classification for the rumen microbiome. Animal Microbiome, 4(1). doi:https://doi.org/10.1186/s42523-022-00207-7.

Song, Chin-Hee, Kim, N., Ryoung Hee Nam, Soo In Choi, Jeong Eun Yu, Nho, H. and Young Joon Surh (2021). Changes in Microbial Community Composition Related to Sex and Colon Cancer by Nrf2 Knockout. Frontiers in Cellular and Infection Microbiology, 11. doi:https://doi.org/10.3389/fcimb.2021.636808.

Sottas, C., Reif, J., Lechosław Kuczyński and Radka Reifová (2018). Interspecific competition promotes habitat and morphological divergence in a secondary contact zone between two hybridizing songbirds. 31(6), pp.914–923. doi:https://doi.org/10.1111/jeb.13275.

Spelberg, M.S. (2013). *Metabolic engineering of Corynebacterium glutamicum for production of the adipate precursor 2-oxoadipate*. [online] Available at: https://docserv.uni-duesseldorf.de/servlets/DerivateServlet/Derivate-31750/Dissertation_Spelberg_final_CYMK.pdf [Accessed 24 Sep. 2024].

Speruda, M., Piecuch, A., Borzęcka, J., Kadej, M. and Ogórek, R. (2022). Microbial traces and their role in forensic science. Journal of Applied Microbiology, 132(4), pp.2547–2557. doi:https://doi.org/10.1111/jam.15426.

Stankovic, M., Katarina Veljović, Nikola Popović, Snežana Kojić, Sofija Dunjić Manevski, Dragica Radojković and Nataša Golić (2022). Lactobacillus brevis BGZLS10-17 and Lb. plantarum BGPKM22 Exhibit Anti-Inflammatory Effect by Attenuation of NF-κB and MAPK Signaling in Human Bronchial Epithelial Cells. International Journal of Molecular Sciences, 23(10), pp.5547–5547. doi:https://doi.org/10.3390/ijms23105547.

Sui, H., Weil, A.A., Nuwagira, E., Qadri, F., Ryan, E.T., Mezzari, M.P., Phipatanakul, W. and Lai, P.S. (2020). Impact of DNA Extraction Method on Variation in Human and Built Environment Microbial Community and Functional Profiles Assessed by Shotgun Metagenomics Sequencing. Frontiers in Microbiology, 11. doi:https://doi.org/10.3389/fmicb.2020.00953.

Takemura, A.F., Chien, D.M. and Polz, M.F. (2014). Associations and dynamics of Vibrionaceae in the environment, from the genus to the population level. Frontiers in Microbiology, 5. doi:https://doi.org/10.3389/fmicb.2014.00038.

Teixeira, L.M., Merquior, V.L.C. (2014). The Family Moraxellaceae . In: Rosenberg, E., DeLong, E.F., Lory, S., Stackebrandt, E., Thompson, F. (eds) The Prokaryotes. Springer, Berlin, Heidelberg. https://doi.org/10.1007/978-3-642-38922-1_245

Tenzin, S., Ogunniyi, A.D., Ferro, S., Deo, P. and Trott, D.J. (2020). Effects of an Eco-Friendly Sanitizing Wash on Spinach Leaf Bacterial Community Structure and Diversity. Applied Sciences, [online] 10(8), p.2986. doi:https://doi.org/10.3390/app10082986.

The Norwegian National Research Ethics Committees (2019). Ethical Guidelines for the Use of Animals in Research. [online] Forskningsetikk. Available at: https://www.forskningsetikk.no/en/guidelines/science-and-technology/ethical-guidelines-for-the-use-of-animals-in-research/.

THOMAS, J.D. (1997). The role of dissolved organic matter, particularly free amino acids and humic substances, in freshwater ecosystems. *Freshwater Biology*, 38(1), pp.1–36. doi:https://doi.org/10.1046/j.1365-2427.1997.00206.x.

Tozzo, P., Amico, I., Delicati, A., Toselli, F. and Caenazzo, L. (2022). Post-Mortem Interval and Microbiome Analysis through 16S rRNA Analysis: A Systematic Review. Diagnostics, 12(11), p.2641. doi:https://doi.org/10.3390/diagnostics12112641.

Tseng, A., Nguyen, V. and Lin, Y. (2023). Metabolic Engineering of Microorganisms Towards the Biomanufacturing of Non-Natural C5 and C6 Chemicals. *Synthetic biology and engineering*, 1(3), pp.1–23. doi:https://doi.org/10.35534/sbe.2023.10015.

Tsurumaki, M., Saito, M., Maruyama, S. and Kanai, A. (2020). Importance of Candidate Phyla Radiation (CPR) Bacteria for the Origin of Life. Journal of Geography (Chigaku Zasshi), 129(6), pp.881–898. doi:https://doi.org/10.5026/jgeography.129.881.

Tuon, F.F., Dantas, L.R., Suss, P.H. and Tasca Ribeiro, V.S. (2022). Pathogenesis of the Pseudomonas aeruginosa Biofilm: A Review. *Pathogens*, 11(3), p.300. doi:https://doi.org/10.3390/pathogens11030300.

Tuttle, J.T., Bruce, T.J., Ian A.E. Butts, Roy, L.A., Abdelrahman, H.A., Beck, B.H. and Kelly, A.M. (2023). Investigating the Ability of Edwardsiella ictaluri and Flavobacterium covae to Persist within Commercial Catfish Pond Sediments under Laboratory Conditions. Pathogens, 12(7), pp.871–871. doi:https://doi.org/10.3390/pathogens12070871.

Unno, T. (2015). Bioinformatic Suggestions on MiSeq-Based Microbial Community Analysis. Journal of Microbiology and Biotechnology, 25(6), pp.765-770.

Ursell, L.K., Metcalf, J.L., Parfrey, L.W. and Knight, R. (2012). Defining the human microbiome. Nutrition Reviews, 70(1), pp.S38–S44.

Vartoukian, S.R., Palmer, R.M. and Wade, W.G. (2010). Strategies for culture of 'unculturable' bacteria. FEMS Microbiology Letters, 309(1), p.no-no. doi:https://doi.org/10.1111/j.1574-6968.2010.02000.x.

Vass A (2001) Beyond the Grave - Understanding Human Decomposition. Microbiology Today 28: 190–192.

Verheggen, F., Perrault, K., Megido, R., Dubois, L., Francis, F., Haubruge, E., Forbes, S., Focant, J. and Stefanuto, P. (2017). The Odor of Death: An Overview of Current Knowledge on Characterization and Applications. BioScience, 67(7), pp.600-613.

Wagg, C., Hautier, Y., Pellkofer, S., Banerjee, S., Schmid, B. and van der Heijden, M.G. (2021). Diversity and asynchrony in soil microbial communities stabilizes ecosystem functioning. eLife, 10. doi:https://doi.org/10.7554/elife.62813.

Wagner, B.D., Grunwald, G.K., Zerbe, G.O., Mikulich-Gilbertson, S.K., Robertson, C.E., Zemanick, E.T. and Harris, J.K. (2018). On the Use of Diversity Measures in Longitudinal Sequencing Studies of Microbial Communities. Frontiers in Microbiology, 9. doi:https://doi.org/10.3389/fmicb.2018.01037.

Wagner, M. and Horn, M. (2006). The Planctomycetes, Verrucomicrobia, Chlamydiae and sister phyla comprise a superphylum with biotechnological and medical relevance. Current Opinion in Biotechnology, 17(3), pp.241–249. doi:https://doi.org/10.1016/j.copbio.2006.05.005.

Wallace, J.R., Receveur, J.P., Hutchinson, P.H., Kaszubinski, S.F., Wallace, H.E. and Benbow, M.E. (2021). Microbial community succession on submerged vertebrate carcasses in a tidal river habitat: Implications for aquatic forensic investigations. Journal of Forensic Sciences, 66(6), pp.2307–2318. doi:https://doi.org/10.1111/1556-4029.14869.

Wandrag, E.M., Catford, J.A. and Duncan, R.P. (2022). Niche partitioning overrides interspecific competition to determine plant species distributions along a nutrient gradient. Oikos, 2023(2). doi:https://doi.org/10.1111/oik.08943.

Wang, B., Yao, M., Lv, L., Ling, Z. and Li, L. (2017). The Human Microbiota in Health and Disease. Engineering, [online] 3(1), pp.71–82. doi:https://doi.org/10.1016/j.eng.2017.01.008.

Wang, G., Huang, D., Ji, J., Völker, C. and Wurm, F.R. (2020). Seawater-Degradable Polymers—Fighting the Marine Plastic Pollution. Advanced Science, [online] 8(1), p.2001121. doi:https://doi.org/10.1002/advs.202001121.

Wang, H., Li, J., Wu, G., Zhang, F., Yin, J. and He, Y. (2022). The effect of intrinsic factors and mechanisms in shaping human gut microbiota. Medicine in Microecology, 12, p.100054. doi:https://doi.org/10.1016/j.medmic.2022.100054.

Wang, Q., Liu, Y. and Yin X (2022). Comparison of Gut Bacterial Communities of Locusta migratoria manilensis (Meyen) Reared on Different Food Plants. Biology, 11(9), pp.1347–1347. doi:https://doi.org/10.3390/biology11091347.

Wang, Y., Huang, J.-M., Zhou, Y.-L., Almeida, A., Finn, R.D., Danchin, A. and He, L.-S. (2020). Phylogenomics of expanding uncultured environmental Tenericutes provides insights into their pathogenicity and evolutionary relationship with Bacilli. BMC Genomics, 21(1). doi:https://doi.org/10.1186/s12864-020-06807-4.

Wang, Y., Wang, M., Xu, W., Wang, Y., Zhang, Y. and Wang, J. (2022). Estimating the Post-mortem Interval of Carcasses in the Water Using the Carrion Insect, Brain Tissue RNA, Bacterial Biofilm, and Algae. Frontiers in Microbiology, 12. doi:https://doi.org/10.3389/fmicb.2021.774276.

Wang, Z., Xue, T., Hu, D. and Ma, Y. (2020). A Novel Butanol Tolerance-Promoting Function of the Transcription Factor Rob in Escherichia coli. Frontiers in Bioengineering and Biotechnology, 8. doi:https://doi.org/10.3389/fbioe.2020.524198.

Waters, J.L. and Ley, R.E. (2019). The human gut bacteria Christensenellaceae are widespread, heritable, and associated with health. BMC Biology, 17(1). doi:https://doi.org/10.1186/s12915-019-0699-4.

Weber, J., 2002. Definition of soil organic matter. Humintech: Humic acids based products.

Wydro, U. (2022). Soil Microbiome Study Based on DNA Extraction: A Review. Water, 14(24), p.3999. doi:https://doi.org/10.3390/w14243999.

Yadav, H.M. and Jawahar, A. (2023). Environmental Factors and Obesity. [online] PubMed. Available at: http://www.ncbi.nlm.nih.gov/books/nbk580543/ [Accessed 2 Dec. 2023].

Yang, F., Hou, C., Zeng, X. and Qiao, S. (2015). The Use of Lactic Acid Bacteria as a Probiotic in Swine Diets. Pathogens, 4(1), pp.34–45. doi:https://doi.org/10.3390/pathogens4010034.

Yang, Park, Park, Baek and Chun (2019). Introducing Murine Microbiome Database (MMDB): A Curated Database with Taxonomic Profiling of the Healthy Mouse Gastrointestinal Microbiome. Microorganisms, 7(11), p.480. doi:https://doi.org/10.3390/microorganisms7110480.

Yang, X., Dai, Z., Yuan, R., Guo, Z., Xi, H., He, Z. and Wei, M. (2023). Effects of Salinity on Assembly Characteristics and Function of Microbial Communities in the Phyllosphere and Rhizosphere of Salt-Tolerant Avicennia marina Mangrove Species. 11(2). doi:https://doi.org/10.1128/spectrum.03000-22.

Yang, Y., Xie, B. and Yan, J. (2014). Application of Next-generation Sequencing Technology in Forensic Science. Genomics, Proteomics & Bioinformatics, [online] 12(5), pp.190–197. doi:https://doi.org/10.1016/j.gpb.2014.09.001.

Yao, T., Chen, M.-H. and Lindemann, S.R. (2020). Structurally complex carbohydrates maintain diversity in gut-derived microbial consortia under high dilution pressure. *FEMS Microbiology Ecology*, 96(9). doi:https://doi.org/10.1093/femsec/fiaa158.

Yao, T., Xia, H., Guan, T., Zhai, C., Liu, C., Liu, C., Zhu, B. and Chen, L. (2020). Exploration of the microbiome community for saliva, skin, and a mixture of both from a population living in Guangdong. International Journal of Legal Medicine, 135(1), pp.53–62. doi:https://doi.org/10.1007/s00414-020-02329-6.

Yin, B., Crowley, D., Sparovek, G., De Melo, W.J. and Borneman, J. (2000). Bacterial Functional Redundancy along a Soil Reclamation Gradient. Applied and Environmental Microbiology, 66(10), pp.4361–4365. doi:https://doi.org/10.1128/aem.66.10.4361-4365.2000.

Yoon, S. H., Ha, S. M., Kwon, S., Lim, J., Kim, Y., Seo, H., & Chun, J. (2017). Introducing EzBioCloud: a taxonomically united database of 16S rRNA gene sequences and whole-genome assemblies. International Journal of Systematic and Evolutionary Microbiology, 67(5), 1613-1617.

Yuan, H., Wang, Z., Wang, Z., Zhang, F., Guan, D. and Zhao, R. (2023). Trends in forensic microbiology: From classical methods to deep learning. Frontiers in Microbiology, 14. doi:https://doi.org/10.3389/fmicb.2023.1163741.

Zapico, S.C., Dytso, A., Rubio, L. and Roca, G. (2022). The Perfect Match: Assessment of Sample Collection Efficiency for Immunological and Molecular Findings in Different Types of Fabrics. International Journal of Molecular Sciences, [online] 23(18), pp.10686–10686. doi:https://doi.org/10.3390/ijms231810686.

Zhang, Z. (2003). Mutualism or cooperation among competitors promotes coexistence and competitive ability. Ecological Modelling, 164(2-3), pp.271–282. doi:https://doi.org/10.1016/s0304-3800(03)00069-3.

Zhao, A., Sun, J. and Liu, Y. (2023). Understanding bacterial biofilms: From definition to treatment strategies. Frontiers in Cellular and Infection Microbiology, 13. doi:https://doi.org/10.3389/fcimb.2023.1137947.

Zhao, L., Cunningham, C., Andruska, A., Schimmel, K., Ali, K., Kim, D.-E., Gu, S., Chang, J.Y., Spiekerkoetter, E. and Nicolls, M.R. (2023). Rat microbial biogeography and age-dependent lactic acid bacteria in healthy lungs. bioRxiv (Cold Spring Harbor Laboratory). doi:https://doi.org/10.1101/2023.05.19.541527.

Zheng, D., Liwinski, T. and Elinav, E. (2020). Interaction between microbiota and immunity in health and disease. Cell Research, 30(6), pp.492–506. doi:https://doi.org/10.1038/s41422-020-0332-7.

Zheng, R., Wang, C., Zhang, T., Tan, Y. and Sun, C. (2021). Cultured deep-sea PVC bacteria shed light on eukaryogenesis. bioRxiv (Cold Spring Harbor Laboratory). doi:https://doi.org/10.1101/2021.11.19.469327.

Zheng, W., Xue, D., Li, X., Deng, Y., Rui, J., Feng, K. and Wang, Z. (2017). The responses and adaptations of microbial communities to salinity in farmland soils: A molecular ecological network analysis. Applied Soil Ecology, 120, pp.239–246. doi:https://doi.org/10.1016/j.apsoil.2017.08.019.

Zhou, W. and Bian, Y. (2018). Thanatomicrobiome composition profiling as a tool for forensic investigation. Forensic Sciences Research, 3(2), pp.105–110. doi:https://doi.org/10.1080/20961790.2018.1466430.

Zhu, Q., Song, M., Azad, Md.A.K., Cheng, Y., Liu, Y., Liu, Y., Blachier, F., Yin, Y. and Kong, X. (2022). Probiotics or synbiotics addition to sows' diets alters colonic microbiome composition and metabolome profiles of offspring pigs. Frontiers in Microbiology, 13. doi:https://doi.org/10.3389/fmicb.2022.934890.

Zou, K.-N., Ren, L.-J., Ping, Y., Ma, K., Li, H., Cao, Y., Zhou, H.-G. and Wei, Y.-L. (2016). Identification of vaginal fluid, saliva, and feces using microbial signatures in a Han Chinese population. Journal of Forensic and Legal Medicine, 43, pp.126–131. doi:https://doi.org/10.1016/j.jflm.2016.08.003.

APPENDICES

APPENDIX 1: NANODROP DATA

Table A1 Showing nanodrop results from nanodrop quantification. p1-3 represent the replicate pigs, s2-23 codes the soil samples, d0-d23 represents dissected tissues sampling day followed by sample type (liv= liver, l= lung, be=belly, m=mouth, an=anus, while w are the water samples, x=seawater sample, y=brackish water sample, z=freshwater sample) For instance, p2.s4 means soil sample of pig 2 on the fourth sampling day, p1.d0.liv means dissected liver sample of pig 1 on day 0, p3.2.be means belly sample of pig 3 on day 2 and x1.0.w means seawater sample on day 0 sampling day. Nucleic Acid Factor (50), Baseline Correction (nm) (340)

SAMPLE	NUCLEIC ACID (NG/µL)	A260/A280	A260/A230	A260	A280	BASELINE ABSORBANCE
P1.0.BE	4.874	2.869	0.591	0.097	0.034	0.148
P1.2.BE	8.462	2.632	0.179	0.169	0.064	-0.042
P3.0.BE	11.566	2.509	0.179	0.231	0.092	0.214
P2.2.BE	23.576	2.137	0.323	0.472	0.221	0.078
P3.2.BE	20.473	2.259	0.295	0.409	0.181	0.032
P2.4.BE	8.809	3.044	0.135	0.176	0.058	0.051
P3.4.BE	4.584	2.449	0.091	0.092	0.037	0.038
P1.7.BE	39.67	1.643	0.423	0.793	0.483	1.186
P2.7.BE	10.157	2.509	0.129	0.203	0.081	0.058
P3.7.BE	7.484	1.507	1.061	0.15	0.099	0.549
P1.14.BE	7.814	1.415	0.553	0.156	0.11	0.303
P2.14.BE	10.873	1.602	0.43	0.217	0.136	0.191
P3.14.BE	65.686	1.388	0.569	1.314	0.946	2.111
P1.23.BE	53.929	2.07	1.391	1.079	0.521	0.111
P3.23.BE	38.615	2.227	0.473	0.772	0.347	0.042
P2.0.AN	202.6595	1.8165	1.43	4.053	2.232	1.186
P1.2.AN	148.819	1.866	1.438	2.976	1.595	0.498
P3.0.AN	146.613	1.771	1.182	2.932	1.656	1.341
P2.2.AN	28.517	1.625	0.629	0.57	0.351	0.529
P3.2.AN	329.326	1.896	1.943	6.587	3.473	0.197
P2.4.AN	339.312	2.017	2.174	6.786	3.364	0.091
P3.4.AN	607.349	2.078	1.888	12.147	5.845	8.805
P1.7.AN	26.787	1.577	0.85	0.536	0.34	0.214
P1.4.AN	58.047	2.018	1.206	1.161	0.575	0.145
P2.7.AN	16.782	1.629	1.524	0.336	0.206	0.128
P3.7.AN	11.604	1.524	0.378	0.232	0.152	0.452
P1.14.AN	20.091	1.389	0.711	0.402	0.289	0.993
P2.14.AN	16.382	1.394	0.895	0.328	0.235	0.191
P3.14.AN	308.181	1.469	0.649	6.164	4.196	12.143
P2.23.AN	55.338	1.814	1.344	1.107	0.61	0.965
P3.23.AN	1.07	0.787	0.466	0.021	0.027	0.101

P1.0.AN	84.4725	1.7465	0.7695	1.6895	0.9675	1.0465
P1.0.M	10.78	2.02	0.342	0.216	0.107	0.037
P2.0.M	97.3045	1.8055	1.2755	1.946	1.078	0.5365
P1.2.M	62.285	1.585	0.596	1.246	0.786	1.319
P2.2.M	14.772	1.921	0.523	0.295	0.154	0.048
P3.0.M	43.067	1.497	0.495	0.861	0.575	1.392
P1.4.M	31.316	1.984	0.873	0.626	0.316	0.108
P2.4.M	82.07	1.838	0.968	1.641	0.893	0.744
P3.4.M	22.099	1.926	1.13	0.442	0.229	0.034
P1.7.M	181.385	1.404	0.751	3.628	2.584	7.885
P2.7.M	19.542	1.669	1.822	0.391	0.234	0.297
P3.7.M	15.753	1.428	1.178	0.315	0.221	0.244
P1.14.M	24.911	1.452	0.39	0.498	0.343	0.548
P2.14.M	28.166	1.369	0.745	0.563	0.412	0.491
P3.14.M	17.315	1.283	1.112	0.346	0.27	0.346
P1.23.M	3.107	1.118	12.694	0.062	0.056	0.173
P2.23.M	15.294	1.976	1.291	0.306	0.155	0.093
P3.23.M	6.558	1.461	0.765	0.131	0.09	0.406
P1.D0.LIV	6.633	1.729	0.675	0.133	0.077	0.121
P2.D0.LIV	14.421	1.744	0.941	0.288	0.165	0.193
P3.D0.LIV	7.425	1.708	0.758	0.148	0.087	0.04
P1.D2.LIV	12.473	1.574	0.475	0.249	0.158	0.283
P2.D2.LIV	10.731	1.236	0.437	0.215	0.174	0.319
P3.D2.LIV	54.429	1.528	0.563	1.089	0.712	2.385
P1.D4.LIV	2.407	1.993	0.286	0.048	0.024	-0.108
P2.D4.LIV	5.943	1.454	0.229	0.119	0.082	0.042
P3.D4.LIV	8.914	1.121	0.302	0.178	0.159	0.226
P1.D0.L	6.144	2.083	0.476	0.123	0.059	0.042
P2.D0.L	17.483	1.69	0.95	0.35	0.207	0.202
P3.D0.L	10.07	1.633	0.669	0.201	0.123	0.089
P1.D2.L	11.334	1.294	0.255	0.227	0.175	0.335
P2.D2.L	2.825	2.145	0.439	0.057	0.026	-0.001
P3.D2.L	47.815	1.857	1.909	0.956	0.515	-0.05
P1.D4.L	12.657	1.481	0.539	0.253	0.171	0.46
P2.D4.L	12.874	1.233	0.261	0.257	0.209	0.1
P3.D4.L	1.825	1.336	0.689	0.036	0.027	0.192
P1.S2	52.842	1.826	7.418	1.057	0.579	-0.011
P2.S2	40.819	1.844	0.237	0.816	0.443	0.019
P3.S2	38.305	1.796	0.682	0.766	0.427	-0.018
P1.S4	46.404	1.819	0.254	0.928	0.51	0.025
P2.S4	41.511	1.81	0.549	0.83	0.459	-0.004
P3.S4	44.446	1.858	1.033	0.889	0.478	0.008
P1.S7	43.486	1.836	0.767	0.87	0.474	0.004

P2.S7	29.947	1.731	-12.899	0.599	0.346	0.011
P3.S7	38.777	1.855	3.581	0.776	0.418	-0.023
P2.S14	41.603	1.793	1.192	0.832	0.464	0.002
P3.S14	30.527	1.817	1.776	0.611	0.336	-0.028
P1.S23	52.617	1.797	3.606	1.052	0.586	-0.021
P2.S23	48.472	1.821	3.427	0.969	0.532	0.004
P1.S14	31.197	1.75	0.817	0.624	0.357	0.033
X1.0.W	4.175	1.476	0.562	0.083	0.057	0.219
X2.0.W	33.338	1.762	1.151	0.667	0.378	0.015
Y2.0.W	4.022	1.821	0.581	0.08	0.044	0.057
Z2.0.W	28.172	1.522	0.545	0.563	0.37	0.98
X1.7.W	22.224	1.654	1.003	0.444	0.269	0.46
X2.7.W	117.974	1.912	1.515	2.359	1.234	0.92
Y1.7.W	12.186	1.761	0.748	0.244	0.138	0.277
Y2.7W	53.477	1.498	0.649	1.07	0.714	2.172
Z1.7.W	6.619	2.138	0.72	0.132	0.062	-0.004
Z2.7.W	24.547	1.436	0.616	0.491	0.342	1.56
X1.14.W	37.56	1.435	0.633	0.751	0.524	2.995
X2.14.W	4.155	1.863	0.439	0.083	0.045	-0.02
Y1.14.W	9.432	1.947	0.317	0.189	0.097	0.048
Y2.14.W	141.254	1.442	0.667	2.825	1.959	8.114
Z1.14.W	21.743	1.485	0.5	0.435	0.293	0.797
Z2.14.W	1.456	2.654	0.102	0.029	0.011	0.039
Z1.0.W	1.283	0.97	0.19	0.026	0.026	0.083
Y1.0.W	1.835	2.189	0.268	0.037	0.017	0.051
AVERAGE	47.94	1.7532	0.8863	0.9588	0.5525	0.7316

APPENDIX 2: CHANGES TO BACTERIAL NOMENCLATURE

Table A2 shows previous and current nomenclature of bacterial phylum, including families, and summaries their life classification ranking.

Old name	***new name***	***Reference***	***Class***	***order***	***family***	***genus***	***species***
Proteobacteria	Pseudomonadota	NCBI	12	80	264	1915	207592
Firmicutes	Bacillota	NCBI	9	18	80	998	75654
Actinobacteria:	Actinomycetota	NCBI	9	44	97	550	75951
Bacteroidetes	Bacteroidota	NCBI	6	10	57	565	22173
Acidobacteria	Acidobacteriota	NCBI	6	15	16	48	1113
Fusobacteria	Fusobacteriota	NCBI	1	1	2	15	373
Armatimonadetes	Armatimonadota	NCBI	3	4	4	5	116
Chlamydiae	Chlamydiota	NCBI	1	3	11	23	387
Fibrobacteres	Fibrobacterota	NCBI	3	4	4	5	96
Verrucomicrobia	Verrucomicrobiota	NCBI	5	6	10	49	1637
Planctomycetes	Planctomycetota	NCBI	4	9	15	75	1149
lentisphaerae	Lentisphaerota	NCBI	2	3	4	5	101
Elusimicrobia (TG1)	Elusimicrobiota	NCBI	2	2	2	3	138
Chloroflexi	Chloroflexota	NCBI	11	16	23	55	1373
Chlorobi	Chlorobiota	NCBI	1	1	3	8	281
Acidobacteria	Acidobacteriota	NCBI	6	15	16	48	1113
Gemmatimonadetes	Gemmatimonadota	NCBI	2	3	2	4	212

APPENDIX 3: SAMPLE SPECIFIC BACTERIAL IDENTIFICATION

Table A3.1 Displays Bacterial families found only in the Anus sample on Day 0

Bacterial Families only Found in the anus sample	**Abundance Percentage**	**Description**
Veillonellaceae, and Christensenellaceae	1.4%	Veillonellaceae and Christensenellaceae are of the Bacterial phylum Firmicutes and Its emergence as a group with a focus on health was examined (Waters & Ley, 2019).
RF16_f	1.2%	RF16_f is an uncultured group of Bacteroidales (Cendron *et al*., 2020)
Rhizobiaceae, and Muribaculaceae	1.1%	Muribaculaceae was previously known as S24-7 under Bacteroidales (Lagkouvardos *et al*., 2019) and has a specialty for complex polysaccharide breakdown (Smith *et al*., 2021). Rhizobiaceae is a group belonging to the order of Rhizobiales from the class of Alphaproteobacteria class that houses genera linked with plants and soil hosts (Carareto Alves *et al*., 2014).
Succinivibrionaceae	1.0%	Succinivibrionaceae are gammaproteobacteria microbes whose species members have been studied to be strictly anaerobic, Gram-negative bacteria that do not produce spores can ferment carbohydrates to produce acetate and succinate (Santos & Thompson, 2014, Hailemariam *et al*., 2020).
Helicobacteraceae	0.8%	Helicobacteraceae family is from the Campylobacterales order and host a lot of pathogenic members have been detected in faeces together with dental plaque and saliva of an infected person (Berman, 2019).

Table A3.2 Displays Bacterial other Families not mentioned initially and only Found in the mouth sample on Day 0

Bacterial Families found only in the mouth	**Abundance Percentage**	**Description**
Fusobacteriaceae	5.7%	Fusobacteriaceae are fermentative gram-negative rods that range from being microaerophilic to being obligately anaerobic and make up the family Fusobacteriaceae, which belongs to the Fusobacteria class and the order Fusobacteriales (Olsen, 2014).
Pasteurellaceae	5.5%	Pasteurellaceae is a family belonging to the gamma-proteobacteria and consisting of numerous aerobic, non-spore-producing, coccoid- or rod-shaped genera of which some houses pathogenic species to humans and animals (Naushad et al., 2015; De Luca et al., 2021; Dousse *et al*., 2008).
DQ413083_f, and Neisseriaceae	1.1%	DQ413083_f has no viable information but has been constructed and referenced by Ezbiocloud as a family group under the class Peribacteria. Neisseriaceae are gram-negative bacteria that equally exhibit lipopolysaccharides at their outer membrane and pathogenic species have been discovered (Nyongesa *et al*., 2022)
Leptotrichiaceae	2.4%	Leptotrichiaceae are group of microbes within the phylum Fusobacteria and seem to colonise mucous membranes but also likely understudied and occasionally isolated (Eisenberg *et al*., 2016).

Table A3.3 Displays Bacterial other Families not mentioned initially and only Found in the soil sample on Day 0

Bacterial Families found only in the soil	**Percentage**	**Description**
Gemmataceae	4.0%	Gemmataceae includes ellipsoidal or spherical microbes that are strictly aerobic, chemo-organotrophic and can be found arranged in huge rosette-like clusters and dendriform-like formations, in singles or pairs (Kulichevskaya *et al*., 2020).
Chitinophagaceae	3.7%	Chitinophagaceae is described as a rod shaped and non-motile facultatively anaerobic or aerobic with some species observed to have fermentative abilities (KäMPfer *et al*., 2011).
Vicinamibacteraceae, and Solibacteraceae	3.4%, 3.1%	Vicinamibacteraceae (Vicinamibacter_f, as referenced by Ezbiocloud) and Solibacteraceae are from the phylum Acidobacteria that appeared on 3.4% and 3.1% respectively. Vicinamibacteraceae's members are non-sporing, gram negative aerobes presenting to be psychrotolerant to mesophilic chemoheterotrophs or neutrophilic organisms (Huber & Overmann, 2018).
Planctomycetaceae	2.8%	Planctomycetaceae contains members in which some genera have bacteriochlorophyll and can perform photosynthesis and others found not to need light to survive and can utilise oxygen for respiration (Newton *et al*., 2011).
Acidobacteriaceae	2.7%	Acidobacteriaceae bacteria are aerobic, microaerobic, or facultatively anaerobic non-spore forming gram negative rod bacteria also known to be chemoorganotrophic mesophiles and some employ monomeric sugars as carbon and energy sources, although many may also disintegrate complex polysaccharides (Huber *et al*., 2017).
Pedosphaera_f	2.6%	Pedosphaera_f is referenced by ezbiocloud as a family and hosts the genus Pedosphaera from the order Verrucomicrobiae. The genus includes aerobically cultured representative from pasture soil (Kant *et al*., 2011)
Bryobacteraceae	2.1%	Bryobacteraceae are a group that houses mesophilic and psychrotolerant bacteria which are aerobic and facultatively anaerobic, non-spore-producing, slightly acidophilic and Gram-negative bacteria (Dedysh, 2019). Species from the of this this family are chemoheterotrophs and some members can potentially reduce and nitrate Iron (III) (Dedysh, 2019).

Bacterial Families found only in the soil	Percentage	Description
Beijerinckiaceae	1.7%	Beijerinckiaceae comprises of aerobic and non-symbiotic species that range from obligate methanotrophs to chemoorganoheterotrophs, also they also possess the ability to commerce nitrogen fixation (Marín & Arahal, 2014).
Isosphaeraceae, Cytophagaceae	1.6%	Isosphaeraceae and Cytophagaceae were mesophilic families, although some species of Cytophagaceae are psychrophilic. Isosphaeraceae are non-motile, oval to pear formed cells and divide by polar budding. Despite some members' ability to develop in microoxic environments, most of them are chemoorganotrophic aerobes (Dedysh & Ivanova, 2020). Cytophagaceae isolates are Gram-negatives, chemoorganotrophic aerobic bacteria with a few anaerobes (Octaviana *et al*., 2022). Macromoclecules such as proteins or polysaccharide are digested by members of this family (McBride *et al*., 2017).
PAC000121_f	1.5%	PAC000121_f is categorised by Ezbiocloud as a family group under class Solibacteres (Acidobacteria) and has been discovered amidst other families that are also prominent in soil samples (Liu *et al*., 2022, Choi, *et al*., 2020).
Rhodomicrobium_f, Hyphomicrobiaceae	1.3%, 1.0%	(Rhodomicrobium_f as referenced by ezbiocloud):1.3% and Hyphomicrobiaceae: 1.0%, The majority are aerobic chemoheterotrophs. By denitrification or mixed-acid fermentation, a few examples can grow anaerobically (Oren & Xu, 2014). When the author checked, (https://www.genome.jp/tools-bin/taxsummary and other sources) Rhodomicrobium is a genus under Hyphomicrobiaceae family, hereby making it confusing.
Steroidobacteraceae	1.3%	Steroidobacteraceae (Steroidobacter_f, as referenced by ezbiocloud) Strains are characterised by gram negative cells that are strictly aerobic or facultatively anaerobic, chemoorganotrophic, rod-like, and non-spore manufacturing (Liu et al., 2019). Species are positive for oxidase and catalase reactions can breakdown nitrate to dinitrogen monoxide and then to dinitrogen or ammonia (Liu *et al*., 2019).
Rhodospirillaceae	1.2%	Rhodospirillaceae, otherwise named purple non-sulfur bacteria, are a Gram-negative family that grow photoheterotrophically or heterotrophically and with strictly aerobic and facultative anaerobic genera and possess rod to spirillum-shaped cells. (Baldani *et al*., 2014)

Bacterial Families found only in the soil	Percentage	Description
Tepidisphaeraceae	1.1%	Tepidisphaeraceae occur as facultative anaerobes, aerobes, Gram-negative, fairly thermophilic, neutrophiles, shapeless aggregates or single cocci member that splits by binary fission (Kovaleva *et al*., 2019)
Haliangiaceae, Polyangiaceae	1.1%, 0.9%	Haliangiaceae (1.1%) and Polyangiaceae (0.9%) descend from the class Myxococcia whose members are known to produce novel bioactive compounds that cause predatory effects towards microbes. For instance, most species in the Polyangiaceae group produces a variety of novel secondary metabolites that are cytotoxic and antimicrobial that also impacts on environmental biocontrol (Garcia & Müller, 2018). They have been discovered to be dominate in soil samples (Petters et al., 2021). The Haliangiaceae family has no established proper nomenclature, but it is frequently utilised as a taxonomic category (Petters *et al*., 2021).
Gaiellaceae	1.0%	Gaiellaceae: Members of this family form rod-shaped cells, aerobic and chemoorganotrophic and have Gram-negative staining (Albuquerque & da Costa, 2014).
PAC001907_f	1.0%	PAC001907_f, is categorised by Ezbiocloud as a family group under Betaproteobacteria (proteobacteria) and has been discovered amidst other families that are also promising.
Acetobacteraceae	1.0%	Acetobacteraceae, bacteria can perform oxidation of ethanol to acetic acid in neutral or acidic conditions and are strictly aerobic, non-spore forming, Gram-negative or Gram-variable (older cells). (Hommel, 2014)

Table A3.4 Displays Bacterial other Families not mentioned initially and only Found in the Water sample on Day 0

Bacterial families found only in the water	Seawater Percentage	Brackish Water Percentage	Fresh Water Percentage	Description
Rickettsiaceae	16.2%	1.3%	-	Rickettsiaceae are characterised as obligating intracellular parasites on a large range of eukaryotic organisms and are Gram-negative, coccoid and rod-shaped bacteria (Driscoll *et al*., 2021). They were the second biggest occupiers of the seawater community and in brackish water were among least dominating family.
Oxalobacteraceae	1.3%	-	-	Oxalobacteraceae are mostly aerobic/microaerobic to facultative anaerobic although some genus members of Oxalobacter showcase strictly anaerobic lifestyle. Endophytic nitrogen-fixing and opportunistic human pathogens bacteria have also been detected in some genera of this group. been found within the group human pathogens. (Baldani *et al*., 2014)
Yersiniaceae	1.0%	-	-	Yersiniaceae are catalase-positive, motile, and not able to create hydrogen disulfide (Gupta, 2014). According to Brenner & Farmer III (2005) description of order Enterobacterales, members of this group are like in features to its family-mate 'Enterobacteriaceae' (Adeolu *et al*., 2016). They are distinguished from other bacteria by their peculiar monophyletic genome cluster and multigene based phylogenetic trees created because of their three conserved Signature Indels (CSIs) in the hypothetical and TetR family transcriptional regulator protein (Gupta, 2014).
Vibrionaceae	0.4%	-	-	Vibrionaceae consists of a variety of heterotrophic bacteria with different genetic and metabolic make-up (Takemura *et al.*, 2014), such as being able to perform nitrogen fixation, phototrophy and gas production (Gomez-Gil *et al*., 2014). They are commonly detected in estuarine and warm waters (Kingsley, 2014). Several species in the Vibrionaceae family

Bacterial families found only in the water	Seawater Percentage	Brackish Water Percentage	Fresh Water Percentage	Description
				elicit intestinal and extraintestinal infections in humans as well as animals (Farmer & Michael Janda, 2015).
Shewanellaceae	0.1%	3.8%	-	Most species of Shewanellaceae detected are Gram-negative, motile, rod-shaped, facultatively anaerobic with positive oxidase and catalase reaction (Satomi, 2014). Shewanellaceae are extensively dispersed in nature and can be found in iced fish, protein-rich foods, the deep oceans, marine environments, and sometimes in clinical samples (Satomi, 2014). The majority of marine-related species produce polyunsaturated fatty acids in their cytoplasmic membranes and are psychrophile and halophile while others are a psychrotolerant and non-halophilic, and psychrotolerant (Satomi, 2014) .
Sphingobacteriaceae	0.3%	2.4%	0.3%	Sphingobacteriaceae Gram-negative, non-spore forming bacilli that can generate lipids (not common in eukaryotes), and because the specific sphingolipids in their cell walls which resembles lipopolysaccharides (LPS) in structure and function, the family classification was proposed (Figueiredo *et al*., 2021). Sphingolipid bacteria that reside gut microbiome can influence how the host metabolise lipids and since various strains have been identified as promising agents for increasing crop yields, some genera are well-known for promoting plant development (Figueiredo *et al*., 2021).
Aeromonadaceae	0.4%	3.7%	-	Aeromonadaceae are rod shaped Gram-negative, facultative anaerobic and non-spore-forming group (D'Agostino & Cook, 2016).

APPENDIX 4: NGS DATA

Table A4.1 Showing NGS data using the curated from EzbioCloud using the FASTQ data. p1-3 represent the replicate pigs, s2-23 codes the soil samples, d0-d23 represents dissected tissues sampling day followed by sample type (liv= liver, l= lung, be=belly, m=mouth, an=anus, while w are the water samples, x=seawater sample, y=brackish water sample, z=freshwater sample) For instance, p2.s4 means soil sample of pig 2 on the fourth sampling day, p1.d0.liv means dissected liver sample of pig 1 on day 0, p3.2.be means belly sample of pig 3 on day 2 and x1.0.w means seawater sample on day 0 sampling day.

Samples	Total Reads After Pre-Filter	Total Valid Reads	Low Quality Amplicon	Non-Target Amplicons	Chimeric Amplicons
p1.d0.liv	100000	1529	97867	41	563
p2.d0.liv	19404	16,236	205	2949	14
p3.d0.liv	39518	24,916	7716	6841	45
p1.d2.liv	100000	99729	146	12	113
p2.d2.liv	100000	98811	212	148	829
p3.d2.liv	100000	99540	158	7	295
p1.d4.liv	93885	93,534	231	18	102
p2.d4.liv	100000	99,445	130	15	410
p3.d4.liv	89178	74743	221	61	14153
p1.d0.l	35,565	31,361	1624	2480	100
p2.d0.l	94440	92,331	904	757	448
p3.d0.l	57998	49,826	4951	3105	116
p1.d2.l	85384	84,804	202	34	244
p2.d2.l	100000	94,474	743	4536	247
p3.d2.l	85715	84,615	564	321	215
p1.d4.l	81640	80,511	141	17	971
p2.d4.l	100000	94,639	508	2	4851
p3.d4.l	100000	99,687	86	18	209
p1.0.be	100000	83,745	597	73	15585
p2.0.be	100000	34,182	3824	52	61942
p3.0.be	100000	75,506	662	84	23748
p1.2.be	100000	76,603	425	8	22964
p2.2.be	100000	26,512	3048	18	70422
p3.2.be	100000	72,079	598	1	27322
p1.4.be	87,084	84,607	291	199	1987
p2.4.be	100,000	95,189	325	179	4307
p3.4.be	100000	95,246	185	10	4559
p1.7.be	100000	37,272	3860	30	58838
p3.7.be	100000	91,903	496	2	7599
p1.23.be	100000	78,905	718	41	20336
p2.23.be	100000	89,585	471	168	9776
p3.23.be	100000	71,810	772	36	27 382
p1.0.an	100000	81775	686	142	17397

p3.0.an	72,674	51688	1091	0	19895
p1.2.an	92,643	72264	540	5	19834
p2.2.an	100000	70724	945	0	28331
p1.4.an	100000	86077	429	16	13473
p3.4.an	100000	36010	3541	4511	55938
p1.23.an	100000	44481	3328	11	52180
p2.23.an	88,259	40218	2091	597	45353
p3.23.an	100000	92076	492	7	7425
p1.0.m	100000	75380	995	125	23500
p2.0.m	91,848	71991	778	0	19079
p3.0.m	100000	73594	1231	9	25166
p1.2.m	95,137	47712	1297	2	46126
p2.2.m	100000	65087	978	14	33921
p3.2.m	100000	64415	1119	9	34457
p1.4.m	89,648	62377	801	13	26457
p2.4.m	84,883	80289	341	2	4251
p3.4.m	100000	60220	909	0	38871
p1.7.m	100000	78124	1308	1	20567
p2.7.m	100000	71072	2621	0	26307
p2.23.m	100000	48158	2791	32	49019
p3.23.m	83,998	83154	424	106	314
p1.s2	100000	85507	2762	171	11560
p2.s2	100000	87833	2486	179	9502
p3.s2	100000	87652	2407	138	9803
p1.s4	100,000	86590	2568	223	10619
p2.s4	100,000	85188	2906	199	11707
p3.s4	100000	85767	2732	201	11300
p1.s7	100000	86454	2394	188	10964
p2.s7	100000	81674	2117	102	16107
p3.s7	100000	86251	2716	200	10813
p1.s14	83,409	71888	1903	119	9499
p2.s14	100000	84207	1729	67	13997
p3.s14	100000	85556	2661	279	11504
p1.s23	100000	86191	2450	248	11111
p2.s23	100000	84726	2472	572	12230
p3.23	100000	85411	1990	92	12507
x1.0.w	69,005	68009	192	616	188
x2.0.w	54,519	54024	165	296	34
y1.0.w	53,939	52929	186	490	334
y2.0.w	100000	98131	397	1411	61
z1.0.w	100000	99626	236	104	34

z2.0.w	31,302	30687	92	362	161
x1.7.w	100000	86296	371	0	13333
x2.7.w	100000	84734	287	0	14979
y1.7.w	100000	77418	373	0	22209
y2.7.w	91,302	77579	323	1	13399
z1.7.w	100000	82949	2044	1775	13232
z2.7.w	100000	89720	444	222	9614
x1.14.w	100000	85007	453	11	14529
x2.14.w	100000	85427	827	86	13660
y1.14.w	100000	84192	634	25	15149
y2.14.w	94,270	71590	484	40	22156
z1.14.w	100000	98633	245	42	1080
z2.14.w	100000	90260	760	393	8587
Mean ± SD	92490.20 ± 16755.71	74469.74 ± 21470.24	2372.68 ± 10439.33	422.03 ± 1104.65	15082.94 ± 16084.46
% of total reads after filter		80.52	2.57	0.46	16.31

Table A4.2 Displays the number of reads, species identified, operational taxonomic units (OTUs), and Good's coverage percentage for multiple samples collected at different time points and treatments. Sample codes are same as table A4.1 and numerical values are curated from the EZbioCloud 16S-based MTP application.

Samples	No Of Reads Identified at Species Level	No. of Species Found	OTUs	Good's Coverage of Library (%)
p1.d0.liv	1191	145	207	96.4
p2.d0.liv	14135	289	418	99.8
p3.d0.liv	18351	203	315	99.92
p1.d2.liv	98454	237	339	99.97
p2.d2.liv	98570	180	257	99.95
p3.d2.liv	99194	158	218	99.94
p1.d4.liv	93447	116	168	99.95
p2.d4.liv	99138	170	250	99.95
p3.d4.liv	73749	130	261	99.97
p1.d0.l	25,609	318	477	99.86
p2.d0.l	88800	357	544	99.97
p3.d0.l	40556	331	497	99.89

p1.d2.l	84471	173	249	99.94
p2.d2.l	92,845	155	257	99.97
p3.d2.l	81 914	226	312	99.96
p1.d4.l	80141	386	502	99.72
p2.d4.l	94206	499	638	99.67
p3.d4.l	97,808	289	434	99.94
p1.0.be	75,989	1,375	1916	99.45
p2.0.be	28,828	743	2043	99.14
p3.0.be	69,014	1193	1693	99.4
p1.2.be	75,700	403	592	99.8
p2.2.be	19,719	377	1479	99.35
p3.2.be	50,983	449	696	99.76
p1.4.be	83,018	802	1036	99.75
p2.4.be	91,729	833	1102	99.72
p3.4.be	93,681	700	895	99.72
p1.7.be	25,330	601	2167	99.42
p3.7.be	74,143	258	497	99.85
p1.23.be	63,446	230	602	99.89
p2.23.be	72,948	281	569	99.85
p3.23.be	63,762	169	499	99.91
p1.0.an	68,609	1,303	1923	99.61
p3.0.an	33,081	754	1581	99.62
p1.2.an	64681	997	1466	99.69
p2.2.an	61,496	722	1286	99.71
p1.4.an	81,911	691	889	99.71
p3.4.an	30,780	474	1298	99.51
p1.23.an	20,668	317	2034	99.68
p2.23.an	29,044	329	1576	99.66
p3.23.an	79,509	372	614	99.8
p1.0.m	56,075	819	1577	99.6

p2.0.m	41,075	41,075	1294	99.78
p3.0.m	40,061	475	1321	99.71
p1.2.m	39,358	328	953	99.75
p2.2.m	39,560	381	959	99.79
p3.2.m	45,662	414	961	99.75
p1.4.m	44,767	516	1053	99.72
p2.4.m	84,883	309	739	99.88
p3.4.m	28169	207	672	99.89
p1.7.m	16,502	210	1155	99.87
p2.7.m	4,112	88	2897	99.93
p2.23.m	38,489	332	1339	99.69
p3.23.m	78,305	500	694	99.9
p1.s2	67,198	2,640	4930	99.14
p2.s2	69,208	2,594	4899	99.2
p3.s2	69,429	2,406	4570	99.27
p1.s4	67,951	2,693	5126	99.17
p2.s4	66,591	2,740	5191	99.1
p3.s4	65,410	2,436	5028	99.34
p1.s7	65,945	2,508	4722	99.2
p2.s7	54,176	1,922	3482	99.31
p3.s7	66,543	2,417	4767	99.26
p1.s14	57,879	2,223	4000	99.13
p2.s14	67,189	1,820	3088	99.29
p3.s14	65,964	2,460	4710	99.21
p1.s23	68,555	2,621	4899	99.21
p2.s23	64,896	2,742	4837	99.06
p3.23	70,402	2,402	4011	99.18
x1.0.w	62,560	283	446	99.95
x2.0.w	46,664	254	399	99.9
y1.0.w	48,553	574	803	99.58

y2.0.w	91,168	330	534	99.97
z1.0.w	30,734	235	410	99.97
z2.0.w	24,705	201	325	99.8
x1.7.w	85,290	238	374	99.9
x2.7.w	82,113	192	350	99.9
y1.7.w	75,917	263	420	99.89
y2.7.w	74,142	268	425	99.9
z1.7.w	70,626	2,609	4131	98.93
z2.7.w	69,928	425	628	99.77
x1.14.w	79,807	426	707	99.73
x2.14.w	70,982	981	1546	99.46
y1.14.w	79,421	511	871	99.69
y2.14.w	68,259	481	797	99.69
z1.14.w	68,162	390	566	99.86
z2.14.w	59,941	1,214	1764	99.45
Mean ± SD	64029.03 ± 25013.07	811.78 ± 839.88	1542.14 ± 1540.1	99.63 ± 0.45

APPENDIX 5 – R OUTPUT RESULTS FOR CHAPTER 4

RICHNESS BETWEEN PIG SAMPLES ON DAY 0

```
pigaov <- aov(Jackknife~SAMPLE.TYPE,data=pigonly)
> summary(pigaov)
             Df  Sum Sq Mean Sq F value   Pr(>F)
SAMPLE.TYPE  4 8660355 2165089   74.77 6.68e-07 ***
Residuals    9  260622   28958
---
Signif. codes:  0 ‘***’ 0.001 ‘**’ 0.01 ‘*’ 0.05 ‘.’ 0.1 ‘ ’ 1
> tukey_pigaov <- TukeyHSD(pigaov)
> print(tukey_pigaov)
  Tukey multiple comparisons of means
    95% family-wise confidence level

Fit: aov(formula = Jackknife ~ SAMPLE.TYPE, data = pigonly)

$SAMPLE.TYPE
                diff       lwr       upr     p adj
BELLY-ANUS    278.1300  -244.2259   800.4859 0.4332284
LIVER-ANUS  -1662.0133 -2184.3692 -1139.6575 0.0000151
LUNG-ANUS   -1462.3633 -1984.7192  -940.0075 0.0000435
MOUTH-ANUS   -388.6667  -911.0225   133.6892 0.1734351
LIVER-BELLY -1940.1433 -2407.3526 -1472.9340 0.0000016
LUNG-BELLY  -1740.4933 -2207.7026 -1273.2840 0.0000040
MOUTH-BELLY  -666.7967 -1134.0060  -199.5874 0.0065483
LUNG-LIVER    199.6500  -267.5593   666.8593 0.6218904
MOUTH-LIVER  1273.3467   806.1374  1740.5560 0.0000541
MOUTH-LUNG   1073.6967   606.4874  1540.9060 0.0002114
```

RESIDUAL NORMALITY TEST

pigaov$residuals ### Shows you the residuals for each sample

1	2	3	4	5	6	7
233.000000	-233.000000	91.970000	47.870000	-139.840000	-87.676667	101.013333
8	9	10	11	12	13	14
-13.336667	-28.146667	22.363333	5.783333	256.666667	-170.333333	-86.333333

hist(pigaov$residuals) ### plots a histogram of the residuals

> shapiro.test(pigaov$residuals)

Shapiro-Wilk normality test

data: pigaov$residuals

W = 0.97211, p-value = 0.9035

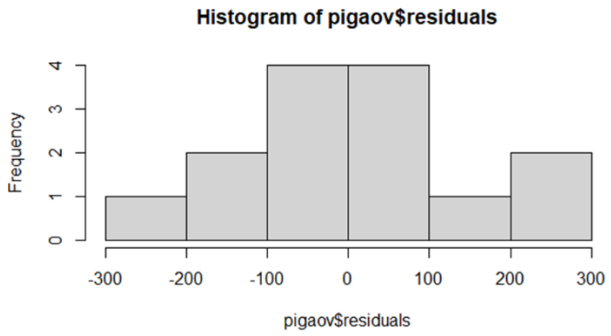

Figure A1 A histogram of the ANOVA residuals of richness of pig samples

EVENNESS BETWEEN PIG SAMPLES DAY 0

	Df	Sum Sq	Mean Sq	F value	Pr(>F)
SAMPLE.TYPE	4	1.298	0.3245	0.751	0.582
Residuals	9	3.888	0.4320		

> pigaov <- aov(NPShannon~SAMPLE.TYPE,data=pigonly)

> summary(pigaov)

Df Sum Sq Mean Sq F value Pr(>F)

```
SAMPLE.TYPE  4  1.298  0.3245   0.751  0.582
Residuals    9  3.888  0.4320
> tukey_pigaov <- TukeyHSD(pigaov)
> print(tukey_pigaov)
  Tukey multiple comparisons of means
    95% family-wise confidence level

Fit: aov(formula = NPShannon ~ SAMPLE.TYPE, data = pigonly)

$SAMPLE.TYPE
                diff       lwr      upr     p adj
BELLY-ANUS  -0.43166667 -2.449175 1.585842 0.9466562
LIVER-ANUS  -0.37500000 -2.392508 1.642508 0.9671669
LUNG-ANUS   -0.90166667 -2.919175 1.115842 0.5851885
MOUTH-ANUS  -0.80166667 -2.819175 1.215842 0.6780520
LIVER-BELLY  -0.05666667 -1.747848 1.861181 0.9999658
LUNG-BELLY  -0.47000000 -2.274514 1.334514 0.8988433
MOUTH-BELLY -0.37000000 -2.174514 1.434514 0.9538436
LUNG-LIVER  -0.52666667 -2.331181 1.277848 0.8571724
MOUTH-LIVER -0.42666667 -2.231181 1.377848 0.9256943
MOUTH-LUNG   0.10000000 -1.704514 1.904514 0.999673

RESIDUAL NORMALITY TEST
 pigaov$residuals            ### Shows you the residuals for each sample.
         1          2          3          4          5          6
 0.30500000 -0.30500000  0.14666667  0.23666667 -0.38333333 -0.20000000
         7          8          9         10         11         12
 0.26000000 -0.06000000  0.77666667 -1.40333333  0.62666667  0.41666667
        13         14
 0.05666667 -0.47333333
> hist(pigaov$residuals) ### plots a histogram of the residuals
```

> shapiro.test(pigaov$residuals)

Shapiro-Wilk normality test

data: pigaov$residuals

W = 0.9257, p-value = 0.2653

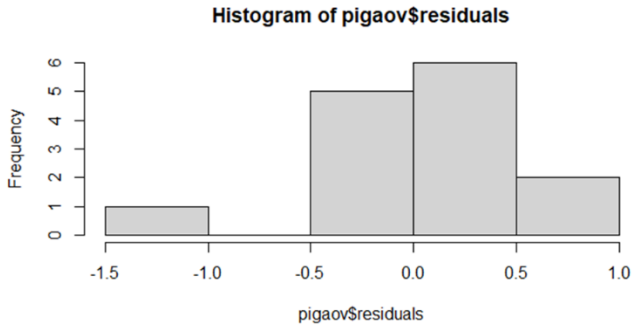

Figure A2 A histogram of the ANOVA residuals of evenness of pig samples

PHYLOGENETIC COMPARISON BETWEEN SAMPLES ON DAY 0

Df Sum Sq Mean Sq F value Pr(>F)

SAMPLE.TYPE 4 4504685 1126171 7.252 0.00678 **

Residuals 9 1397646 155294

Signif. codes: 0 '***' 0.001 '**' 0.01 '*' 0.05 '.' 0.1 ' ' 1

> tukey_pigaov <- TukeyHSD(pigaov)

> print(tukey_pigaov)

Tukey multiple comparisons of means

95% family-wise confidence level

Fit: aov(formula = Phylogenetic.Diversity ~ SAMPLE.TYPE, data = pigonly)

$SAMPLE.TYPE

diff lwr upr p adj

BELLY-ANUS 262.1667 -947.4817 1471.81499 0.9442946

LIVER-ANUS -1235.5000 -2445.1483 -25.85168 0.0450124

LUNG-ANUS -955.8333 -2165.4817 253.81499 0.1393659

MOUTH-ANUS -625.5000 -1835.1483 584.14832 0.4590228

LIVER-BELLY -1497.6667 -2579.6090 -415.72432 0.0079611

LUNG-BELLY -1218.0000 -2299.9424 -136.05765 0.0270198

MOUTH-BELLY -887.6667 -1969.6090 194.27568 0.1204861

LUNG-LIVER 279.6667 -802.2757 1361.60902 0.9012182

MOUTH-LIVER 610.0000 -471.9424 1691.94235 0.3832501

MOUTH-LUNG 330.3333 -751.6090 1412.27568 0.8372574

NORMALITY TEST FOR RESIDUAL

> pigaov$residuals ### Shows you the residuals for each sample

1	2	3	4	5	6
553.500000	-553.500000	408.333333	-558.666667	150.333333	-170.000000
7	8	9	10	11	12
174.000000	-4.000000	-7.666667	17.333333	-9.666667	366.000000
13	14				
-290.000000	-76.000000				

> hist(pigaov$residuals) ### plots a histogram of the residuals

> shapiro.test(pigaov$residuals)

Shapiro-Wilk normality test

data: pigaov$residuals

W = 0.957, p-value = 0.6736

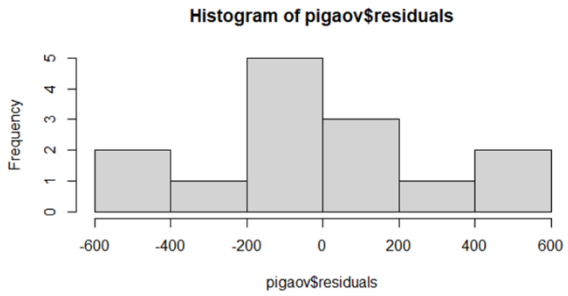

Figure A3 A histogram of the ANOVA residuals of phylogenetic diversity of pig samples

RICHNESS BETWEEN ENVIRONMENTAL SAMPLES ON DAY 0

Df Sum Sq Mean Sq F value Pr(>F)

SAMPLE.TYPE 3 48190897 16063632 330.7 3.62e-06 ***

Residuals 5 242901 48580

Signif. codes: 0 '***' 0.001 '**' 0.01 '*' 0.05 '.' 0.1 ' ' 1

> tukey_environaov <- TukeyHSD(environaov)

> print(tukey_environaov)

Tukey multiple comparisons of means

95% family-wise confidence level

Fit: aov(formula = Jackknife ~ SAMPLE.TYPE, data = environ)

$SAMPLE.TYPE

	diff	lwr	upr	p adj
Fresh -Brackish	-327.070	-1140.3603	486.2203	0.5084410
Sea-Brackish	-329.235	-1142.5253	484.0553	0.5037388
Soil-Brackish	4682.625	3940.1959	5425.0541	0.0000137
Sea-Fresh	-2.165	-815.4553	811.1253	0.9999996
Soil-Fresh	5009.695	4267.2659	5752.1241	0.0000110
Soil-Sea	5011.860	4269.4309	5754.2891	0.0000110

NORMALITY TEST FOR RESIDUAL

> environaov$residuals ### Shows you the residuals for each sample

```
      1       2       3       4       5       6       7       8
175.000 109.000 -284.000   6.060  -6.060 240.375 -240.375 -45.305
      9
 45.305
```

> hist(environaov$residuals) ### plots a histogram of the residuals

> shapiro.test(environaov$residuals)

```
        Shapiro-Wilk normality test

data:  environaov$residuals
W = 0.94397, p-value = 0.6243
```

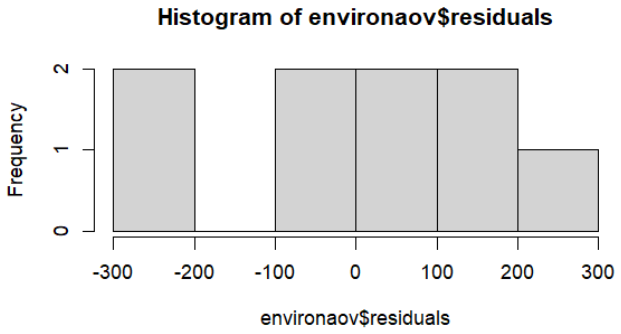

Figure A4 A histogram of the ANOVA residuals of evenness of environmental samples

EVENNESS BETWEEN ENVIRONMENTAL SAMPLES ON DAY 0

```
            Df Sum Sq Mean Sq F value   Pr(>F)
SAMPLE.TYPE  3 18.541   6.180   43.15 0.000536 ***
Residuals    5  0.716   0.143
---
Signif. codes:  0 ‘***’ 0.001 ‘**’ 0.01 ‘*’ 0.05 ‘.’ 0.1 ‘ ’ 1
```

> tukey_environaov <- TukeyHSD(environaov)

> print(tukey_environaov)

Tukey multiple comparisons of means

95% family-wise confidence level

Fit: aov(formula = NPShannon ~ SAMPLE.TYPE, data = environ)

$SAMPLE.TYPE

	diff	lwr	upr	p adj
Fresh -Brackish	-0.255	-1.651426	1.1414261	0.9027521
Sea-Brackish	-0.420	-1.816426	0.9764261	0.6998921
Soil-Brackish	2.805	1.530243	4.0797568	0.0017649
Sea-Fresh	-0.165	-1.561426	1.2314261	0.9695748
Soil-Fresh	3.060	1.785243	4.3347568	0.0011749
Soil-Sea	3.225	1.950243	4.4997568	0.0009170

NORMALITY TEST FOR RESIDUAL

```
> environaov$residuals     ### Shows you the residuals for each sample
    1     2     3     4     5     6     7     8     9
 0.120 -0.040 -0.080  0.265 -0.265 -0.215  0.215 -0.480  0.480
> hist(environaov$residuals) ### plots a histogram of the residuals
> shapiro.test(environaov$residuals)

        Shapiro-Wilk normality test

data:  environaov$residuals
W = 0.9882, p-value = 0.9931
```

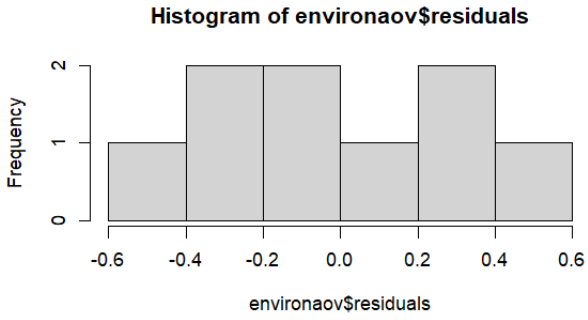

Figure A5 A histogram of the ANOVA residuals of evenness of environmental samples

PHYLOGENETIC DIVERSITY BETWEEN ENVIRONMENTAL SAMPLES ON DAY 0

```
            Df   Sum Sq  Mean Sq F value   Pr(>F)
SAMPLE.TYPE  3 32612702 10870901   238.9 8.12e-06 ***
Residuals    5   227550    45510
---
Signif. codes:  0 ‘***’ 0.001 ‘**’ 0.01 ‘*’ 0.05 ‘.’ 0.1 ‘ ’ 1
> tukey_environaov <- TukeyHSD(environaov)
> print(tukey_environaov)
  Tukey multiple comparisons of means
    95% family-wise confidence level

Fit: aov(formula = Phylogenetic.Diversity ~ SAMPLE.TYPE, data = environ)

$SAMPLE.TYPE
                    diff       lwr       upr     p adj
Fresh -Brackish  -491.000 -1278.1721  296.1721 0.2166434
Sea-Brackish     -387.000 -1174.1721  400.1721 0.3657393
Soil-Brackish    3728.833  3010.2468 4447.4199 0.0000277
Sea-Fresh         104.000  -683.1721  891.1721 0.9585900
Soil-Fresh       4219.833  3501.2468 4938.4199 0.0000173
Soil-Sea         4115.833  3397.2468 4834.4199 0.0000189

NORMALITY TEST FOR RESIDUAL
> environaov$residuals     ### Shows you the residuals for each sample
       1        2        3        4        5        6        7
 134.6667  117.6667 -252.3333   43.5000  -43.5000  249.5000 -249.5000
       8        9
  42.5000  -42.5000
> hist(environaov$residuals) ### plots a histogram of the residuals
```

> shapiro.test(environaov$residuals)

Shapiro-Wilk normality test

data: environaov$residuals

W = 0.93034, p-value = 0.4846

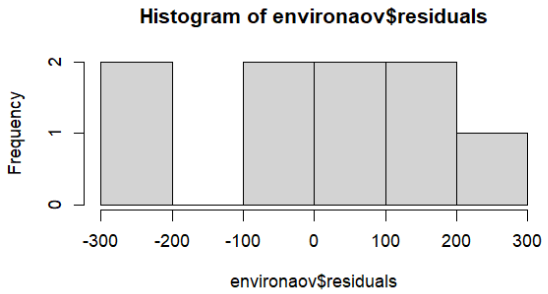

Figure A6 A histogram of the ANOVA residuals of evenness of environmental samples

RICHNESS (SIGNIFICANT SAMPLES) BETWEEN PIG SAMPLES OVER TIME

BELLY

Df Sum Sq Mean Sq F value Pr(>F)

DAYf 4 4391201 1097800 4.7673 0.02428 *

Residuals 9 2072497 230277

Signif. codes: 0 '***' 0.001 '**' 0.01 '*' 0.05 '.' 0.1 ' ' 1

> summary(belly_AN_JK)

Call:

lm(formula = Jackknife ~ DAYf, data = belly)

Residuals:

Min 1Q Median 3Q Max

-873.08 -128.68 9.44 82.73 873.08

Coefficients:

	Estimate	Std. Error	t value	Pr(>|t|)	
(Intercept)	2290.1	277.1	8.266	1.7e-05	***
DAYf2	-1200.8	391.8	-3.065	0.01347	*
DAYf4	-1029.0	391.8	-2.626	0.02753	*
DAYf7	-781.2	438.1	-1.783	0.10820	
DAYf23	-1638.1	391.8	-4.181	0.00237	**

Signif. codes: 0 '***' 0.001 '**' 0.01 '*' 0.05 '.' 0.1 ' ' 1

Residual standard error: 479.9 on 9 degrees of freedom

Multiple R-squared: 0.6794, Adjusted R-squared: 0.5369

F-statistic: 4.767 on 4 and 9 DF, p-value: 0.02428

NORMALITY TEST FOR RESIDUAL

belly

```
> belly_AN_JK$residuals          ### Shows you the residuals for each sample
     10       11       12       13       14       15       16       17
 91.9700  47.8700 -139.8400 -345.3333  562.6667 -217.3333  -17.1100  112.3100
     18       19       20       21       22       23
-95.2000  873.0800 -873.0800   36.0000   55.0000  -91.0000
> hist(belly_AN_JK$residuals) ### plots a histogram of the residuals
> shapiro.test(belly_AN_JK$residuals)

        Shapiro-Wilk normality test

data:  belly_AN_JK$residuals
W = 0.90699, p-value = 0.1425
```

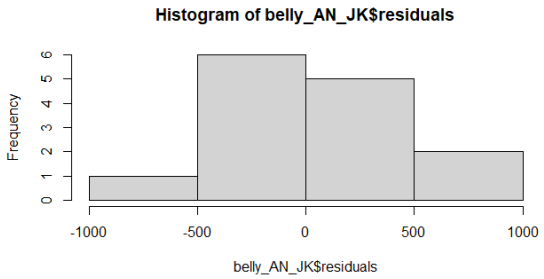

Figure A7 A histogram of the ANOVA residuals of richness of belly samples

LUNG

Response: Jackknife

	Df	Sum Sq	Mean Sq	F value	Pr(>F)	
DAYf	2	392335	196168	5.7853	0.03982	*
Residuals	6	203447	33908			

Signif. codes: 0 '***' 0.001 '**' 0.01 '*' 0.05 '.' 0.1 ' ' 1

> summary(lung_AN_JK)

Call:

lm(formula = Jackknife ~ DAYf, data = lung)

Residuals:

Min	1Q	Median	3Q	Max
-328.96	-28.15	5.78	27.66	301.29

Coefficients:

	Estimate	Std. Error	t value	Pr(>|t|)	
(Intercept)	549.6	106.3	5.170	0.00207	**
DAYf2	-236.6	150.4	-1.574	0.16657	
DAYf4	274.3	150.4	1.825	0.11788	

Signif. codes: 0 '***' 0.001 '**' 0.01 '*' 0.05 '.' 0.1 ' ' 1

Residual standard error: 184.1 on 6 degrees of freedom

Multiple R-squared: 0.6585, Adjusted R-squared: 0.5447

F-statistic: 5.785 on 2 and 6 DF, p-value: 0.03982

NORMALITY TEST FOR RESIDUAL

lung_AN_JK$residuals ### Shows you the residuals for each sample

33	34	35	36	37	38
-28.146667	22.363333	5.783333	-6.013333	-30.993333	37.006667

39	40	41
27.663333	301.293333	-328.956667

> hist(lung_AN_JK$residuals) ### plots a histogram of the residuals

> shapiro.test(lung_AN_JK$residuals)

Shapiro-Wilk normality test

data: lung_AN_JK$residuals

W = 0.81347, p-value = 0.02907

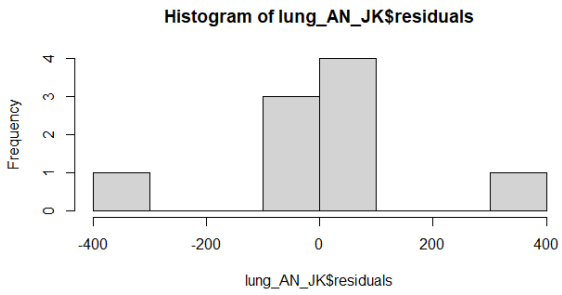

Figure A8 A histogram of the ANOVA residuals of richness of lung samples

EVENNESS (SIGNIFICANT SAMPLES) BETWEEN PIG SAMPLES OVER TIME

LIVER

	Df	Sum Sq	Mean Sq	F value	Pr(>F)
DAYf	2	17.8845	8.9422	55.765	0.000133 ***

```
Residuals  6  0.9621  0.1604
---
Signif. codes:  0 ‘***’ 0.001 ‘**’ 0.01 ‘*’ 0.05 ‘.’ 0.1 ‘ ’ 1
> summary(liver_AN_NP)

Call:
lm(formula = NPShannon ~ DAYf, data = liver)

Residuals:
   Min     1Q  Median     3Q    Max
-0.5267 -0.2000  0.1633  0.2600  0.3633

Coefficients:
            Estimate Std. Error t value Pr(>|t|)
(Intercept)   4.7400     0.2312  20.502 8.76e-07 ***
DAYf2        -3.0167     0.3270  -9.226 9.15e-05 ***
DAYf4        -2.9633     0.3270  -9.063 0.000101 ***
---
Signif. codes:  0 ‘***’ 0.001 ‘**’ 0.01 ‘*’ 0.05 ‘.’ 0.1 ‘ ’ 1
Residual standard error: 0.4004 on 6 degrees of freedom
Multiple R-squared:  0.9489,            Adjusted R-squared:  0.9319
F-statistic: 55.77 on 2 and 6 DF,  p-value: 0.000133

NORMALITY TEST FOR RESIDUAL
liver_AN_NP$residuals            ### Shows you the residuals for each sample
       24         25         26         27         28         29         30
-0.2000000  0.2600000 -0.0600000  0.2166667 -0.5233333  0.3066667 -0.5266667
       31         32
 0.3633333  0.1633333
> hist(liver_AN_NP$residuals) ### plots a histogram of the residuals
> shapiro.test(liver_AN_NP$residuals)
```

Shapiro-Wilk normality test

data: liver_AN_NP$residuals

W = 0.86171, p-value = 0.1001

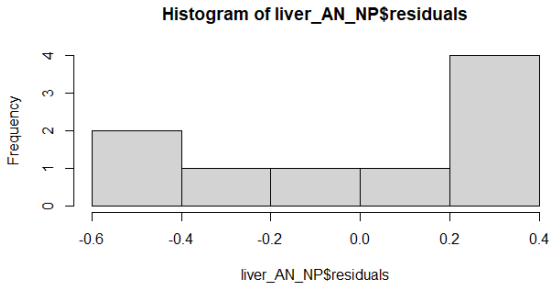

Figure A9 A histogram of the ANOVA residuals of evenness of liver samples

LUNG

Df Sum Sq Mean Sq F value Pr(>F)

DAYf 2 9.3544 4.6772 7.7785 0.02156 *

Residuals 6 3.6078 0.6013

Signif. codes: 0 ‘***’ 0.001 ‘**’ 0.01 ‘*’ 0.05 ‘.’ 0.1 ‘ ’ 1

> summary(lung_AN_NP)

Call:

lm(formula = NPShannon ~ DAYf, data = lung)

Residuals:

Min 1Q Median 3Q Max

-1.40333 -0.22333 0.02333 0.50333 0.77667

Coefficients:

```
            Estimate Std. Error t value Pr(>|t|)
(Intercept)   4.2133     0.4477   9.411 8.18e-05 ***
DAYf2        -1.9067     0.6331  -3.011  0.02366 *
DAYf4        -2.3500     0.6331  -3.712  0.00995 **
---
Signif. codes:  0 ‘***’ 0.001 ‘**’ 0.01 ‘*’ 0.05 ‘.’ 0.1 ‘ ’ 1

Residual standard error: 0.7754 on 6 degrees of freedom
Multiple R-squared:  0.7217,           Adjusted R-squared:  0.6289
F-statistic: 7.778 on 2 and 6 DF,  p-value: 0.02156

NORMALITY TEST FOR RESIDUAL
> lung_AN_NP$residuals           ### Shows you the residuals for each sample
        33         34         35         36         37         38
 0.77666667 -1.40333333  0.62666667 -0.52666667  0.02333333  0.50333333
        39         40         41
-0.02333333 -0.22333333  0.24666667
> hist(lung_AN_NP$residuals) ### plots a histogram of the residuals
> shapiro.test(lung_AN_NP$residuals)

            Shapiro-Wilk normality test
data:  lung_AN_NP$residuals
W = 0.92517, p-value = 0.4368
```

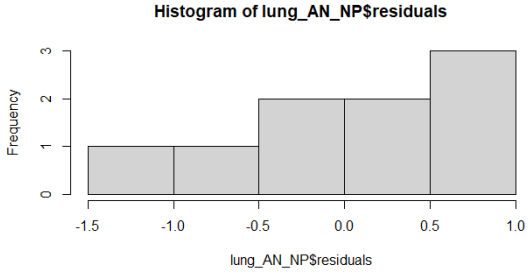

Figure A10 A histogram of the ANOVA residuals of evenness of lung samples

EVENNESS (SIGNIFICANT SAMPLES) BETWEEN ENVIRONMENTAL SAMPLES OVER TIME

BRAKISH WATER

```
        Df Sum Sq Mean Sq F value  Pr(>F)
DAYf       2 1.0407 0.52035  14.938 0.02756 *
Residuals  3 0.1045 0.03483
---
Signif. codes:  0 ‘***’ 0.001 ‘**’ 0.01 ‘*’ 0.05 ‘.’ 0.1 ‘ ’ 1
> summary(brackishwater_AN_NP)

Call:
lm(formula = NPShannon ~ DAYf, data = brackishwater)

Residuals:
   76    77    78    79    80    81
-0.215  0.215 -0.020  0.020  0.075 -0.075

Coefficients:
          Estimate Std. Error t value Pr(>|t|)
(Intercept)   4.0150     0.1320  30.423  7.8e-05 ***
DAYf7        -0.4950     0.1866  -2.652   0.0768 .
DAYf14       -1.0200     0.1866  -5.465   0.0120 *
---
Signif. codes:  0 ‘***’ 0.001 ‘**’ 0.01 ‘*’ 0.05 ‘.’ 0.1 ‘ ’ 1

Residual standard error: 0.1866 on 3 degrees of freedom
Multiple R-squared:  0.9087,            Adjusted R-squared:  0.8479
F-statistic: 14.94 on 2 and 3 DF,  p-value: 0.02756
```

NORMALITY TEST FOR RESIDUAL

```
brackishwater_AN_NP$residuals            ### Shows you the residuals for each sample
```

```
   76    77    78    79    80    81
-0.215  0.215 -0.020  0.020  0.075 -0.075
> hist(brackishwater_AN_NP$residuals) ### plots a histogram of the residuals
> shapiro.test(brackishwater_AN_NP$residuals)

        Shapiro-Wilk normality test

data:  brackishwater_AN_NP$residuals
W = 0.9929, p-value = 0.995
```

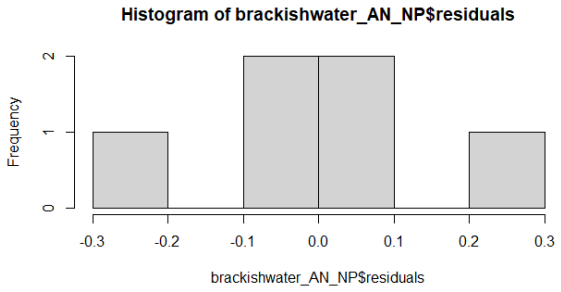

Figure A11 A histogram of the ANOVA residuals of evenness of brackish water samples

PHYLOGENETIC DIVERSITY (SIGNIFICANT SAMPLES) BETWEEN PIG SAMPLES OVER TIME

BELLY

```
        Df  Sum Sq Mean Sq F value    Pr(>F)
DAYf     4 4887759 1221940  14.679 0.0005576 ***
Residuals  9  749192   83244
---
Signif. codes:  0 ‘***’ 0.001 ‘**’ 0.01 ‘*’ 0.05 ‘.’ 0.1 ‘ ’ 1
> summary(belly_AN_PD)
Call:
lm(formula = Phylogenetic.Diversity ~ DAYf, data = belly)

Residuals:
    Min      1Q  Median      3Q     Max
```

-558.67 -119.75 17.17 140.58 408.33

Coefficients:

	Estimate	Std. Error	t value	Pr(>|t|)	
(Intercept)	2192.7	166.6	13.163	3.49e-07	***
DAYf2	-1285.7	235.6	-5.458	0.000402	***
DAYf4	-502.0	235.6	-2.131	0.061925	.
DAYf7	-1181.7	263.4	-4.487	0.001518	**
DAYf23	-1578.0	235.6	-6.698	8.87e-05	***

Signif. codes: 0 ‘***’ 0.001 ‘**’ 0.01 ‘*’ 0.05 ‘.’ 0.1 ‘ ’ 1

Residual standard error: 288.5 on 9 degrees of freedom

Multiple R-squared: 0.8671, Adjusted R-squared: 0.808

F-statistic: 14.68 on 4 and 9 DF, p-value: 0.0005576

NORMALITY TEST FOR RESIDUAL

```
> belly_AN_PD$residuals          ### Shows you the residuals for each sample
       10         11         12         13         14
 4.083333e+02 -5.586667e+02  1.503333e+02 -4.200000e+01 -1.847411e-13
       15         16         17         18         19
 4.200000e+01  3.433333e+01  1.113333e+02 -1.456667e+02  2.780000e+02
       20         21         22         23
-2.780000e+02 -2.666667e+01  1.773333e+02 -1.506667e+02
> hist(belly_AN_PD$residuals) ### plots a histogram of the residuals
> shapiro.test(belly_AN_PD$residuals)

        Shapiro-Wilk normality test

data:  belly_AN_PD$residuals
W = 0.96683, p-value = 0.8317
```

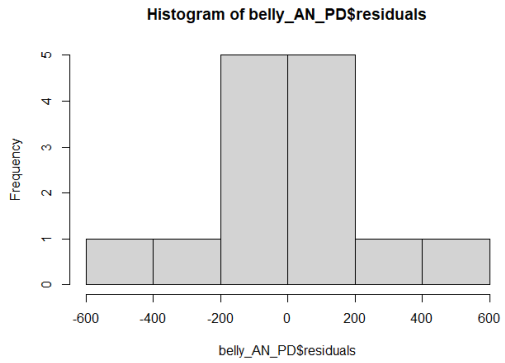

Figure A12 A histogram of the ANOVA residuals PD of Belly samples

LUNGS

Df Sum Sq Mean Sq F value Pr(>F)

DAYf 2 371538 185769 14.374 0.005148 **

Residuals 6 77544 12924

Signif. codes: 0 '***' 0.001 '**' 0.01 '*' 0.05 '.' 0.1 ' ' 1

> summary(lung_AN_PD)

Call:

lm(formula = Phylogenetic.Diversity ~ DAYf, data = lung)

Residuals:

Min 1Q Median 3Q Max

-190.333 -13.333 -7.667 17.333 188.667

Coefficients:

Estimate Std. Error t value Pr(>|t|)

(Intercept) 974.67 65.64 14.850 5.87e-06 ***

DAYf2 -384.33 92.82 -4.141 0.00608 **

DAYf4 81.67 92.82 0.880 0.41281

Signif. codes: 0 ‘***’ 0.001 ‘**’ 0.01 ‘*’ 0.05 ‘.’ 0.1 ‘ ’ 1

Residual standard error: 113.7 on 6 degrees of freedom

Multiple R-squared: 0.8273, Adjusted R-squared: 0.7698

F-statistic: 14.37 on 2 and 6 DF, p-value: 0.005148

NORMALITY TEST FOR RESIDUAL

> lung_AN_PD$residuals ### Shows you the residuals for each sample

33	34	35	36	37	38
-7.666667	17.333333	-9.666667	-13.333333	-43.333333	56.666667

39	40	41
1.666667	188.666667	-190.333333

> hist(lung_AN_PD$residuals) ### plots a histogram of the residuals

> shapiro.test(lung_AN_PD$residuals)

Shapiro-Wilk normality test

data: lung_AN_PD$residuals

W = 0.88988, p-value = 0.1989

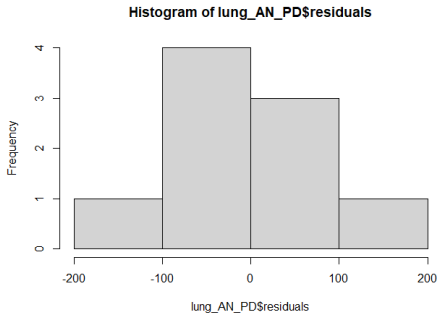

Figure A13 A histogram of the ANOVA residuals PD of lung samples

PHYLOGENETIC DIVERSITY (SIGNIFICANT SAMPLES) BETWEEN PIG SAMPLES OVER TIME

No samples with significant values for phylogenetic samples in the environmental samples over time.

APPENDIX 6: R OUTPUT RESULT FOR CHAPTER 5 (SIGNIFICANT TAXA)

PIG AND BODY SITE SAMPLES (PHYLUM)

ACTINOBACTERIA

summary(Actinobacteria)

```
             Df    Sum Sq  Mean Sq F value Pr(>F)
Sample.Type  4 306178178 76544545    4.76 0.0244 *
Residuals    9 144732133 16081348
---
Signif. codes:  0 ‘***’ 0.001 ‘**’ 0.01 ‘*’ 0.05 ‘.’ 0.1 ‘ ’ 1
> Tukey_Actinobacteria <- TukeyHSD(Actinobacteria)
> print (Tukey_Actinobacteria)
  Tukey multiple comparisons of means
    95% family-wise confidence level

Fit: aov(formula = Actinobacteria ~ Sample.Type, data = day0taxa)

$Sample.Type
                    diff        lwr       upr     p adj
Belly-Anus   11516.00000   -793.5745 23825.5745 0.0686675
Liver-Anus      10.33333 -12299.2412 12319.9079 1.0000000
Lung-Anus     2780.33333  -9529.2412 15089.9079 0.9360632
Mouth-Anus    -822.00000 -13131.5745 11487.5745 0.9993194
Liver-Belly -11505.66667 -22515.6848  -495.6485 0.0400780
Lung-Belly   -8735.66667 -19745.6848  2274.3515 0.1372106
Mouth-Belly -12338.00000 -23348.0182 -1327.9818 0.0277027
Lung-Liver    2770.00000  -8240.0182 13780.0182 0.9092873
Mouth-Liver   -832.33333 -11842.3515 10177.6848 0.9988927
Mouth-Lung   -3602.33333 -14612.3515  7407.6848 0.8025992
```

NORMALITY TEST FOR RESIDUAL

```
> Actinobacteria$residuals                    ### Shows you the residuals for each sample
       1        2        3        4        5        6        7
 845.0000 1788.0000 7655.0000 -193.0000 -652.0000  209.0000  368.6667
       8        9       10       11       12       13       14
-1788.0000 -2632.3333   124.6667  2263.6667 -1556.3333  1431.6667 -7864.0000
> hist(Actinobacteria$residuals)              ### plots a histogram of the residuals
> shapiro.test(Actinobacteria$residuals)    ### test for normality >0.05 =  normal

        Shapiro-Wilk normality test

data:  Actinobacteria$residuals
W = 0.90093, p-value = 0.1164
```

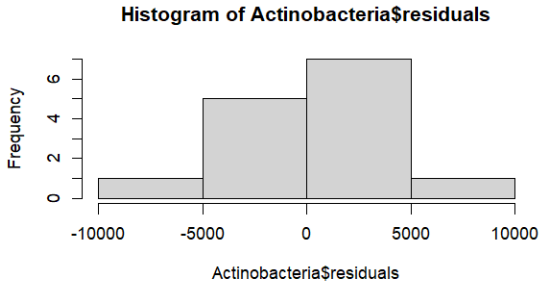

Figure A14 A histogram of the ANOVA residuals of Actinobacteria between pig samples on day 0

BACTEROIDETES

```
> summary(Bacteroidetes)
            Df    Sum Sq   Mean Sq F value   Pr(>F)
Sample.Type  4 1.580e+09 394991142   19.28 0.000194 ***
Residuals    9 1.844e+08  20491277
---
Signif. codes:  0 ‘***’ 0.001 ‘**’ 0.01 ‘*’ 0.05 ‘.’ 0.1 ‘ ’ 1
> Tukey_Bacteroidetes <- TukeyHSD(Bacteroidetes)
> print (Tukey_Bacteroidetes)
```

```
  Tukey multiple comparisons of means
    95% family-wise confidence level
Fit: aov(formula = Bacteroidetes ~ Sample.Type, data = day0taxa)
$Sample.Type
                diff       lwr       upr     p adj
Belly-Anus  -18871.833 -32767.082 -4976.585 0.0089746
Liver-Anus  -22274.833 -36170.082 -8379.585 0.0030197
Lung-Anus   -20081.167 -33976.415 -6185.918 0.0060381
Mouth-Anus    2628.833 -11266.415 16524.082 0.9650651
Liver-Belly  -3403.000 -15831.288  9025.288 0.8819925
Lung-Belly   -1209.333 -13637.622 11218.955 0.9970447
Mouth-Belly  21500.667   9072.378 33928.955 0.0017733
Lung-Liver    2193.667 -10234.622 14621.955 0.9726569
Mouth-Liver  24903.667  12475.378 37331.955 0.0006052
Mouth-Lung   22710.000  10281.712 35138.288 0.0011966

NORMALITY TEST FOR RESIDUAL
> Bacteroidetes$residuals                    ### Shows you the residuals for each sample
        1         2         3         4         5         6
-5928.33333  6784.50000  3343.33333   -90.33333  6018.66667 -1954.66667
        7         8         9        10        11        12
-1079.33333 -6784.50000   940.66667  1009.33333   138.66667  -984.66667
       13        14
  -24.66667 -1388.66667
> hist(Bacteroidetes$residuals)              ### plots a histogram of the residuals
> shapiro.test(Bacteroidetes$residuals)    ### test for normality >0.05 =  normal

            Shapiro-Wilk normality test

data:  Bacteroidetes$residuals
W = 0.93883, p-value = 0.4035
```

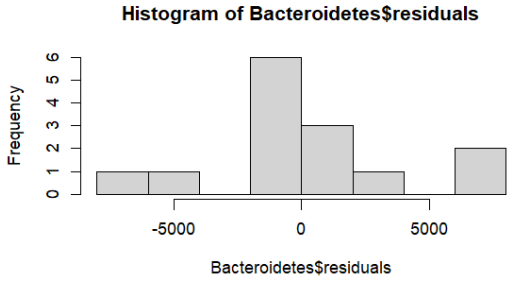

Figure A15 A histogram of the ANOVA residuals of Bacteroidetes between pig samples on day 0

CYANOBACTERIA

summary(Cyanobacteria)

Df Sum Sq Mean Sq F value Pr(>F)

Sample.Type 4 33607 8402 4.773 0.0242 *

Residuals 9 15842 1760

Signif. codes: 0 '***' 0.001 '**' 0.01 '*' 0.05 '.' 0.1 ' ' 1

> Tukey_Cyanobacteria <- TukeyHSD(Cyanobacteria)

> print (Tukey_Cyanobacteria)

Tukey multiple comparisons of means

95% family-wise confidence level

Fit: aov(formula = Cyanobacteria ~ Sample.Type, data = day0taxa)

$Sample.Type

diff lwr upr p adj

Belly-Anus -122.16667 -250.95107 6.61774 0.0643876

Liver-Anus -100.50000 -229.28441 28.28441 0.1460472

Lung-Anus -35.50000 -164.28441 93.28441 0.8795625

Mouth-Anus -133.16667 -261.95107 -4.38226 0.0422991

Liver-Belly 21.66667 -93.52161 136.85494 0.9657661

Lung-Belly 86.66667 -28.52161 201.85494 0.1667729

Mouth-Belly -11.00000 -126.18827 104.18827 0.9972513

Lung-Liver 65.00000 -50.18827 180.18827 0.3824949

Mouth-Liver -32.66667 -147.85494 82.52161 0.8688212

Mouth-Lung -97.66667 -212.85494 17.52161 0.1054719

NORMALITY TEST FOR RESIDUAL

```
> Cyanobacteria$residuals                    ### Shows you the residuals for each sample
        1         2         3         4         5         6
-0.3333333 35.5000000  0.6666667 -0.3333333  0.6666667  6.6666667
        7         8         9        10        11        12
44.0000000 -35.5000000 -86.0000000  -3.0000000  42.0000000 -31.0000000
       13        14
34.0000000  -7.3333333
> hist(Cyanobacteria$residuals)              ### plots a histogram of the residuals
> shapiro.test(Cyanobacteria$residuals)    ### test for normality >0.05 =  normal
            Shapiro-Wilk normality test

data:  Cyanobacteria$residuals
W = 0.89484, p-value = 0.09495
```

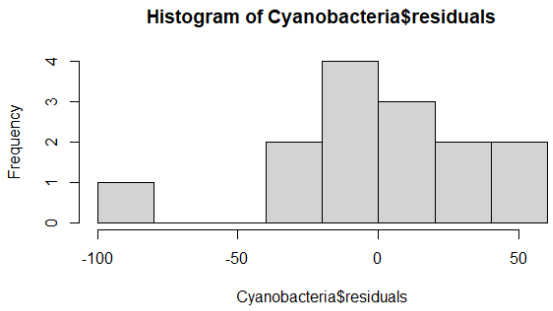

Figure A16 A histogram of the ANOVA residuals of Cyanobacteria between pig samples on day 0

PEREGRINIBACTERIA

```
> summary(Peregrinibacteria)
            Df  Sum Sq Mean Sq F value Pr(>F)
Sample.Type  4 1552435  388109   5.448 0.0165 *
Residuals    9  641203   71245
---
Signif. codes:  0 ‘***’ 0.001 ‘**’ 0.01 ‘*’ 0.05 ‘.’ 0.1 ‘ ’ 1
> Tukey_Peregrinibacteria <- TukeyHSD(Peregrinibacteria)
> print (Tukey_Peregrinibacteria)
  Tukey multiple comparisons of means
    95% family-wise confidence level

Fit: aov(formula = Peregrinibacteria ~ Sample.Type, data = day0taxa)

$Sample.Type
                  diff        lwr      upr     p adj
Belly-Anus   1.666667e+00 -817.662132  820.9955 1.0000000
Liver-Anus  -1.421085e-13 -819.328798  819.3288 1.0000000
Lung-Anus   -8.526513e-14 -819.328798  819.3288 1.0000000
Mouth-Anus   8.120000e+02   -7.328798 1631.3288 0.0522497
Liver-Belly -1.666667e+00 -734.496622  731.1633 1.0000000
Lung-Belly  -1.666667e+00 -734.496622  731.1633 1.0000000
Mouth-Belly  8.103333e+02   77.503378 1543.1633 0.0297795
Lung-Liver   5.684342e-14 -732.829956  732.8300 1.0000000
Mouth-Liver  8.120000e+02   79.170044 1544.8300 0.0294515
Mouth-Lung   8.120000e+02   79.170044 1544.8300 0.0294515
```

NORMALITY TEST FOR RESIDUAL

```
> Peregrinibacteria$residuals                    ### Shows you the residuals for each sample
         1          2          3          4          5          6
-6.410000e+02 -1.421085e-13  3.333333e+00  2.090000e+02  4.320000e+02 -1.666667e+00
```

```
         7          8          9         10         11         12
2.842171e-14 -2.273737e-13  2.842171e-14  2.842171e-14  2.842171e-14  2.842171e-14
        13         14
2.842171e-14 -1.666667e+00
> hist(Peregrinibacteria$residuals)                ### plots a histogram of the residuals
> shapiro.test(Peregrinibacteria$residuals)    ### test for normality >0.05 =  normal

            Shapiro-Wilk normality test

data:  Peregrinibacteria$residuals
W = 0.6279, p-value = 7.272e-05
```

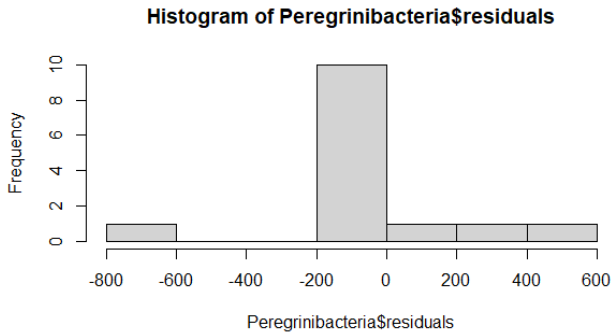

Figure A17 A histogram of the ANOVA residuals of Peregrinibacteria between pig samples on day 0

ENVIRONMENTAL SAMPLES (PHYLUM)

VERRUCOMICROBIA

```
summary(Verrucomicrobia)
             Df    Sum Sq  Mean Sq F value   Pr(>F)
Sample.Type  3 111767981 37255994   109.8 5.53e-05 ***
Residuals    5   1695901   339180
---
Signif. codes:  0 ‘***’ 0.001 ‘**’ 0.01 ‘*’ 0.05 ‘.’ 0.1 ‘ ’ 1
> Tukey_Verrucomicrobia <- TukeyHSD(Verrucomicrobia)
> print (Tukey_Verrucomicrobia)
  Tukey multiple comparisons of means
```

95% family-wise confidence level

Fit: aov(formula = Verrucomicrobia ~ Sample.Type, data = day0taxa)

$Sample.Type

	diff	lwr	upr	p adj
Fresh-Brackish	-230.5	-2379.475	1918.475	0.9768034
Sea-Brackish	-295.5	-2444.475	1853.475	0.9538249
Soil-Brackish	7297.0	5335.263	9258.737	0.0001416
Sea-Fresh	-65.0	-2213.975	2083.975	0.9994341
Soil-Fresh	7527.5	5565.763	9489.237	0.0001211
Soil-Sea	7592.5	5630.763	9554.237	0.0001160

RESIDUAL NORMALITY TEST

```
> Verrucomicrobia$residuals                    ### Shows you the residuals for each sample
    1     2     3     4     5     6     7     8     9
 -28.5  460.0  202.5  476.0 -936.0 -386.0 -202.5  386.0   28.5
> hist(Verrucomicrobia$residuals)              ### plots a histogram of the residuals
> shapiro.test(Verrucomicrobia$residuals)    ### test for normality >0.05 =  normal
```

Shapiro-Wilk normality test

data: Verrucomicrobia$residuals

W = 0.9127, p-value = 0.3352

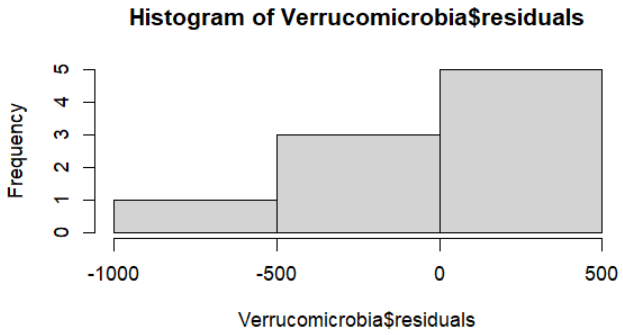

Figure A18 A histogram of the ANOVA residuals of Verrucomicrobia between environmental samples on day 0

CHLAMYDIAE

> summary(Chlamydiae)

Df Sum Sq Mean Sq F value Pr(>F)

Sample.Type 3 1475974 491991 575.6 9.11e-07 ***

Residuals 5 4274 855

Signif. codes: 0 '***' 0.001 '**' 0.01 '*' 0.05 '.' 0.1 ' ' 1

> Tukey_Chlamydiae <- TukeyHSD(Chlamydiae)

> print (Tukey_Chlamydiae)

Tukey multiple comparisons of means

95% family-wise confidence level

Fit: aov(formula = Chlamydiae ~ Sample.Type, data = day0taxa)

$Sample.Type

	diff	lwr	upr	p adj
Fresh-Brackish	3.5000	-104.37764	111.3776	0.9993023
Sea-Brackish	14.0000	-93.87764	121.8776	0.9605694
Soil-Brackish	864.8333	766.35497	963.3117	0.0000038
Sea-Fresh	10.5000	-97.37764	118.3776	0.9823892
Soil-Fresh	861.3333	762.85497	959.8117	0.0000039
Soil-Sea	850.8333	752.35497	949.3117	0.0000041

NORMALITY TEST FOR RESIDUAL

```
> Chlamydiae$residuals                    ### Shows you the residuals for each sample
      1       2       3       4       5       6       7
-25.50000 -10.33333 -18.00000  36.66667 -26.33333   9.50000  18.00000
      8       9
 -9.50000  25.50000
> hist(Chlamydiae$residuals)              ### plots a histogram of the residuals
> shapiro.test(Chlamydiae$residuals)    ### test for normality >0.05 =  normal

            Shapiro-Wilk normality test

data:  Chlamydiae$residuals
W = 0.91826, p-value = 0.378
```

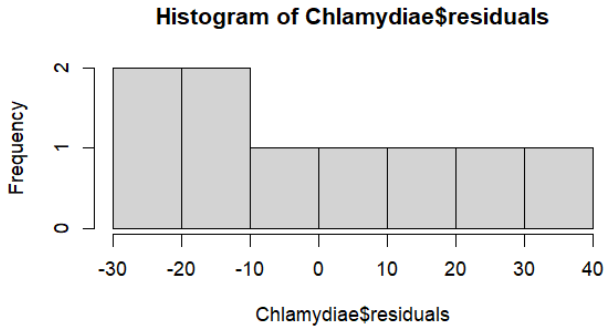

Figure A19 A histogram of the ANOVA residuals of Chlamydiae between environmental samples on day 0

PLANCTOMYCETES

```
summary(Planctomycetes)
            Df    Sum Sq  Mean Sq F value   Pr(>F)
Sample.Type  3 178848013 59616004   198.8 1.28e-05 ***
Residuals    5   1499759   299952
---
Signif. codes:  0 ‘***’ 0.001 ‘**’ 0.01 ‘*’ 0.05 ‘.’ 0.1 ‘ ’ 1
```

```
> Tukey_Planctomycetes <- TukeyHSD(Planctomycetes)
> print (Tukey_Planctomycetes)
  Tukey multiple comparisons of means
    95% family-wise confidence level

Fit: aov(formula = Planctomycetes ~ Sample.Type, data = day0taxa)

$Sample.Type
                diff       lwr       upr     p adj
Fresh-Brackish  -64.500 -2085.386  1956.386 0.9993356
Sea-Brackish     33.000 -1987.886  2053.886 0.9999105
Soil-Brackish  9445.667  7600.858 11290.475 0.0000293
Sea-Fresh        97.500 -1923.386  2118.386 0.9977295
Soil-Fresh     9510.167  7665.358 11354.975 0.0000285
Soil-Sea       9412.667  7567.858 11257.475 0.0000298

Planctomycetes$residuals                    ### Shows you the residuals for each sample
      1       2       3       4       5       6       7
-128.0000 -942.6667  145.5000  685.3333  257.3333   -8.0000 -145.5000
      8       9
  8.0000  128.0000
> hist(Planctomycetes$residuals)              ### plots a histogram of the residuals
> shapiro.test(Planctomycetes$residuals)    ### test for normality >0.05 =  normal

            Shapiro-Wilk normality test

data:  Planctomycetes$residuals
W = 0.8912, p-value = 0.2053
```

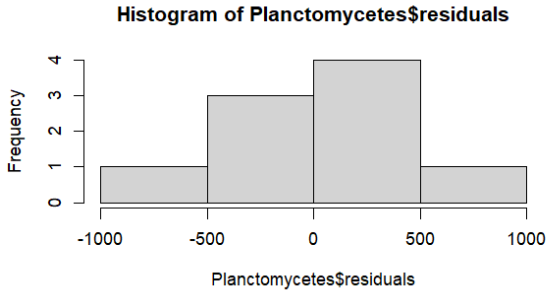

Figure A20 A histogram of the ANOVA residuals of Planctomycetes between environmental samples on day 0

CHLOROFLEXI

summary(Chloroflexi)

	Df	Sum Sq	Mean Sq	F value	Pr(>F)	
Sample.Type	3	15374968	5124989	88.02	9.53e-05	***
Residuals	5	291143	58229			

Signif. codes: 0 '***' 0.001 '**' 0.01 '*' 0.05 '.' 0.1 ' ' 1

> Tukey_Chloroflexi <- TukeyHSD(Chloroflexi)

> print (Tukey_Chloroflexi)

Tukey multiple comparisons of means

95% family-wise confidence level

Fit: aov(formula = Chloroflexi ~ Sample.Type, data = day0taxa)

$Sample.Type

	diff	lwr	upr	p adj
Fresh-Brackish	-89.5	-979.8982	800.8982	0.9806992
Sea-Brackish	143.0	-747.3982	1033.3982	0.9301165
Soil-Brackish	2785.5	1972.6813	3598.3187	0.0002127
Sea-Fresh	232.5	-657.8982	1122.8982	0.7750378
Soil-Fresh	2875.0	2062.1813	3687.8187	0.0001820
Soil-Sea	2642.5	1829.6813	3455.3187	0.0002754

NORMALITY TEST FOR RESIDUAL

```
> Cyanobacteria$residuals                    ### Shows you the residuals for each sample
       1        2        3        4        5        6        7
-36.000000   5.666667  37.500000  15.666667 -21.333333 -28.000000 -37.500000
       8        9
 28.000000  36.000000
> day0taxa=read.csv("environmental.csv",header=T, stringsAsFactors=TRUE)
> plot(Chloroflexi~Sample.Type,data=day0taxa)          ###  generates a boxplot
> Chloroflexi <- aov(Chloroflexi~Sample.Type,data=day0taxa)
> summary(Chloroflexi)
             Df   Sum Sq Mean Sq F value   Pr(>F)
Sample.Type  3 15374968 5124989   88.02 9.53e-05 ***
Residuals    5   291143   58229
---
Signif. codes:  0 ‘***’ 0.001 ‘**’ 0.01 ‘*’ 0.05 ‘.’ 0.1 ‘ ’ 1
> Tukey_Chloroflexi <- TukeyHSD(Chloroflexi)
> print (Tukey_Chloroflexi)
  Tukey multiple comparisons of means
    95% family-wise confidence level

Fit: aov(formula = Chloroflexi ~ Sample.Type, data = day0taxa)

$Sample.Type
                diff       lwr       upr     p adj
Fresh-Brackish  -89.5 -979.8982  800.8982 0.9806992
Sea-Brackish    143.0 -747.3982 1033.3982 0.9301165
Soil-Brackish  2785.5 1972.6813 3598.3187 0.0002127
Sea-Fresh       232.5 -657.8982 1122.8982 0.7750378
Soil-Fresh     2875.0 2062.1813 3687.8187 0.0001820
Soil-Sea       2642.5 1829.6813 3455.3187 0.0002754
```

> Chloroflexi$residuals ### Shows you the residuals for each sample

1 2 3 4 5 6 7 8 9

-136.5 -93.0 30.0 383.0 -290.0 -79.5 -30.0 79.5 136.5

> hist(Chloroflexi$residuals) ### plots a histogram of the residuals

> shapiro.test(Chloroflexi$residuals) ### test for normality >0.05 = normal

Shapiro-Wilk normality test

data: Chloroflexi$residuals

W = 0.96226, p-value = 0.8217

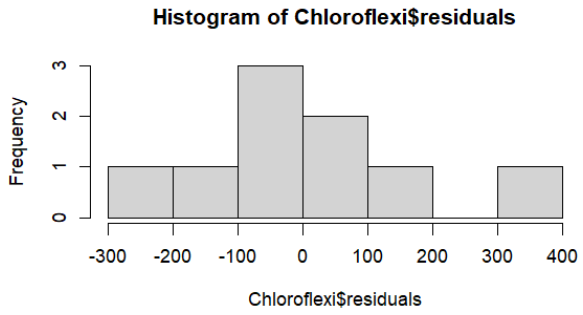

Figure A21 A histogram of the ANOVA residuals of Chloroflexi between environmental samples on day 0

ACIDOBACTERIA

> summary(Acidobacteria)

Df Sum Sq Mean Sq F value Pr(>F)

Sample.Type 3 281042296 93680765 88.33 9.44e-05 ***

Residuals 5 5302867 1060573

Signif. codes: 0 '***' 0.001 '**' 0.01 '*' 0.05 '.' 0.1 ' ' 1

> Tukey_Acidobacteria <- TukeyHSD(Acidobacteria)

> print (Tukey_Acidobacteria)

Tukey multiple comparisons of means

95% family-wise confidence level

Fit: aov(formula = Acidobacteria ~ Sample.Type, data = day0taxa)

$Sample.Type

	diff	lwr	upr	p adj
Fresh-Brackish	157.00	-3643.025	3957.025	0.9985669
Sea-Brackish	365.00	-3435.025	4165.025	0.9830422
Soil-Brackish	12025.33	8556.401	15494.266	0.0002010
Sea-Fresh	208.00	-3592.025	4008.025	0.9967022
Soil-Fresh	11868.33	8399.401	15337.266	0.0002145
Soil-Sea	11660.33	8191.401	15129.266	0.0002339

NORMALITY TEST FOR RESIDUAL

Acidobacteria$residuals ### Shows you the residuals for each sample

1	2	3	4	5	6	7
-179.0000	-389.3333	137.0000	1771.6667	-1382.3333	3.0000	-137.0000

8	9
-3.0000	179.0000

> hist(Acidobacteria$residuals) ### plots a histogram of the residuals

> shapiro.test(Acidobacteria$residuals) ### test for normality >0.05 = normal

Shapiro-Wilk normality test

data: Acidobacteria$residuals

W = 0.84505, p-value = 0.06571

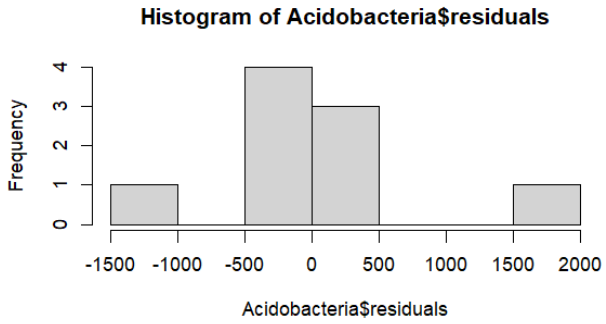

Figure A22 A histogram of the ANOVA residuals of Acidobacteria between environmental samples on day 0

TENERICUTES

> summary(Tenericutes)

Df Sum Sq Mean Sq F value Pr(>F)

Sample.Type 3 20966 6989 154.2 2.4e-05 ***

Residuals 5 227 45

Signif. codes: 0 '***' 0.001 '**' 0.01 '*' 0.05 '.' 0.1 ' ' 1

> Tukey_Tenericutes <- TukeyHSD(Tenericutes)

> print (Tukey_Tenericutes)

Tukey multiple comparisons of means

95% family-wise confidence level

Fit: aov(formula = Tenericutes ~ Sample.Type, data = day0taxa)

$Sample.Type

	diff	lwr	upr	p adj
Fresh-Brackish	4.000000e+00	-20.84420	28.8442	0.9296584
Sea-Brackish	-3.552714e-15	-24.84420	24.8442	1.0000000
Soil-Brackish	1.036667e+02	80.98712	126.3462	0.0000499
Sea-Fresh	-4.000000e+00	-28.84420	20.8442	0.9296584
Soil-Fresh	9.966667e+01	76.98712	122.3462	0.0000608
Soil-Sea	1.036667e+02	80.98712	126.3462	0.0000499

NORMALITY TEST FOR RESIDUAL

```
> Tenericutes$residuals                    ### Shows you the residuals for each sample
         1          2          3          4          5
 1.480297e-15 -4.666667e+00 -4.000000e+00  1.133333e+01 -6.666667e+00
         6          7          8          9
-1.184238e-15  4.000000e+00 -1.184238e-15 -2.516506e-15
> hist(Tenericutes$residuals)              ### plots a histogram of the residuals
> shapiro.test(Tenericutes$residuals)    ### test for normality >0.05 =  normal

        Shapiro-Wilk normality test

data:  Tenericutes$residuals
W = 0.88947, p-value = 0.197
```

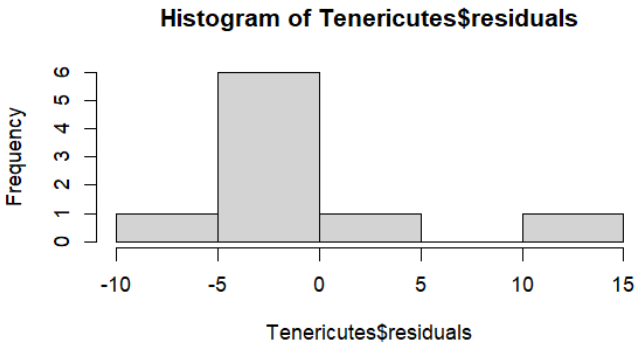

Figure A23 A histogram of the ANOVA residuals of Tenericutes between environmental samples on day 0

PIG AND BOBY SITES (FAMILIES)

ENTEROCOCCACEAE

```
plot(Enterococcaceae~Sample.Type,data=day0taxa)          ###  generates a boxplot
> Enterococcaceae <- aov(Enterococcaceae~Sample.Type,data=day0taxa)
> summary(Enterococcaceae)
             Df  Sum Sq Mean Sq F value Pr(>F)
Sample.Type  4 1041450  260362   5.108 0.0199 *
Residuals    9  458760   50973
```

```
---
Signif. codes:  0 ‘***’ 0.001 ‘**’ 0.01 ‘*’ 0.05 ‘.’ 0.1 ‘ ’ 1
> Tukey_Enterococcaceae <- TukeyHSD(Enterococcaceae)
> print (Tukey_Enterococcaceae)
  Tukey multiple comparisons of means
    95% family-wise confidence level

Fit: aov(formula = Enterococcaceae ~ Sample.Type, data = day0taxa)

$Sample.Type
                diff        lwr       upr     p adj
Belly-Anus   589.50000  -103.53194 1282.53194 0.1040838
Liver-Anus   132.83333  -560.19861  825.86528 0.9634383
Lung-Anus    603.16667   -89.86528 1296.19861 0.0945419
Mouth-Anus     9.50000  -683.53194  702.53194 0.9999988
Liver-Belly -456.66667 -1076.53328  163.19995 0.1795108
Lung-Belly    13.66667  -606.19995  633.53328 0.9999917
Mouth-Belly -580.00000 -1199.86662   39.86662 0.0686158
Lung-Liver   470.33333  -149.53328 1090.19995 0.1618297
Mouth-Liver -123.33333  -743.19995  496.53328 0.9583757
Mouth-Lung  -593.66667 -1213.53328   26.19995 0.0615619

NORMALITY TEST FOR RESIDUAL
> Enterococcaceae$residuals                    ### Shows you the residuals for each sample
       1        2        3        4        5        6        7
 77.00000   49.50000  192.00000  -32.00000  -45.00000  -93.00000 -461.66667
       8        9       10       11       12       13       14
 -49.50000   80.33333  -87.33333  381.33333  -37.33333  124.66667  -99.00000
> hist(Enterococcaceae$residuals)              ### plots a histogram of the residuals
> shapiro.test(Enterococcaceae$residuals)    ### test for normality >0.05 =  normal
```

Shapiro-Wilk normality test

data: Enterococcaceae$residuals

W = 0.90857, p-value = 0.1502

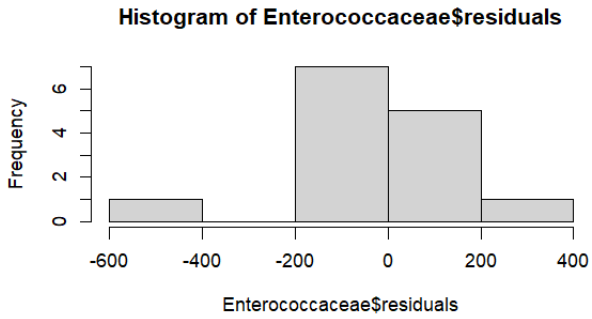

Figure A24 A histogram of the ANOVA residuals of Enterococcaceae between environmental samples on day 0

CARNOBACTERIACEAE

summary(Carnobacteriaceae)

Df Sum Sq Mean Sq F value Pr(>F)

Sample.Type 4 15754566 3938641 12.74 0.000948 ***

Residuals 9 2781646 309072

Signif. codes: 0 '***' 0.001 '**' 0.01 '*' 0.05 '.' 0.1 ' ' 1

> Tukey_Carnobacteriaceae <- TukeyHSD(Carnobacteriaceae)

> print (Tukey_Carnobacteriaceae)

Tukey multiple comparisons of means

95% family-wise confidence level

Fit: aov(formula = Carnobacteriaceae ~ Sample.Type, data = day0taxa)

$Sample.Type

diff lwr upr p adj

Belly-Anus 2598.16667 891.6463 4304.6870 0.0042824

Liver-Anus 54.83333 -1651.6870 1761.3537 0.9999626

Lung-Anus 146.50000 -1560.0204 1853.0204 0.9981813

Mouth-Anus -120.50000 -1827.0204 1586.0204 0.9991525

Liver-Belly -2543.33333 -4069.6916 -1016.9751 0.0023100

Lung-Belly -2451.66667 -3978.0249 -925.3084 0.0029791

Mouth-Belly -2718.66667 -4245.0249 -1192.3084 0.0014397

Lung-Liver 91.66667 -1434.6916 1618.0249 0.9995519

Mouth-Liver -175.33333 -1701.6916 1351.0249 0.9944166

Mouth-Lung -267.00000 -1793.3582 1259.3582 0.9735191

NORMALITY TEST FOR RESIDUAL

> Carnobacteriaceae $residuals ### Shows you the residuals for each sample

1 2 3 4 5 6 7

98.00000 201.50000 1249.33333 -50.00000 -48.00000 -296.66667 -143.00000

8 9 10 11 12 13 14

-201.50000 9.00000 155.66667 134.00000 -243.33333 87.66667 -952.66667

> hist(Carnobacteriaceae $residuals) ### plots a histogram of the residuals

> shapiro.test(Carnobacteriaceae $residuals) ### test for normality >0.05 = normal

Shapiro-Wilk normality test

data: Carnobacteriaceae$residuals

W = 0.83199, p-value = 0.01276

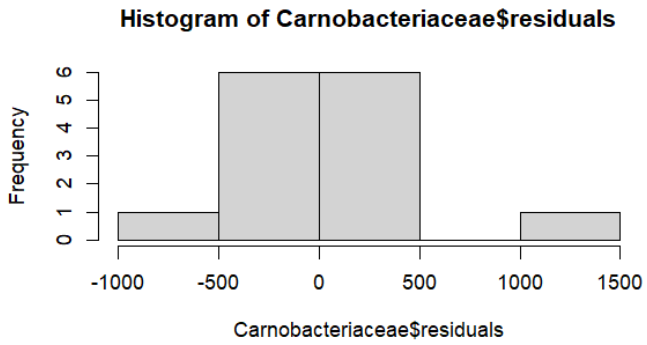

Figure A25 A histogram of the ANOVA residuals of Carnobacteriaceae between environmental samples on day 0

AEROCOCCACEAE

> summary(Aerococcaceae)

	Df	Sum Sq	Mean Sq	F value	Pr(>F)	
Sample.Type	4	18782154	4695538	9.112	0.00315	**
Residuals	9	4637971	515330			

Signif. codes: 0 ‘***’ 0.001 ‘**’ 0.01 ‘*’ 0.05 ‘.’ 0.1 ‘ ’ 1

> Tukey_Aerococcaceae <- TukeyHSD(Aerococcaceae)

> print (Tukey_Aerococcaceae)

Tukey multiple comparisons of means

95% family-wise confidence level

Fit: aov(formula = Aerococcaceae ~ Sample.Type, data = day0taxa)

$Sample.Type

	diff	lwr	upr	p adj
Belly-Anus	3056.33333	852.775	5259.8917	0.0078612
Liver-Anus	-23.66667	-2227.225	2179.8917	0.9999995
Lung-Anus	518.33333	-1685.225	2721.8917	0.9269347
Mouth-Anus	631.33333	-1572.225	2834.8917	0.8647701
Liver-Belly	-3080.00000	-5050.923	-1109.0775	0.0035929
Lung-Belly	-2538.00000	-4508.923	-567.0775	0.0124549

Mouth-Belly -2425.00000 -4395.923 -454.0775 0.0163332

Lung-Liver 542.00000 -1428.923 2512.9225 0.8804304

Mouth-Liver 655.00000 -1315.923 2625.9225 0.7940803

Mouth-Lung 113.00000 -1857.923 2083.9225 0.9996269

NORMALITY TEST FOR RESIDUAL

> Aerococcaceae $residuals ### Shows you the residuals for each sample

```
       1        2        3        4        5        6
 338.66667  200.00000 1081.66667   21.66667 -360.33333   19.66667
       7        8        9       10       11       12
-684.33333 -200.00000 -425.33333  133.66667 1109.66667 -172.33333
      13       14
  38.66667 -1101.33333
```

> hist(Aerococcaceae $residuals) ### plots a histogram of the residuals

> shapiro.test(Aerococcaceae $residuals) ### test for normality >0.05 = normal

Shapiro-Wilk normality test

data: Aerococcaceae$residuals

W = 0.94422, p-value = 0.4751

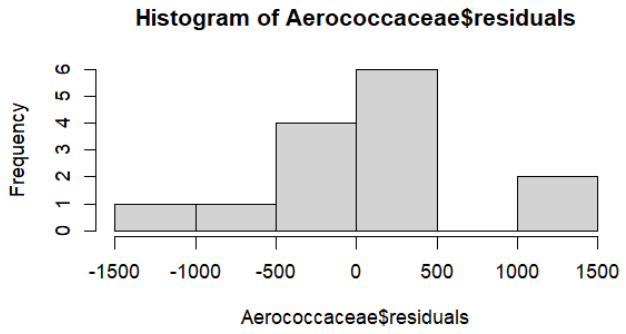

Figure A26 A histogram of the ANOVA residuals of Aerococcaceae between environmental samples on day 0

CORYNEBACTERIACEAE

```
> summary(Corynebacteriaceae)
             Df    Sum Sq  Mean Sq F value Pr(>F)
Sample.Type  4 111463103 27865776   5.574 0.0154 *
Residuals    9  44995071  4999452
---
Signif. codes:  0 ‘***’ 0.001 ‘**’ 0.01 ‘*’ 0.05 ‘.’ 0.1 ‘ ’ 1
> Tukey_Corynebacteriaceae <- TukeyHSD(Corynebacteriaceae)
> print (Tukey_Corynebacteriaceae)
  Tukey multiple comparisons of means
    95% family-wise confidence level

Fit: aov(formula = Corynebacteriaceae ~ Sample.Type, data = day0taxa)

$Sample.Type
                diff         lwr        upr     p adj
Belly-Anus   6937.3333     73.87456 13800.79210 0.0474219
Liver-Anus   -176.6667  -7040.12544  6686.79210 0.9999845
Lung-Anus     732.3333  -6131.12544  7595.79210 0.9957875
Mouth-Anus   -147.6667  -7011.12544  6715.79210 0.9999924
Liver-Belly -7114.0000 -13252.86415  -975.13585 0.0230183
Lung-Belly  -6205.0000 -12343.86415   -66.13585 0.0474196
Mouth-Belly -7085.0000 -13223.86415  -946.13585 0.0235497
Lung-Liver    909.0000  -5229.86415  7047.86415 0.9855351
Mouth-Liver    29.0000  -6109.86415  6167.86415 1.0000000
Mouth-Lung   -880.0000  -7018.86415  5258.86415 0.9871674
```

NORMALITY TEST FOR RESIDUAL

```
> Corynebacteriaceae$residuals                    ### Shows you the residuals for each sample
        1         2         3         4         5         6
 247.66667  486.00000 3830.66667  -77.33333 -170.33333 1259.66667
        7         8         9        10        11        12
-584.33333 -486.00000 -610.33333  183.66667 1194.66667 -268.33333
       13        14
  84.66667 -5090.33333
> hist(Corynebacteriaceae$residuals)              ### plots a histogram of the residuals
> shapiro.test(Corynebacteriaceae$residuals)    ### test for normality >0.05 =  normal

        Shapiro-Wilk normality test

data:  Corynebacteriaceae$residuals
W = 0.80286, p-value = 0.005415
```

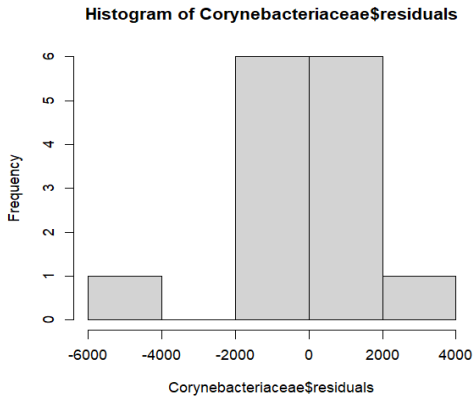

Figure A27 A histogram of the ANOVA residuals of Corynebacteriaceae between environmental samples on day 0

MORAXELLACEAE

```
summary(Moraxellaceae)
             Df    Sum Sq  Mean Sq F value  Pr(>F)
Sample.Type  4 336044781 84011195   7.375 0.00642 **
Residuals    9 102527515 11391946
```

Signif. codes: 0 ‘***’ 0.001 ‘**’ 0.01 ‘*’ 0.05 ‘.’ 0.1 ‘ ’ 1

> Tukey_Moraxellaceae <- TukeyHSD(Moraxellaceae)

> print (Tukey_Moraxellaceae)

  Tukey multiple comparisons of means

    95% family-wise confidence level

Fit: aov(formula = Moraxellaceae ~ Sample.Type, data = day0taxa)

$Sample.Type

                diff   lwr   upr   p adj

Belly-Anus   4900.000 -5460.501 15260.501 0.5371177

Liver-Anus   88.000 -10272.501 10448.501 0.9999998

Lung-Anus   1121.667 -9238.835 11482.168 0.9955462

Mouth-Anus 12772.667   2412.165 23133.168 0.0161450

Liver-Belly -4812.000 -14078.714 4454.714 0.4553042

Lung-Belly -3778.333 -13045.048 5488.381 0.6586650

Mouth-Belly 7872.667 -1394.048 17139.381 0.1046151

Lung-Liver   1033.667 -8233.048 10300.381 0.9950077

Mouth-Liver 12684.667   3417.952 21951.381 0.0085436

Mouth-Lung 11651.000   2384.286 20917.714 0.0143754

NORMALITY TEST FOR RESIDUAL

> Moraxellaceae$residuals   ### Shows you the residuals for each sample

       1   2   3   4   5   6   7

-1645.6667 1077.0000   44.0000 -5950.6667 7596.3333   892.0000 -268.6667

       8   9   10   11   12   13   14

-1077.0000 -320.6667   848.0000   589.3333 -1169.0000   321.0000 -936.0000

> hist(Moraxellaceae$residuals)   ### plots a histogram of the residuals

> shapiro.test(Moraxellaceae$residuals)   ### test for normality >0.05 = normal

Shapiro-Wilk normality test

data: Moraxellaceae$residuals

W = 0.81004, p-value = 0.00666

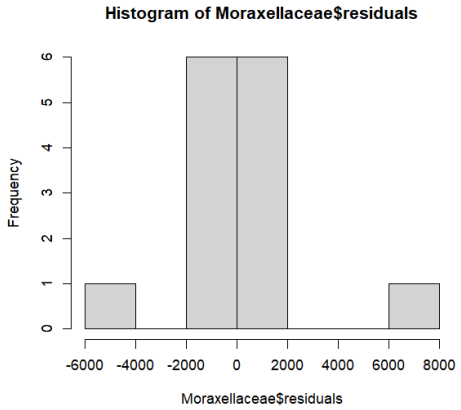

Figure A28 A histogram of the ANOVA residuals of Moraxellaceae between environmental samples on day 0

RUMINOCOCCACEAE

summary(Ruminococcaceae)

	Df	Sum Sq	Mean Sq	F value	Pr(>F)	
Sample.Type	4	159461177	39865294	18.48	0.000229	***
Residuals	9	19416664	2157407			

Signif. codes: 0 ‘***’ 0.001 ‘**’ 0.01 ‘*’ 0.05 ‘.’ 0.1 ‘ ’ 1

> Tukey_Ruminococcaceae <- TukeyHSD(Ruminococcaceae)

> print (Tukey_Ruminococcaceae)

 Tukey multiple comparisons of means

  95% family-wise confidence level

Fit: aov(formula = Ruminococcaceae ~ Sample.Type, data = day0taxa)

$Sample.Type

```
                diff       lwr       upr     p adj
Belly-Anus  -8328.50000 -12837.164 -3819.836 0.0011057
Liver-Anus  -9912.16667 -14420.831 -5403.503 0.0002984
Lung-Anus   -9830.83333 -14339.497 -5322.169 0.0003180
Mouth-Anus  -9856.50000 -14365.164 -5347.836 0.0003117
Liver-Belly -1583.66667  -5616.338  2449.005 0.6866913
Lung-Belly  -1502.33333  -5535.005  2530.338 0.7237539
Mouth-Belly -1528.00000  -5560.672  2504.672 0.7121500
Lung-Liver     81.33333  -3951.338  4114.005 0.9999942
Mouth-Liver    55.66667  -3977.005  4088.338 0.9999987
Mouth-Lung    -25.66667  -4058.338  4007.005 0.9999999
```

NORMALITY TEST FOR RESIDUAL

```
> Ruminococcaceae$residuals                    ### Shows you the residuals for each sample
        1         2         3         4         5         6
  99.00000 -2692.50000   914.00000   258.00000  -357.00000   693.00000
        7         8         9        10        11        12
 -25.66667  2692.50000  -169.66667   694.66667   195.33333  -457.33333
       13        14
-237.33333 -1607.00000
> hist(Ruminococcaceae$residuals)              ### plots a histogram of the residuals
> shapiro.test(Ruminococcaceae$residuals)    ### test for normality >0.05 =  normal

            Shapiro-Wilk normality test

data:  Ruminococcaceae$residuals
W = 0.92046, p-value = 0.2233
```

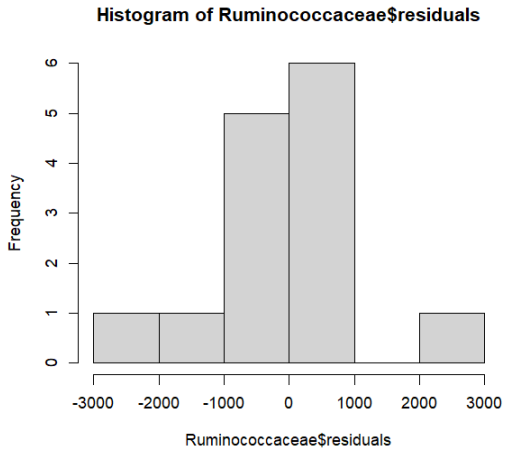

Figure A29 A histogram of the ANOVA residuals of Ruminococcaceae between environmental samples on day 0

LACHNOSPIRACEAE

> summary(Lachnospiraceae)

	Df	Sum Sq	Mean Sq	F value	Pr(>F)	
Sample.Type	4	114507606	28626901	6.924	0.00788	**
Residuals	9	37208799	4134311			

Signif. codes: 0 '***' 0.001 '**' 0.01 '*' 0.05 '.' 0.1 ' ' 1

> Tukey_Lachnospiraceae <- TukeyHSD(Lachnospiraceae)

> print (Tukey_Lachnospiraceae)

Tukey multiple comparisons of means

95% family-wise confidence level

Fit: aov(formula = Lachnospiraceae ~ Sample.Type, data = day0taxa)

$Sample.Type

	diff	lwr	upr	p adj
Belly-Anus	-7321.6667	-13563.086	-1080.247	0.0214914
Liver-Anus	-8647.6667	-14889.086	-2406.247	0.0079143

Lung-Anus -8479.3333 -14720.753 -2237.914 0.0089577

Mouth-Anus -7738.3333 -13979.753 -1496.914 0.0156158

Liver-Belly -1326.0000 -6908.495 4256.495 0.9245805

Lung-Belly -1157.6667 -6740.162 4424.829 0.9520249

Mouth-Belly -416.6667 -5999.162 5165.829 0.9989467

Lung-Liver 168.3333 -5414.162 5750.829 0.9999709

Mouth-Liver 909.3333 -4673.162 6491.829 0.9795057

Mouth-Lung 741.0000 -4841.495 6323.495 0.9903630

NORMALITY TEST FOR RESIDUAL

```
> Lachnospiraceae$residuals                    ### Shows you the residuals for each sample
       1        2        3        4        5        6
 636.33333 -4118.00000   716.66667   264.33333  -900.66667   372.66667
       7        8        9       10       11       12
-206.66667  4118.00000    21.33333   199.66667   185.33333  -223.33333
      13       14
  23.66667 -1089.33333
> hist(Lachnospiraceae$residuals)              ### plots a histogram of the residuals
> shapiro.test(Lachnospiraceae$residuals)    ### test for normality >0.05 =  normal

        Shapiro-Wilk normality test

data:  Lachnospiraceae$residuals
W = 0.80822, p-value = 0.006318
```

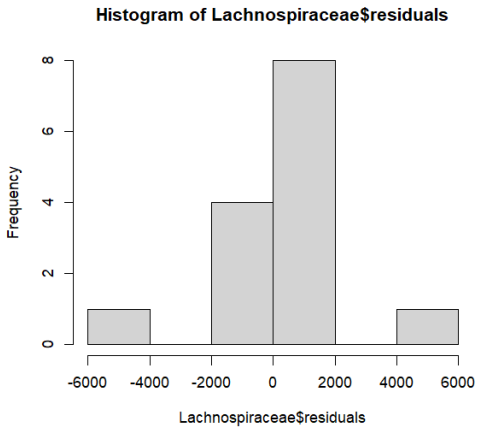

Figure A30 A histogram of the ANOVA residuals of Lachnospiraceae between environmental samples on day 0

PORPHYROMONADACEAE

summary(Porphyromonadaceae)

	Df	Sum Sq	Mean Sq	F value	Pr(>F)	
Sample.Type	4	163735347	40933837	4.741	0.0247	*
Residuals	9	77713696	8634855			

Signif. codes: 0 '***' 0.001 '**' 0.01 '*' 0.05 '.' 0.1 ' ' 1

> Tukey_Porphyromonadaceae <- TukeyHSD(Porphyromonadaceae)

> print (Tukey_Porphyromonadaceae)

Tukey multiple comparisons of means

95% family-wise confidence level

Fit: aov(formula = Porphyromonadaceae ~ Sample.Type, data = day0taxa)

$Sample.Type

	diff	lwr	upr	p adj
Belly-Anus	-4165.3333	-13185.391584	4854.725	0.5576037
Liver-Anus	-5196.0000	-14216.058250	3824.058	0.3647648
Lung-Anus	-4513.3333	-13533.391584	4506.725	0.4879814

Mouth-Anus 3558.6667 -5461.391584 12578.725 0.6833121

Liver-Belly -1030.6667 -9098.452030 7037.119 0.9916525

Lung-Belly -348.0000 -8415.785364 7719.785 0.9998792

Mouth-Belly 7724.0000 -343.785364 15791.785 0.0616666

Lung-Liver 682.6667 -7385.118697 8750.452 0.9982807

Mouth-Liver 8754.6667 686.881303 16822.452 0.0329308

Mouth-Lung 8072.0000 4.214636 16139.785 0.0498717

NORMALITY TEST FOR RESIDUAL

> Porphyromonadaceae$residuals ### Shows you the residuals for each sample

```
       1        2        3        4        5        6        7
-5135.6667 -4124.0000  -225.6667  3605.3333  1530.3333  -121.6667  -850.6667
       8        9       10       11       12       13       14
 4124.0000   988.3333   137.0000  -137.6667  -226.0000    89.0000   347.3333
```

> hist(Porphyromonadaceae$residuals) ### plots a histogram of the residuals

> shapiro.test(Porphyromonadaceae$residuals) ### test for normality >0.05 = normal

Shapiro-Wilk normality test

data: Porphyromonadaceae$residuals

W = 0.89238, p-value = 0.08749

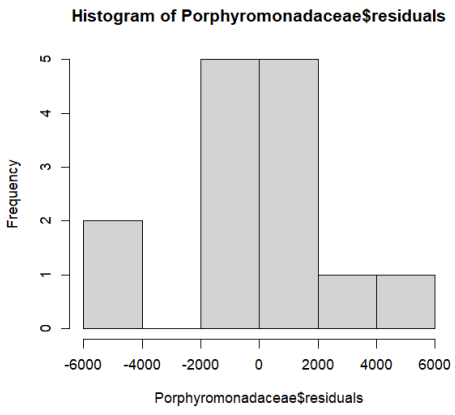

Figure A31 A histogram of the ANOVA residuals of Porphyromonadaceae between environmental samples on day 0

MICROCOCCACEAE

```
> summary(Micrococcaceae)
            Df  Sum Sq Mean Sq F value Pr(>F)
Sample.Type  4 2794402  698601   5.378 0.0172 *
Residuals    9 1169023  129891
---
Signif. codes:  0 ‘***’ 0.001 ‘**’ 0.01 ‘*’ 0.05 ‘.’ 0.1 ‘ ’ 1
> Tukey_Micrococcaceae  <- TukeyHSD(Micrococcaceae)
> print (Tukey_Micrococcaceae)
  Tukey multiple comparisons of means
    95% family-wise confidence level

Fit: aov(formula = Micrococcaceae ~ Sample.Type, data = day0taxa)

$Sample.Type
                diff        lwr       upr     p adj
Belly-Anus   1151.83333    45.53535 2258.13131 0.0408439
Liver-Anus    -26.16667 -1132.46465 1080.13131 0.9999890
Lung-Anus     250.16667  -856.13131 1356.46465 0.9358173
Mouth-Anus    104.16667 -1002.13131 1210.46465 0.9973972
Liver-Belly -1178.00000 -2167.50299 -188.49701 0.0197646
Lung-Belly   -901.66667 -1891.16966   87.83633 0.0773773
Mouth-Belly -1047.66667 -2037.16966  -58.16367 0.0374631
Lung-Liver    276.33333  -713.16966 1265.83633 0.8747333
Mouth-Liver   130.33333  -859.16966 1119.83633 0.9906375
Mouth-Lung   -146.00000 -1135.50299  843.50299 0.9857228
```

NORMALITY TEST FOR RESIDUAL

```
> Micrococcaceae$residuals                    ### Shows you the residuals for each sample
        1         2         3         4         5         6
 82.333333   87.500000  797.666667   69.333333 -151.666667 -548.333333
```

```
        7         8         9        10        11        12
-69.666667  -87.500000 -199.666667    7.666667  269.333333  -40.333333
       13        14
 32.666667 -249.333333
> hist(Micrococcaceae$residuals)              ### plots a histogram of the residuals
> shapiro.test(Micrococcaceae$residuals)    ### test for normality >0.05 =  normal

        Shapiro-Wilk normality test

data:  Micrococcaceae$residuals
W = 0.88941, p-value = 0.07926
```

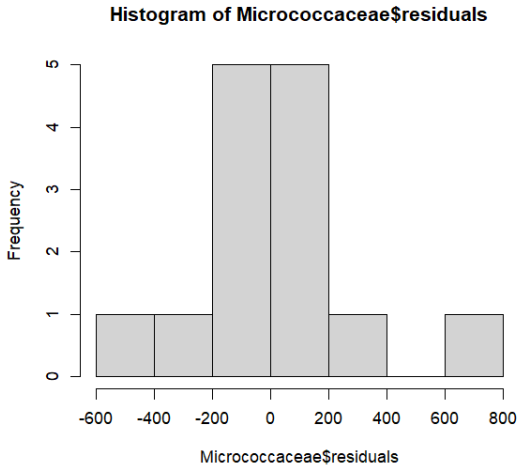

Figure A32 A histogram of the ANOVA residuals of Micrococcaceae between environmental samples on day 0

```
BIFIDOBACTERIACEAE
summary(Bifidobacteriaceae)
          Df  Sum Sq Mean Sq F value Pr(>F)
Sample.Type  4 1323850  330963    5.45 0.0165 *
Residuals    9  546532   60726
---
Signif. codes:  0 ‘***’ 0.001 ‘**’ 0.01 ‘*’ 0.05 ‘.’ 0.1 ‘ ’ 1
```

```
> Tukey_Bifidobacteriaceae <- TukeyHSD(Bifidobacteriaceae)
> print (Tukey_Bifidobacteriaceae)
  Tukey multiple comparisons of means
    95% family-wise confidence level

Fit: aov(formula = Bifidobacteriaceae ~ Sample.Type, data = day0taxa)

$Sample.Type
                diff        lwr        upr     p adj
Belly-Anus   718.00000   -38.42933 1474.429326 0.0642033
Liver-Anus   -97.33333  -853.76266  659.095993 0.9914233
Lung-Anus    -32.66667  -789.09599  723.762660 0.9998786
Mouth-Anus    50.33333  -706.09599  806.762660 0.9993289
Liver-Belly -815.33333 -1491.90429 -138.762376 0.0184288
Lung-Belly  -750.66667 -1427.23762  -74.095709 0.0292395
Mouth-Belly -667.66667 -1344.23762    8.904291 0.0533451
Lung-Liver    64.66667  -611.90429  741.237624 0.9972419
Mouth-Liver  147.66667  -528.90429  824.237624 0.9429653
Mouth-Lung    83.00000  -593.57096  759.570957 0.9928352

NORMALITY TEST FOR RESIDUAL
> Bifidobacteriaceae $residuals                    ### Shows you the residuals for each sample
        1         2         3         4         5         6
 307.666667  119.000000  262.000000 -134.333333 -173.333333  234.000000
        7         8         9        10        11        12
  17.666667 -119.000000  -50.333333   -3.666667   32.666667  -30.666667
       13        14
  34.333333 -496.000000
> hist(Bifidobacteriaceae $residuals)              ### plots a histogram of the residuals
> shapiro.test(Bifidobacteriaceae $residuals)    ### test for normality >0.05 =  normal
```

Shapiro-Wilk normality test

data: Bifidobacteriaceae$residuals

W = 0.93665, p-value = 0.3771

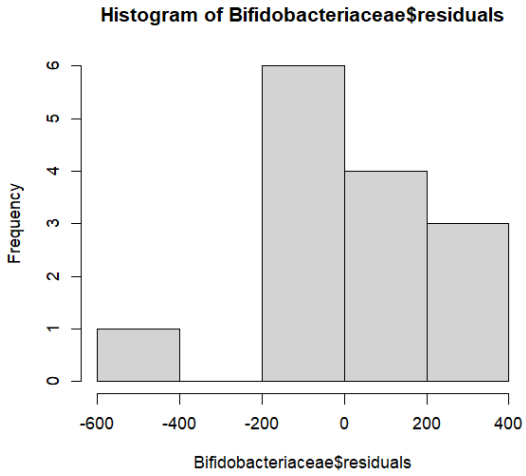

Figure A33 A histogram of the ANOVA residuals of Bifidobacteriaceae between environmental samples on day 0

TISSIERELLACEAE

summary(Tissierellaceae)

Df Sum Sq Mean Sq F value Pr(>F)

Sample.Type 4 7094107 1773527 4.24 0.0335 *

Residuals 9 3764256 418251

Signif. codes: 0 ‘***’ 0.001 ‘**’ 0.01 ‘*’ 0.05 ‘.’ 0.1 ‘ ’ 1

> Tukey_Tissierellaceae <- TukeyHSD(Tissierellaceae)

> print (Tukey_Tissierellaceae)

Tukey multiple comparisons of means

95% family-wise confidence level

Fit: aov(formula = Tissierellaceae ~ Sample.Type, data = day0taxa)

$Sample.Type

```
                diff       lwr       upr     p adj
Belly-Anus    736.66667 -1248.5145 2721.8478 0.7263972
Liver-Anus    289.00000 -1696.1811 2274.1811 0.9864137
Lung-Anus    1857.33333  -127.8478 3842.5145 0.0686449
Mouth-Anus    -54.66667 -2039.8478 1930.5145 0.9999798
Liver-Belly  -447.66667 -2223.2666 1327.9333 0.9086777
Lung-Belly   1120.66667  -654.9333 2896.2666 0.2893114
Mouth-Belly  -791.33333 -2566.9333  984.2666 0.5875207
Lung-Liver   1568.33333  -207.2666 3343.9333 0.0887459
Mouth-Liver  -343.66667 -2119.2666 1431.9333 0.9621738
Mouth-Lung  -1912.00000 -3687.6000 -136.4000 0.0342973
```

NORMALITY TEST FOR RESIDUAL

```
> Tissierellaceae$residuals                    ### Shows you the residuals for each sample
        1         2         3         4         5         6
  73.66667   110.00000  -185.66667   -44.33333   -29.33333   511.33333
        7         8         9        10        11        12
 655.66667  -110.00000 -1343.33333  -265.00000   687.66667  -376.00000
       13        14
 641.00000  -325.66667
> hist(Tissierellaceae$residuals)              ### plots a histogram of the residuals
> shapiro.test(Tissierellaceae$residuals)    ### test for normality >0.05 =  normal

        Shapiro-Wilk normality test

data:  Tissierellaceae$residuals
W = 0.89614, p-value = 0.09915
```

Figure A34 A histogram of the ANOVA residuals of Tissierellaceae between environmental samples on day 0

PREVOTELLACEAE

summary(Prevotellaceae)

	Df	Sum Sq	Mean Sq	F value	Pr(>F)	
Sample.Type	4	429146835	107286709	4.638	0.0262	*
Residuals	9	208197264	23133029			

Signif. codes: 0 '***' 0.001 '**' 0.01 '*' 0.05 '.' 0.1 ' ' 1

> Tukey_Prevotellaceae <- TukeyHSD(Prevotellaceae)

> print (Tukey_Prevotellaceae)

Tukey multiple comparisons of means

95% family-wise confidence level

Fit: aov(formula = Prevotellaceae ~ Sample.Type, data = day0taxa)

$Sample.Type

	diff	lwr	upr	p adj
Belly-Anus	-11648.83333	-26412.630	3114.964	0.1401424
Liver-Anus	-12040.50000	-26804.297	2723.297	0.1233682

Lung-Anus -12066.83333 -26830.630 2696.964 0.1223108

Mouth-Anus -624.50000 -15388.297 14139.297 0.9998882

Liver-Belly -391.66667 -13596.808 12813.475 0.9999728

Lung-Belly -418.00000 -13623.142 12787.142 0.9999647

Mouth-Belly 11024.33333 -2180.808 24229.475 0.1123657

Lung-Liver -26.33333 -13231.475 13178.808 1.0000000

Mouth-Liver 11416.00000 -1789.142 24621.142 0.0972660

Mouth-Lung 11442.33333 -1762.808 24647.475 0.0963239

NORMALITY TEST FOR RESIDUAL

> Prevotellaceae$residuals ### Shows you the residuals for each sample

1	2	3	4	5	6
2663.00000	9775.50000	977.33333	181.00000	-2844.00000	-378.66667

7	8	9	10	11	12
-203.66667	-9775.50000	-60.66667	432.00000	264.33333	-293.00000

13	14
-139.00000	-598.66667

> hist(Prevotellaceae$residuals) ### plots a histogram of the residuals

> shapiro.test(Prevotellaceae$residuals) ### test for normality >0.05 = normal

Shapiro-Wilk normality test

data: Prevotellaceae$residuals

W = 0.77779, p-value = 0.002686

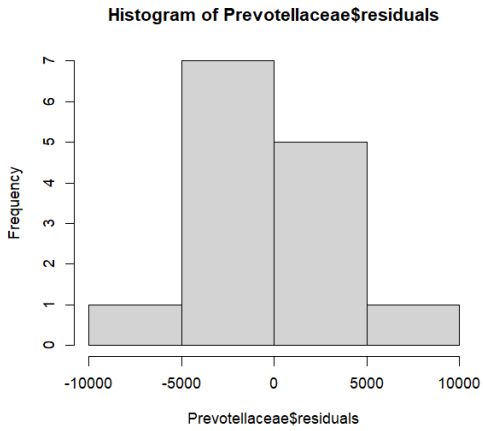

Figure A35 A histogram of the ANOVA residuals of Prevotellaceae between environmental samples on day 0

AC160630_f

summary(AC160630_f)

	Df	Sum Sq	Mean Sq	F value	Pr(>F)	
Sample.Type	4	7059048	1764762	16.89	0.000326	***
Residuals	9	940437	104493			

Signif. codes: 0 '***' 0.001 '**' 0.01 '*' 0.05 '.' 0.1 ' ' 1

> Tukey_AC160630_f <- TukeyHSD(AC160630_f)

> print (Tukey_AC160630_f)

Tukey multiple comparisons of means

95% family-wise confidence level

Fit: aov(formula = AC160630_f ~ Sample.Type, data = day0taxa)

$Sample.Type

	diff	lwr	upr	p adj
Belly-Anus	-2021.83333	-3014.0933	-1029.5734	0.0005335
Liver-Anus	-1955.50000	-2947.7599	-963.2401	0.0006855
Lung-Anus	-2042.50000	-3034.7599	-1050.2401	0.0004940
Mouth-Anus	-2082.50000	-3074.7599	-1090.2401	0.0004263

```
Liver-Belly    66.33333  -821.1709   953.8376 0.9989410
Lung-Belly    -20.66667  -908.1709   866.8376 0.9999896
Mouth-Belly   -60.66667  -948.1709   826.8376 0.9992539
Lung-Liver    -87.00000  -974.5043   800.5043 0.9969591
Mouth-Liver  -127.00000 -1014.5043   760.5043 0.9872505
Mouth-Lung    -40.00000  -927.5043   847.5043 0.9998562
```

NORMALITY TEST FOR RESIDUAL

```
> AC160630_f$residuals                    ### Shows you the residuals for each sample
       1        2        3        4        5        6        7
 32.00000 -643.50000  126.33333   15.00000  -47.00000  -34.66667  -18.00000
       8        9       10       11       12       13       14
 643.50000   16.00000  221.00000    2.00000 -179.00000  -42.00000  -91.66667
> hist(AC160630_f$residuals)              ### plots a histogram of the residuals
> shapiro.test(AC160630_f$residuals)    ### test for normality >0.05 =  normal

            Shapiro-Wilk normality test

data:  AC160630_f$residuals
W = 0.83769, p-value = 0.01518
```

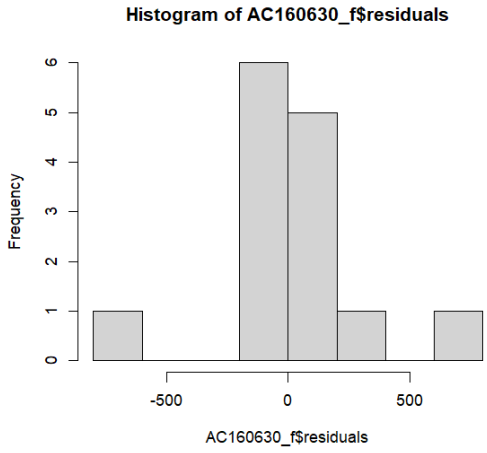

Figure A36 A histogram of the ANOVA residuals of AC160630_f between environmental samples on day 0

ENVIRONMENTAL SAMPLES (FAMILIES)

LACTOBACILLACEAE

summary(Lactobacillaceae)

```
            Df Sum Sq Mean Sq F value Pr(>F)
Sample.Type  3 612022  204007   5.911 0.0424 *
Residuals    5 172565   34513
---
Signif. codes:  0 ‘***’ 0.001 ‘**’ 0.01 ‘*’ 0.05 ‘.’ 0.1 ‘ ’ 1
```

> Tukey_Lactobacillaceae <- TukeyHSD(Lactobacillaceae)

> print (Tukey_Lactobacillaceae)

```
  Tukey multiple comparisons of means
    95% family-wise confidence level

Fit: aov(formula = Lactobacillaceae ~ Sample.Type, data = day0taxa)

$Sample.Type
                          diff       lwr      upr     p adj
Freshwater-Brackishwater   51.50000  -634.0004 737.00035 0.9916523
Seawater-Brackishwater   -445.00000 -1130.5004 240.50035 0.1955344
Soil-Brackishwater       -527.33333 -1153.1067  98.44001 0.0904772
Seawater-Freshwater      -496.50000 -1182.0004 189.00035 0.1444865
Soil-Freshwater          -578.83333 -1204.6067  46.94001 0.0660309
Soil-Seawater             -82.33333  -708.1067 543.44001 0.9590581
```

> Lactobacillaceae$residuals ### Shows you the residuals for each sample

```
        1         2         3         4         5         6
 -64.000000   24.333333 -254.500000  -20.666667   -3.666667 -130.000000
        7         8         9
 254.500000  130.000000   64.000000
```

> hist(Lactobacillaceae$residuals) ### plots a histogram of the residuals

> shapiro.test(Lactobacillaceae$residuals) ### test for normality >0.05 = normal

Shapiro-Wilk normality test

data: Lactobacillaceae$residuals

W = 0.99125, p-value = 0.9976

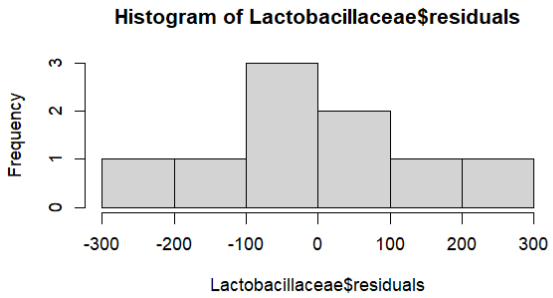

Figure A37 A histogram of the ANOVA residuals of Lactobacillaceae between environmental samples on day 0

AEROCOCCACEAE

summary(Aerococcaceae)

Df Sum Sq Mean Sq F value Pr(>F)

Sample.Type 3 7493 2497.5 5.777 0.0443 *

Residuals 5 2162 432.3

Signif. codes: 0 ‘***’ 0.001 ‘**’ 0.01 ‘*’ 0.05 ‘.’ 0.1 ‘ ’ 1

> Tukey_Aerococcaceae <- TukeyHSD(Aerococcaceae)

> print (Tukey_Aerococcaceae)

Tukey multiple comparisons of means

95% family-wise confidence level

Fit: aov(formula = Aerococcaceae ~ Sample.Type, data = day0taxa)

$Sample.Type

```
                  diff       lwr       upr     p adj
Fresh-Brackish -72.5000000 -149.22298  4.222982 0.0612655
Sea-Brackish   -58.0000000 -134.72298 18.722982 0.1273027
Soil-Brackish  -71.8333333 -141.87151 -1.795153 0.0455621
Sea-Fresh       14.5000000  -62.22298 91.222982 0.8940004
Soil-Fresh       0.6666667  -69.37151 70.704847 0.9999822
Soil-Sea       -13.8333333  -83.87151 56.204847 0.8817849
```

STREPTOCOCCACEAE

```
summary(Streptococcaceae)
            Df Sum Sq Mean Sq F value Pr(>F)
Sample.Type  3  56006   18669   6.609 0.0343 *
Residuals    5  14123    2825
---
Signif. codes:  0 ‘***’ 0.001 ‘**’ 0.01 ‘*’ 0.05 ‘.’ 0.1 ‘ ’ 1
> Tukey_Streptococcaceae <- TukeyHSD(Streptococcaceae)
> print (Tukey_Streptococcaceae)
  Tukey multiple comparisons of means
    95% family-wise confidence level

Fit: aov(formula = Streptococcaceae ~ Sample.Type, data = day0taxa)

$Sample.Type
                  diff       lwr       upr     p adj
Fresh-Brackish -128.00000 -324.10536  68.105362 0.1927530
Sea-Brackish    -10.00000 -206.10536 186.105362 0.9973251
Soil-Brackish  -179.66667 -358.68555  -0.647783 0.0493450
Sea-Fresh       118.00000  -78.10536 314.105362 0.2367449
Soil-Fresh      -51.66667 -230.68555 127.352217 0.7232825
Soil-Sea       -169.66667 -348.68555   9.352217 0.0606284
```

NORMALITY TEST FOR RESIDUAL

```
> Streptococcaceae$residuals                    ### Shows you the residuals for each sample
       1        2        3        4        5        6
-73.0000000  -0.3333333  24.0000000  -0.3333333   0.6666667  34.0000000
       7        8        9
-24.0000000 -34.0000000  73.0000000
> hist(Streptococcaceae$residuals)              ### plots a histogram of the residuals
> shapiro.test(Streptococcaceae$residuals)    ### test for normality >0.05 =  normal

            Shapiro-Wilk normality test

data:  Streptococcaceae$residuals
W = 0.97931, p-value = 0.9606
```

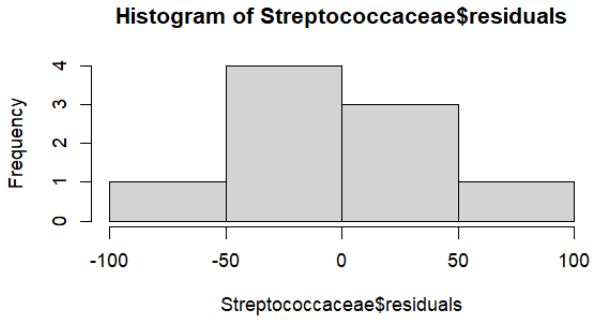

Figure A38 A histogram of the ANOVA residuals of Streptococcaceae between environmental samples on day 0

RUMINOCOCCACEAE

```
plot(Ruminococcaceae~Sample.Type,data=day0taxa)          ###  generates a boxplot
> Ruminococcaceae <- aov(Ruminococcaceae~Sample.Type,data=day0taxa)
> summary(Ruminococcaceae)
            Df Sum Sq Mean Sq F value  Pr(>F)
Sample.Type  3  17262    5754   16.17 0.00525 **
Residuals    5   1779     356
---
```

```
Signif. codes:  0 ‘***’ 0.001 ‘**’ 0.01 ‘*’ 0.05 ‘.’ 0.1 ‘ ’ 1
> Tukey_Ruminococcaceae <- TukeyHSD(Ruminococcaceae)
> print (Tukey_Ruminococcaceae)
  Tukey multiple comparisons of means
    95% family-wise confidence level

Fit: aov(formula = Ruminococcaceae ~ Sample.Type, data = day0taxa)

$Sample.Type
                 diff       lwr       upr     p adj
Fresh-Brackish -58.50000 -128.1048  11.10484 0.0912654
Sea-Brackish   -91.00000 -160.6048 -21.39516 0.0176100
Soil-Brackish   16.33333  -47.2069  79.87357 0.7824914
Sea-Fresh      -32.50000 -102.1048  37.10484 0.4017965
Soil-Fresh      74.83333   11.2931 138.37357 0.0268383
Soil-Sea       107.33333   43.7931 170.87357 0.0058757

 NORMALITY TEST FOR RESIDUAL
> Ruminococcaceae$residuals                    ### Shows you the residuals for each sample
         1          2          3          4          5
-1.694940e-14  8.666667e+00 -3.500000e+00  9.666667e+00 -1.833333e+01
         6          7          8          9
 2.500000e+01  3.500000e+00 -2.500000e+01  1.463644e-14
> hist(Ruminococcaceae$residuals)              ### plots a histogram of the residuals
> shapiro.test(Ruminococcaceae$residuals)    ### test for normality >0.05 =  normal

            Shapiro-Wilk normality test

data:  Ruminococcaceae$residuals
W = 0.95671, p-value = 0.7633
```

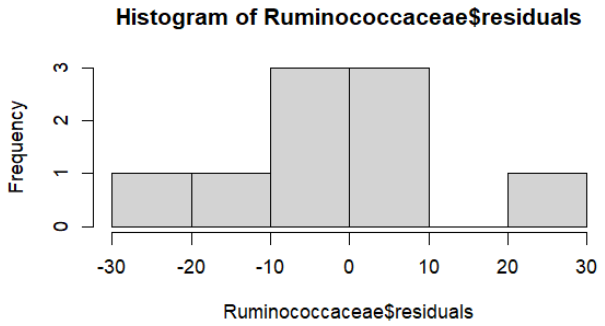

Figure A39 A histogram of the ANOVA residuals of Ruminococcaceae between environmental samples on day 0

LACHNOSPIRACEAE

> summary(Lachnospiraceae)

Df Sum Sq Mean Sq F value Pr(>F)

Sample.Type 3 26132 8711 9.624 0.0161 *

Residuals 5 4526 905

Signif. codes: 0 '***' 0.001 '**' 0.01 '*' 0.05 '.' 0.1 ' ' 1

> Tukey_Lachnospiraceae <- TukeyHSD(Lachnospiraceae)

> print (Tukey_Lachnospiraceae)

Tukey multiple comparisons of means

95% family-wise confidence level

Fit: aov(formula = Lachnospiraceae ~ Sample.Type, data = day0taxa)

$Sample.Type

	diff	lwr	upr	p adj
Fresh-Brackish	-159.50000	-270.51263	-48.48737	0.0118673
Sea-Brackish	-88.00000	-199.01263	23.01263	0.1100443
Soil-Brackish	-99.83333	-201.17354	1.50687	0.0527960
Sea-Fresh	71.50000	-39.51263	182.51263	0.1995929
Soil-Fresh	59.66667	-41.67354	161.00687	0.2493757
Soil-Sea	-11.83333	-113.17354	89.50687	0.9705621

NORMALITY TEST FOR RESIDUAL

```
> Lachnospiraceae$residuals                    ### Shows you the residuals for each sample
      1        2        3        4        5        6        7
-33.500000 -13.666667 -22.000000  -7.666667  21.333333  17.500000  22.000000
      8        9
-17.500000  33.500000
> hist(Lachnospiraceae$residuals)              ### plots a histogram of the residuals
> shapiro.test(Lachnospiraceae$residuals)    ### test for normality >0.05 =  normal

        Shapiro-Wilk normality test

data:  Lachnospiraceae$residuals
W = 0.91551, p-value = 0.3564
```

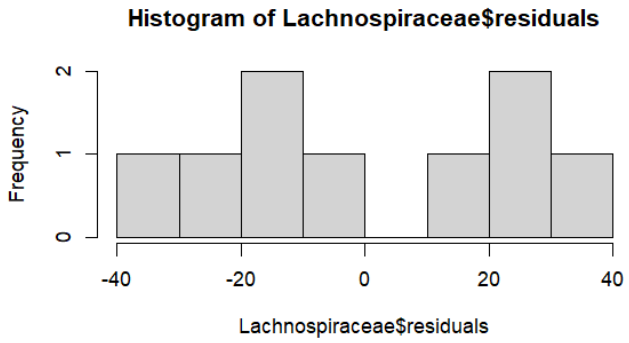

Figure A40 A histogram of the ANOVA residuals of Lachnospiraceae between environmental samples on day 0

BIFIDOBACTERIACEAE

```
> summary(Bifidobacteriaceae)
             Df Sum Sq Mean Sq F value Pr(>F)
Sample.Type  3 1419.1   473.0   8.679   0.02 *
Residuals    5  272.5    54.5
---
Signif. codes:  0 ‘***’ 0.001 ‘**’ 0.01 ‘*’ 0.05 ‘.’ 0.1 ‘ ’ 1
> Tukey_Bifidobacteriaceae <- TukeyHSD(Bifidobacteriaceae)
> print (Tukey_Bifidobacteriaceae)
```

```
  Tukey multiple comparisons of means
    95% family-wise confidence level

Fit: aov(formula = Bifidobacteriaceae ~ Sample.Type, data = day0taxa)

$Sample.Type
                    diff       lwr      upr     p adj
Fresh-Brackish  2.350000e+01  -3.740456 50.740456 0.0837366
Sea-Brackish   -8.000000e+00 -35.240456 19.240456 0.7135513
Soil-Brackish  -8.000000e+00 -32.867020 16.867020 0.6593289
Sea-Fresh      -3.150000e+01 -58.740456 -4.259544 0.0288428
Soil-Fresh     -3.150000e+01 -56.367020 -6.632980 0.0200391
Soil-Sea       -2.072416e-15 -24.867020 24.867020 1.0000000

NORMALITY TEST FOR RESIDUAL
Bifidobacteriaceae$residuals                    ### Shows you the residuals for each sample
         1           2           3           4           5
-2.450769e-15 -2.285692e-15 -8.500000e+00  1.410543e-15  7.827560e-17
         6           7           8           9
 8.000000e+00  8.500000e+00 -8.000000e+00  7.827560e-17
> hist(Bifidobacteriaceae$residuals)              ### plots a histogram of the residuals
> shapiro.test(Bifidobacteriaceae$residuals)    ### test for normality >0.05 =  normal

            Shapiro-Wilk normality test

data:  Bifidobacteriaceae$residuals
W = 0.8474, p-value = 0.06975
```

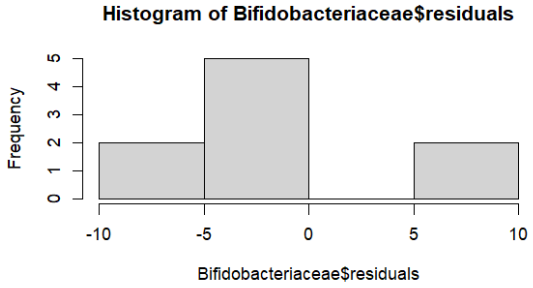

Figure A41 A histogram of the ANOVA residuals of Bifidobacteriaceae between environmental samples on day 0

ALCALIGENACEAE

> summary(Alcaligenaceae)

Df Sum Sq Mean Sq F value Pr(>F)

Sample.Type 3 1625418 541806 16.14 0.00527 **

Residuals 5 167842 33568

Signif. codes: 0 '***' 0.001 '**' 0.01 '*' 0.05 '.' 0.1 ' ' 1

> Tukey_Alcaligenaceae <- TukeyHSD(Alcaligenaceae)

> print (Tukey_Alcaligenaceae)

Tukey multiple comparisons of means

95% family-wise confidence level

Fit: aov(formula = Alcaligenaceae ~ Sample.Type, data = day0taxa)

$Sample.Type

	diff	lwr	upr	p adj
Fresh-Brackish	160.5000	-515.5534	836.5534	0.8175248
Sea-Brackish	-126.0000	-802.0534	550.0534	0.8976295
Soil-Brackish	-866.8333	-1483.9828	-249.6838	0.0130616
Sea-Fresh	-286.5000	-962.5534	389.5534	0.4709827
Soil-Fresh	-1027.3333	-1644.4828	-410.1838	0.0062693
Soil-Sea	-740.8333	-1357.9828	-123.6838	0.024882

NORMALITY TEST FOR RESIDUAL

> Alcaligenaceae$residuals ### Shows you the residuals for each sample

```
        1         2         3         4         5         6
-166.500000    4.333333 -128.000000   -2.666667   -1.666667  199.500000
        7         8         9
 128.000000 -199.500000  166.500000
```

> hist(Alcaligenaceae$residuals) ### plots a histogram of the residuals

> shapiro.test(Alcaligenaceae$residuals) ### test for normality >0.05 = normal

```
        Shapiro-Wilk normality test

data:  Alcaligenaceae$residuals
W = 0.92611, p-value = 0.4452
```

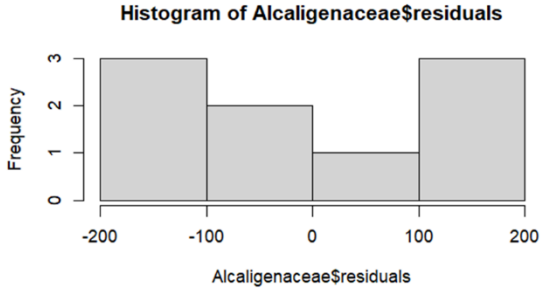

Figure A42 A histogram of the ANOVA residuals of Alcaligenaceae between environmental samples on day 0

BRADYRHIZOBIACEAE

> summary(Bradyrhizobiaceae)

```
             Df    Sum Sq  Mean Sq F value   Pr(>F)
Sample.Type  3 107838120 35946040   975.9 2.44e-07 ***
Residuals    5    184166    36833
---
Signif. codes:  0 ‘***’ 0.001 ‘**’ 0.01 ‘*’ 0.05 ‘.’ 0.1 ‘ ’ 1
```

> Tukey_Bradyrhizobiaceae <- TukeyHSD(Bradyrhizobiaceae)

> print (Tukey_Bradyrhizobiaceae)

```
  Tukey multiple comparisons of means
    95% family-wise confidence level

Fit: aov(formula = Bradyrhizobiaceae ~ Sample.Type, data = day0taxa)

$Sample.Type
                diff       lwr       upr     p adj
Fresh-Brackish   66.000 -642.1666  774.1666 0.9844432
Sea-Brackish    -23.500 -731.6666  684.6666 0.9992538
Soil-Brackish  7356.833 6710.3686 8003.2980 0.0000010
Sea-Fresh       -89.500 -797.6666  618.6666 0.9633402
Soil-Fresh     7290.833 6644.3686 7937.2980 0.0000010
Soil-Sea       7380.333 6733.8686 8026.7980 0.0000010

NORMALITY TEST FOR RESIDUAL
> Bradyrhizobiaceae$residuals                    ### Shows you the residuals for each sample
       1        2        3        4        5        6        7
 40.00000 -153.33333   80.50000   43.66667  109.66667 -255.50000  -80.50000
       8        9
 255.50000  -40.00000
> hist(Bradyrhizobiaceae$residuals)              ### plots a histogram of the residuals
> shapiro.test(Bradyrhizobiaceae$residuals)    ### test for normality >0.05 =  normal

            Shapiro-Wilk normality test

data:  Bradyrhizobiaceae$residuals
W = 0.98519, p-value = 0.9856
```

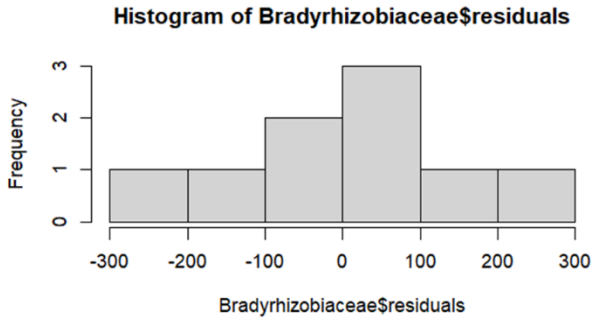

Figure A43 A histogram of the ANOVA residuals of Bradyrhizobiaceae between environmental samples on day

CHTHONIOBACTERACEAE

```
> summary(Chthoniobacteraceae)
            Df   Sum Sq  Mean Sq F value   Pr(>F)
Sample.Type  3 42289485 14096495   56.08 0.000285 ***
Residuals    5  1256913   251383
---
Signif. codes:  0 ‘***’ 0.001 ‘**’ 0.01 ‘*’ 0.05 ‘.’ 0.1 ‘ ’ 1
> Tukey_Chthoniobacteraceae  <- TukeyHSD(Chthoniobacteraceae)
> print (Tukey_Chthoniobacteraceae)
  Tukey multiple comparisons of means
    95% family-wise confidence level

Fit: aov(formula = Chthoniobacteraceae ~ Sample.Type, data = day0taxa)

$Sample.Type
                    diff       lwr      upr     p adj
Fresh-Brackish -254.500 -2104.551 1595.551 0.9537736
Sea-Brackish   -306.000 -2156.051 1544.051 0.9245350
Soil-Brackish  4405.667  2716.809 6094.525 0.0007930
Sea-Fresh       -51.500 -1901.551 1798.551 0.9995583
Soil-Fresh     4660.167  2971.309 6349.025 0.0006069
```

Soil-Sea 4711.667 3022.809 6400.525 0.0005759

NORMALITY TEST FOR RESIDUAL

Chthoniobacteraceae$residuals ### Shows you the residuals for each sample

1 2 3 4 5 6 7

-58.0000 487.3333 174.5000 337.3333 -824.6667 -281.0000 -174.5000

8 9

281.0000 58.0000

> hist(Chthoniobacteraceae$residuals) ### plots a histogram of the residuals

> shapiro.test(Chthoniobacteraceae$residuals) ### test for normality >0.05 = normal

Shapiro-Wilk normality test

data: Chthoniobacteraceae$residuals

W = 0.93698, p-value = 0.5505

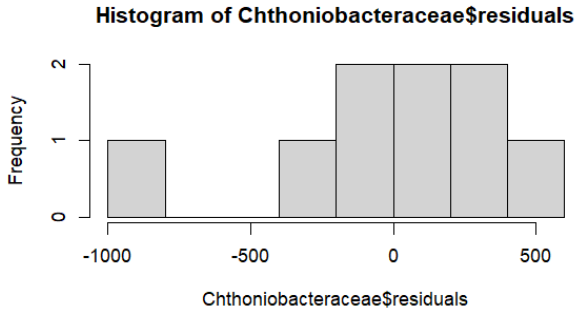

Figure A44 A histogram of the ANOVA residuals of Chthoniobacteraceae between environmental samples on day

BACILLACEAE

> summary(Bacillaceae)

Df Sum Sq Mean Sq F value Pr(>F)

Sample.Type 3 58609179 19536393 7.66 0.0257 *

Residuals 5 12751558 2550312

Signif. codes: 0 '***' 0.001 '**' 0.01 '*' 0.05 '.' 0.1 ' ' 1

> Tukey_Bacillaceae <- TukeyHSD(Bacillaceae)

```
> print (Tukey_Bacillaceae)
  Tukey multiple comparisons of means
    95% family-wise confidence level

Fit: aov(formula = Bacillaceae ~ Sample.Type, data = day0taxa)

$Sample.Type
                 diff       lwr       upr     p adj
Fresh-Brackish  2278.000 -3614.6784  8170.678 0.5364259
Sea-Brackish    1138.000 -4754.6784  7030.678 0.8881541
Soil-Brackish   6306.833   927.5785 11686.088 0.0273199
Sea-Fresh      -1140.000 -7032.6784  4752.678 0.8876673
Soil-Fresh      4028.833 -1350.4215  9408.088 0.1309102
Soil-Sea        5168.833  -210.4215 10548.088 0.0577389

NORMALITY TEST FOR RESIDUAL
> Bacillaceae$residuals                    ### Shows you the residuals for each sample
       1        2        3        4        5        6        7
 -177.5000  1270.6667 -1727.5000   807.6667 -2078.3333  -258.5000  1727.5000
       8        9
  258.5000   177.5000
> hist(Bacillaceae$residuals)              ### plots a histogram of the residuals
> shapiro.test(Bacillaceae$residuals)    ### test for normality >0.05 =  normal

            Shapiro-Wilk normality test

data:  Bacillaceae$residuals
W = 0.94175, p-value = 0.6004
```

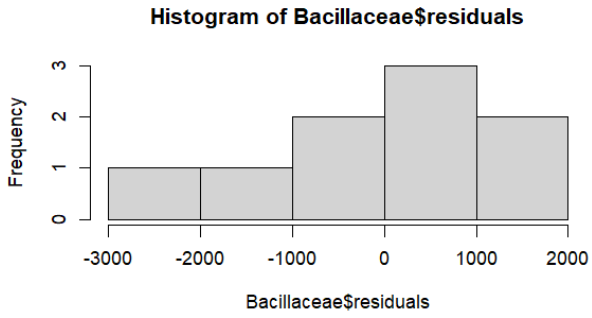

Figure A45 A histogram of the ANOVA residuals of Bacillaceae between environmental samples on day

APPENDIX 7 – R OUTPUT RESULTS FOR CHAPTER 6

BELLY

BACTEROIDETES

Analysis of Variance Table

Response: Bacteroidetes

	Df	Sum Sq	Mean Sq	F value	Pr(>F)
Dayf	4	1269540246	317385061	4.499	0.02853 *
Residuals	9	634914493	70546055		

Signif. codes: 0 '***' 0.001 '**' 0.01 '*' 0.05 '.' 0.1 ' ' 1

> summary(Bacteroidetes)

Call:

lm(formula = Bacteroidetes ~ Dayf, data = bellyphyla)

Residuals:

Min	1Q	Median	3Q	Max
-10372.7	-3473.8	-982.2	1248.2	17439.3

Coefficients:

	Estimate	Std. Error	t value	Pr(>|t|)
(Intercept)	4390	4849	0.905	0.38887
Dayf2	2028	6858	0.296	0.77412
Dayf4	-1312	6858	-0.191	0.85253
Dayf7	-1840	7667	-0.240	0.81569
Dayf23	22847	6858	3.332	0.00878 **

Signif. codes: 0 '***' 0.001 '**' 0.01 '*' 0.05 '.' 0.1 ' ' 1

Residual standard error: 8399 on 9 degrees of freedom

Multiple R-squared: 0.6666, Adjusted R-squared: 0.5184

F-statistic: 4.499 on 4 and 9 DF, p-value: 0.02853

NORMALITY TEST FOR RESIDUAL

> Bacteroidetes$residuals ### Shows you the residuals for each sample

1	2	3	4	5	6
-191.3333	-1367.3333	-3979.6667	-1956.3333	1418.6667	-737.0000
7	8	9	10	11	12
-7066.6667	-10372.6667	737.0000	17439.3333	9993.3333	-1227.3333
13	14				
-6013.6667	3323.6667				

> hist(Bacteroidetes$residuals) ### plots a histogram of the residuals

> shapiro.test(Bacteroidetes$residuals)

Shapiro-Wilk normality test

data: Bacteroidetes$residuals

W = 0.9045, p-value = 0.1311

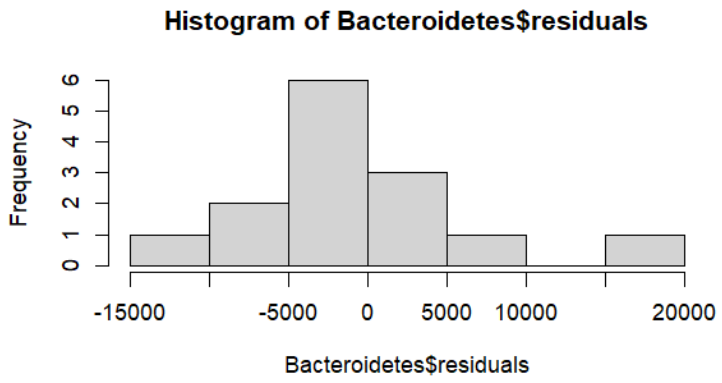

Figure A46 A histogram of the ANOVA residuals of Bacteroidetes in the belly samples across of decomposition

ACTINOBACTERIA

Analysis of Variance Table

Response: Actinobacteria

	Df	Sum Sq	Mean Sq	F value	Pr(>F)	
Dayf	4	318247681	79561920	5.2329	0.01859	*
Residuals	9	136837178	15204131			

Signif. codes: 0 '***' 0.001 '**' 0.01 '*' 0.05 '.' 0.1 ' ' 1

> summary(Actinobacteria)

Call:

lm(formula = Actinobacteria ~ Dayf, data = bellyphyla)

Residuals:

Min	1Q	Median	3Q	Max
-7878.7	-534.2	67.0	768.3	7690.3

Coefficients:

	Estimate	Std. Error	t value	Pr(>|t|)	
(Intercept)	13433	2251	5.967	0.000211	***
Dayf2	-12180	3184	-3.826	0.004054	**
Dayf4	-9997	3184	-3.140	0.011929	*
Dayf7	-13105	3560	-3.682	0.005063	**
Dayf23	-10668	3184	-3.351	0.008513	**

Signif. codes: 0 '***' 0.001 '**' 0.01 '*' 0.05 '.' 0.1 ' ' 1

Residual standard error: 3899 on 9 degrees of freedom

Multiple R-squared: 0.6993, Adjusted R-squared: 0.5657

F-statistic: 5.233 on 4 and 9 DF, p-value: 0.01859

NORMALITY TEST FOR RESIDUAL

Actinobacteria$residuals ### Shows you the residuals for each sample

```
       1        2        3        4        5        6        7
 -34.0000 -7878.6667  -283.6667   188.3333 -1279.0000   168.0000  2127.3333
       8        9       10       11       12       13       14
 369.3333  -168.0000 -2496.6667  -617.6667  1313.0000   901.3333  7690.3333
```

> hist(Actinobacteria$residuals) ### plots a histogram of the residuals

> shapiro.test(Actinobacteria$residuals)

Shapiro-Wilk normality test

data: Actinobacteria$residuals

W = 0.84162, p-value = 0.01712

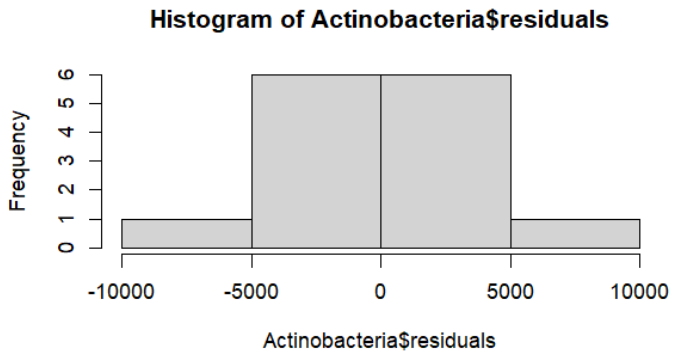

Figure A47 A histogram of the ANOVA residuals of Actinobacteria in the belly samples across days of decomposition

MOUTH

FIRMICUTES

Analysis of Variance Table

Response: Firmicutes

```
          Df    Sum Sq   Mean Sq F value   Pr(>F)
Dayf       4 3814777430 953694357  11.413 0.002177 **
Residuals  8  668503550  83562944
```

```
---
Signif. codes:  0 ‘***’ 0.001 ‘**’ 0.01 ‘*’ 0.05 ‘.’ 0.1 ‘ ’ 1
> summary(Firmicutes)

Call:
lm(formula = Firmicutes ~ Dayf, data = mouthphyla)

Residuals:
   Min     1Q Median     3Q    Max
-15075  -4080    -27   5896  12281

Coefficients:
            Estimate Std. Error t value Pr(>|t|)
(Intercept)    19384       5278   3.673  0.00628 **
Dayf2         -12272       7464  -1.644  0.13875
Dayf4          -1447       7464  -0.194  0.85114
Dayf7          41060       8345   4.920  0.00116 **
Dayf23         -5286       8345  -0.633  0.54416
---
Signif. codes:  0 ‘***’ 0.001 ‘**’ 0.01 ‘*’ 0.05 ‘.’ 0.1 ‘ ’ 1

Residual standard error: 9141 on 8 degrees of freedom
Multiple R-squared:  0.8509,            Adjusted R-squared:  0.7763
F-statistic: 11.41 on 4 and 8 DF,  p-value: 0.002177

NORMALITY TEST FOR RESIDUAL
> Firmicutes$residuals            ### Shows you the residuals for each sample
       1        2        3        4        5        6        7
 -7509.333  -2264.333 -15075.000  -4079.667  -1816.667  12281.000   2794.000
       8        9       10       11       12       13
  -27.000    27.000  -5952.500   9773.667   5952.500   5896.333
```

> hist(Firmicutes$residuals) ### plots a histogram of the residuals

> shapiro.test(Firmicutes$residuals)

Shapiro-Wilk normality test

data: Firmicutes$residuals

W = 0.98305, p-value = 0.9911

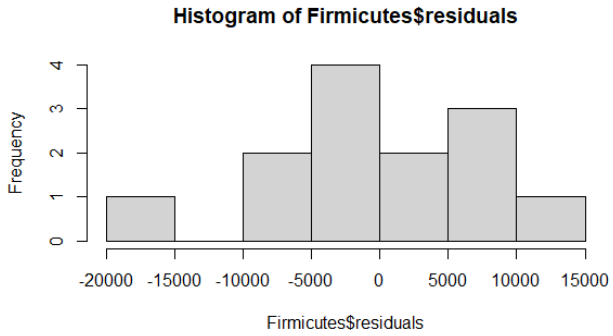

Figure A48 A histogram of the ANOVA residuals of Firmicutes in the mouth samples across days of decomposition

LIVER

FIRMICUTES

Analysis of Variance Table

Response: Firmicutes

	Df	Sum Sq	Mean Sq	F value	Pr(>F)
Dayf	2	1.4300e+10	7149921308	89.911	3.366e-05 ***
Residuals	6	4.7713e+08	79522176		

Signif. codes: 0 '***' 0.001 '**' 0.01 '*' 0.05 '.' 0.1 ' ' 1

> summary(Firmicutes)

Call:

lm(formula = Firmicutes ~ Dayf, data = liverphyla)

Residuals:

Min	1Q	Median	3Q	Max
-15699.7	-3667.3	603.7	5262.3	10437.3

Coefficients:

	Estimate	Std. Error	t value	Pr(>|t|)	
(Intercept)	7074	5148	1.374	0.219	
Dayf2	87811	7281	12.060	1.97e-05	***
Dayf4	80876	7281	11.108	3.17e-05	***

Signif. codes: 0 '***' 0.001 '**' 0.01 '*' 0.05 '.' 0.1 ' ' 1

Residual standard error: 8918 on 6 degrees of freedom

Multiple R-squared: 0.9677, Adjusted R-squared: 0.9569

F-statistic: 89.91 on 2 and 6 DF, p-value: 3.366e-05

NORMALITY TEST FOR RESIDUAL

> Firmicutes$residuals ### Shows you the residuals for each sample

1	2	3	4	5	6	7
-3667.3333	603.6667	3063.6667	-6133.3333	-15699.6667	5262.3333	10437.3333

8	9
383.6667	5749.6667

> hist(Firmicutes$residuals) ### plots a histogram of the residuals

> shapiro.test(Firmicutes$residuals)

Shapiro-Wilk normality test

data: Firmicutes$residuals

W = 0.94764, p-value = 0.6641

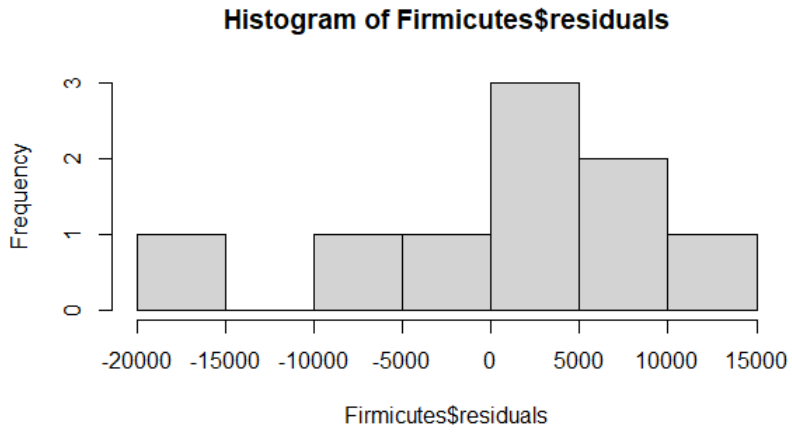

Figure A49 A histogram of the ANOVA residuals of Firmicutes in the liver samples across days of decomposition

LUNGS

BACTEROIDETES

Analysis of Variance Table

Response: Bacteroidetes

	Df	Sum Sq	Mean Sq	F value	Pr(>F)	
Dayf	2	13683087	6841543	9.4767	0.0139	*
Residuals	6	4331591	721932			

Signif. codes: 0 '***' 0.001 '**' 0.01 '*' 0.05 '.' 0.1 ' ' 1

> summary(Bacteroidetes)

Call:

lm(formula = Bacteroidetes ~ Dayf, data = lungphyla)

Residuals:

Min	1Q	Median	3Q	Max
-1079.3	-261.3	-193.0	412.0	1106.7

Coefficients:

	Estimate	Std. Error	t value	Pr(>|t|)	
(Intercept)	3191.3	490.6	6.506	0.000628	***
Dayf2	-2298.0	693.7	-3.312	0.016156	*
Dayf4	-2846.3	693.7	-4.103	0.006337	**

Signif. codes: 0 '***' 0.001 '**' 0.01 '*' 0.05 '.' 0.1 ' ' 1

Residual standard error: 849.7 on 6 degrees of freedom

Multiple R-squared: 0.7596, Adjusted R-squared: 0.6794

F-statistic: 9.477 on 2 and 6 DF, p-value: 0.0139

NORMALITY TEST FOR RESIDUAL

```
> Bacteroidetes$residuals          ### Shows you the residuals for each sample
      1       2       3       4       5       6       7
 1106.6667  -219.0000  -193.0000   940.6667   138.6667  -845.3333  -261.3333
      8       9
  412.0000 -1079.3333
> hist(Bacteroidetes$residuals) ### plots a histogram of the residuals
> shapiro.test(Bacteroidetes$residuals)

        Shapiro-Wilk normality test

data:  Bacteroidetes$residuals
W = 0.95459, p-value = 0.7403
```

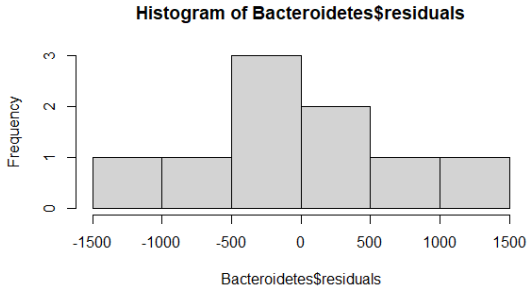

Figure A50 A histogram of the ANOVA residuals of Bacteroidetes in the liver samples across decomposition days

ACTINOBACTERIA

Analysis of Variance Table

Response: Actinobacteria

	Df	Sum Sq	Mean Sq	F value	Pr(>F)
Dayf	2	32405064	16202532	7.0959	0.02624 *
Residuals	6	13700241	2283373		

Signif. codes: 0 '***' 0.001 '**' 0.01 '*' 0.05 '.' 0.1 ' ' 1

> summary(Actinobacteria)

Call:

lm(formula = Actinobacteria ~ Dayf, data = lungphyla)

Residuals:

Min	1Q	Median	3Q	Max
-2632.3	-475.0	-88.0	368.7	2263.7

Coefficients:

	Estimate	Std. Error	t value	Pr(>|t|)
(Intercept)	4619.3	872.4	5.295	0.00184 **

Dayf2 -3718.3 1233.8 -3.014 0.02359 *

Dayf4 -4274.3 1233.8 -3.464 0.01340 *

Signif. codes: 0 '***' 0.001 '**' 0.01 '*' 0.05 '.' 0.1 ' ' 1

Residual standard error: 1511 on 6 degrees of freedom

Multiple R-squared: 0.7028, Adjusted R-squared: 0.6038

F-statistic: 7.096 on 2 and 6 DF, p-value: 0.02624

NORMALITY TEST FOR RESIDUAL

plot(Actinobacteria~Dayf,data=lungphyla)

> Actinobacteria$residuals ### Shows you the residuals for each sample

1	2	3	4	5	6	7
954.0000	-88.0000	-215.0000	-2632.3333	2263.6667	-479.0000	-475.0000

8	9
303.0000	368.6667

> hist(Actinobacteria$residuals) ### plots a histogram of the residuals

> shapiro.test(Actinobacteria$residuals)

Shapiro-Wilk normality test

data: Actinobacteria$residuals

W = 0.92675, p-value = 0.4511

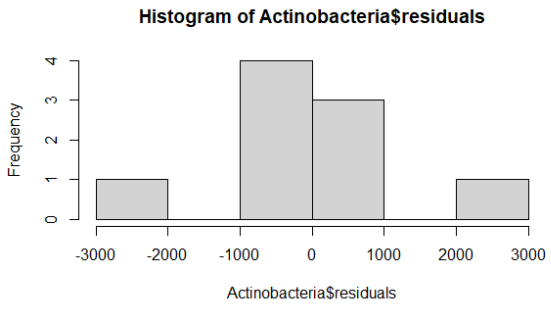

Figure A51 A histogram of the ANOVA residuals of Actinobacteria in the lung samples across of decomposition

Families

Belly

CORYNEBACTERIACEAE

Analysis of Variance Table

Response: Corynebacteriaceae

	Df	Sum Sq	Mean Sq	F value	Pr(>F)	
Dayf	4	96383911	24095978	3.8152	0.04419	*
Residuals	9	56842549	6315839			

Signif. codes: 0 ‘***’ 0.001 ‘**’ 0.01 ‘*’ 0.05 ‘.’ 0.1 ‘ ’ 1

> summary(Corynebacteriaceae)

Call:

lm(formula = Corynebacteriaceae ~ Dayf, data = bellyphyla)

Residuals:

Min	1Q	Median	3Q	Max
-5113.7	-275.9	0.0	1093.1	3836.3

Coefficients:

	Estimate	Std. Error	t value	Pr(>|t|)	
(Intercept)	7502	1451	5.170	0.000587	***
Dayf2	-6773	2052	-3.301	0.009219	**
Dayf4	-5481	2052	-2.671	0.025576	*
Dayf7	-7463	2294	-3.253	0.009951	**
Dayf23	-4931	2052	-2.403	0.039687	*

Signif. codes: 0 ‘***’ 0.001 ‘**’ 0.01 ‘*’ 0.05 ‘.’ 0.1 ‘ ’ 1

Residual standard error: 2513 on 9 degrees of freedom

Multiple R-squared: 0.629, Adjusted R-squared: 0.4642

F-statistic: 3.815 on 4 and 9 DF, p-value: 0.04419

NORMALITY TEST FOR RESIDUAL

> Corynebacteriaceae$residuals ### Shows you the residuals for each sample

1	2	3	4	5	6	7
-154.6667	-5113.6667	-281.6667	1277.3333	-1178.6667	20.0000	2187.6667

8	9	10	11	12	13	14
235.6667	-20.0000	-2423.3333	-258.6667	1333.3333	540.3333	3836.3333

> hist(Corynebacteriaceae$residuals) ### plots a histogram of the residuals

> shapiro.test(Corynebacteriaceae$residuals)

Shapiro-Wilk normality test

data: Corynebacteriaceae$residuals

W = 0.92634, p-value = 0.2709

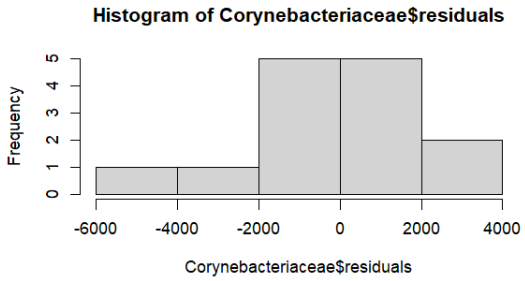

Figure A52 A histogram of the ANOVA residuals of Corynebacteriaceae in the belly samples across of decomposition

CLOSTRIDIACEAE

Analysis of Variance Table

Response: Clostridiaceae

	Df	Sum Sq	Mean Sq	F value	Pr(>F)
Dayf	4	688293583	172073396	23.338	9.049e-05 ***

```
Residuals  9  66358350   7373150
---
Signif. codes:  0 ‘***’ 0.001 ‘**’ 0.01 ‘*’ 0.05 ‘.’ 0.1 ‘ ’ 1
> summary(Clostridiaceae)

Call:
lm(formula = Clostridiaceae ~ Dayf, data = bellyphyla)

Residuals:
   Min     1Q  Median     3Q    Max
-6043.7  -999.0   120.3  1253.1  3861.3

Coefficients:
            Estimate Std. Error t value Pr(>|t|)
(Intercept)   2220.7     1567.7   1.417    0.190
Dayf2         -438.7     2217.1  -0.198    0.848
Dayf4        16553.0     2217.1   7.466 3.83e-05 ***
Dayf7         -811.7     2478.8  -0.327    0.751
Dayf23        -915.3     2217.1  -0.413    0.689
---
Signif. codes:  0 ‘***’ 0.001 ‘**’ 0.01 ‘*’ 0.05 ‘.’ 0.1 ‘ ’ 1

Residual standard error: 2715 on 9 degrees of freedom
Multiple R-squared:  0.9121,            Adjusted R-squared:  0.873
F-statistic: 23.34 on 4 and 9 DF,  p-value: 9.049e-05

NORMALITY TEST FOR RESIDUAL
> Clostridiaceae$residuals            ### Shows you the residuals for each sample
       1        2        3        4        5        6        7
 2182.3333 -1308.6667 -1205.0000   786.3333  3861.3333  -476.0000  -235.3333
       8        9       10       11       12       13       14
```

1408.6667 476.0000 -1173.3333 1471.0000 -6043.6667 -266.0000 522.3333

> hist(Clostridiaceae$residuals) ### plots a histogram of the residuals

> shapiro.test(Clostridiaceae$residuals)

Shapiro-Wilk normality test

data: Clostridiaceae$residuals

W = 0.89659, p-value = 0.1006

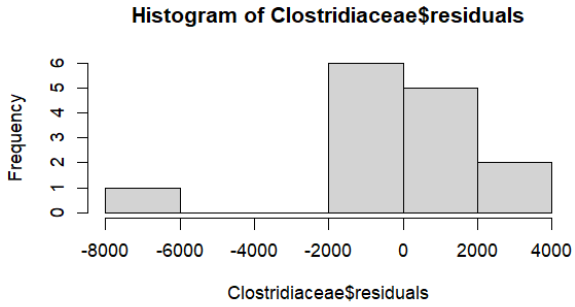

Figure A53 A histogram of the ANOVA residuals of Clostridiaceae in the belly samples across of decomposition

TISSIERELLACEAE

Analysis of Variance Table

Response: Tissierellaceae

Df Sum Sq Mean Sq F value Pr(>F)

Dayf 4 27488394 6872099 11.946 0.001202 **

Residuals 9 5177185 575243

Signif. codes: 0 ‘***’ 0.001 ‘**’ 0.01 ‘*’ 0.05 ‘.’ 0.1 ‘ ’ 1

> summary(Tissierellaceae)

Call:

lm(formula = Tissierellaceae ~ Dayf, data = bellyphyla)

```
Residuals:
    Min      1Q  Median      3Q     Max
-1391.67 -151.42    5.17  327.33  968.33

Coefficients:
            Estimate Std. Error t value Pr(>|t|)
(Intercept)    845.7      437.9   1.931  0.08550 .
Dayf2         -835.3      619.3  -1.349  0.21033
Dayf4         -785.0      619.3  -1.268  0.23675
Dayf7         3186.3      692.4   4.602  0.00129 **
Dayf23         1347.0      619.3   2.175  0.05763 .
---
Signif. codes:  0 ‘***’ 0.001 ‘**’ 0.01 ‘*’ 0.05 ‘.’ 0.1 ‘ ’ 1

Residual standard error: 758.4 on 9 degrees of freedom
Multiple R-squared:  0.8415,            Adjusted R-squared:  0.7711
F-statistic: 11.95 on 4 and 9 DF,  p-value: 0.001202
```

NORMALITY TEST FOR RESIDUAL

```
> Tissierellaceae$residuals            ### Shows you the residuals for each sample
        1         2         3         4         5         6
  39.333333  -332.666667    -1.333333   516.333333   -54.666667   924.000000
        7         8         9        10        11        12
 968.333333   423.333333  -924.000000 -1391.666667   -10.333333    15.333333
       13        14
  11.666667  -183.666667
> hist(Tissierellaceae$residuals) ### plots a histogram of the residuals
> shapiro.test(Tissierellaceae$residuals)

            Shapiro-Wilk normality test
```

data: Tissierellaceae$residuals

W = 0.92166, p-value = 0.2323

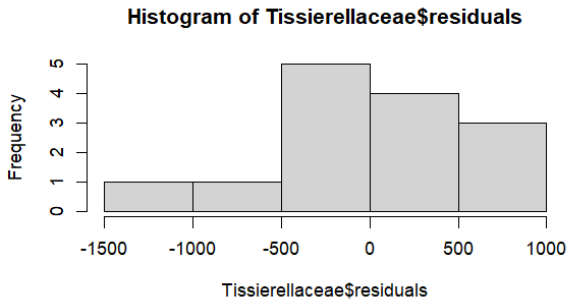

Figure A54 A histogram of the ANOVA residuals of Tissierellaceae in the belly samples across day of decomposition

ANUS

RUMINOCOCCACEAE

Analysis of Variance Table

Response: Ruminococcaceae

	Df	Sum Sq	Mean Sq	F value	Pr(>F)
Dayf	3	359283330	119761110	7.7358	0.02518 *
Residuals	5	77407230	15481446		

Signif. codes: 0 ‘***’ 0.001 ‘**’ 0.01 ‘*’ 0.05 ‘.’ 0.1 ‘ ’ 1

> summary(Ruminococcaceae)

Call:

lm(formula = Ruminococcaceae ~ Dayf, data = anusphyla)

Residuals:

1	2	3	4	5	6	7
2719.500	-5537.500	802.500	-802.500	5537.500	-3.667	5.333

```
      8       9
  -1.667 -2719.500


Coefficients:
            Estimate Std. Error t value Pr(>|t|)
(Intercept)    10342       2782   3.717   0.0137 *
Dayf2           4922       3935   1.251   0.2663
Dayf4          -8937       3935  -2.271   0.0723 .
Dayf23        -10334       3592  -2.877   0.0347 *
---
Signif. codes:  0 ‘***’ 0.001 ‘**’ 0.01 ‘*’ 0.05 ‘.’ 0.1 ‘ ’ 1


Residual standard error: 3935 on 5 degrees of freedom
Multiple R-squared:  0.8227,            Adjusted R-squared:  0.7164
F-statistic: 7.736 on 3 and 5 DF,  p-value: 0.02518


NORMALITY TEST FOR RESIDUAL
> Ruminococcaceae$residuals            ### Shows you the residuals for each sample
        1         2         3         4         5         6
 2719.500000 -5537.500000   802.500000  -802.500000  5537.500000    -3.666667
        7         8         9
    5.333333    -1.666667 -2719.500000
> hist(Ruminococcaceae$residuals) ### plots a histogram of the residuals
> shapiro.test(Ruminococcaceae$residuals)


            Shapiro-Wilk normality test


data:  Ruminococcaceae$residuals
W = 0.95594, p-value = 0.7551
```

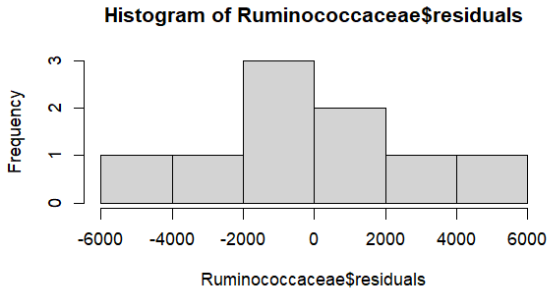

Figure A55 A histogram of the ANOVA residuals of Ruminococcaceae in the anus samples across of decomposition

BACTEROIDACEAE

Analysis of Variance Table

Response: Bacteroidaceae

	Df	Sum Sq	Mean Sq	F value	Pr(>F)
Dayf	3	164105095	54701698	8.918	0.01888 *
Residuals	5	30669429	6133886		

Signif. codes: 0 '***' 0.001 '**' 0.01 '*' 0.05 '.' 0.1 ' ' 1

> summary(Bacteroidaceae)

Call:

lm(formula = Bacteroidaceae ~ Dayf, data = anusphyla)

Residuals:

1	2	3	4	5	6	7	8	9
16.0	81.5	-3648.0	3648.0	-81.5	-776.7	1640.3	-863.7	-16.0

Coefficients:

	Estimate	Std. Error	t value	Pr(>|t|)
(Intercept)	96.0	1751.3	0.055	0.95841
Dayf2	22.5	2476.7	0.009	0.99310

Dayf4 10613.0 2476.7 4.285 0.00782 **

Dayf23 876.7 2260.9 0.388 0.71416

Signif. codes: 0 '***' 0.001 '**' 0.01 '*' 0.05 '.' 0.1 ' ' 1

Residual standard error: 2477 on 5 degrees of freedom

Multiple R-squared: 0.8425, Adjusted R-squared: 0.7481

F-statistic: 8.918 on 3 and 5 DF, p-value: 0.01888

NORMALITY TEST FOR RESIDUAL

> Bacteroidaceae$residuals ### Shows you the residuals for each sample

1	2	3	4	5	6	7
16.0000	81.5000	-3648.0000	3648.0000	-81.5000	-776.6667	1640.3333

8	9
-863.6667	-16.0000

> hist(Bacteroidaceae$residuals) ### plots a histogram of the residuals

> shapiro.test(Bacteroidaceae$residuals)

Shapiro-Wilk normality test

data: Bacteroidaceae$residuals

W = 0.91114, p-value = 0.32

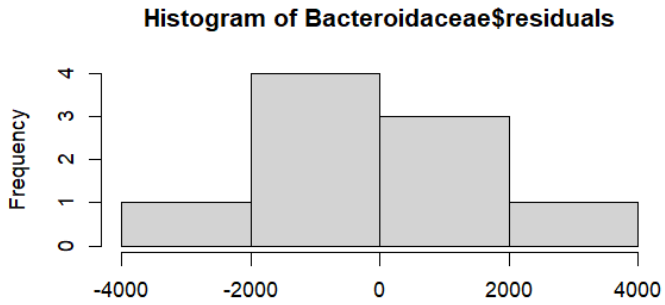

Figure A56 A histogram of the ANOVA residuals of Bacteroidaceae in the anus samples across of decomposition

MOUTH

TISSIERELLACEAE

Analysis of Variance Table

Response: Tissierellaceae

	Df	Sum Sq	Mean Sq	F value	Pr(>F)	
Dayf	4	4541852895	1135463224	240.73	2.289e-08	***
Residuals	8	37733508	4716689			

Signif. codes: 0 '***' 0.001 '**' 0.01 '*' 0.05 '.' 0.1 ' ' 1

> summary(Tissierellaceae)

Call:

lm(formula = Tissierellaceae ~ Dayf, data = mouthphyla)

Residuals:

Min	1Q	Median	3Q	Max
-4289.5	-30.0	-4.7	53.7	4289.5

Coefficients:

	Estimate	Std. Error	t value	Pr(>|t|)	
(Intercept)	57.00	1253.89	0.045	0.965	
Dayf2	-52.33	1773.26	-0.030	0.977	
Dayf4	-21.67	1773.26	-0.012	0.991	
Dayf7	51904.50	1982.57	26.180	4.87e-09	***
Dayf23	680.50	1982.57	0.343	0.740	

Signif. codes: 0 '***' 0.001 '**' 0.01 '*' 0.05 '.' 0.1 ' ' 1

Residual standard error: 2172 on 8 degrees of freedom

Multiple R-squared: 0.9918, Adjusted R-squared: 0.9876

F-statistic: 240.7 on 4 and 8 DF, p-value: 2.289e-08

NORMALITY TEST FOR RESIDUAL

> Tissierellaceae$residuals ### Shows you the residuals for each sample

1	2	3	4	5
-26.3333333	-27.3333333	-30.0000000	-4.6666667	5.3333333
6	7	8	9	10
76.0000000	-46.0000000	-4289.5000000	4289.5000000	-678.5000000
11	12	13		
53.6666667	678.5000000	-0.6666667		

> hist(Tissierellaceae$residuals) ### plots a histogram of the residuals

> shapiro.test(Tissierellaceae$residuals)

Shapiro-Wilk normality test

data: Tissierellaceae$residuals

W = 0.68842, p-value = 0.0004261

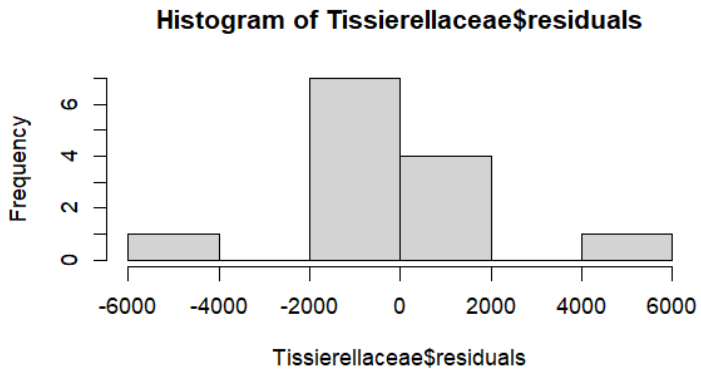

Figure A57 A histogram of the ANOVA residuals of Tissierellaceae in the mouth samples across of decomposition

PSEUDOMONADACEAE

Analysis of Variance Table

Response: Pseudomonadaceae

	Df	Sum Sq	Mean Sq	F value	Pr(>F)	
Dayf	4	110535048	27633762	202.94	4.5e-08	***
Residuals	8	1089343	136168			

Signif. codes: 0 '***' 0.001 '**' 0.01 '*' 0.05 '.' 0.1 ' ' 1

> summary(Pseudomonadaceae)

Call:

lm(formula = Pseudomonadaceae ~ Dayf, data = mouthphyla)

Residuals:

Min	1Q	Median	3Q	Max
-504.3	-123.3	-72.0	120.0	721.7

Coefficients:

	Estimate	Std. Error	t value	Pr(>|t|)	
(Intercept)	124.00	213.05	0.582	0.5766	
Dayf2	937.33	301.29	3.111	0.0144	*
Dayf4	97.33	301.29	0.323	0.7549	
Dayf7	62.00	336.86	0.184	0.8586	
Dayf23	8312.00	336.86	24.675	7.78e-09	***

Signif. codes: 0 '***' 0.001 '**' 0.01 '*' 0.05 '.' 0.1 ' ' 1

Residual standard error: 369 on 8 degrees of freedom

Multiple R-squared: 0.9902, Adjusted R-squared: 0.9854

F-statistic: 202.9 on 4 and 8 DF, p-value: 4.5e-08

NORMALITY TEST FOR RESIDUAL

> Pseudomonadaceae$residuals ### Shows you the residuals for each sample

```
      1       2       3       4       5       6       7
-123.3333  342.6667  -72.0000 -217.3333 -504.3333  184.0000 -112.0000
      8       9      10      11      12      13
-120.0000  120.0000  -54.0000 -219.3333   54.0000  721.6667
```

> hist(Pseudomonadaceae$residuals) ### plots a histogram of the residuals

> shapiro.test(Pseudomonadaceae$residuals)

```
        Shapiro-Wilk normality test

data:  Pseudomonadaceae$residuals
W = 0.92605, p-value = 0.3023
```

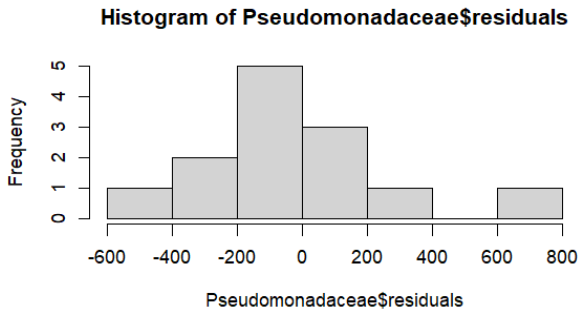

Figure A58 A histogram of the ANOVA residuals of Pseudomonadaceae in the mouth samples across of decomposition

LIVER

LACTOBACILLACEAE

Analysis of Variance Table

Response: Lactobacillaceae

```
      Df    Sum Sq    Mean Sq F value  Pr(>F)
Dayf   2 3894930963 1947465481  7.4356 0.02376 *
```

```
Residuals  6 1571471673  261911946
---
Signif. codes:  0 ‘***’ 0.001 ‘**’ 0.01 ‘*’ 0.05 ‘.’ 0.1 ‘ ’ 1
> summary( Lactobacillaceae)

Call:
lm(formula = Lactobacillaceae ~ Dayf, data = liverphyla)

Residuals:
   Min     1Q Median     3Q    Max
-16613 -10599   -568    495  27211

Coefficients:
            Estimate Std. Error t value Pr(>|t|)
(Intercept)     759       9344   0.081   0.9379
Dayf2         44620      13214   3.377   0.0149 *
Dayf4         43624      13214   3.301   0.0164 *
---
Signif. codes:  0 ‘***’ 0.001 ‘**’ 0.01 ‘*’ 0.05 ‘.’ 0.1 ‘ ’ 1

Residual standard error: 16180 on 6 degrees of freedom
Multiple R-squared:  0.7125,            Adjusted R-squared:  0.6167
F-statistic: 7.436 on 2 and 6 DF,  p-value: 0.02376

NORMALITY TEST FOR RESIDUAL
> Lactobacillaceae$residuals            ### Shows you the residuals for each sample
       1        2        3        4        5        6        7
-11118.667  -5769.667  16888.333   -568.000 -16612.667  27211.333 -10598.667
       8        9
  495.000    73.000
> hist(Lactobacillaceae$residuals) ### plots a histogram of the residuals
```

```
> shapiro.test(Lactobacillaceae$residuals)

        Shapiro-Wilk normality test

data:  Lactobacillaceae$residuals
W = 0.90127, p-value = 0.2594
```

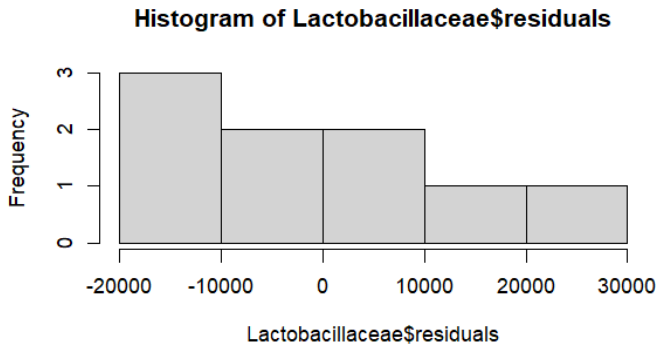

Figure A59 A histogram of the ANOVA residuals of Lactobacillaceae in the liver samples across of decomposition

APPENDIX 8 – R OUTPUT RESULTS FOR CHAPTER 7

SEAWATER

PROTEOBACTERIA

Analysis of Variance Table

Response: Proteobacteria

	Df	Sum Sq	Mean Sq	F value	Pr(>F)	
Dayf	2	1149240628	574620314	13.474	0.03171	*
Residuals	3	127939814	42646605			

Signif. codes: 0 '***' 0.001 '**' 0.01 '*' 0.05 '.' 0.1 ' ' 1

> summary(Proteobacteria)

Call:

lm(formula = Proteobacteria ~ Dayf, data = seawaterphyla)

Residuals:

1	2	3	4	5	6
4255	-4255	6741	-6741	-651	651

Coefficients:

	Estimate	Std. Error	t value	Pr(>|t|)	
(Intercept)	40455	4618	8.761	0.00313	**
Dayf7	-26879	6530	-4.116	0.02598	*
Dayf14	-31330	6530	-4.798	0.01723	*

Signif. codes: 0 '***' 0.001 '**' 0.01 '*' 0.05 '.' 0.1 ' ' 1

Residual standard error: 6530 on 3 degrees of freedom

Multiple R-squared: 0.8998, Adjusted R-squared: 0.833

F-statistic: 13.47 on 2 and 3 DF, p-value: 0.03171

NORMALITY TEST FOR RESIDUAL

> Proteobacteria$residuals ### Shows you the residuals for each sample

1 2 3 4 5 6

4255 -4255 6741 -6741 -651 651

> hist(Proteobacteria$residuals) ### plots a histogram of the residuals

> shapiro.test(Proteobacteria$residuals)

Shapiro-Wilk normality test

data: Proteobacteria$residuals

W = 0.97562, p-value = 0.9278

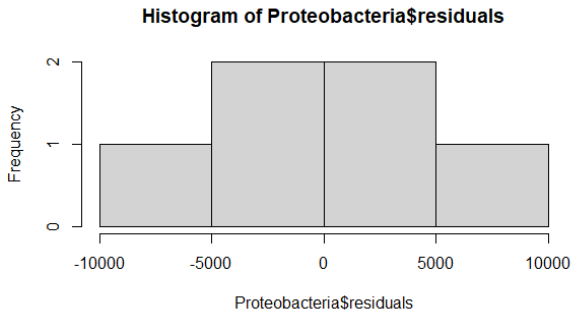

Figure A60 A histogram of the ANOVA residuals of Proteobacteria in the seawater samples across of decomposition

FIRMICUTES

Analysis of Variance Table

Response: Firmicutes

Df Sum Sq Mean Sq F value Pr(>F)

Dayf 2 84355050 42177525 35.452 0.008179 **

```
Residuals  3  3569163  1189721
---
Signif. codes:  0 ‘***’ 0.001 ‘**’ 0.01 ‘*’ 0.05 ‘.’ 0.1 ‘ ’ 1
> summary(Firmicutes)

Call:
lm(formula = Firmicutes ~ Dayf, data = brackishwaterphyla)

Residuals:
    1      2      3      4      5      6
 -211.0   211.0  -434.5   434.5  1245.5 -1245.5

Coefficients:
            Estimate Std. Error t value Pr(>|t|)
(Intercept)   8996.5      771.3  11.664  0.00135 **
Dayf7         9155.0     1090.7   8.393  0.00355 **
Dayf14        5214.5     1090.7   4.781  0.01740 *
---
Signif. codes:  0 ‘***’ 0.001 ‘**’ 0.01 ‘*’ 0.05 ‘.’ 0.1 ‘ ’ 1

Residual standard error: 1091 on 3 degrees of freedom
Multiple R-squared:  0.9594,            Adjusted R-squared:  0.9323
F-statistic: 35.45 on 2 and 3 DF,  p-value: 0.008179

NORMALITY TEST FOR RESIDUAL
Firmicutes$residuals            ### Shows you the residuals for each sample
    1      2      3      4      5      6
 -211.0   211.0  -434.5   434.5  1245.5 -1245.5
> hist(Firmicutes$residuals) ### plots a histogram of the residuals
> shapiro.test(Firmicutes$residuals)
```

Shapiro-Wilk normality test

data: Firmicutes$residuals

W = 0.99324, p-value = 0.9956

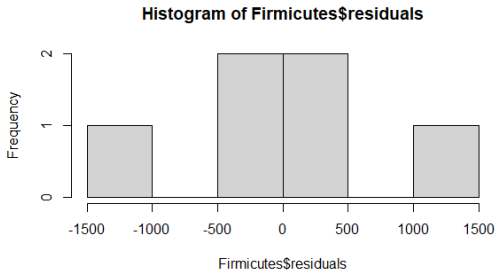

Figure A61 A histogram of the ANOVA residuals of Firmicutes in the seawater samples across of decomposition

BRACKISH WATER

FIRMICUTES

Analysis of Variance Table

Response: Firmicutes

	Df	Sum Sq	Mean Sq	F value	Pr(>F)
Dayf	2	84355050	42177525	35.452	0.008179 **
Residuals	3	3569163	1189721		

Signif. codes: 0 ‘***’ 0.001 ‘**’ 0.01 ‘*’ 0.05 ‘.’ 0.1 ‘ ’ 1

> summary(Firmicutes)

Call:

lm(formula = Firmicutes ~ Dayf, data = brackishwaterphyla)

Residuals:

1 2 3 4 5 6

```
 -211.0   211.0  -434.5   434.5  1245.5 -1245.5


Coefficients:
            Estimate Std. Error t value Pr(>|t|)
(Intercept)   8996.5      771.3  11.664  0.00135 **
Dayf7         9155.0     1090.7   8.393  0.00355 **
Dayf14        5214.5     1090.7   4.781  0.01740 *
---
Signif. codes:  0 ‘***’ 0.001 ‘**’ 0.01 ‘*’ 0.05 ‘.’ 0.1 ‘ ’ 1


Residual standard error: 1091 on 3 degrees of freedom
Multiple R-squared:  0.9594,            Adjusted R-squared:  0.9323
F-statistic: 35.45 on 2 and 3 DF,  p-value: 0.008179



NORMALITY TEST FOR RESIDUAL
Firmicutes$residuals            ### Shows you the residuals for each sample
     1      2      3      4      5      6
 -211.0   211.0  -434.5   434.5  1245.5 -1245.5
> hist(Firmicutes$residuals) ### plots a histogram of the residuals
> shapiro.test(Firmicutes$residuals)

            Shapiro-Wilk normality test


data:  Firmicutes$residuals
W = 0.99324, p-value = 0.9956
```

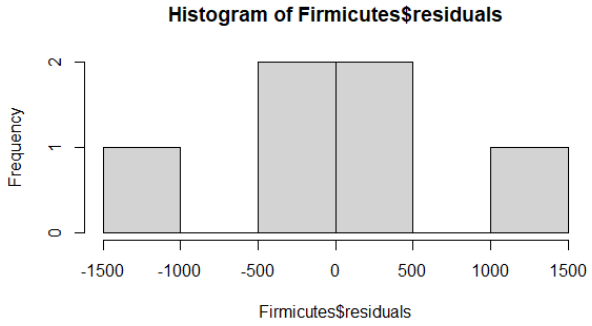

Figure A62 A histogram of the ANOVA residuals of Firmicutes in the brackish water samples across of decomposition

BACTEROIDETES

Analysis of Variance Table

Response: Bacteroidetes

	Df	Sum Sq	Mean Sq	F value	Pr(>F)
Dayf	2	578727466	289363733	12.522	0.03499 *
Residuals	3	69325917	23108639		

Signif. codes: 0 '***' 0.001 '**' 0.01 '*' 0.05 '.' 0.1 ' ' 1

> summary(Bacteroidetes)

Call:

lm(formula = Bacteroidetes ~ Dayf, data = brackishwaterphyla)

Residuals:

1	2	3	4	5	6
-3024	3024	1546	-1546	-4810	4809

Coefficients:

	Estimate	Std. Error	t value	Pr(>|t|)
(Intercept)	6908	3399	2.032	0.1351

Dayf7 17429 4807 3.626 0.0361 *

Dayf14 23075 4807 4.800 0.0172 *

Signif. codes: 0 ‘***’ 0.001 ‘**’ 0.01 ‘*’ 0.05 ‘.’ 0.1 ‘ ’ 1

Residual standard error: 4807 on 3 degrees of freedom

Multiple R-squared: 0.893, Adjusted R-squared: 0.8217

F-statistic: 12.52 on 2 and 3 DF, p-value: 0.03499

NORMALITY TEST FOR RESIDUAL

> Bacteroidetes$residuals ### Shows you the residuals for each sample

1 2 3 4 5 6

-3023.5 3023.5 1546.0 -1546.0 -4809.5 4809.5

> hist(Bacteroidetes$residuals) ### plots a histogram of the residuals

> shapiro.test(Bacteroidetes$residuals)

Shapiro-Wilk normality test

data: Bacteroidetes$residuals

W = 0.95932, p-value = 0.8144

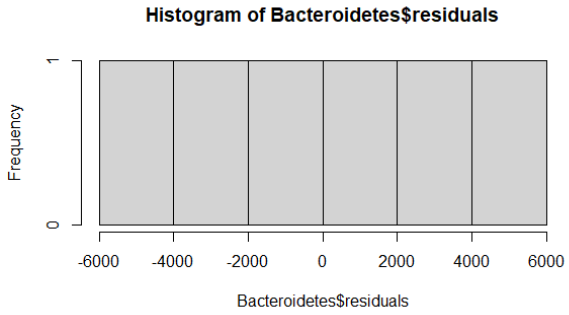

Figure A63 A histogram of the ANOVA residuals of Bacteroidetes in the brackish water samples across of decomposition

FRESH WATER

PROTEOBACTERIA

Analysis of Variance Table

Response: Proteobacteria

	Df	Sum Sq	Mean Sq	F value	Pr(>F)
Dayf	2	617920417	308960208	10.937	0.04188 *
Residuals	3	84745663	28248554		

Signif. codes: 0 '***' 0.001 '**' 0.01 '*' 0.05 '.' 0.1 ' ' 1

> summary(Proteobacteria)

Call:

lm(formula = Proteobacteria ~ Dayf, data = freshwaterphyla)

Residuals:

1	2	3	4	5	6
-5283.0	5283.0	3759.5	-3759.5	-573.5	573.5

Coefficients:

	Estimate	Std. Error	t value	Pr(>|t|)
(Intercept)	12622	3758	3.358	0.0438 *
Dayf7	24817	5315	4.669	0.0185 *
Dayf14	11172	5315	2.102	0.1263

Signif. codes: 0 '***' 0.001 '**' 0.01 '*' 0.05 '.' 0.1 ' ' 1

Residual standard error: 5315 on 3 degrees of freedom

Multiple R-squared: 0.8794, Adjusted R-squared: 0.799

F-statistic: 10.94 on 2 and 3 DF, p-value: 0.04188

NORMALITY TEST FOR RESIDUAL

> Proteobacteria$residuals ### Shows you the residuals for each sample

1 2 3 4 5 6

-5283.0 5283.0 3759.5 -3759.5 -573.5 573.5

> hist(Proteobacteria$residuals) ### plots a histogram of the residuals

> shapiro.test(Proteobacteria$residuals)

Shapiro-Wilk normality test

data: Proteobacteria$residuals

W = 0.95698, p-value = 0.7962

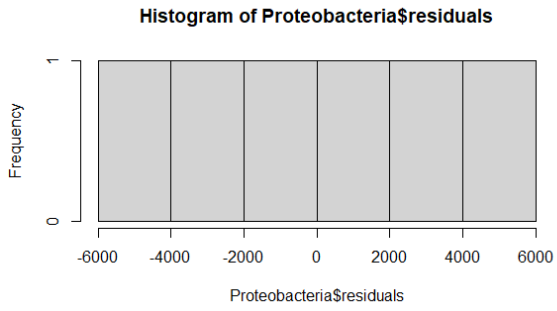

Figure A64 A histogram of the ANOVA residuals of Proteobacteria in the freshwater samples across of decomposition

BACTEROIDETES

Analysis of Variance Table

Response: Bacteroidetes

Df Sum Sq Mean Sq F value Pr(>F)

Dayf 2 195185649 97592825 36.662 0.007793 **

Residuals 3 7985862 2661954

Signif. codes: 0 '***' 0.001 '**' 0.01 '*' 0.05 '.' 0.1 ' ' 1

> summary(Bacteroidetes)

```
Call:
lm(formula = Bacteroidetes ~ Dayf, data = freshwaterphyla)

Residuals:
   1    2    3    4    5    6
-645   645   192  -192 -1882  1882

Coefficients:
            Estimate Std. Error t value Pr(>|t|)
(Intercept)     990       1154   0.858  0.45392
Dayf7         12362       1632   7.577  0.00477 **
Dayf14          543       1632   0.333  0.76118
---
Signif. codes:  0 ‘***’ 0.001 ‘**’ 0.01 ‘*’ 0.05 ‘.’ 0.1 ‘ ’ 1

Residual standard error: 1632 on 3 degrees of freedom
Multiple R-squared:  0.9607,           Adjusted R-squared:  0.9345
F-statistic: 36.66 on 2 and 3 DF,  p-value: 0.007793

NORMALITY TEST FOR RESIDUAL
> Bacteroidetes$residuals            ### Shows you the residuals for each sample
     1      2      3      4      5      6
 -645.0   645.0   192.0  -192.0 -1881.5  1881.5
> hist(Bacteroidetes$residuals) ### plots a histogram of the residuals
> shapiro.test(Bacteroidetes$residuals)

            Shapiro-Wilk normality test

data:  Bacteroidetes$residuals
W = 0.99264, p-value = 0.9946
```

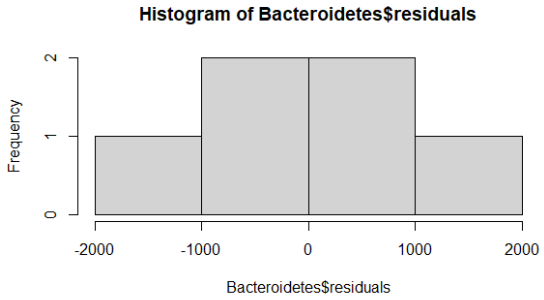

Figure A65 A histogram of the ANOVA residuals of Bacteroidetes in the freshwater samples across of decomposition

SOIL

CHTHONIOBACTERACEAE

Analysis of Variance Table

Response: Chthoniobacteraceae

	Df	Sum Sq	Mean Sq	F value	Pr(>F)
Dayf	4	6854048	1713512	3.7544	0.04083 *
Residuals	10	4564056	456406		

Signif. codes: 0 ‘***’ 0.001 ‘**’ 0.01 ‘*’ 0.05 ‘.’ 0.1 ‘ ’ 1

> summary(Chthoniobacteraceae)

Call:

lm(formula = Chthoniobacteraceae ~ Dayf, data = soilphyla)

Residuals:

Min	1Q	Median	3Q	Max
-1109.3	-293.8	121.7	404.7	987.7

Coefficients:

```
          Estimate Std. Error t value Pr(>|t|)
(Intercept)   4863.0      390.0  12.468 2.04e-07 ***
Dayf4         -607.3      551.6  -1.101  0.29668
Dayf7         -734.3      551.6  -1.331  0.21265
Dayf14       -1924.7      551.6  -3.489  0.00583 **
Dayf23       -1468.0      551.6  -2.661  0.02385 *
---
Signif. codes:  0 ‘***’ 0.001 ‘**’ 0.01 ‘*’ 0.05 ‘.’ 0.1 ‘ ’ 1

Residual standard error: 675.6 on 10 degrees of freedom
Multiple R-squared:  0.6003,            Adjusted R-squared:  0.4404
F-statistic: 3.754 on 4 and 10 DF,  p-value: 0.04083
```

NORMALITY TEST FOR RESIDUAL

```
> Chthoniobacteraceae$residuals            ### Shows you the residuals for each sample
        1         2         3         4         5         6
 322.00000   466.00000  -222.66667  -788.00000   -32.66667   255.33333
        7         8         9        10        11        12
 121.66667 -1109.33333  -810.66667   403.33333   407.33333   987.66667
       13        14        15
 406.00000   -41.00000  -365.00000
> hist(Chthoniobacteraceae$residuals) ### plots a histogram of the residuals
> shapiro.test(Chthoniobacteraceae$residuals)

            Shapiro-Wilk normality test

data:  Chthoniobacteraceae$residuals
W = 0.9426, p-value = 0.4162
```

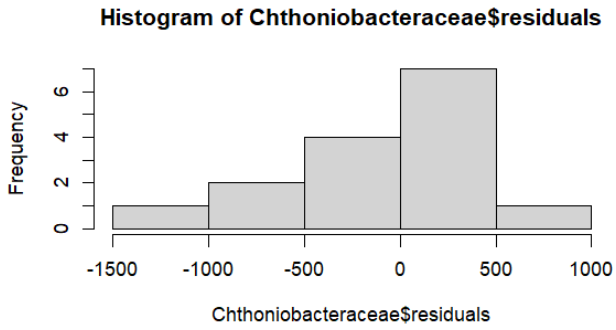

Figure A66 A histogram of the ANOVA residuals of Chthoniobacteraceae in the soil samples across of decomposition

CHITINOPHAGACEAE

Analysis of Variance Table

Response: Chitinophagaceae

	Df	Sum Sq	Mean Sq	F value	Pr(>F)	
Dayf	4	8707545	2176886	7.7095	0.004205	**
Residuals	10	2823649	282365			

Signif. codes: 0 '***' 0.001 '**' 0.01 '*' 0.05 '.' 0.1 ' ' 1

> summary(Chitinophagaceae)

Call:

lm(formula = Chitinophagaceae ~ Dayf, data = soilphyla)

Residuals:

Min	1Q	Median	3Q	Max
-761.0	-279.8	71.0	323.7	636.0

Coefficients:

	Estimate	Std. Error	t value	Pr(>|t|)	
(Intercept)	3249.0	306.8	10.590	9.37e-07	***
Dayf4	382.7	433.9	0.882	0.39849	

```
Dayf7        -960.0      433.9  -2.213  0.05133 .
Dayf14       -1802.0      433.9  -4.153  0.00197 **
Dayf23        -651.7      433.9  -1.502  0.16400
---
Signif. codes:  0 ‘***’ 0.001 ‘**’ 0.01 ‘*’ 0.05 ‘.’ 0.1 ‘ ’ 1

Residual standard error: 531.4 on 10 degrees of freedom
Multiple R-squared:  0.7551,           Adjusted R-squared:  0.6572
F-statistic: 7.709 on 4 and 10 DF,  p-value: 0.004205
```

NORMALITY TEST FOR RESIDUAL

```
> Chitinophagaceae$residuals            ### Shows you the residuals for each sample
       1        2        3        4        5        6        7
 71.0000  -88.0000  338.3333   17.0000  213.3333 -551.6667  452.0000
       8        9       10       11       12       13       14
-761.0000 -756.0000  636.0000  120.0000  309.0000  559.6667 -339.3333
      15
-220.3333
> hist(Chitinophagaceae$residuals) ### plots a histogram of the residuals
> shapiro.test(Chitinophagaceae$residuals)

            Shapiro-Wilk normality test

data:  Chitinophagaceae$residuals
W = 0.94644, p-value = 0.4702
```

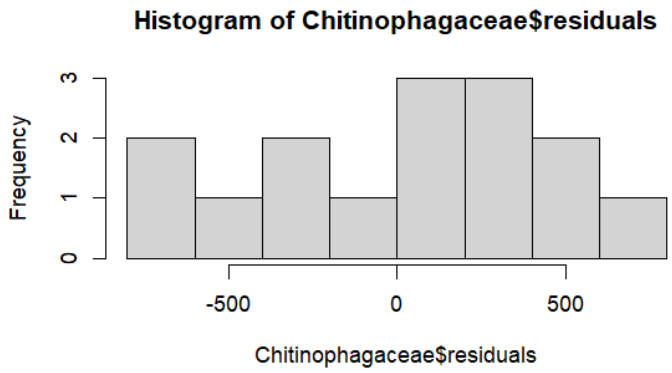

Figure A67 A histogram of the ANOVA residuals of Chitinophagaceae in the soil samples across of decomposition

BRACKISH WATER family

BACTEROIDACEAE

Analysis of Variance Table

Response: Bacteroidaceae

	Df	Sum Sq	Mean Sq	F value	Pr(>F)	
Dayf	2	781947877	390973939	97.451	0.001866	**
Residuals	3	12036029	4012010			

Signif. codes: 0 '***' 0.001 '**' 0.01 '*' 0.05 '.' 0.1 ' ' 1

> summary(Bacteroidaceae)

Call:

lm(formula = Bacteroidaceae ~ Dayf, data = brackishwaterphyla)

Residuals:

1	2	3	4	5	6
-2110.0	2110.0	406.5	-406.5	-1183.5	1183.5

Coefficients:

	Estimate	Std. Error	t value	Pr(>|t|)

(Intercept) 1708 1416 1.206 0.314396

Dayf7 19637 2003 9.804 0.002256 **

Dayf14 27060 2003 13.509 0.000877 ***

Signif. codes: 0 ‘***’ 0.001 ‘**’ 0.01 ‘*’ 0.05 ‘.’ 0.1 ‘ ’ 1

Residual standard error: 2003 on 3 degrees of freedom

Multiple R-squared: 0.9848, Adjusted R-squared: 0.9747

F-statistic: 97.45 on 2 and 3 DF, p-value: 0.001866

NORMALITY TEST FOR RESIDUAL

> Bacteroidaceae$residuals ### Shows you the residuals for each sample

1 2 3 4 5 6

-2110.0 2110.0 406.5 -406.5 -1183.5 1183.5

> hist(Bacteroidaceae$residuals) ### plots a histogram of the residuals

> shapiro.test(Bacteroidaceae$residuals)

Shapiro-Wilk normality test

data: Bacteroidaceae$residuals

W = 0.98864, p-value = 0.9856

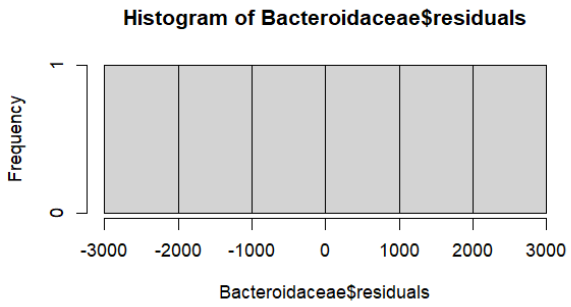

Figure A68 A histogram of the ANOVA residuals of Bacteroidaceae in the brackish water samples across of decomposition

ACIDAMINOCOCCACEAE

Analysis of Variance Table

Response: Acidaminococcaceae

	Df	Sum Sq	Mean Sq	F value	Pr(>F)	
Dayf	2	11749971	5874986	20.399	0.01793	*
Residuals	3	864009	288003			

Signif. codes: 0 ‘***’ 0.001 ‘**’ 0.01 ‘*’ 0.05 ‘.’ 0.1 ‘ ’ 1

> summary(Acidaminococcaceae)

Call:

lm(formula = Acidaminococcaceae ~ Dayf, data = brackishwaterphyla)

Residuals:

1	2	3	4	5	6
-647.5	647.5	-76.0	76.0	-83.5	83.5

Coefficients:

	Estimate	Std. Error	t value	Pr(>|t|)	
(Intercept)	112.5	379.5	0.296	0.78622	
Dayf7	985.5	536.7	1.836	0.16363	
Dayf14	3336.0	536.7	6.216	0.00839	**

Signif. codes: 0 ‘***’ 0.001 ‘**’ 0.01 ‘*’ 0.05 ‘.’ 0.1 ‘ ’ 1

Residual standard error: 536.7 on 3 degrees of freedom

Multiple R-squared: 0.9315, Adjusted R-squared: 0.8858

F-statistic: 20.4 on 2 and 3 DF, p-value: 0.01793

NORMALITY TEST FOR RESIDUAL

> Acidaminococcaceae$residuals ### Shows you the residuals for each sample

   1   2   3   4   5   6

-647.5 647.5 -76.0   76.0 -83.5   83.5

> hist(Acidaminococcaceae$residuals) ### plots a histogram of the residuals

> shapiro.test(Acidaminococcaceae$residuals)

Shapiro-Wilk normality test

data: Acidaminococcaceae$residuals

W = 0.92284, p-value = 0.5261

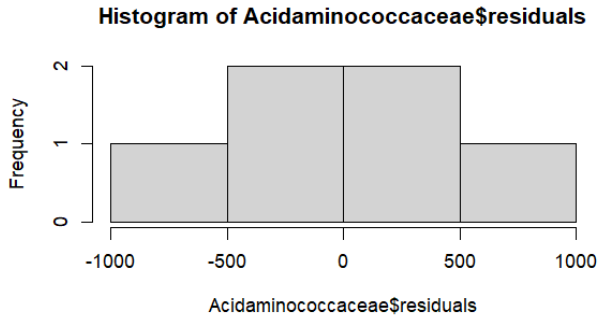

Figure A69 A histogram of the ANOVA residuals of Acidaminococcaceae in the brackish water samples across of decomposition

FRESH WATER

PSEUDOMONADACEAE

Analysis of Variance Table

Response: Pseudomonadaceae

	Df	Sum Sq	Mean Sq	F value	Pr(>F)	
Dayf	2	176466633	88233317	46.87	0.005461	**
Residuals	3	5647570	1882523			

Signif. codes: 0 ‘***’ 0.001 ‘**’ 0.01 ‘*’ 0.05 ‘.’ 0.1 ‘ ’ 1

> summary(Pseudomonadaceae)

Call:

lm(formula = Pseudomonadaceae ~ Dayf, data = freshwaterphyla)

Residuals:

1	2	3	4	5	6
-133	133	600	-600	1564	-1564

Coefficients:

	Estimate	Std. Error	t value	Pr(>|t|)	
(Intercept)	2826.0	970.2	2.913	0.06185	.
Dayf7	9965.0	1372.1	7.263	0.00539	**
Dayf14	-2625.0	1372.1	-1.913	0.15165	

Signif. codes: 0 ‘***’ 0.001 ‘**’ 0.01 ‘*’ 0.05 ‘.’ 0.1 ‘ ’ 1

Residual standard error: 1372 on 3 degrees of freedom

Multiple R-squared: 0.969, Adjusted R-squared: 0.9483

F-statistic: 46.87 on 2 and 3 DF, p-value: 0.005461

NORMALITY TEST FOR RESIDUAL

> Pseudomonadaceae$residuals ### Shows you the residuals for each sample

   1   2   3   4   5   6

 -133   133   600 -600 1564 -1564

> hist(Pseudomonadaceae$residuals) ### plots a histogram of the residuals

> shapiro.test(Pseudomonadaceae$residuals)

Shapiro-Wilk normality test

data: Pseudomonadaceae$residuals

W = 0.99587, p-value = 0.9986

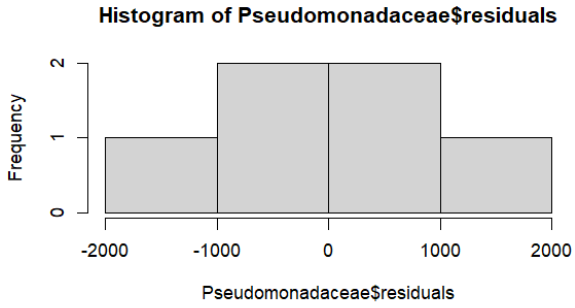

Figure A70 A histogram of the ANOVA residuals of Pseudomonadaceae in the freshwater samples across of decomposition

SIGNIFICANT BETADISPER MULTIPLE DISPERSION RESULTS FOR CHAPTER SEVEN

SEAWATER

> seawaterphyla=read.csv("seawater.csv",header=T, stringsAsFactors=TRUE)

> group <- c("Day 0", "Day 0", "Day 7", "Day 7", "Day 14", "Day 14")

> seawaterdist <- vegdist(seawaterphyla) ## creates distance matrix

```
> as.matrix (seawaterdist) ## show distance matrix
        1         2         3         4         5         6
1 0.0000000 0.1194677 0.5613562 0.7246350 0.7106319 0.6800130
2 0.1194677 0.0000000 0.5191089 0.6983101 0.6829803 0.6503496
3 0.5613562 0.5191089 0.0000000 0.3871986 0.2722444 0.1748766
4 0.7246350 0.6983101 0.3871986 0.0000000 0.1168224 0.3755509
5 0.7106319 0.6829803 0.2722444 0.1168224 0.0000000 0.2615128
6 0.6800130 0.6503496 0.1748766 0.3755509 0.2615128 0.0000000
> seawatermod <- betadisper(seawaterdist, group)    ## Calculate multivariate dispersion
> seawatermod

             Homogeneity of multivariate dispersions

Call: betadisper(d = seawaterdist, group = group)

No. of Positive Eigenvalues: 4
No. of Negative Eigenvalues: 1

Average distance to median:
  Day 0  Day 14   Day 7
0.05973 0.13076 0.19360

Eigenvalues for PCoA axes:
    PCoA1     PCoA2     PCoA3     PCoA4     PCoA5
 0.552004  0.093459  0.010984  0.004585 -0.003344
> anova(seawatermod)    ## Perform test
Analysis of Variance Table

Response: Distances
         Df   Sum Sq   Mean Sq    F value    Pr(>F)
Groups     2 0.017942 0.0089711 3.0052e+30 < 2.2e-16 ***
```

```
Residuals  3 0.000000 0.0000000
---
Signif. codes:  0 ‘***’ 0.001 ‘**’ 0.01 ‘*’ 0.05 ‘.’ 0.1 ‘ ’ 1
Warning message:
In anova.lm(lm(Distances ~ Groups, data = model.dat)) :
  ANOVA F-tests on an essentially perfect fit are unreliable
> permutest(seawatermod, pairwise = TRUE, permutations = 99) ## Permutation test for F
Set of permutations < 'minperm'. Generating entire set.

Permutation test for homogeneity of multivariate dispersions
Permutation: free
Number of permutations: 719

Response: Distances
        Df   Sum Sq   Mean Sq         F N.Perm Pr(>F)
Groups     2 0.017942 0.0089711 3.0052e+30     99   0.01 **
Residuals  3 0.000000 0.0000000
---
Signif. codes:  0 ‘***’ 0.001 ‘**’ 0.01 ‘*’ 0.05 ‘.’ 0.1 ‘ ’ 1

Pairwise comparisons:
(Observed p-value below diagonal, permuted p-value above diagonal)
          Day 0     Day 14 Day 7
Day 0            8.0000e-02  0.05
Day 14 5.0113e-31            0.09
Day 7  5.5080e-32 5.8521e-31
Warning messages:
1: In anova.lm(lm(Distances ~ Groups, data = model.dat)) :
  ANOVA F-tests on an essentially perfect fit are unreliable
2: In summary.lm(mod) : essentially perfect fit: summary may be unreliable
> (seawatermod.HSD <- TukeyHSD(seawatermod) ## Tukey's Honest Significant Differences
```

Tukey multiple comparisons of means

95% family-wise confidence level

Fit: aov(formula = distances ~ group, data = df)

$group

	diff	lwr	upr	p adj
Day 14-Day 0	0.07102257	0.07102257	0.07102257	0
Day 7-Day 0	0.13386547	0.13386547	0.13386547	0
Day 7-Day 14	0.06284289	0.06284289	0.06284289	0

BRACKISH WATER

```
> brackishwaterphyla=read.csv ("brackishwater.csv",header=T, stringsAsFactors=TRUE)
> group <- c("Day 14", "Day 14", "Day 7", "Day 7", "Day 0", "Day 0")
> brackishwaterdist <- vegdist(brackishwaterphyla) ## creates distance matrix
> as.matrix (brackishwaterdist) ## show distance matrix
          1         2         3         4         5         6
1 0.00000000 0.08471857 0.05658630 0.09904149 0.5774293 0.4298406
2 0.08471857 0.00000000 0.11002221 0.09954757 0.6161593 0.3992223
3 0.05658630 0.11002221 0.00000000 0.06246653 0.5993986 0.4345622
4 0.09904149 0.09954757 0.06246653 0.00000000 0.5990346 0.3889720
5 0.57742928 0.61615926 0.59939856 0.59903459 0.0000000 0.6332715
6 0.42984063 0.39922232 0.43456219 0.38897204 0.6332715 0.0000000
> brackishwatermod <- betadisper(brackishwaterdist, group)    ## Calculate multivariate dispersion
> brackishwatermod

             Homogeneity of multivariate dispersions

Call: betadisper(d = brackishwaterdist, group = group)

No. of Positive Eigenvalues: 4
```

No. of Negative Eigenvalues: 1

Average distance to median:

Day 0 Day 14 Day 7

0.31664 0.04236 0.03123

Eigenvalues for PCoA axes:

PCoA1 PCoA2 PCoA3 PCoA4 PCoA5

0.2851242 0.1333400 0.0066244 0.0023376 -0.0003228

> anova(brackishwatermod) ## Perform test

Analysis of Variance Table

Response: Distances

Df Sum Sq Mean Sq F value Pr(>F)

Groups 2 0.10454 0.052269 1.1308e+31 < 2.2e-16 ***

Residuals 3 0.00000 0.000000

Signif. codes: 0 '***' 0.001 '**' 0.01 '*' 0.05 '.' 0.1 ' ' 1

Warning message:

In anova.lm(lm(Distances ~ Groups, data = model.dat)) :

ANOVA F-tests on an essentially perfect fit are unreliable

> permutest(brackishwatermod, pairwise = TRUE, permutations = 99) ## Permutation test for F

Set of permutations < 'minperm'. Generating entire set.

Permutation test for homogeneity of multivariate dispersions

Permutation: free

Number of permutations: 719

Response: Distances

Df Sum Sq Mean Sq F N.Perm Pr(>F)

Groups 2 0.10454 0.052269 1.1308e+31 99 0.01 **

```
Residuals  3 0.00000 0.000000
---
Signif. codes:  0 ‘***’ 0.001 ‘**’ 0.01 ‘*’ 0.05 ‘.’ 0.1 ‘ ’ 1

Pairwise comparisons:
(Observed p-value below diagonal, permuted p-value above diagonal)
          Day 0     Day 14 Day 7
Day 0            4.0000e-02  0.06
Day 14 3.2002e-34            0.08
Day 7  5.9111e-34 5.8343e-31
Warning messages:
1: In anova.lm(lm(Distances ~ Groups, data = model.dat)) :
  ANOVA F-tests on an essentially perfect fit are unreliable
2: In summary.lm(mod) : essentially perfect fit: summary may be unreliable
> (brackishwatermod.HSD <- TukeyHSD(brackishwatermod))  ## Tukey's Honest Significant Differences
  Tukey multiple comparisons of means
    95% family-wise confidence level

Fit: aov(formula = distances ~ group, data = df)

$group
                 diff        lwr        upr p adj
Day 14-Day 0 -0.27427649 -0.27427649 -0.27427649     0
Day 7-Day 0  -0.28540251 -0.28540251 -0.28540251     0
Day 7-Day 14 -0.01112602 -0.01112602 -0.01112602
FRESHWATER
> freshwaterphyla=read.csv("freshwater.csv",header=T, stringsAsFactors=TRUE)
> group <- c("Day 14", "Day 14", "Day 0", "Day 0", "Day 7", "Day 7")
> freshwaterdist <- vegdist(freshwaterphyla) ## creates distance matrix
> as.matrix (freshwaterdist) ## show distance matrix
          1         2         3         4         5         6
```

1 0.00000000 0.1872370 0.03311091 0.6670172 0.5848857 0.4067440

2 0.18723699 0.0000000 0.20282254 0.6228371 0.4089592 0.2473931

3 0.03311091 0.2028225 0.00000000 0.6195314 0.5706368 0.4292670

4 0.66701718 0.6228371 0.61953144 0.0000000 0.5433243 0.6544422

5 0.58488571 0.4089592 0.57063675 0.5433243 0.0000000 0.2370644

6 0.40674403 0.2473931 0.42926703 0.6544422 0.2370644 0.0000000

> freshwatermod <- betadisper(freshwaterdist, group) ## Calculate multivariate dispersion

> freshwatermod

Homogeneity of multivariate dispersions

Call: betadisper(d = freshwaterdist, group = group)

No. of Positive Eigenvalues: 4

No. of Negative Eigenvalues: 1

Average distance to median:

Day 0 Day 14 Day 7

0.30977 0.09362 0.11853

Eigenvalues for PCoA axes:

PCoA1 PCoA2 PCoA3 PCoA4 PCoA5

0.331457 0.219604 0.005651 0.001383 -0.004842

> anova(freshwatermod) ## Perform test

Analysis of Variance Table

Response: Distances

Df Sum Sq Mean Sq F value Pr(>F)

Groups 2 0.05594 0.02797 6.6013e+30 < 2.2e-16 ***

Residuals 3 0.00000 0.00000

Signif. codes: 0 ‘***’ 0.001 ‘**’ 0.01 ‘*’ 0.05 ‘.’ 0.1 ‘ ’ 1

```
Warning message:
In anova.lm(lm(Distances ~ Groups, data = model.dat)) :
  ANOVA F-tests on an essentially perfect fit are unreliable
> permutest(freshwatermod, pairwise = TRUE, permutations = 99) ## Permutation test for F
Set of permutations < 'minperm'. Generating entire set.

Permutation test for homogeneity of multivariate dispersions
Permutation: free
Number of permutations: 719

Response: Distances
          Df  Sum Sq Mean Sq          F N.Perm Pr(>F)
Groups     2 0.05594 0.02797 6.6013e+30     99   0.01 **
Residuals  3 0.00000 0.00000
---
Signif. codes:  0 ‘***’ 0.001 ‘**’ 0.01 ‘*’ 0.05 ‘.’ 0.1 ‘ ’ 1

Pairwise comparisons:
(Observed p-value below diagonal, permuted p-value above diagonal)
           Day 0     Day 14 Day 7
Day 0            3.0000e-02  0.08
Day 14 0.0000e+00            0.11
Day 7  1.3166e-32 7.7572e-31
Warning messages:
1: In anova.lm(lm(Distances ~ Groups, data = model.dat)) :
  ANOVA F-tests on an essentially perfect fit are unreliable
2: In summary.lm(mod) : essentially perfect fit: summary may be unreliable
> (freshwatermod.HSD <- TukeyHSD(freshwatermod))  ## Tukey's Honest Significant Differences
  Tukey multiple comparisons of means
    95% family-wise confidence level
```

Fit: aov(formula = distances ~ group, data = df)

$group

	diff	lwr	upr	p adj
Day 14-Day 0	-0.21614722	-0.21614722	-0.21614722	0
Day 7-Day 0	-0.19123349	-0.19123349	-0.19123349	0
Day 7-Day 14	0.02491373	0.02491373	0.02491373	0